IRON HOMEOSTASIS
IN THE CENTRAL NERVOUS SYSTEM

Suh Young Jeong, M.Sc.

Centre for Research in Neuroscience
The Research Institute of the McGill University Health Center
Department of Neurology and Neurosurgery
McGill University, Montréal, Canada
August 2007

A thesis submitted to the Faculty of Graduate and Postdoctoral Studies
in partial fulfillment of the requirements of the degree of Doctor of Philosophy

Your file Votre référence
ISBN: 978-0-494-50836-7
Our file Notre référence
ISBN: 978-0-494-50836-7

To my parents, with all my heart

TABLE OF CONTENTS

Abstract

Iron is an essential, yet highly reactive, metal that needs to be tightly regulated. Excess iron in the central nervous system (CNS) can lead to free radical formation and neurodegeneration. My Ph.D. thesis work is focused on two animal models of neurodegeneration: one uses a null mutation of ceruloplasmin (*CP*), which in humans causes iron accumulation and neurodegeneration in the CNS; and the other is a gain of function mutation in the superoxide dismutase 1 (*SOD1*), which causes amyotrophic lateral sclerosis (ALS) in mice/humans. CP is a ferroxidase that converts highly toxic ferrous iron to its non-toxic ferric form. A GPI-anchored form of CP (GPI-CP), expressed by astrocytes, is the major form of CP in the CNS. In my Master's work, the role of CP in iron influx and efflux *in vitro* using astrocyte cultures from $CP^{-/-}$ and $CP^{+/+}$ mice was characterized and revealed that iron efflux is completely absent while iron influx into astrocytes is unaffected in the absence of CP.

For my Doctoral thesis, I continued to study the role of GPI-CP in astrocytes and showed that GPI-CP is physically associated with the iron efflux transporter ferroportin (FPN). I also assessed whether FPN, a transmembrane protein, is mobilized from non-lipid raft to lipid raft regions of the membrane in response to cellular iron status. Using astrocyte cultures incubated in different iron concentrations, I found that under high iron conditions, there is a rapid relocation of FPN into lipid rafts containing GPI-CP. On the other hand, cells treated with an iron chelator showed decreased FPN expression on the membrane. Therefore, formation of the GPI-CP/FPN complex is essential for cellular iron efflux and the generation of this complex is regulated by cellular iron levels.

To understand how the lack of CP causes iron accumulation and neurodegeneration, I carried out a detailed analysis of iron accumulation, dysregulation of

iron homeostasis proteins, and loss of astrocytes and neurons in the cerebellum of $CP^{-/-}$ mice during aging. Abnormal iron accumulation is first detected in $CP^{-/-}$ mice by 12 months and peaks at 24 months. Iron accumulation occurs in astrocytes, but not in Purkinje neurons and large neurons in the deep nuclei. The iron importer DMT1 is abnormally increased in these large neurons but not in astrocytes, while ferritin expression is increased in astrocytes. There is also a marked loss of astrocytes and Purkinje neurons in $CP^{-/-}$ mice with age. The loss of astrocytes is likely to be related to iron accumulation while the loss of the Purkinje neurons is likely due to the loss of astrocytic support and lack of sufficient supply of iron from astrocytes.

To assess the contribution of iron to the pathogenesis of ALS, I studied the involvement of iron accumulation and the dysregulation of iron homeostasis in a mouse model of ALS ($SOD1^{G37R}$). I found excessive iron accumulation in the large motor neurons and glia in the spinals cords of 12-month old SOD1 mice. There was dysregulation in the expression of iron homeostasis proteins, which correlate with the progression of the disease. This iron accumulation in the motor neurons may be due to impaired anterograde axonal transport, as evidenced by a nerve ligation study I carried out. Furthermore, purified mitochondria from *SOD1* mice show increased iron accumulation, suggesting a role for iron in mitochondrial dysfunction. Importantly, treatment with a lipophilic iron chelator before the onset of clinical symptoms (8 months of age) extended lifespan by an extra 4.8 weeks, thus pointing to an important role for iron in the progression of disease.

Iron in the CNS is thought to play an important role in many neuroinflammatory conditions due to its redox activity. My work will help further the understanding of how disruption of iron homeostasis can contribute to cell death under various neurodegenerative conditions.

Résumé

Le fer est un métal essentiel, mais très réactif, qui nécessite un règlement très étroit. Un excès de fer dans le system nerveux centrale (SNC) peut induire la formation de radicaux libres et la neurodegénération. Ma thèse doctorale c'est concentré sur deux modèles animale de neurodegénération : le premier modèle fut l'utilisation d'une souris avec une inactivation du gène de la ceruloplasmine (CP), qui chez l'humain cause l'accumulation du fer et de la neurodegénération dans le SNC; le deuxième modèle fut l'utilisation d'une souris avec une mutation causant un gain de fonction dans le gène de la superoxide dismutase 1 (SOD1), qui cause la sclérose latérale amyotrophique (SLA) chez la souris et l'homme. CP est une ferroxidase qui convertit le hautement toxique fer ferreux en le non toxique fer ferrique. Une forme ancrée par GPI du CP (GPI-CP), exprimé par les astrocytes, est la forme majeure de la CP dans le SNC. Mon travaille de thèse de maîtrise était de caractérisé le rôle de la CP dans le flux du fer des cultures *in vitro* d'astrocytes de souris $CP^{-/-}$ et $CP^{+/+}$. Ce travaille a révélé que l'absence de CP n'affect pas l'influx du fer mais plutôt abolit complètement l'efflux du fer des astrocytes.

Pour ma thèse doctorale, j'ai continué à étudier le rôle de la GPI-CP dans les astrocytes et j'ai démontré que la GPI-CP est associé physiquement avec la transporteuse efflux de fer, la ferroportine (FPN). J'ai aussi déterminé si FPN, une protéine transmembranaire, est immobilisé dans les radeaux lipidiques de la membrane cytoplasmique en réponse au statut du fer cellulaire. En utilisant des cultures d'astrocytes incubés dans de différentes concentrations de fer, j'ai trouvé que sous haute concentration il y a une relocalisation de la FPN vers les radeaux lipidiques contentent des GPI-CP. D'un autre côté, des cellules traitées avec un chélateur de fer ont démontré une diminution d'expression de la FPN à la membrane cytoplasmique. Donc, la formation du complexe

GPI-CP/FPN est essentielle pour le flux cellulaire du fer et la génération de ce complexe est réglée par les niveaux cellulaires du fer.

Pour comprendre comment un manque de la CP cause une accumulation de fer et de la neurodegénération, j'ai performé une analyse détaillé de l'accumulation du fer, le dérèglement des protéines de la l'homéostasie du fer, et la perte d'astrocytes et de neurones dans le cervelet, pendant le vieillissement de souris $CP^{-/-}$. Une accumulation anormale de fer est premièrement détecté dans les souris $CP^{-/-}$ à 12 mois et sommet à 24 mois. Une accumulation de fer ce produit dans les astrocytes, mais pas dans les neurones Purkinje et les neurones large des noyaux profonds. L'importatrice de fer DMT1 est anormalement augmentée dans les neurones larges mais pas les astrocytes, pendant que l'expression de la ferratine est augmentée dans les astrocytes. Il y aussi une perte d'astrocyte et de neurones Purkinje chez la souris $CP^{-/-}$. La perte d'astrocyte est probablement relié à l'accumulation de fer, pendent que la perte de neurones Purkinje est probablement relié à un manque de support des astrocytes et un manque de provision de fer provenant des astrocytes.

Pour évaluer la contribution du fer à la pathogenèse de la SLA, j'ai étudié la participation de l'accumulation du fer et le dérèglement de l'homéostasie du fer chez la souris $SOD1^{G37R}$, un modèle de SLA. J'ai trouvé une accumulation excessive de fer dans les motoneurones larges et les cellules gliales de la moelle épinière chez les souris SOD1 âgées de 12 mois. Il y avait un dérèglement dans l'expression de protéines contribuant à l'homéostasie du fer qui corrélait avec le progrès de la maladie. Cette accumulation de fer dans les motoneurones larges peut être du à la détérioration de transport axonale antérograde, démontré par l'étude de ligature neuronale que j'ai performé. De plus, des mitochondries purifiées de la souris SOD1 a démontré une augmentation dans l'accumulation de fer, suggérant un rôle pour le fer dans le dérèglement des mitochondries.

Le traitement avec un chélateur de fer lipophilique avant le début des symptômes cliniques (à l'age de 8 mois) a allonger la longévité par un extra 4.8 semaines, indiquant un rôle important pour le fer dans la progression de la maladie.

Dans le SNC le fer, due à sa réaction d'oxydo-réductrice, est cru de jouer un rôle important dans plusieurs conditions neuroinflammatoire. Mon travaille va aider à approfondir les connaissances de la l'homéostasie du fer et comment son dérèglement peut contribuer à la mort cellulaire dans de différentes conditions de neurodegénération.

Acknowledgments

I would like to express my sincere gratitude to all the people who helped me during my Ph.D. training although I may not be able to mention all their names here.

All my work would not be possible without the enormous support, encouragement, patience and guidance from my supervisor, Dr. Samuel David. He showed me how exciting science can be through the many scientific discussions we shared.

I would like to thank my advisory committee members, Drs Prem Ponka and Josephine Nalbantoglu for their help and thoughtful discussions. I am also grateful to Dr. Yong Rao for serving as my mentor and chairing my Ph.D. seminar.

Many advices and collaborations helped me along my training period. I would like to thank Drs Robert J. Dunn, Sangwon Kim, and Manuela Santos for their help and advice. I also would like to thank Drs Prem Ponka, Paolo Arosio and Kostas Pantopoulos for kindly supplying key reagents.

I would like to thank all the members of the David lab for their help and friendship. I am particularly indebted to Drs Bharatkumar Patel and Shalina Ousman for their kind help when I first started in the lab. I am thankful to Ms. Margaret Attiwell, Ourania Tsatas, and Hiba Kazak for not only their assistance but also their love and encouragement. I would like to thank Mr. Khizr Rathore for his help in the SOD1 project and wonderful discussions we shared.

I would like to say a special thank you to Mr. Nader Ghasemlou and Ms. Ourania Tsatas for their excellent editorial assistance for this thesis. I am grateful to Ms. Nadia Melián for translating my abstract in French, and Mr. Michael Haber for his help with one of the illustrations.

I would like to thank my best friend Chung Keun Yim for his encouragement. Finally, a special thank you to my parents for their love, encouragement, and support, which have made this long journey possible.

Contribution of authors

Chapter 2:

The first part of this chapter is published. Jeong SY, David S. (2003) GPI-anchored ceruloplasmin is required for iron efflux from cells in the central nervous system. *J Biol. Chem.* 278: 27144-8. The second part of this chapter is work that will be submitted for publication soon. Jeong SY, Ponka P, David S. (2007) Mobilization of the iron exporter Ferroportin to lipid raft is regulated by iron. (manuscript in preparation). All the experimental work described in these manuscripts and writing of the initial manuscripts was done by me. Dr. Prem Ponka provided an iron chelator and gave advice in designing the protocol for the *in vitro* chelator experiment. The planning of the experiments and the editing of the manuscripts were done jointly with my supervisor, Dr. Samuel David.

Chapter 3:

Jeong SY, David S. (2006) Age-related changes in iron homeostasis and cell death in the cerebellum of ceruloplasmin-deficient mice. *J Neurosci.*26: 9810-9. All the experimental work described in this manuscript and writing of the initial manuscript was done by me. The planning of the experiments and editing of the manuscript was done jointly with my supervisor, Dr. Samuel David.

Chapter 4:

Jeong SY, Rathore KI, Arosio P, Ponka P, David S (2007) Disruption of iron homeostasis contributes disease progression in a mouse model of Amyotrophic Lateral Sclerosis. (manuscript in preparation). All the experimental work described in this manuscript was done by me, except for the sciatic nerve ligation experiment, which was done by another graduate student in the lab, Mr. Khizr Rathore. I have also written the initial manuscript. Drs Paolo Arosio and Prem Ponka provided antibodies and an iron chelator for the experiments. The planning of the experiments and editing of the manuscript was done jointly with my supervisor, Dr. Samuel David.

Publications

Publications based on Ph. D. thesis work:

1. **Jeong SY**, David S. (2003) GPI-anchored ceruloplasmin is required for iron efflux from cells in the central nervous system. *J Biol. Chem.* 278: 27144-8.
2. **Jeong SY**, David S. (2006) Age-related changes in iron homeostasis and cell death in the cerebellum of ceruloplasmin-deficient mice. *J Neurosci.*26: 9810-9.
3. **Jeong SY**, Rathore KI, Arosio P, Ponka P, David S (2007) Disruption of iron homeostasis contributes disease progression in a mouse model of Amyotrophic Lateral Sclerosis. (manuscript in preparation).
4. **Jeong SY**, Ponka P, David S. (2007) Mobilization of the iron exporter Ferroportin1 to lipid raft is regulated by iron. (manuscript in preparation).

Publications based on other projects on ceruloplasmin:

5. Patel BN, Dunn RJ, **Jeong SY**, Zhu Q, Julien JP, David S. (2002) Ceruloplasmin regulates iron levels in the CNS and prevents free radical injury. *J Neurosci.* 22(15): 6578-86.
6. Mittal B, Doroudchi MM, **Jeong SY**, Patel BN, David S. (2003) Expression of a membrane-bound form of the ferroxidase ceruloplasmin by leptomeningeal cells. *Glia.* 41(4): 337-46.
7. De Domenico I, McVey Ward D, Bonaccorsi di Patti MC, **Jeong SY**, David S, Musci G, and Kaplan J. (2007) Ceruloplasmin is required for the stability of cell surface ferroportin. *EMBO J.* 26(12): 2823-31.
8. Rathore KI, Kerr BJ, López-Vales R, **Jeong SY**, Ponka P, David S. (2007) Ceruloplasmin protects the injured spinal cord from iron-mediated oxidative damage. *Nat. Neurosci.* (under review)

Other collaborations:

9. Sicotte M, Tsatas O, **Jeong SY**, Cai C-Q, He Z, David S. (2003) Immunization with myelin or Nogo-66/MAG in alum promotes axon regeneration and sprouting after corticospinal tract lesions in the spinal cord. *Mol. Cell Neurosci.* 23: 251-63.

10. Ghasemlou N, **Jeong SY**, Lacroix S, David S. (2007) T cells contribute to lysophosphatidylcholine-induced macrophage activation and demyelination in the CNS. *Glia*, 55: 294-302.
11. Kerr BJ, Girolami EI, Ghasemlou N, **Jeong SY**, David S. (2007) 15-Deoxy-Δ-12,14-Prostaglandin J2 reduces tissue damage and promotes functional recovery after spinal cord injury. *J. Immunol.* (under review)

Claims for originality

My Ph. D. thesis research includes the following original findings and observations.

1. GPI-anchored ceruloplasmin (CP) promotes iron efflux from astrocytes in the CNS and is an essential factor for the function of the iron exporter ferroportin (FPN).
2. GPI-CP and FPN form an iron efflux complex and the generation of this complex is regulated by cellular iron concentration. High iron drives translocation of FPN into the lipid raft regions of the cell membrane where GPI-CP is located.
3. I have characterized the changes in the cerebellum of ceruloplasmin null mice during aging and found these mice to have progressive accumulation of iron starting from 12 months of age.
4. *CP* null mice show age-dependent dysregulation of proteins involved in iron homeostasis and the pattern of dysregulation was similar to the normal aging process suggesting an exaggerated aging process in the *CP* null mice.
5. There is an extensive loss of both astrocytes and Pukinje neurons in the *CP* null mice cerebellum although large neurons did not accumulate excess iron.
6. I have provided the first evidence of abnormal iron accumulation in the spinal cord of $SOD1^{G37R}$ mice, which is a mouse model for Amyotrophic lateral sclerosis (ALS). Iron accumulation was found in both neurons and glia, but the pattern of accumulation was different in these cells.
7. I also discovered that $SOD1^{G37R}$ mice showed dysregulation of proteins involved in iron homeostasis, which followed the caudal to rostral progression of the disease.
8. I also show that there is an abnormal increase in mitochondrial ferritin (MtF) expression in $SOD1^{G37R}$ mice, suggesting that excess iron may be one of the possibilities for mitochondrial oxidative damage. This increase of MfF was found in both neurons and

glia.

9. I provide the first direct evidence that blockage of axonal transport can cause iron accumulation in the neuronal cell bodies, also indicating that iron is normally transported down axons via anterograde axonal transport.

10. I show that treatment with the iron chelator salicylaldehyde isonicotinoyl hydrazone (SIH) starting before the onset of symptoms is effective in increasing the lifespan of $SOD1^{G37R}$ mice, indicating the important role of iron in the pathogenesis of the disease and its potential role in ALS.

Abbreviations

ALS	amyotrophic lateral sclerosis
ARE	antioxidant responsive element
ATP	adenosine triphosphate
BBB	blood-brain-barrier
BPS	bathophenanthroline disulfonate
CNS	central nervous system
CP	ceruloplasmin
CSF	cerebrospinal fluid
DCYTB	duodenal cytochrome b
DMT1	divalent metal transporter 1
Fe-S	iron-sulfur
FLVCR	feline leukemia virus subgroup C receptor
FPN	ferroportin
FTH, FTL	ferritin heavy (light) chain
GAIT	IFN-γ activated inhibitor of translation
GPI	glycosylphosphatidylinositol
HEPC	hepcidin
HEPH	hephaestin
HH	hereditary hemochromatosis
HIF	hypoxia-inducible factor
IRE	iron-responsive element
IRP	iron-regulatory protein
LIP	labile iron pool
NBIA	Neurodegeneration with brain iron accumulation
NTBI	non-transferrin-bound iron
PANK2	pantothenate kinase 2
PKAN	Pantothenate kinase-associated neurodegeneration
ROS	reactive oxygen species
s.e.m.	standard error of the mean
SIH	salicylaldehyde isonicotinoyl hydrazone
SOD1	superoxide dismutase 1

Steap3	Six-transmembrane epithelial antigen of the prostate 3
TF	transferrin
TfR1	transferrin receptor 1
Tim-2	T cell immunoglobulin-domain and mucin-domain protein2
UTR	untranslated region

CHAPTER 1

Literature Review

1.1 Introduction

Iron is an essential element that is required for organisms to live in an oxygen-rich environment. Iron imparts to haemoglobin its oxygen-carrying capacity by providing specific binding sites for oxygen [1]. The ability to donate and accept electrons gives iron the capacity to serve as an important co-factor for various enzymes, such as those involved in DNA, RNA, and protein synthesis, mitochondrial oxidation reactions, and a variety of other metabolic processes (reviewed in [2]). However, its redox-active character allows ferrous iron to generate toxic free radicals that can cause cell and DNA damage. Therefore, iron needs to be properly handled and shielded to prevent tissue injury. There are several examples in the literature linking excess iron with neurodegeneration in the central nervous system (CNS) [3, 4]. My Ph.D. thesis research is focused on the ferroxidase ceruloplasmin (CP) and a variety of molecules involved in maintaining iron homeostasis in the CNS. In this introductory chapter, I will provide an overview of the various proteins involved in iron homeostasis and of various CNS diseases that show disruption in iron homeostasis mechanisms.

1.2 A double-edged sword

Iron is necessary for life, as it functions as a necessary cofactor for many proteins containing heme including cytochrome and cytochrome oxidase. Iron is also involved in adenosine triphosphate (ATP) synthesis in mitochondria, the major energy generator in cells. Three complexes of the electron transport chain contain iron-sulfur clusters (Fe-S clusters) as a cofactor. These Fe-S clusters are involved in promoting electron transfer between proteins [5]. Other Fe-S cluster-containing proteins are involved in DNA repair (e.g. endonuclease), heme synthesis (e.g. ferrochelatase), and iron

metabolism (e.g. iron-regulatory protein 1) in cytosol as well as in mitochondria (reviewed in [6]). Other iron-dependent enzymes include ribonucleotide reductase, which is required for DNA synthesis, succinate dehydrogenase and aconitase of the TCA cycle [7]. Furthermore, iron is a cofactor for tyrosine hydroxylase and tryptophan hydroxylase, which are involved in synthesis of neurotransmitters in the CNS [8]. Iron is also necessary for oligodendrocytes to generate and maintain myelin in the CNS [9-11].

Although it is clear that iron is important for many normal cellular activities, excess or inappropriately shielded iron can cause devastating toxic effects. Ferrous iron (Fe^{2+}), which is more soluble at a physiological pH, can react with hydrogen peroxide to produce ferric iron (Fe^{3+}) leading to the formation of hydroxyl radicals (via the Fenton reaction). Iron can also react with molecular oxygen to yield superoxide anions, hydrogen peroxide, and hydroxyl radicals that are potentially toxic to cells (via the Haber-Weiss reaction).

Fenton reaction

$$Fe^{2+} + H_2O_2 \rightarrow Fe^{3+} + {\cdot}OH + OH^-$$

Haber-Weiss Reaction

$$O_2 + Fe^{2+} \rightarrow O_2^{-}{\cdot} + Fe^{3+}$$

$$2O_2^{-}{\cdot} + 2H^+ \rightarrow O_2 + H_2O_2$$

$$Fe^{2+} + H_2O_2 \rightarrow Fe^{3+} + {\cdot}OH + OH^-$$

These reactive oxygen species are thought to play important pathogenic roles in a variety of diseases with excess iron such as Parkinson's and Alzheimer's diseases [12-

16] (see section 1.7). Free radical formation can trigger lipid peroxidation, DNA damage, protein oxidation and eventually cause cell death [17-20]. Therefore, the safe conversion of Fe^{2+} to Fe^{3+} is necessary and is mainly carried out by various ferroxidases. In addition there are a number of other proteins that are involved in the binding, transport, influx and efflux, and storage of iron that help maintain iron homeostasis and keep it from producing toxic free radicals. Organisms have developed mechanisms to prevent increase of the iron-pool while maintaining sufficient levels for metabolic use. However, these homeostatic mechanisms can become dysregulated and can cause iron deficiency or iron overload.

1.3 Proteins involved in iron homeostasis

Since iron is essential for cellular metabolism, but can be potentially toxic at the same time, it is very important for iron homeostasis to be maintained. There are many proteins involved in transporting and storing iron as well as enzymes that oxidize or reduce the two forms of iron (ferrous and ferric). I will therefore provide a brief summary of some of those proteins involved in iron homeostasis. Protein names and abbreviations in this section are based on the recent recommendations set forth by the BioIron Society and published in the Society's website (http://www.bioiron.org).

1.3.1 Transferrin (TF) and transferrin receptor (TfR)

Most of the iron in plasma is bound to transferrin (TF), while very little is associated with ferritin, albumin or low-molecular weight carriers [21]. It is via TF that much of the iron is carried to organs and tissues throughout the body. Human TF is a 80kDa glycoprotein with two iron binding domains that can bind tightly, but reversibly, to two

ferric iron atoms [22]. To form diferric-TF, ferrous iron has to be converted into the ferric form, which can be achieved by the ferroxidase ceruloplasmin, which is abundant in plasma (see section 1.3.6), or by TF's own ferroxidase activity [23]. Two different transferrin receptors (TfR) have been cloned and reported in both human and mouse: the classical TfR1 is more ubiquitously expressed in many cell types while TfR2 is mainly expressed in hepatocytes [24]. Mammalian TfR1 is a homodimer of 760 amino acid subunits connected by disulfide bonds [25, 26]. The binding affinity between TF and TfR1 depends on the iron status of TF and the pH. Diferric-TF has a high affinity for its receptor (TfR1) under normal pH but apo-TF has a low affinity for the receptor. Therefore, diferric-TF/TfR complex formation can occur on the cell surface membrane and apo-TF can be released back into circulation when it is returned to the cell membrane (for details, see section 1.4.1). Therefore, transferrin-bound iron can be rapidly cleared from the circulation ($t_{1/2}$ = 1.7h) and TF is recycled more than one hundred times in the lifetime of the protein [27]. In addition to binding to TF, both TfRs also bind to HFE, a protein found to be defective in type 1 hereditary hemochromatosis (HH) [28, 29]. HH patients show increases in iron absorption and accumulation in the liver (reviewed in [30]). HFE can decrease TfR1-mediated iron uptake by 33% in HeLa cells [31], suggesting that it plays a role as a "brake" for TfR-mediated iron uptake. While most non-CNS mammalian cells, except for duodenal enterocytes, absorb iron via TF/TfR endocytosis, cells acquire iron through the endocytosis of the diferric-TF and TfR complex. Iron is released from the TF/TfR complex in the endosome and then gets translocated into the cytosol and the complex is recycled to the membrane (reviewed in [32], see section 1.4.1 for more details of this processing).

The intracellular levels of iron mainly regulate the amount of TfR1 expressed by cells. TfR1 mRNA contains five iron-responsive elements (IREs) in the 3' untranslated region. Under iron-deprived conditions, iron-regulatory proteins (IRPs) bind to IREs and stabilize TfR1 mRNA, thus promoting increased expression of TfR1 [33, 34] and resulting in increased iron uptake into the cell. The mechanisms through which IRPs are regulated by intracellular iron level will be discussed later in section 1.5.2. There are no IREs reported in the mRNA of TfR2 and its expression does not appear to be regulated by iron [24]. However, mutations in TfR2 have been reported to cause hemochromatosis with severe liver iron overload [35]. It has been suggested that TfR2 may play a role as an "iron sensor" for hepatocytes and might regulate expression of the peptide hepcidin, a negative regulator of iron absorption (see below for more details), but currently the biological roles of TfR2 are unclear.

Endothelial cells in the CNS express TfR1 and are able to import TF-bound iron ([36], for details, see section 1.6.1). TfR1 is also expressed in neurons and oligodendrocytes, although the TF concentration in the CSF is very low compared to the plasma (about 1/100-200) [37]. Unlike the normal human plasma TF saturation of between 20-50%, which leaves a significant amount of plasma TF capable of responding to increases in body iron, TF in the CSF is estimated to be fully saturated [37]. Interestingly, aside from the CNS, it has been recently reported that TF is expressed in Schwann cells of the peripheral nervous system [38]. The authors showed that TF mRNA is increased after nerve injury suggesting pro-differentiation role of TF. Taken together, TF plays an important role in sequestering iron safely in the plasma and delivering it to cells throughout the body.

1.3.2 Divalent metal transporter 1 (DMT1, DCT, Nramp2)

DMT1 is a transmembrane protein with 2 glycosylation sites and a consensus transport motif that is found in common with other cation transporters [39, 40]. Therefore, as expected, DMT1 transports various divalent metals including zinc, copper, iron and others [41]. Animal models with DMT1 mutations (*mk* mice and Belgrade rat) show problems with intestinal iron absorption and erythrocyte iron utilization resulting in severe anemia [41, 42]. *mk* mice not only show iron deficiency but also lower levels of manganese in the liver [43]. DMT1 is found on the brush border membrane of mature enterocytes, where its expression is tightly regulated by body iron status [44, 45] and where it functions as an iron importer. Besides the duodenum, DMT1 transcripts are found in many other tissues including kidney and brain [41]. To date, at least 4 transcripts of DMT1 have been identified, all of which are generated from one gene by combination of two sets of alternative splicing (Figure 1, reviewed in [46]). A 3' alternative splicing generates DMT1 with IRE (+IRE) sequence transcripts that are regulated by cellular iron levels (see section 1.5.2), and transcripts without IRE (-IRE) that may be independent of cellular iron status. Interestingly, in two types of neurons that express both forms of DMT1, the +IRE form was mainly found in intracellular vesicles while the –IRE form was found in neurites, the cell membrane, and the nucleus [47]. It is not clear whether there is any signal to trigger alternative splicing of DMT1 mRNA, but the duodenum, liver and testes all mainly express the +IRE form while other tissues express both forms, suggesting different roles for the two isoforms. Another alternative splicing at the 5' end of DMT1 mRNA generates the 1A and IB isoforms, the former having a longer N-terminus than the latter [48]. It is not clear whether 1A and 1B isoforms have different functions in cells or how they are regulated,

but nitric oxide was reported recently to downregulate only the 1B isoform via the NF-κB pathway *in vitro* [49]. DMT1 is also involved in the release of iron from the TF/TfR1 endocytosis pathway in the endosome (see section 1.4.1) [42]. It therefore plays an important role in the acquisition of iron into the cytosol.

In the CNS, DMT1 is found in neurons and astrocytes, and weak immunoreactivity was also detected in oligodendrocytes [50]. Interestingly, strong DMT1 immunostaining was found in ependymal cells lining the third ventricle, suggesting a role in the transfer of iron across the blood-brain barrier (BBB) possibly releasing transferrin-bound iron within the endothelial cells (see section 1.6.1). Moreover, it has been demonstrated recently that NMDA toxicity is mediated through increased expression of DMT1 in neurons and iron uptake via a nitric oxide regulatory pathway [51]. Both forms of DMT1 are also upregulated in the neuronal injury model induced by kainate [52]. Therefore, these data indicate that the non-transferrin-bound iron transporter DMT1 may play an important role in maintaining CNS iron homeostasis.

1.3.3 Ferrireductases

After the identification of the ferrous iron importer DMT1 in the duodenum, the existence of a ferrireductase expressed on the brush border of the duodenal enterocytes was speculated due to the preferred solubility of ferric iron under acidic conditions. Using a subtractive cloning method, McKie and colleagues identified a ferrireductase in duodenum whose expression is controlled by body iron status and named the protein duodenal cytochrome b (DCYTB) [53]. Although DCYTB expression is increased in a mouse model of hemochromatosis, a mouse model lacking DCYTB did not alter body

iron homeostasis [54, 55], suggesting that there may be other ferrireductases helping DMT1 under normal iron conditions.

While transferrin-bound iron is released in the endosome by acidification, this ferric iron must be reduced to be transported out through DMT1 on the endosomal membrane (see section 1.4.1). Six-transmembrane epithelial antigen of the prostate 3 (Steap3), a newly identified protein that has ferrireductase activity [56, 57], is highly expressed in hematopoietic tissue, and co-localizes with endogenous TF and TfR1, and facilitates TF-bound iron uptake [56].

1.3.4 Ferritin

Ferritin is a multimeric protein composed of 24 symmetrically arranged heavy (FTH) and light (FTL) chain subunits [58-60]. These polypeptide subunits of ferritin fold into four helix bundles and assemble into a hollow sphere-like structure that resembles a small spherical virus (reviewed in [61, 62]). The H to L chain ratio differs in different tissues [61-63]. One molecule of ferritin can store up to 4500 atoms of iron in this nano-cavity structure [64]. This high Fe:ferritin ratio (much higher than hemoglobin) makes ferritin a safe and efficient cytosolic iron storage protein. Studies *in vitro* show that the H and L chains of ferritin have different functions; FTH has ferroxidase activity that converts relatively soluble ferrous iron into the ferric form, while FTL can induce iron-core nucleation (see below) [65-67]. To incorporate iron into ferritin, two atoms of ferrous iron enter through one of two entry pores and are transported to the ferroxidase centre in FTH where they are oxidized to two atoms of ferric iron. They are then transferred to the inner cavity of ferritin where they interact with FTL and form the mineralized iron core [68]. It is not clear how iron travels between these sites or how

iron gets demineralized and released from ferritin under low iron conditions. It was originally shown that degradation of ferritin in the lysosome is necessary for iron to be released in rat hepatoma cells [69, 70]. More recently, it was shown that iron that is bound to ferritin can be released autonomously before the protein gets ubiquitinated and degraded in the proteasome when there is low iron in the cytosol [71]. There are two iron exit pores in ferritin [72] and mutations in one of these pores enables ferritin to release iron 30-times faster than wildtype ferritin [73]. Therefore, iron that is bound to ferritin can be released by at least two different mechanisms.

Although most ferritin is found in the cytosol, a minor proportion in vertebrates is found in plasma and secretory fluids [74]. This plasma ferritin is a clinically important index of body iron storage but the mechanism and the role of ferritin release into plasma is not yet clear. Recently, a receptor for FTH was identified that is expressed in liver, kidney and B lymphocytes [75]. This receptor called 'T cell immunoglobulin-domain and mucin-domain protein2' (Tim-2) can bind and cause internalization of FTH but not FTL. Therefore, while it is not a dominant pathway for iron uptake into cells, some cells might have the ability to take up ferritin-bound iron in the plasma. Another minor proportion of ferritin is also found in the nucleus that is translocated from cytosol [76]. This nuclear ferritin is mainly composed of FTH and inhibition of O-glycosylation decreases the amount of nuclear ferritin in astrocytoma cells [76, 77]. It has been suggested that this nuclear ferritin may play a role in protecting DNA from iron-induced oxidative damage [78, 79].

As a major iron storage protein in the cytosol, expression of ferritin is mainly controlled by intracellular iron status. This iron-based regulation of ferritin expression is achieved by regulation of an IRE in the 5' untranslated region of the ferritin mRNA.

Briefly, under low intracellular iron conditions, IRP binds to the IRE in ferritin mRNA and blocks the access of ribosomes, which in turn suppresses ferritin synthesis. Under high iron conditions, IRP no longer binds to the IRE and allows the ribosome to initiate ferritin synthesis (reviewed in [80, 81], for details see section 1.5.2). Moreover, it has been reported that nitrogen monoxide can increase translational efficiency of ferritin before IRE/IRP binding is modified [82]. Besides the translational regulation of ferritin, there is evidence that ferritin expression is also regulated transcriptionally. Tumor necrosis factor α (TNF-α) and interleukin-1α (IL-1α) are able to increase ferritin mRNA expression via the NF-κB pathway [83-85]. Both H and L ferritin mRNAs also contain an 'antioxidant responsive element' (ARE) sequence [86], which is found in the promoter region and enables a gene to respond to the oxidant stressors. This may explain how hydrogen peroxide has been shown to increase ferritin mRNA expression [87]. Moreover, treatment of cells with iron changed not only the IRP binding activity to IRE and induction of translation of ferritin, but also increased FTL mRNA levels [88]. This data suggests that many factors, including iron, can regulate ferritin expression not only translationally but also transcriptionally to obtain iron homeostasis.

In the CNS, most cell types express ferritin, including neurons, although most ferritin immunoreactivity is found in oligodendrocytes [89, 90]. Strikingly, mutations in L-ferritin (FTL) cause severe iron accumulation in basal ganglia and low plasma ferritin levels (see section 1.7.1) [91]. It was also suggested recently that iron-bound ferritin might cross the BBB and deliver iron into the CNS [92].

A new member of the ferritin family has been reported that is specifically located in mitochondria [93]. This mitochondrial ferritin (MtF) shares ~80% homology with FTH, and also has ferroxidase activity. Unlike cytosolic ferritin, which is composed of

both FTH and FTL, MtF forms homopolymers and does not contain an IRE sequence for iron-dependent regulation of expression (see section 1.5.2) [93]. Originally, MtF was reported to be highly expressed in human testis though a recent study in mice showed that it is widely expressed in other organs including the heart and brain [94]. Interestingly, the authors also reported that MtF is not found in the liver and spleen where cytosolic ferritin is highly expressed. MtF incorporates iron with higher efficiency than cytosolic ferritin [95], and has also been reported to have tumor growth suppressing activity by reducing cytosolic iron [96].

1.3.5 Ferroportin (FPN, IREG1, MTP1)

Ferroportin (FPN) is a glycoprotein consisting of 571-amino acids which was cloned by three different groups which is able to efflux ferrous iron *in vitro* [97-99]. To date, FPN is the only known ferrous iron exporter found in duodenum, liver, spleen, placenta, brain and many other tissues which can export iron [50, 99]. Lack of FPN expression in animal models causes embryonic lethality, likely due to a defect in maternal iron export to the fetus [98, 100]. Moreover, conditional knock-out mice suppressing FPN expression postnatally in the duodenum showed duodenal iron accumulation and severe iron-deficiency anemia [100] confirming that FPN is a major iron exporter from the small intestine. FPN requires the activity of a ferroxidase to efflux iron [98, 99, 101]. I have shown in my thesis work that in the CNS, FPN is associated with the GPI-anchored form of the ferroxidase, ceruloplasmin (GPI-CP), on astrocyte membranes [101]. The function of GPI-CP in promoting iron efflux and association with FPN will be discussed in detail in chapter 2.

It is still not clear how FPN expression is regulated in different cells and tissues. FPN mRNA transcripts contain IRE sequences in the 5' end [97, 99] which is likely regulated by IRP post-transcriptionally by inhibiting access of ribosomes (see section 1.5.2). This IRE sequence in FPN is functional and can compete with ferritin IRE *in vitro*. Consistent with the IRP data, iron depletion decreases FPN expression in the liver [97]. However, iron deficiency increases FPN expression in the duodenum and in a duodenal cell line showing differences in FPN regulation [97, 99, 102]. In addition to changes at the protein level, mRNA changes have also been reported following iron loading [99] suggesting that regulatory mechanisms other than IRE/IRP might also exist. On the other hand, binding of the anti-bacterial peptide hepcidin (see section 1.5.1), or lack of GPI-CP on astrocyte membranes, can also cause FPN internalization and degradation [103, 104]. These differences in regulation of FPN can be due to differences between intracellular (IRP) and extracellular factors (such as plasma iron, hepcidin or inflammation). Therefore, cell type-specific regulation of FPN may exist to meet the need of cells in terms of maintaining global iron homeostasis in the body.

1.3.6 Ceruloplasmin (CP)

The glycoprotein ceruloplasmin (CP, EC 1.16.3.1, [105]) is a ferroxidase that converts toxic Fe^{2+} to Fe^{3+}. It is one of the most abundant proteins in plasma (300-450μg/ml, [106]) and carries about 95% of the copper found in plasma. It is not involved in copper metabolism, but failure to incorporate copper leads to rapid degradation of the protein [107, 108]. CP has six domains that are arranged in a triangular shape [109]. Each domain consists of a β-barrel, composed of eight anti-parallel strands that are similar in arrangement to other oxidases [109, 110]. There are three mononuclear copper centers

in domains 2, 4, and 6, and a trinuclear copper center at the interface between domains 1 and 6 (Figure 2, [109-114]). An electron transfer pathway was proposed [109] in which the mononuclear copper atoms in domains 4 and 6 serve to translocate electrons from ferrous iron (Fe^{2+}), which binds to a nearby site, to the trinuclear copper center, resulting in the reduction of dioxygen to two molecules of water [109, 113].

$$4Fe^{2+} + 4Cu^{2+} \rightarrow 4Fe^{3+} + 4\ Cu^{+}$$

$$4H^{+} + O_2 + 4Cu^{+} \rightarrow 2H_2O + 4Cu^{2+}$$

Therefore, CP safely converts highly reactive and toxic ferrous iron to ferric iron and water without any harmful byproducts [114].

Since free radicals and ferrous iron can induce cell damage under inflammatory conditions, CP expression has been shown to be regulated by inflammatory signaling molecules. Inflammatory conditions including photic injury [115], and inflammatory chemokines and cytokines including interferon-γ (IFN- γ), tumor necrosis factor-α (TNF- α), as well as interleukin-6 (IL-6), have been found to increase CP expression [116-118]. Fox and colleagues reported that there is a translational silencing machinery sequence in the 3' UTR of the CP gene [119]. They reported that a complex named GAIT (IFN-γ activated inhibitor of translation) is silencing CP by binding to a specific 256 bp sequence in 3' UTR 24 hours after IFN-γ treatment. Interestingly, this complex was only found in myeloid cells but lysates from non-myeloid cells did not have this CP silencing effect. Although CP is expected to play a role in maintaining iron homeostasis (see below) no IRE sequence is found in CP mRNA transcripts like other proteins

involved in iron homeostasis (see section 1.5.2), and cellular iron levels does not affect expression of CP in the CNS (for details, see chapter 2).

CP was originally reported as a soluble 132kDa protein secreted by the liver into the plasma and by the choroid plexus into the cerebrospinal fluid (CSF) [120-128]. Several earlier studies demonstrated the expression of CP mRNA in the brain by Northern blotting [128-131] and RNase protection assay [129]. While CP is expressed mostly in astrocytes throughout the brain, its expression appears to be higher in certain areas, including the brainstem and deep nuclei. The cells of the pia mater, the ependymal cells lining the ventricles, and the choroid plexus also express CP [128, 129]. Our lab reported that astrocytes and leptomeningeal cells that line the brain and spinal cord express a membrane-bound glycosylphosphatidylinositol (GPI) anchored form of CP [132]. GPI-CP is generated by alternative splicing of the primary ceruloplasmin transcript, and is the major form in the rat brain [133]. GPI-CP is also present on the surface of Schwann cells in peripheral nerves system [134] and on the surface of Sertoli cells in the testes [134]. Expression of human GPI-CP has also been confirmed [135]. These findings suggest that CP is likely to play an important role as a ferroxidase in a variety of cells and tissues.

Moreover, the role of CP in preventing iron-mediated injury is evident in patients with mutations in the CP gene, who develop a disease known as aceruloplasminemia, which is an autosomal recessive genetic disorder with undetectable CP in plasma [136]. Interestingly, while CP is abundant in plasma, it does not cross the blood-brain barrier, and yet these patients show abnormal CNS iron accumulation and neurological symptoms suggesting that GPI-CP may play an important role in maintaining iron homeostasis in the CNS. Detailed discussion about aceruloplasminemia and role of

GPI-CP in maintaining iron homeostasis in the CNS will follow in section 1.7.1 and chapter 2, respectively.

1.3.7 Hephaestin (HEPH)

Hephaestin (HEPH) is another ferroxidase and shares 50% sequential homology with CP, but unlike CP, it is predicted to have one transmembrane domain [137]. It was originally identified as the gene responsible for a defect in sex-linked anemia (*sla*) mice [138]. These mice have microcytic hypochromic anemia due to the inability of the duodenal enterocytes to release iron into the circulation resulting in abnormal iron accumulation in duodenal enterocytes. By immunohistochemistry, HEPH has been shown to be localized to the basolateral membrane of the enterocytes [138]. Dietary iron is taken into the enterocytes via DMT1 on the side of the cell facing the lumen of the gut (the brush border) and then released into the circulation at the basolateral side of the cell via FPN and HEPH. Therefore, HEPH is expected to play a role in releasing iron from the duodenal enterocytes probably by partnering with FPN and providing the ferroxidase activity required to oxidize Fe^{2+} released by FPN to Fe^{3+}. HEPH and FPN have also been shown to co-localize in Caco cells *in vitro* [139]. HEPH is mainly expressed by mature enterocytes and low expression is also detected in the spleen, lung, placenta, and CNS [137, 140, 141]. Since no IRE sequence was identified in HEPH mRNA transcript, its expression does not appear to be regulated by the IRE/IRP mechanism (see section 1.5.2) but is rather regulated by cellular iron level [140, 142, 143]. How iron regulates HEPH expression is currently unknown.

1.3.8 Hepcidin (HEPC, LEAP-1)

Hepcidin is a small peptide that was identified in human urine and plasma that is mainly produced by the liver [144-146]. It is a 25 amino acid peptide stabilized by 4 disulfide bonds. It also has structural similarities with typical antibacterial peptides such as porcine protegrins [147] and shows antibacterial activity at a high, non-physiological concentration range [144]. The role of HEPC was identified in two mouse models: a mouse model lacking HEPC shows a hemochromatosis phenotype with iron deposition in the liver, while over-expression of HEPC1 in a transgenic mouse model caused severe iron deficiency [148, 149]. Moreover, humans with disruption of *HEPC* show a severe, juvenile form of iron overload disease (juvenile hemochromatosis) [150]. Therefore, HEPC plays a role as a negative regulator of iron absorption. How HEPC can regulate iron release from cells will be discussed in detail in section 1.5.1. There are several factors regulating HEPC expression in hepatocytes: iron concentration, oxygen concentration and inflammation [151]. HEPC is expressed by neurons and astrocytes in the murine CNS [152] though its role in the CNS is currently not known.

1.3.9 Other proteins

In the above sections, I have reviewed the major proteins involved in iron homeostasis in mammals. There are several other proteins also shown to play important roles in maintaining iron homeostasis in mammals, which for the sake of completeness I have listed in Table 1.

1.4 Iron uptake and release by cells

1.4.1 Transferrin-mediated uptake

Most cells acquire the iron that they need from the iron-bound to transferrin (TF). Transferrin binds two atoms of ferric iron and becomes diferric TF, which has a higher affinity at physiological pH for its receptor (TfR) than mono-iron or apo forms of TF (Figure 3) [153]. Therefore, cellular iron uptake can be controlled by the saturation level of transferrin in the circulation. When diferric TF binds to the TfR, clathrin-coated vesicles are formed and the TF/TfR complex undergoes endocytosis [32]. Once inside the cell, the coated-vesicles move within the cytoplasm, likely along microtubules, until they fuse with trans-reticular Golgi elements to form an endosome [154]. The pH of this endocytic vesicle is lowered to 5 - 5.5 through a proton (H^+) pump and the reduction in pH causes dissociation of iron bound to TF, but the TF/TfR complex remains intact because of the high affinity of apoTF to the receptor at low pH [153, 155]. There is also evidence that TfR may help iron release from TF at this step [156]. The iron released from TF is reduced and translocated from the endosome to the cytosol by an iron transporter DMT1 [157]. Since iron released from transferrin is in the ferric form while DMT1 can only transport the ferrous form of iron, a ferrireductase is required in the endosome to transfer iron out of the endosome into the cytosol. Recently, an endosomal protein called six-transmembrane epithelial antigen of the prostate 3 (Steap3) was cloned that has ferrireductase activity. Mice lacking this protein show microcytic, hypochromic anemia [56, 158]. After the release of iron from TF in the endosome, the apoTF/TfR complex is then returned to the cell surface. Upon encountering neutral pH, apoTF is released from the receptor, which is then recycled [32, 155]. In erythroid cells,

the iron-carrying endosomes have also been shown to be able to directly contact mitochondria to deliver iron to mitochondria [159, 160].

1.4.2 Non-transferrin-mediated uptake

In cells involved in the acquisition of iron for the body, such as duodenal enterocytes, iron is available in a non-transferrin bound form (NTBI) or in the heme form. Therefore, another uptake pathway (the non-transferrin mediated pathway) is found in duodenal enterocytes and also in several other cell types. These cells take up non-heme iron through DMT1. This function of DMT1 was identified by phenotypic analysis of two mutant animals. Microcytic anemia (*mk*) mice and the Belgrade (*b*) rat have mutations in DMT1 and have defects in transporting iron from the lumen of the gut into enterocytes, and from plasma transferrin to erythroid precursors [41, 42, 157]. DMT1 transports ferrous iron (Fe^{2+}) instead of ferric (Fe^{3+}) iron, which is bioavailable (Figure 4). To facilitate this, the ferric reductase DCYTB is localized in the brush border membrane and catalyses the reduction of ferric to ferrous iron for transport via DMT1. In addition, duodenal enterocytes also express a heme transporter that has been reported to take up heme directly into the cell [161].

1.4.3 Iron release from cells

Iron that is absorbed into a cell can be used by mitochondria for ATP synthesis, heme synthesis and generation of Fe-S clusters, stored in ferritin or available in the labile iron pool (LIP). To date, the only known ferrous iron exporter is FPN [97-99]. As described above, FPN is found in many cell types including CNS cells [98] and FPN cRNA injected into *Xenopus* oocytes with DMT1 led to a marked increase in iron efflux.

Interestingly, these iron export experiments demonstrated that FPN needs either soluble transferrin and/or ceruloplasmin [98, 99], suggesting that the ferroxidase activity is necessary for iron efflux from cells. In chapter 2, I show that GPI-CP is necessary for iron efflux from CNS astrocytes [101]. Another ferroxidase, hephaestin (HEPH), was identified as the gene affected in the sex-linked anemia (*sla*) mouse. Loss of HEPH in this mouse, which has microcytic hypochromic anemia, leads to iron accumulation in enterocytes but the absorption from the intestinal lumen is normal [162]. Mutation of HEPH in the *sla* mice causes mis-localization of HEPH in the duodenum and results in entrapment of iron in the duodenum [138]. Therefore, HEPH is involved in release of iron from the duodenal enterocytes.

Recently, the heme transporting capacity of the receptor for feline leukemia virus subgroup C (FLVCR) was reported [163]. This cell membrane protein shows heme exporting activity *in vitro*, and inhibition of FLVCR expression causes a decrease in heme export, impairment in erythroid maturation, and cell death in a haematopoietic cell line. Therefore, FLVCR might play a role in exporting excess free heme during erythroid differentiation. ABCG2, a protein that belongs to the ABC transporter family [164] was also reported to have heme exporting capacity [165]. The protein is also expressed on the cell surface membrane of haematopoietic cells, liver and intestine. Interestingly, ABCG2 null mice showed high photosensitivity due to excess pheophorbide a [166]. Pheophorbide a is a porphyin derived from chlorophoyll and can function as a phototoxin. ABCG2 was shown to be capable of exporting these porphyrins. Another study also showed that ABCG2 interacts with heme and protects cells under hypoxic conditions [167]. Whether these heme transporters are involved in heme trafficking in cells other than haematopoietic cells is currently not known.

1.5 Maintaining iron homeostasis

The iron balance for the whole body is maintained by the regulation of iron absorption from the intestine because there is no regulated pathway for iron excretion. Iron leaves the body by menstrual blood loss in females and through the sloughing of epithelial cells, such as the skin. The greatest portion of body iron, ranging from 65-75%, is found in hemoglobin in red blood cells. Macrophages phagocytose senescent red blood cells and recycle iron from heme (reviewed in [168]). Therefore, these two bone-marrow derived cells cycle most of the body iron. Liver stores most of the body's excess iron, normally 0.5-1g in a normal adult male. Other tissues use smaller amounts of iron, but the brain's iron requirement is relatively high, consistent with its high energy need. The brain, which only weighs 2% of the total body weight, accounts for 20% of the total oxygen consumption, making the brain the highest oxygen-consuming organ in the body [169]. An important aspect of iron metabolism is that although cells in different tissues have different needs for iron, they appear to share many of the same molecules and general regulatory mechanisms to maintain iron homeostasis.

1.5.1 Extracellular iron homeostasis.

The average human male acquires about 1-2mg of iron per day, and maintains about 4g for essential metabolism [170]. As mentioned above, total body iron has to be tightly regulated due to its redox active nature but there are no particular mechanisms to release iron from the body. Therefore maintaining iron homeostasis is achieved at the point of entry - duodenum enterocytes. An important, and as yet unanswered, question is how the iron storage cells (hepatocytes) and iron absorbing cells (duodenal enterocytes) communicate with each other. Since the 1960s, it has been thought that

nascent enterocytes in the crypts of the duodenum detect body (or circulating) iron levels and get 'programmed' to absorb adequate amounts of iron when they mature (reviewed in [171]). Recently, an antimicrobial peptide hepcidin (HEPC) was identified that acts as a negative regulator of iron absorption [144, 145]. Systemic injection of HEPC can decrease plasma iron levels in four hours, showing that it can modulate iron absorption before crypt cells are matured [172]. Two animal models lacking HEPC demonstrated that it is not only a negative regulator for iron absorption but that it also suppresses macrophage iron release [148, 173]. HEPC binds to the iron exporter FPN and causes internalization and degradation of this iron efflux transporter [104], thus suppressing iron release from macrophages and enterocytes into the circulation. Mutations in FPN that are resistant to HEPC regulation cause hemochromatosis, where iron accumulates in Kupffer cells or hepatocytes [174]. HEPC mRNA does not contain IREs, suggesting that the body iron status is not signaled through the classical IRE/IRP regulatory mechanism but by some other mechanism. HEPC expression is decreased in hypoxic conditions *in vitro* and *in vivo* [175]. Under hypoxic conditions, renal erythropoietin synthesis is stimulated by the transcription factor hypoxia-inducible factor (HIF) that in turn stimulates erythropoiesis [176]. Whether this increased erythropoiesis can directly lead to HEPC down-regulation, or if decreased plasma iron will lead to HEPC down-regulation, is not clear. HEPC expression increases during inflammation causing a phenomenon called 'anemia of inflammation' [177]. This is one of the body's defensive mechanisms to fight infection by limiting the supply of iron to microorganisms and thus prevent their proliferation. Nemeth *et al.* showed that this upregulation of HEPC is modulated via IL-6 [178, 179]. Although HEPC has been

demonstrated to work as a body iron sensor and a negative regulator [175], the exact sensing mechanism is not known.

1.5.2 Intracellular iron homeostasis.

As mentioned above, the uptake, sequestration, and export of iron must be properly orchestrated. In mammalian cells, two cytosolic proteins "sense" intracellular iron levels and regulate expression of iron-regulated proteins. These "iron-regulatory proteins 1 and 2" (IRP1 and IRP2) bind to RNA stem loops known as "iron-responsive elements" (IRE) found in either the 5' or 3' locations within the mRNA transcripts of proteins involved in iron homeostasis [34]. The IREs are found in proteins whose expression is regulated by iron, such as ferritin, TfR1, DMT1, FPN, and erythroid 5-aminolevulinate synthase (eALAS) [34, 41, 97]. IREs contain a six-membered loop with the sequence 5'-CAGUGX-3', where X can be an A, C, or U, but never a G, and a base-paired stem composed of double helices (reviewed in [180]). In the case of ferritin, a single IRE is found near the 5' end of the transcript and binding of IRP to this IRE inhibits new protein synthesis (Figure 5, [34, 181]). In the TfR1 transcript, there are five IREs in the 3' untranslated region (UTR), named A-E [33, 34, 182, 183] and IRP binding protects the transcript from endonucleolytic cleavage and degradation. As a result, TfR1 mRNA transcript levels increase, leading to a concomitant increase in TfR1 biosynthesis [184, 185]. Conversely, under conditions of excess iron, the RNA-binding activity of IRP is decreased, and TfR1 mRNA is degraded. Treating cells with an iron source confirmed that the degradation of TfR1 mRNA occurs due to the destabilization of the 3' UTR instead of shortening of the poly(A) tail [185]. These data suggest that cellular iron homeostasis is maintained in part by cytosolic iron levels. In

addition, there is evidence that IRE/IRP binding can be modulated not only by cellular iron levels but also by chemokines and cytokines via a nitric oxide signaling pathway [186, 187]. On the other hand, the expression of these IRE-containing proteins can also be regulated via IRP-independent pathways including cytokines, hydrogen peroxide, and nitric monoxide and under hypoxia [82, 188-190].

But how do IRPs sense cellular iron status? IRP1 is a bi-functional protein in which function is determined by the presence or absence of an iron-sulfur cluster, which is generally linked to cysteines of the protein [191]. When the iron-sulfur cluster is formed, IRP1 functions as cytosolic aconitase, an interconverting enzyme for citrate and isocitrate. Absence of the iron-sulfur cluster causes a conformational change in IRP1, and the active site of IRP1 then becomes a high-affinity binding motif for IREs. Although iron is the major regulator for IRP1 and aconitase conversion, the iron-sulfur cluster can also be disassembled due to oxidation or by phosphorylation [192-196] despite intracellular iron levels. Moreover, phosphorylation of Ser711 can modulate aconitase activity of IRP1 [197, 198]. IRP2 differs from IRP1 in the mechanism by which iron levels are sensed as IRP2 undergoes ubiquitination and proteasomal degradation in iron-replete cells [199]. Originally, this iron-dependent degradation was thought to be due to a 73-amino acid sequence called a "degradation domain" that is unique to IRP2 [200, 201]. It was shown that when this cysteine-rich sequence was inserted into IRP1, it also acquired the ability to undergo iron-dependent ubiquitination and degradation [201]. This cysteine-oxidation model has been challenged since complete deletion of 73-amino acid sequence and specific mutations to cysteine residues did not alter the degradation kinetics of IRP2 [202, 203]. Alternatively, a 2-

oxoglutarate-dependent oxygenase-induced IRP2 degradation pathway has recently been demonstrated [202, 203].

1.6 Maintaining iron homeostasis in the central nervous system (CNS)

As mentioned above, the CNS consumes about 20% of the total body energy at a rate 10 times faster per gram of tissue as compared to non-CNS areas [169]. Therefore, a high amount of iron is needed in the CNS to fulfill the needs of the mitochondrial oxidative chain. However, the CNS is isolated by a tight epithelial barrier called the blood-brain-barrier (BBB), and so the cells in the CNS do not have direct access to plasma borne iron. Moreover, the CNS is particularly sensitive to oxidative stress due to the low level of antioxidant enzymes (e.g. glutathione-peroxidase), high levels of polyunsaturated lipids on the membranes, and generation of high levels of reactive oxygen species (ROS) during neurochemical reactions such as dopamine oxidation [204]. It seems likely that the BBB allows the CNS to have exclusive regulatory mechanisms for iron that are independent from the liver-dependent regulatory mechanism operational in non-CNS areas. For example, hereditary hemochromatosis patients with very high iron accumulation in the liver do not seem to have CNS involvement [30]. On the contrary, patients with aceruloplasminemia resulting form mutations in the *CP* gene have iron-overload in the CNS, while the plasma iron level is often anemic [205]. Therefore, the CNS seems to have a unique mechanism for regulating the uptake and release of iron to maintain the metabolic needs of this highly specialized organ.

1.6.1 Iron uptake into the CNS.

For iron to enter the CNS, iron must pass through the endothelial cells forming the BBB. The iron importing protein TfR1 has been reported to be expressed on the luminal membrane of CNS endothelial cells [36, 37, 206, 207]. Experiments using radiolabeled or horseradish peroxidase (HRP)-conjugated TF were used to show that TF can enter CNS endothelial cells [208, 209]. Several reports also showed that non-transferrin bound iron (NTBI) can also enter into the CNS [210-212]. However, under normal conditions, there is very little NTBI available in the plasma. It has also been suggested, based on *in vitro* evidence, that ferritin-bound iron might be able to cross the BBB [92]. Therefore, although CNS iron uptake is thought to occur mainly via the transferrin-bound iron-endocytosis pathway, under certain conditions (e.g., hypotransferrinemic mice) non-transferrin bound iron uptake might also occur to fulfill the high metabolic demands of the CNS. It is still unclear whether this TF-bound iron is released from the endosomes of endothelial cells [50, 213] or as has been suggested the Fe/TF complex is transcytosed and released from the abluminal side of the cells [207, 208, 214]. On the other hand, once iron is released from the Fe/TF complex within the endothelial cells, the iron exporter FPN, which is found in the endothelial cells, can efflux iron [215] into the CNS tissue. However, the expression of FPN in the CNS endothelial cells is still under debate [210, 216] and the exact localization of FPN on the endothelial membrane is still not known. Hypotransferrinemic mice with very low TF levels show iron accumulation in the choroid plexus, suggesting that TF is needed for proper iron transport into the cerebrospinal fluid (CSF) [217].

1.6.2 CNS iron circulation.

Most of the CNS capillaries (95%, [218]) are in contact with astrocytic end-feet which induce the development of tight junctions between CNS endothelial cells that form the BBB. Once iron has traveled through endothelial cells and been released, most of it might be imported into the astrocytic end-feet that surround CNS capillaries or bind to transferrin (TF) in the CSF. This iron buffering capacity of astrocytes will be discussed further in chapter 3. Although there is TF in the CSF, its levels are very low compared to the plasma (about 1/100-200; 0.2-0.6μM in human lumbar spinal cord [219-222]) and is estimated to be fully saturated. Therefore, CNS iron might be either distributed directly via cell-cell contact or by other carrier proteins or low molecular weight chaperons in the CSF. One of these transport proteins can be lactoferrin (LF) that is a member of TF family and has higher affinity for iron than TF. LF uptake is mediated by a receptor that is found in neurons, cerebral vasculature and some glial cells [223, 224]. Non-transferrin bound, low-molecular weight iron has also been detected in the CSF of neonatal animals [225].

1.6.3 Iron release from the CNS

Once iron enters the CNS, it seems likely to be conserved within the CNS since there is very minimal decrease in brain iron content in anemic animal models induced by switching to the low-iron diet. Furthermore, the CNS cannot lower its iron content in animal models showing iron overload in the CNS [226, 227]. Therefore, the CNS might have a mechanism to conserve iron efficiently and also lack a mechanism to efficiently release iron. The probable route of iron exiting the CNS might be the efflux of iron from the arachnoid cells that form tight junction and outlining the CNS. Iron can be

exported via vacuolization of arachnoid villi [218] or actively transported through iron exporter. It is not known whether these cells express known iron exporting proteins, but we have previously reported that these cells express GPI-CP that is essential for iron efflux in astrocytes [228].

1.7 Iron and neurodegenerative diseases

There are a number of diseases that show iron accumulation in the CNS [3, 4, 229, 230]. Some of these are caused by genetic mutations in genes involved in regulating iron levels, while the reasons for the iron accumulation in others is not fully known and may be a secondary consequence of the disease process. Nevertheless, the increased iron accumulation and iron-mediated free radical injury may contribute to the neurodegeneration seen in these diseases. A brief description of some of these neurological conditions is provided below.

1.7.1 Neurodegenerative diseases caused by genes involved in iron metabolism

Neuroferritinopathy. As described above, ferritin is an iron storage protein that can accommodate up to 4500 atoms of iron. The heavy (FTH) and light (FTL) chains of ferritin form a 24-subunit symmetrical complex to make up ferritin's barrel-like structure. The FTH subunit has ferroxidase activity while FTL is involved in stabilizing the structure (reviewed in [80]). Insertion mutations of FTL in humans cause a basal ganglia disease with excess iron in various parts of the brain [91]. These patients show abundant accumulation of iron and ferritin, mainly in the neurons of the globus pallidus, forebrain and cerebellum. Axonal swellings and cytoplasmic inclusions that are positive for iron, ferritin and ubiquitin were particularly seen in the globus pallidus and putamen

but also throughout the CNS [231, 232]. Interestingly, affected patients show low plasma ferritin while plasma iron, hemoglobin, and transferrin levels are normal [91]. These mutations in the FTL are thought to disrupt its C-terminus structure and affect its stability and function, probably resulting in the release of free iron [91]. *In vitro* studies have shown that mutant FTL/wildtype FTH heteropolymer ferritin show less active iron incorporation than normal ferritin [233]. How a mutation in the FTL can cause selective damage in the CNS is currently not known.

Pantothenate kinase-associated neurodegeneration (PKAN). PKAN (also known as Neurodegeneration with brain iron accumulation [NBIA]) and previously known as Hallervorden-Spatz syndrome, is a juvenile neurodegenerative disorder with a large amount of iron accumulation found in the globus pallidus and the pars reticulata of the substantia nigra [234]. These patients have extrapyramidal dysfunction showing rigidity, dystonia, choreoathetosis and characteristic MRI patterns of iron accumulation in the globus pallidus [235]. This disease is caused by mutation in pantothenate kinase 2 (*PANK2*) [236], an essential enzyme for coenzyme A biosynthesis that catalyzes the phosphorylation of pantothenate. Phosphorylated pantothenate normally condenses with cysteine, and therefore, unbound cysteine accumulation occurs in PKAN patients [237]. Iron accumulation in PKAN might be due to the iron-chelating activity of cysteine, and this accumulated iron might cause oxidative damage in affected regions of the CNS [236]. Interestingly, a mouse model lacking *PANK2* showed retinal degeneration, but did not show any neurological symptoms seen in humans [238].

Friedreich's Ataxia. Friedreich's ataxia is characterized by the degeneration of large sensory neurons, spinocerebellar tracts, and cardiomyopathy [239]. It is caused by expansion of a GAA trinucleotide repeat in intron 1 of the *frataxin* gene (*FRDA*) that leads to a reduction in its expression [240]. Frataxin and its yeast homologue Yfh1p are mitochondrial matrix proteins [241-243]. *In vitro* studies in yeast show that a lack of Yfh1p leads to a 10-fold increase in iron accumulation in mitochondria, which can be reversed by re-expression of Yfh1p [242, 244]. These data imply a role for Yfh1p in the mitochondrial iron export machinery. Frataxin is essential for mitochondrial and extra-mitochondrial Fe-S cluster formation. Therefore, mutations in frataxin cause mitochondrial respiratory chain failure due to a lack of Fe-S cluster [245-250]. Taken together, frataxin may play a role in iron-sulfur cluster assembly by providing iron and may also be involved in the export of iron-sulfur clusters to maintain mitochondrial iron homeostasis. An earlier study using an *in vitro* mitochondrial iron overload model generated by a heme synthesis blocker showed that treating these cells with an iron chelator is effective and suggested that this might be a therapeutic approach for Friedreich's ataxia [251]. Treatment of fibroblasts from Friedreich's ataxia patients with an iron chelator was also shown to prevent oxidant-induced cell death [252]. Recent reports show that Friedreich's ataxia patients treated with an iron chelator for 6 months had reduced neuropathy and improved motor functions [253].

Aceruloplasminemia. Aceruloplasminemia is a rare autosomal recessive disorder in which mutations of the CP gene lead to almost undetectable levels of CP [254-256]. The human CP gene is located on chromosome 3q21-25 [125, 257] and plasma CP is encoded by 19 exons spread over 50kb of genomic DNA [258]. To date, more than 10

different mutations in the human CP gene have been identified. These patients develop retinal degeneration, diabetes mellitus and neurological symptoms including dementia, ataxia, and loss of motor coordination between the ages of 45-50 years [254, 256, 259, 260]. Originally, it was considered to be 'atypical Wilson's disease' due to undetectable levels of CP, but liver biopsy showed accumulation of iron, not copper [254]. Liver biopsies from these patients showed granular deposits of iron in the cytoplasm of hepatocytes and Kupffer's cells [256]. Intracellular iron accumulations in a number of organs including the liver, pancreas, heart, spleen, and CNS have also been reported in autopsy material [261]. Iron accumulation in the CNS varied in different regions and occurred particularly in the deep motor nuclei in the brain. Iron deposits were found in both glia and neurons. Another striking feature of the pathology is the neuronal degeneration that occurs in many of the affected regions [256, 262]. Increased levels of iron and lipid peroxidation have also been observed in the cerebrospinal fluid (CSF) of these patients [263]. Mitochondrial dysfunction has also been reported in these patients, which include a decrease of more than 30% in the enzyme activities of complex I and IV of the respiratory chain [264 376].

Mice lacking CP have been generated that develop high iron accumulation in various tissues including liver, retina, and cerebellum [265-267]. Like humans with aceruloplasminemia, these mice also showed mild anemia and low plasma iron levels [265, 267]. Injecting CP into CP null mice and adding CP to astrocytes from null mice triggered iron release from hepatocytes and astrocytes, respectively, confirming the essential role of CP in efficient cellular iron efflux (see also chapter 2) [101, 265]. These mice show deficits in motor coordination as tested with the roto-rod assay [267]. Neonatal cerebellar cells from CP null mice were also shown to be more susceptible to

oxidative damage *in vitro* [267]. Interestingly, while CP is one of the major copper containing proteins, there were no abnormalities in copper metabolism nor accumulation of copper in CP null mice [108]. As part of this thesis work, I carried out a detailed analysis of changes in iron homeostasis in the cerebellum of CP null mice with aging, which will be discussed in chapter 3. In a study carried out by Dunaief's group, double transgenic mice for CP and hephaestin ($Cp^{-/-}/Heph^{-/Y}$) showed high levels of retinal iron accumulation in both glia and the retinal pigment epithelium (RPE) and retinal degeneration [268]. Interestingly, the authors also reported that CP and HEPH are expressed in RPE, which acts as the BBB in the eye, unlike the BBB endothelial cells lining the CNS. It is not clear what the role of ferroxidases is in the BBB in the eye, but these data indicate that they are important in maintaining iron homeostasis in the CNS.

IRP2 deficient mice. A transgenic mouse with a targeted disruption of the IRP2 gene (*Ireb2*) showed neurodegenerative changes at 6 months of age and iron accumulation in cerebellar white matter, caudate-putamen, thalamus and colliculi [269]. Abnormal accumulation of ferritin and iron accumulation was detected in degenerating neurons. $Ireb2^{+/-}$ mice showed milder effects than the homozygote null mice, and $Ireb1^{+/-}/Ireb2^{-/-}$ mice showed worse neurological symptoms suggesting a dose-dependent effect by IRP proteins [270]. Interestingly, IRP1 was not able to repress over-expression of ferritin mRNA translation in the absence of IRP2. Similar data were reported in a macrophage-like cell line [271]. Another group generated $Ireb2^{-/-}$ mice using the cre/lox knock-out method and reported that these mice do not show iron accumulation nor neurodegeneration in the brain but increased ferritin expression and reduced the ability

to stay on the roto-rod assay [272]. It has been suggested that the differences between these two lines of *Ireb2*$^{-/-}$ mice may be due to genetic and technical differences but there is as yet no satisfactory explanation [272].

1.7.2 Neurodegenerative diseases with abnormal iron accumulation not associated with mutations in iron homeostasis genes

Parkinson's disease (PD). Parkinson's disease is a chronic, progressive movement disorder also showing muscle rigidity, language problems, and in extreme cases, akinesia [273]. Loss of dopaminergic neurons and decreased production of the neurotransmitter dopamine are the hallmarks of the disease, but the cause is still not known. Numerous studies have confirmed that there is increased iron accumulation in the substantia nigra pars compacta (SNpc) in the midbrain of PD patients [274-278]. Along with iron accumulation, increased reactive oxygen species have also been reported in these patients, likely caused by abnormal iron accumulation [279-282]. Another hallmark of the disease is the presence of Lewy bodies within neurons which contain an insoluble form of alpha-synuclein (α-syn) [283]. α -syn is found primarily in brain tissue, and mainly localized to the pre-synaptic nerve terminal. Normally, α-syn is a soluble protein with an α-helical structure, but it is found in Lewy body in insoluble β-pleated sheet structure. Interestingly, iron has been shown to interact with α-syn and enhances the conformational change of the protein into the beta-pleated sheet, thereby promoting aggregate formation [284, 285]. Iron can, therefore, not only generate harmful reactive oxygen species but also be involved in aggregate formation in PD pathology.

Alzheimer's disease (AD). AD is a progressive neurodegenerative disease accompanied by dementia and movement impairment. Like PD, abnormal protein aggregation is also found in the brain of AD patients. Amyloid plaques found in AD are mainly composed of amyloid beta (Aβ) a short peptide that is a proteolytic byproduct of the transmembrane protein, amyloid precursor protein (APP). Aβ monomer is normally a soluble peptide, but it can undergo structural change and become a highly insoluble beta-sheet structure and form protein aggregates [286]. Formations of these amyloid plaques appear before the start of clinical symptoms. Interestingly, increased iron and ferritin accumulation is associated with amyloid plaques in the brain in AD [287-290]. As was described in PD, iron can also bind to Aβ and facilitate aggregation of the protein *in vitro* [291, 292]. Moreover, iron can modulate expression of APP and its cleavage by alpha-secretase [293, 294], impacting plaque formation. Intracerebral injection of iron along with Aβ leads to more severe damage to neurons as compared to Aβ alone [295]. It is currently unclear how abnormal iron accumulation occurs in the CNS in AD.

Huntington's disease (HD). This is an autosomal dominant neurodegenerative disease that shows abnormal involuntary body movements, lack of coordination and loss of mental abilities [296]. The cause of the disease was reported to be a CAG expansion in the huntingtin (*Htt*) gene. *In vitro* studies showed that Htt is involved in the formation of nuclear and perinuclear organelle structures [297]. In HD, the brain shows increased iron and ferritin accumulation in the putamen, caudate nucleus, and globus pallidus [298-300] early in the disease process [301]. Since Htt knock-out cells show abnormal recycling of endosomal structures, it was suggested that lack of Htt might disturb the

TF/TfR endocytosis pathway. The expression of Htt is also affected by cellular iron levels [297]. Furthermore, a recent study in zebrafish lacking Htt showed decreased hemoglobin synthesis and increased TfR1 synthesis, suggesting a deficit in cellular iron uptake [302]. The direct mechanism underlying iron accumulation in HD is still not fully understood.

Amyotrophic lateral sclerosis (ALS). This is one of the most common and lethal neurodegenerative diseases. ALS patients develop progressive paralysis due to degeneration of motor neurons in the spinal cord and motor cortex. About 90% of ALS cases are sporadic, although their symptoms are similar to that of the familial cases. Among familial cases, almost 20% of the patients have genetic mutation in superoxide dismutase 1 gene (*SOD1*) [303]. Animal models of the disease have been developed by inducing the over-expression of various human mutant SOD1s in mice [304]. Currently the mechanism of how mutant SOD1 causes neurodegeneration is not fully understood but it appears to be due to a 'toxic gain of function' by mutations. Several possible mechanisms have been proposed including oxidative stress (reviewed in [305]), cytoskeletal abnormalities and disrupted axonal transport [306], excitoxicity by glutamate [307], protein aggregation (reviewed in [308, 309]), mitochondrial dysfunction (reviewed in [306]), and recently extracellular SOD1 toxicity [310] suggesting more than one mechanism is involved in this complex disease. Interestingly, it has been reported that there is abnormal iron accumulation in both familial and sporadic cases [311-314]. Increased expression of lactoferrin and TfR1 in neurons has been reported, suggesting abnormal iron uptake [315, 316]. Polymorphisms in the hemochromatosis gene *Hfe* are also reported in sporadic ALS patients [317, 318],

suggesting a link between iron-caused toxicity and the etiology of ALS. How these iron accumulation occur is currently not known and it will be discussed in detail in chapter 4.

GFAP-IL6 mice. An animal model over-expressing interleukin-6 (IL-6) in astrocytes shows reactive gliosis and defects in the blood-brain-barrier (BBB) [319, 320]. Astrocytic support is very important in forming the BBB during development. Interestingly, these mice show chronic neurodegeneration and iron accumulation in the cerebellum starting from 1 month of age. These mice also show increased ferritin expression and evidence of lipid peroxidation [321]. It is not clear at present if the iron accumulation in these mice is due to defects in the BBB or dysregulation of iron homeostasis proteins as a result of the increased cytokine expression.

1.8 Rationale for the studies

The CNS, which is shielded behind a tight BBB, appears to have a unique ability to acquire and retain iron. Interestingly, many neurodegenerative diseases show signs of iron accumulation. In some cases, this is primarily due to defects in genes involved in regulating iron levels, while in other cases iron accumulation appears to occur secondary to other events that may disrupt normal iron homeostasis in the affected regions of the CNS. In my Ph.D. thesis research, I carried out experiments designed to better understand the mechanisms underlying iron homeostasis in the CNS. For this, I worked on two mouse models of human neurodegenerative diseases: one that involves a protein that regulates iron oxidation (aceruloplasminemia), and the other a disease not directly related to iron (amyotrophic lateral sclerosis).

As described above, humans lacking *CP* (aceruloplasminemia) develop a progressive neurodegenerative disease with iron accumulation in the CNS. Previously, our laboratory identified a membrane-bound GPI-anchored form of CP (GPI-CP) that is the major form in the rat brain and is mainly expressed by astrocytes [132]. Although several studies have examined the role of soluble CP in cellular iron transport in non-CNS cells [322-324], the role of GPI-CP in the CNS was not known. Therefore, I studied the role of GPI-CP in iron efflux from astrocytes and how it partners with the iron transporter FPN. This was done using primary cultures of astrocytes isolated from wildtype and *CP* null mice using a series of biochemical and functional cell culture assays (Chapter 2). Secondly, I carried out a detailed analysis of iron accumulation and changes in expression of a number of proteins involved in regulating iron levels, i.e., iron homeostasis proteins during aging in wildtype and *CP* null mice. The comparison with the two mouse strains has given us important insights into the important role of CP in maintaining iron homeostasis in the CNS and how loss of this protein dysregulates iron homeostasis with age (Chapter 3).

Iron accumulation has also been reported to occur in the CNS in ALS. However, the molecular mechanisms underlying the accumulation of this redox-active metal in ALS has not been studied. Importantly, the role of iron in the pathogenesis and progression of the disease has not been directly evaluated. For this part of my thesis, I used a well known transgenic mouse model of ALS in which the G37R mutant form of human SOD1 is over-expressed in mice ($SOD1^{G37R}$), where the mouse develops hindlimb paralysis at approximately 50 weeks of age. I assessed iron accumulation in the spinal cords of these mice, examined the changes in expression of a number of iron homeostasis proteins with age, and assessed the effects of an iron chelator on the

progression of the disease. These studies provide direct evidence for an important role for iron in the progression of ALS and provide novel insights into some of the potential mechanisms by which iron-mediated toxicity contributes to ALS pathology (Chapter 4).

1.9 References

1. Gibson, Q.H. and D.C. Harrison, *Blood haemoglobin: the relationship between oxygen capacity and iron content of blood in men and women.* Biochem J, 1946. **40**(2): p. 247-9.
2. Kaplan, J. and T.V. O'Halloran, *Iron metabolism in eukaryotes: Mars and Venus at it again.* Science, 1996. **271**(5255): p. 1510-2.
3. Ponka, P., *Hereditary causes of disturbed iron homeostasis in the central nervous system.* Ann N Y Acad Sci, 2004. **1012**: p. 267-81.
4. Zecca, L., et al., *Iron, brain ageing and neurodegenerative disorders.* Nat Rev Neurosci, 2004. **5**(11): p. 863-73.
5. Lill, R., et al., *Mechanisms of iron-sulfur protein maturation in mitochondria, cytosol and nucleus of eukaryotes.* Biochim Biophys Acta, 2006. **1763**(7): p. 652-67.
6. Rouault, T.A. and W.H. Tong, *Iron-sulphur cluster biogenesis and mitochondrial iron homeostasis.* Nat Rev Mol Cell Biol, 2005. **6**(4): p. 345-51.
7. Pinero, D.J. and J.R. Connor, *Iron in the brain: An important contibutor in normal and diseased states.* Neuroscientist, 2000. **6**: p. 435-53.
8. Qing, C., J.L. Beard, and B.C. Jones, *Abnormal brain monoamine metabolism in iron deficiency anemia.* J Nutr Biochem, 1995. **6**(9): p. 486-93.
9. Yu, G.S., et al., *Effect of prenatal iron deficiency on myelination in rat pups.* Am J Pathol, 1986. **125**(3): p. 620-4.
10. Roncagliolo, M., et al., *Evidence of altered central nervous system development in infants with iron deficiency anemia at 6 mo: delayed maturation of auditory brainstem responses.* Am J Clin Nutr, 1998. **68**(3): p. 683-90.

11. Ortiz, E., et al., *Effect of manipulation of iron storage, transport, or availability on myelin composition and brain iron content in three different animal models.* J Neurosci Res, 2004. **77**(5): p. 681-9.

12. Smith, M.A., et al., *Carbonyl-related posttranslational modification of neurofilament protein in the neurofibrillary pathology of Alzheimer's disease.* J Neurochem, 1995. **64**(6): p. 2660-6.

13. Mattson, M.P., J.W. Carney, and D.A. Butterfield, *A tombstone in Alzheimer's?* Nature, 1995. **373**(6514): p. 481.

14. Markesbery, W.R., *Oxidative stress hypothesis in Alzheimer's disease.* Free Radic Biol Med, 1997. **23**(1): p. 134-47.

15. Dexter, D.T., et al., *Increased nigral iron content and alterations in other metal ions occurring in brain in Parkinson's disease.* J Neurochem, 1989. **52**(6): p. 1830-6.

16. Good, P.F., C.W. Olanow, and D.P. Perl, *Neuromelanin-containing neurons of the substantia nigra accumulate iron and aluminum in Parkinson's disease: a LAMMA study.* Brain Res, 1992. **593**(2): p. 343-6.

17. Halliwell, B. and J.M. Gutteridge, *Oxygen toxicity, oxygen radicals, transition metals and disease.* Biochem J, 1984. **219**(1): p. 1-14.

18. Watson, B.D., et al., *Lipid peroxidation in vivo induced by reversible global ischemia in rat brain.* J Neurochem, 1984. **42**(1): p. 268-74.

19. Komara, J.S., et al., *Brain iron delocalization and lipid peroxidation following cardiac arrest.* Ann Emerg Med, 1986. **15**(4): p. 384-9.

20. Siesjo, B.K., *Mechanisms of ischemic brain damage.* Crit Care Med, 1988. **16**(10): p. 954-63.

21. Aisen, P., *Transferrin, the transferrin receptor, and the uptake of iron by cells.* Met Ions Biol Syst, 1998. **35**: p. 585-631.

22. Metz-Boutigue, M.H., et al., *Human lactotransferrin: amino acid sequence and structural comparisons with other transferrins.* Eur J Biochem, 1984. **145**(3): p. 659-76.

23. Bates, G.W., E.F. Workman, Jr., and M.R. Schlabach, *Does transferrin exhibit ferroxidase activity?* Biochem Biophys Res Commun, 1973. **50**(1): p. 84-90.

24. Kawabata, H., et al., *Molecular cloning of transferrin receptor 2. A new member of the transferrin receptor-like family.* J Biol Chem, 1999. **274**(30): p. 20826-32.

25. Hu, H.Y. and P. Aisen, *Molecular characteristics of the transferrin-receptor complex of the rabbit reticulocyte.* J Supramol Struct, 1978. **8**(3): p. 349-60.

26. Seligman, P.A., R.B. Schleicher, and R.H. Allen, *Isolation and characterization of the transferrin receptor from human placenta.* J Biol Chem, 1979. **254**(20): p. 9943-6.

27. Katz, J.H., *Iron and protein kinetics studied by means of doubly labeled human crystalline transferrin.* J Clin Invest, 1961. **40**: p. 2143-52.

28. Goswami, T. and N.C. Andrews, *Hereditary hemochromatosis protein, HFE, interaction with transferrin receptor 2 suggests a molecular mechanism for mammalian iron sensing.* J Biol Chem, 2006. **281**(39): p. 28494-8.

29. Parkkila, S., et al., *Association of the transferrin receptor in human placenta with HFE, the protein defective in hereditary hemochromatosis.* Proc Natl Acad Sci U S A, 1997. **94**(24): p. 13198-202.

30. Pietrangelo, A., *Hereditary hemochromatosis.* Biochim Biophys Acta, 2006. **1763**(7): p. 700-10.

31. Roy, C.N., et al., *The hereditary hemochromatosis protein, HFE, specifically regulates transferrin-mediated iron uptake in HeLa cells.* J Biol Chem, 1999. **274**(13): p. 9022-8.

32. Richardson, D.R. and P. Ponka, *The molecular mechanisms of the metabolism and transport of iron in normal and neoplastic cells.* Biochim Biophys Acta, 1997. **1331**(1): p. 1-40.

33. Casey, J.L., et al., *Iron regulation of transferrin receptor mRNA levels requires iron- responsive elements and a rapid turnover determinant in the 3' untranslated region of the mRNA.* Embo J, 1989. **8**(12): p. 3693-9.

34. Harford, J.B. and R.D. Klausner, *Coordinate post-transcriptional regulation of ferritin and transferrin receptor expression: the role of regulated RNA-protein interaction.* Enzyme, 1990. **44**(1-4): p. 28-41.

35. Fleming, R.E., et al., *Transferrin receptor 2: continued expression in mouse liver in the face of iron overload and in hereditary hemochromatosis.* Proc Natl Acad Sci U S A, 2000. **97**(5): p. 2214-9.

36. Jefferies, W.A., et al., *Transferrin receptor on endothelium of brain capillaries.* Nature, 1984. **312**(5990): p. 162-3.

37. Bradbury, M.W., *Transport of iron in the blood-brain-cerebrospinal fluid system.* J Neurochem, 1997. **69**(2): p. 443-54.

38. Salis, C., et al., *The mRNA of transferrin is expressed in Schwann cells during their maturation and after nerve injury.* Exp Neurol, 2007.

39. Lee, P.L., et al., *The human Nramp2 gene: characterization of the gene structure, alternative splicing, promoter region and polymorphisms.* Blood Cells Mol Dis, 1998. **24**(2): p. 199-215.

40. Picard, V., et al., *Nramp 2 (DCT1/DMT1) expressed at the plasma membrane transports iron and other divalent cations into a calcein-accessible cytoplasmic pool.* J Biol Chem, 2000. **275**(46): p. 35738-45.

41. Gunshin, H., et al., *Cloning and characterization of a mammalian proton-coupled metal-ion transporter.* Nature, 1997. **388**(6641): p. 482-8.

42. Fleming, M.D., et al., *Microcytic anaemia mice have a mutation in Nramp2, a candidate iron transporter gene.* Nat Genet, 1997. **16**(4): p. 383-6.

43. Conrad, M.E., et al., *Separate pathways for cellular uptake of ferric and ferrous iron.* Am J Physiol Gastrointest Liver Physiol, 2000. **279**(4): p. G767-74.

44. Knopfel, M., et al., *Characterization of an integral protein of the brush border membrane mediating the transport of divalent metal ions.* Biophys J, 2000. **79**(2): p. 874-84.

45. Mackenzie, B. and M.A. Hediger, *SLC11 family of H+-coupled metal-ion transporters NRAMP1 and DMT1.* Pflugers Arch, 2004. **447**(5): p. 571-9.

46. Garrick, M.D., et al., *DMT1: a mammalian transporter for multiple metals.* Biometals, 2003. **16**(1): p. 41-54.

47. Roth, J.A., et al., *Differential localization of divalent metal transporter 1 with and without iron response element in rat PC12 and sympathetic neuronal cells.* J Neurosci, 2000. **20**(20): p. 7595-601.

48. Hubert, N. and M.W. Hentze, *Previously uncharacterized isoforms of divalent metal transporter (DMT)-1: implications for regulation and cellular function.* Proc Natl Acad Sci U S A, 2002. **99**(19): p. 12345-50.

49. Paradkar, P.N. and J.A. Roth, *Nitric oxide transcriptionally down-regulates specific isoforms of divalent metal transporter (DMT1) via NF-kappaB.* J Neurochem, 2006. **96**(6): p. 1768-77.

50. Burdo, J.R., et al., *Distribution of divalent metal transporter 1 and metal transport protein 1 in the normal and Belgrade rat.* J Neurosci Res, 2001. **66**(6): p. 1198-207.

51. Cheah, J.H., et al., *NMDA receptor-nitric oxide transmission mediates neuronal iron homeostasis via the GTPase Dexras1.* Neuron, 2006. **51**(4): p. 431-40.

52. Huang, E., et al., *Upregulation of iron regulatory proteins and divalent metal transporter-1 isoforms in the rat hippocampus after kainate induced neuronal injury.* Exp Brain Res, 2006. **170**(3): p. 376-86.

53. McKie, A.T., et al., *An iron-regulated ferric reductase associated with the absorption of dietary iron.* Science, 2001. **291**(5509): p. 1755-9.

54. Gunshin, H., et al., *Cybrd1 (duodenal cytochrome b) is not necessary for dietary iron absorption in mice.* Blood, 2005. **106**(8): p. 2879-83.

55. Muckenthaler, M., et al., *Regulatory defects in liver and intestine implicate abnormal hepcidin and Cybrd1 expression in mouse hemochromatosis.* Nat Genet, 2003. **34**(1): p. 102-7.

56. Ohgami, R.S., et al., *Identification of a ferrireductase required for efficient transferrin-dependent iron uptake in erythroid cells.* Nat Genet, 2005. **37**(11): p. 1264-9.

57. Ohgami, R.S., et al., *The Steap proteins are metalloreductases.* Blood, 2006. **108**(4): p. 1388-94.

58. Costanzo, F., et al., *Cloning and sequencing of a full length cDNA coding for a human apoferritin H chain: evidence for a multigene family.* Embo J, 1984. **3**(1): p. 23-7.

59. Munro, H.N. and M.C. Linder, *Ferritin: structure, biosynthesis, and role in iron metabolism.* Physiol Rev, 1978. **58**(2): p. 317-96.

60. Santoro, C., et al., *Cloning of the gene coding for human L apoferritin.* Nucleic Acids Res, 1986. **14**(7): p. 2863-76.

61. Chasteen, N.D. and P.M. Harrison, *Mineralization in ferritin: an efficient means of iron storage.* J Struct Biol, 1999. **126**(3): p. 182-94.

62. Liu, X. and E.C. Theil, *Ferritins: dynamic management of biological iron and oxygen chemistry.* Acc Chem Res, 2005. **38**(3): p. 167-75.

63. Harrison, P.M. and P. Arosio, *The ferritins: molecular properties, iron storage function and cellular regulation.* Biochim Biophys Acta, 1996. **1275**(3): p. 161-203.

64. Theil, E.C., M. Matzapetakis, and X. Liu, *Ferritins: iron/oxygen biominerals in protein nanocages.* J Biol Inorg Chem, 2006. **11**(7): p. 803-10.

65. Levi, S., et al., *Mechanism of ferritin iron uptake: activity of the H-chain and deletion mapping of the ferro-oxidase site. A study of iron uptake and ferro-oxidase activity of human liver, recombinant H-chain ferritins, and of two H-chain deletion mutants.* J Biol Chem, 1988. **263**(34): p. 18086-92.

66. Levi, S., et al., *The role of the L-chain in ferritin iron incorporation. Studies of homo and heteropolymers.* J Mol Biol, 1994. **238**(5): p. 649-54.

67. Santambrogio, P., et al., *Evidence that a salt bridge in the light chain contributes to the physical stability difference between heavy and light human ferritins.* J Biol Chem, 1992. **267**(20): p. 14077-83.

68. Arosio, P. and S. Levi, *Ferritin, iron homeostasis, and oxidative damage.* Free Radic Biol Med, 2002. **33**(4): p. 457-63.

69. Kidane, T.Z., E. Sauble, and M.C. Linder, *Release of iron from ferritin requires lysosomal activity.* Am J Physiol Cell Physiol, 2006. **291**(3): p. C445-55.

70. Truty, J., R. Malpe, and M.C. Linder, *Iron prevents ferritin turnover in hepatic cells.* J Biol Chem, 2001. **276**(52): p. 48775-80.

71. De Domenico, I., et al., *Ferroportin-mediated mobilization of ferritin iron precedes ferritin degradation by the proteasome.* Embo J, 2006. **25**(22): p. 5396-404.

72. Takagi, H., et al., *Localized unfolding at the junction of three ferritin subunits. A mechanism for iron release?* J Biol Chem, 1998. **273**(30): p. 18685-8.

73. Jin, W., et al., *"Opening" the ferritin pore for iron release by mutation of conserved amino acids at interhelix and loop sites.* Biochemistry, 2001. **40**(25): p. 7525-32.

74. Wohler, F. and F. Schomlau, *[Occurrence of ferritin in plasma.].* Klin Wochenschr, 1959. **37**(8): p. 445-51.

75. Chen, T.T., et al., *TIM-2 is expressed on B cells and in liver and kidney and is a receptor for H-ferritin endocytosis.* J Exp Med, 2005. **202**(7): p. 955-65.

76. Cai, C.X., D.E. Birk, and T.F. Linsenmayer, *Ferritin is a developmentally regulated nuclear protein of avian corneal epithelial cells.* J Biol Chem, 1997. **272**(19): p. 12831-9.

77. Surguladze, N., et al., *Characterization of nuclear ferritin and mechanism of translocation.* Biochem J, 2005. **388**(Pt 3): p. 731-40.

78. Cai, C.X., D.E. Birk, and T.F. Linsenmayer, *Nuclear ferritin protects DNA from UV damage in corneal epithelial cells.* Mol Biol Cell, 1998. **9**(5): p. 1037-51.

79. Thompson, K.J., et al., *Regulation, mechanisms and proposed function of ferritin translocation to cell nuclei.* J Cell Sci, 2002. **115**(Pt 10): p. 2165-77.

80. Hintze, K.J. and E.C. Theil, *Cellular regulation and molecular interactions of the ferritins.* Cell Mol Life Sci, 2006. **63**(5): p. 591-600.

81. Torti, F.M. and S.V. Torti, *Regulation of ferritin genes and protein.* Blood, 2002. **99**(10): p. 3505-16.

82. Mikhael, M., et al., *Iron regulatory protein-independent regulation of ferritin synthesis by nitrogen monoxide.* Febs J, 2006. **273**(16): p. 3828-36.

83. Torti, S.V., et al., *The molecular cloning and characterization of murine ferritin heavy chain, a tumor necrosis factor-inducible gene.* J Biol Chem, 1988. **263**(25): p. 12638-44.

84. Wei, Y., et al., *Interleukin 1 induces ferritin heavy chain in human muscle cells.* Biochem Biophys Res Commun, 1990. **169**(1): p. 289-96.

85. Kwak, E.L., et al., *Role for NF-kappa B in the regulation of ferritin H by tumor necrosis factor-alpha.* J Biol Chem, 1995. **270**(25): p. 15285-93.

86. Wasserman, W.W. and W.E. Fahl, *Functional antioxidant responsive elements.* Proc Natl Acad Sci U S A, 1997. **94**(10): p. 5361-6.

87. Tsuji, Y., et al., *Coordinate transcriptional and translational regulation of ferritin in response to oxidative stress.* Mol Cell Biol, 2000. **20**(16): p. 5818-27.

88. Muckenthaler, M., et al., *Relationships and distinctions in iron-regulatory networks responding to interrelated signals.* Blood, 2003. **101**(9): p. 3690-8.

89. Connor, J.R., et al., *Cellular distribution of transferrin, ferritin, and iron in normal and aged human brains.* J Neurosci Res, 1990. **27**(4): p. 595-611.

90. Zhang, P., et al., *Electron tomography of degenerating neurons in mice with abnormal regulation of iron metabolism.* J Struct Biol, 2005. **150**(2): p. 144-53.

91. Curtis, A.R., et al., *Mutation in the gene encoding ferritin light polypeptide causes dominant adult-onset basal ganglia disease.* Nat Genet, 2001. **28**(4): p. 350-4.

92. Fisher, J.L., et al., *Ferritin - A Novel Mechanism for Delivery of Iron to the Brain and other Organs.* Am J Physiol Cell Physiol, 2007.

93. Levi, S., et al., *A human mitochondrial ferritin encoded by an intronless gene.* J Biol Chem, 2001. **276**(27): p. 24437-40.

94. Santambrogio, P., et al., *Mitochondrial Ferritin Expression in Adult Mouse Tissues.* J Histochem Cytochem, 2007.

95. Corsi, B., et al., *Human mitochondrial ferritin expressed in HeLa cells incorporates iron and affects cellular iron metabolism.* J Biol Chem, 2002. **277**(25): p. 22430-7.

96. Nie, G., et al., *In vivo tumor growth is inhibited by cytosolic iron deprivation caused by the expression of mitochondrial ferritin.* Blood, 2006. **108**(7): p. 2428-34.

97. Abboud, S. and D.J. Haile, *A novel mammalian iron-regulated protein involved in intracellular iron metabolism.* J Biol Chem, 2000. **275**(26): p. 19906-12.

98. Donovan, A., et al., *Positional cloning of zebrafish ferroportin1 identifies a conserved vertebrate iron exporter.* Nature, 2000. **403**(6771): p. 776-81.

99. McKie, A.T., et al., *A novel duodenal iron-regulated transporter, IREG1, implicated in the basolateral transfer of iron to the circulation.* Mol Cell, 2000. **5**(2): p. 299-309.

100. Donovan, A., et al., *The iron exporter ferroportin/Slc40a1 is essential for iron homeostasis.* Cell Metab, 2005. **1**(3): p. 191-200.

101. Jeong, S.Y. and S. David, *Glycosylphosphatidylinositol-anchored ceruloplasmin is required for iron efflux from cells in the central nervous system.* J Biol Chem, 2003. **278**(29): p. 27144-8.

102. Han, O. and M. Wessling-Resnick, *Copper repletion enhances apical iron uptake and transepithelial iron transport by Caco-2 cells.* Am J Physiol Gastrointest Liver Physiol, 2002. **282**(3): p. G527-33.

103. De Domenico, I., et al., *Ferroxidase activity is required for the stability of cell surface ferroportin in cells expressing GPI-ceruloplasmin.* Embo J, 2007. **26**(12): p. 2823-31.

104. Nemeth, E., et al., *Hepcidin regulates cellular iron efflux by binding to ferroportin and inducing its internalization.* Science, 2004. **306**(5704): p. 2090-3.

105. Osaki, S., D.A. Johnson, and E. Frieden, *The possible significance of the ferrous oxidase activity of ceruloplasmin in normal human plasma.* J Biol Chem, 1966. **241**(12): p. 2746-51.

106. Holmberg, C.G. and C.B. Laurell, *Investigations in plasma copper. II. Isolation of the copper containing protein, and a description of some of its properties.* Acta Chem Scand, 1948. **2**: p. 550-6.

107. Hellman, N.E., et al., *Mechanisms of copper incorporation into human ceruloplasmin.* J Biol Chem, 2002. **277**(48): p. 46632-8.

108. Meyer, L.A., et al., *Copper transport and metabolism are normal in aceruloplasminemic mice.* J Biol Chem, 2001. **276**(39): p. 36857-61.

109. Zaitseva, I., et al., *The X-ray structure of human plasma ceruloplasmin at 3.1A:nature of the copper center.* JBIC, 1996. **1**: p. 15-23.

110. Messerschmidt, A. and R. Huber, *The blue oxidases, ascorbate oxidase, laccase and ceruloplasmin. Modelling and structural relationships.* Eur J Biochem, 1990. **187**(2): p. 341-52.

111. Takahashi, N., et al., *Internal triplication in the structure of human ceruloplasmin.* Proc Natl Acad Sci U S A, 1983. **80**(1): p. 115-9.

112. Ortel, T.L., N. Takahashi, and F.W. Putnam, *Structural model of human ceruloplasmin based on internal triplication, hydrophilic/hydrophobic character, and secondary structure of domains.* Proc Natl Acad Sci U S A, 1984. **81**(15): p. 4761-5.

113. Calabrese, L., M. Carbonaro, and G. Musci, *Presence of coupled trinuclear copper cluster in mammalian ceruloplasmin is essential for efficient electron transfer to oxygen.* J Biol Chem, 1989. **264**(11): p. 6183-7.

114. Lindley, P.F., et al., *An X-ray structural study of human ceruloplasmin in relation to feroxidase activity.* JBIC, 1997. **2**: p. 454-463.

115. Chen, L., et al., *Increased expression of ceruloplasmin in the retina following photic injury.* Mol Vis, 2003. **9**: p. 151-8.

116. Fleming, R.E., I.P. Whitman, and J.D. Gitlin, *Induction of ceruloplasmin gene expression in rat lung during inflammation and hyperoxia.* Am J Physiol, 1991. **260**(2 Pt 1): p. L68-74.

117. Mazumder, B., et al., *Induction of ceruloplasmin synthesis by IFN-gamma in human monocytic cells.* J Immunol, 1997. **159**(4): p. 1938-44.

118. Ramadori, G., et al., *Interleukin 6, the third mediator of acute-phase reaction, modulates hepatic protein synthesis in human and mouse. Comparison with interleukin 1 beta and tumor necrosis factor-alpha.* Eur J Immunol, 1988. **18**(8): p. 1259-64.

119. Sampath, P., et al., *Transcript-selective translational silencing by gamma interferon is directed by a novel structural element in the ceruloplasmin mRNA 3' untranslated region.* Mol Cell Biol, 2003. **23**(5): p. 1509-19.

120. Owen, C.A., Jr., *Metabolism of radiocopper (Cu64) in the rat.* Am J Physiol, 1965. **209**(5): p. 900-4.

121. Hsieh, H.S. and E. Frieden, *Evidence for ceruloplasmin as a copper transport protein.* Biochem Biophys Res Commun, 1975. **67**(4): p. 1326-31.

122. Frieden, E. and H.S. Hsieh, *Ceruloplasmin: the copper transport protein with essential oxidase activity.* Adv Enzymol Relat Areas Mol Biol, 1976. **44**: p. 187-236.

123. Cooper, E.H. and A.M. Ward, *Acute phase reactant proteins as aids to monitoring disease.* Invest Cell Pathol, 1979. **2**(4): p. 293-301.

124. Koschinsky, M.L., et al., *Complete cDNA sequence of human preceruloplasmin.* Proc Natl Acad Sci U S A, 1986. **83**(14): p. 5086-90.

125. Yang, F., et al., *Characterization, mapping, and expression of the human ceruloplasmin gene.* Proc Natl Acad Sci U S A, 1986. **83**(10): p. 3257-61.

126. Mercer, J.F. and A. Grimes, *Isolation of a human ceruloplasmin cDNA clone that includes the N- terminal leader sequence.* FEBS Lett, 1986. **203**(2): p. 185-90.

127. Fleming, R.E. and J.D. Gitlin, *Primary structure of rat ceruloplasmin and analysis of tissue-specific gene expression during development.* J Biol Chem, 1990. **265**(13): p. 7701-7.

128. Klomp, L.W., et al., *Ceruloplasmin gene expression in the murine central nervous system.* J Clin Invest, 1996. **98**(1): p. 207-15.

129. Klomp, L.W. and J.D. Gitlin, *Expression of the ceruloplasmin gene in the human retina and brain: implications for a pathogenic model in aceruloplasminemia.* Hum Mol Genet, 1996. **5**(12): p. 1989-96.

130. Thomas, T. and G. Schreiber, *The expression of genes coding for positive acute-phase proteins in the reproductive tract of the female rat. High levels of ceruloplasmin mRNA in the uterus.* FEBS Lett, 1989. **243**(2): p. 381-4.

131. Yang, F.M., et al., *Human ceruloplasmin. Tissue-specific expression of transcripts produced by alternative splicing.* J Biol Chem, 1990. **265**(18): p. 10780-5.

132. Patel, B.N. and S. David, *A novel glycosylphosphatidylinositol-anchored form of ceruloplasmin is expressed by mammalian astrocytes.* J Biol Chem, 1997. **272**(32): p. 20185-90.

133. Patel, B.N., R.J. Dunn, and S. David, *Alternative RNA splicing generates a glycosylphosphatidylinositol- anchored form of ceruloplasmin in mammalian brain.* J Biol Chem, 2000. **275**(6): p. 4305-10.

134. Salzer, J.L., et al., *Ran-2, a glial lineage marker, is a GPI-anchored form of ceruloplasmin.* J Neurosci Res, 1998. **54**(2): p. 147-57.

135. Hellman, N.E., et al., *Biochemical analysis of a missense mutation in aceruloplasminemia.* J Biol Chem, 2002. **277**(2): p. 1375-80.

136. Gitlin, J.D., *Aceruloplasminemia.* Pediatr Res, 1998. **44**(3): p. 271-6.

137. Vulpe, C.D., et al., *Hephaestin, a ceruloplasmin homologue implicated in intestinal iron transport, is defective in the sla mouse.* Nat Genet, 1999. **21**(2): p. 195-9.

138. Kuo, Y.M., et al., *Mislocalisation of hephaestin, a multicopper ferroxidase involved in basolateral intestinal iron transport, in the sex linked anaemia mouse.* Gut, 2004. **53**(2): p. 201-6.

139. Han, O. and E.Y. Kim, *Colocalization of ferroportin-1 with hephaestin on the basolateral membrane of human intestinal absorptive cells.* J Cell Biochem, 2007. **101**(4): p. 1000-10.

140. Frazer, D.M., et al., *Cloning and gastrointestinal expression of rat hephaestin: relationship to other iron transport proteins.* Am J Physiol Gastrointest Liver Physiol, 2001. **281**(4): p. G931-9.

141. Syed, B.A., et al., *Analysis of the human hephaestin gene and protein: comparative modelling of the N-terminus ecto-domain based upon ceruloplasmin.* Protein Eng, 2002. **15**(3): p. 205-14.

142. Chen, H., et al., *Systemic regulation of Hephaestin and Ireg1 revealed in studies of genetic and nutritional iron deficiency.* Blood, 2003. **102**(5): p. 1893-9.

143. Sakakibara, S. and Y. Aoyama, *Dietary iron-deficiency up-regulates hephaestin mRNA level in small intestine of rats.* Life Sci, 2002. **70**(26): p. 3123-9.

144. Krause, A., et al., *LEAP-1, a novel highly disulfide-bonded human peptide, exhibits antimicrobial activity.* FEBS Lett, 2000. **480**(2-3): p. 147-50.

145. Park, C.H., et al., *Hepcidin, a urinary antimicrobial peptide synthesized in the liver.* J Biol Chem, 2001. **276**(11): p. 7806-10.

146. Pigeon, C., et al., *A new mouse liver-specific gene, encoding a protein homologous to human antimicrobial peptide hepcidin, is overexpressed during iron overload.* J Biol Chem, 2001. **276**(11): p. 7811-9.

147. Hunter, H.N., et al., *The solution structure of human hepcidin, a peptide hormone with antimicrobial activity that is involved in iron uptake and hereditary hemochromatosis.* J Biol Chem, 2002. **277**(40): p. 37597-603.

148. Nicolas, G., et al., *Lack of hepcidin gene expression and severe tissue iron overload in upstream stimulatory factor 2 (USF2) knockout mice.* Proc Natl Acad Sci U S A, 2001. **98**(15): p. 8780-5.

149. Nicolas, G., et al., *Severe iron deficiency anemia in transgenic mice expressing liver hepcidin.* Proc Natl Acad Sci U S A, 2002. **99**(7): p. 4596-601.

150. Roetto, A., et al., *Mutant antimicrobial peptide hepcidin is associated with severe juvenile hemochromatosis.* Nat Genet, 2003. **33**(1): p. 21-2.

151. Ganz, T. and E. Nemeth, *Iron imports. IV. Hepcidin and regulation of body iron metabolism.* Am J Physiol Gastrointest Liver Physiol, 2006. **290**(2): p. G199-203.

152. Zechel, S., K. Huber-Wittmer, and O. von Bohlen und Halbach, *Distribution of the iron-regulating protein hepcidin in the murine central nervous system.* J Neurosci Res, 2006. **84**(4): p. 790-800.

153. Dautry-Varsat, A., A. Ciechanover, and H.F. Lodish, *pH and the recycling of transferrin during receptor-mediated endocytosis.* Proc Natl Acad Sci U S A, 1983. **80**(8): p. 2258-62.

154. McClelland, A., L.C. Kuhn, and F.H. Ruddle, *The human transferrin receptor gene: genomic organization, and the complete primary structure of the receptor deduced from a cDNA sequence.* Cell, 1984. **39**(2 Pt 1): p. 267-74.

155. Dautry-Varsat, A., *Receptor-mediated endocytosis: the intracellular journey of transferrin and its receptor.* Biochimie, 1986. **68**(3): p. 375-81.

156. Aisen, P., *Entry of iron into cells: a new role for the transferrin receptor in modulating iron release from transferrin.* Ann Neurol, 1992. **32**(Suppl): p. S62-8.

157. Fleming, M.D., et al., *Nramp2 is mutated in the anemic Belgrade (b) rat: evidence of a role for Nramp2 in endosomal iron transport.* Proc Natl Acad Sci U S A, 1998. **95**(3): p. 1148-53.

158. Ohgami, R.S., et al., *nm1054: a spontaneous, recessive, hypochromic, microcytic anemia mutation in the mouse.* Blood, 2005. **106**(10): p. 3625-31.

159. Sheftel, A.D., et al., *Direct interorganellar transfer of iron from endosome to mitochondrion.* Blood, 2007. **110**(1): p. 125-32.

160. Zhang, A.S., A.D. Sheftel, and P. Ponka, *Intracellular kinetics of iron in reticulocytes: evidence for endosome involvement in iron targeting to mitochondria.* Blood, 2005. **105**(1): p. 368-75.

161. Shayeghi, M., et al., *Identification of an intestinal heme transporter.* Cell, 2005. **122**(5): p. 789-801.

162. Chen, H., et al., *Hephaestin is a ferroxidase that maintains partial activity in sex-linked anemia mice.* Blood, 2004. **103**(10): p. 3933-9.

163. Quigley, J.G., et al., *Identification of a human heme exporter that is essential for erythropoiesis.* Cell, 2004. **118**(6): p. 757-66.

164. Dean, M., A. Rzhetsky, and R. Allikmets, *The human ATP-binding cassette (ABC) transporter superfamily.* Genome Res, 2001. **11**(7): p. 1156-66.

165. Krishnamurthy, P. and J.D. Schuetz, *The ABC transporter Abcg2/Bcrp: role in hypoxia mediated survival.* Biometals, 2005. **18**(4): p. 349-58.

166. Jonker, J.W., et al., *The breast cancer resistance protein protects against a major chlorophyll-derived dietary phototoxin and protoporphyria.* Proc Natl Acad Sci U S A, 2002. **99**(24): p. 15649-54.

167. Krishnamurthy, P., et al., *The stem cell marker Bcrp/ABCG2 enhances hypoxic cell survival through interactions with heme.* J Biol Chem, 2004. **279**(23): p. 24218-25.

168. Andrews, N.C., *Iron homeostasis: insights from genetics and animal models.* Nat Rev Genet, 2000. **1**(3): p. 208-17.

169. Drubach, D., *The Brain Explained.* 1999: Prentice Hall.

170. Anderson, G.J., et al., *Regulation of systemic iron homeostasis: how the body responds to changes in iron demand.* Biometals, 2007. **20**(3-4): p. 665-74.

171. Frazer, D.M. and G.J. Anderson, *The orchestration of body iron intake: how and where do enterocytes receive their cues?* Blood Cells Mol Dis, 2003. **30**(3): p. 288-97.

172. Rivera, S., et al., *Hepcidin excess induces the sequestration of iron and exacerbates tumor-associated anemia.* Blood, 2005. **105**(4): p. 1797-802.

173. Lesbordes-Brion, J.C., et al., *Targeted disruption of the hepcidin 1 gene results in severe hemochromatosis.* Blood, 2006. **108**(4): p. 1402-5.

174. Drakesmith, H., et al., *Resistance to hepcidin is conferred by hemochromatosis-associated mutations of ferroportin.* Blood, 2005. **106**(3): p. 1092-7.

175. Nicolas, G., et al., *The gene encoding the iron regulatory peptide hepcidin is regulated by anemia, hypoxia, and inflammation.* J Clin Invest, 2002. **110**(7): p. 1037-44.

176. Bunn, H.F. and R.O. Poyton, *Oxygen sensing and molecular adaptation to hypoxia.* Physiol Rev, 1996. **76**(3): p. 839-85.

177. Roy, C.N. and N.C. Andrews, *Anemia of inflammation: the hepcidin link.* Curr Opin Hematol, 2005. **12**(2): p. 107-11.

178. Nemeth, E., et al., *IL-6 mediates hypoferremia of inflammation by inducing the synthesis of the iron regulatory hormone hepcidin.* J Clin Invest, 2004. **113**(9): p. 1271-6.

179. Nemeth, E., et al., *Hepcidin, a putative mediator of anemia of inflammation, is a type II acute-phase protein.* Blood, 2003. **101**(7): p. 2461-3.

180. Rouault, T.A., *The role of iron regulatory proteins in mammalian iron homeostasis and disease.* Nat Chem Biol, 2006. **2**(8): p. 406-14.

181. Gray, N.K. and M.W. Hentze, *Iron regulatory protein prevents binding of the 43S translation pre- initiation complex to ferritin and eALAS mRNAs.* Embo J, 1994. **13**(16): p. 3882-91.

182. Schlegl, J., et al., *Probing the structure of the regulatory region of human transferrin receptor messenger RNA and its interaction with iron regulatory protein- 1.* Rna, 1997. **3**(10): p. 1159-72.

183. Theil, E.C., *Regulation of ferritin and transferrin receptor mRNAs.* J Biol Chem, 1990. **265**(9): p. 4771-4.

184. Koeller, D.M., et al., *Translation and the stability of mRNAs encoding the transferrin receptor and c-fos.* Proc Natl Acad Sci U S A, 1991. **88**(17): p. 7778-82.

185. Binder, R., et al., *Evidence that the pathway of transferrin receptor mRNA degradation involves an endonucleolytic cleavage within the 3' UTR and does not involve poly(A) tail shortening.* Embo J, 1994. **13**(8): p. 1969-80.

186. Richardson, D.R., et al., *The effect of redox-related species of nitrogen monoxide on transferrin and iron uptake and cellular proliferation of erythroleukemia (K562) cells.* Blood, 1995. **86**(8): p. 3211-9.

187. Weiss, G., C. Bogdan, and M.W. Hentze, *Pathways for the regulation of macrophage iron metabolism by the anti-inflammatory cytokines IL-4 and IL-13.* J Immunol, 1997. **158**(1): p. 420-5.

188. Andriopoulos, B., et al., *Sustained Hydrogen Peroxide Induces Iron Uptake by Transferrin Receptor-1 Independent of the Iron Regulatory Protein/Iron-responsive Element Network.* J Biol Chem, 2007. **282**(28): p. 20301-8.

189. Irace, C., et al., *Divergent modulation of iron regulatory proteins and ferritin biosynthesis by hypoxia/reoxygenation in neurones and glial cells.* J Neurochem, 2005. **95**(5): p. 1321-31.

190. Yang, F., et al., *Regulation of reticuloendothelial iron transporter MTP1 (Slc11a3) by inflammation.* J Biol Chem, 2002. **277**(42): p. 39786-91.

191. Beinert, H., R.H. Holm, and E. Munck, *Iron-sulfur clusters: nature's modular, multipurpose structures.* Science, 1997. **277**(5326): p. 653-9.

192. Beinert, H. and P. Kiley, *Redox control of gene expression involving iron-sulfur proteins. Change of oxidation-state or assembly/disassembly of Fe-S clusters?* FEBS Lett, 1996. **382**(1-2): p. 218-9; discussion 220-1.

193. Cairo, G., et al., *The iron regulatory proteins: targets and modulators of free radical reactions and oxidative damage.* Free Radic Biol Med, 2002. **32**(12): p. 1237-43.

194. Caltagirone, A., G. Weiss, and K. Pantopoulos, *Modulation of cellular iron metabolism by hydrogen peroxide. Effects of H2O2 on the expression and function of iron-responsive element-containing mRNAs in B6 fibroblasts.* J Biol Chem, 2001. **276**(23): p. 19738-45.

195. Pantopoulos, K. and M.W. Hentze, *Rapid responses to oxidative stress mediated by iron regulatory protein.* Embo J, 1995. **14**(12): p. 2917-24.

196. Rouault, T.A. and R.D. Klausner, *Iron-sulfur clusters as biosensors of oxidants and iron.* Trends Biochem Sci, 1996. **21**(5): p. 174-7.

197. Fillebeen, C., et al., *IRP1 Ser-711 is a phosphorylation site, critical for regulation of RNA-binding and aconitase activities.* Biochem J, 2005. **388**(Pt 1): p. 143-50.

198. Pitula, J.S., et al., *Selective inhibition of the citrate-to-isocitrate reaction of cytosolic aconitase by phosphomimetic mutation of serine-711.* Proc Natl Acad Sci U S A, 2004. **101**(30): p. 10907-12.

199. Guo, B., et al., *Iron regulates the intracellular degradation of iron regulatory protein 2 by the proteasome.* J Biol Chem, 1995. **270**(37): p. 21645-51.

200. Iwai, K., et al., *Iron-dependent oxidation, ubiquitination, and degradation of iron regulatory protein 2: implications for degradation of oxidized proteins.* Proc Natl Acad Sci U S A, 1998. **95**(9): p. 4924-8.

201. Iwai, K., R.D. Klausner, and T.A. Rouault, *Requirements for iron-regulated degradation of the RNA binding protein, iron regulatory protein 2.* Embo J, 1995. **14**(21): p. 5350-7.

202. Hanson, E.S., M.L. Rawlins, and E.A. Leibold, *Oxygen and iron regulation of iron regulatory protein 2.* J Biol Chem, 2003. **278**(41): p. 40337-42.

203. Wang, J., et al., *Iron-mediated degradation of IRP2, an unexpected pathway involving a 2-oxoglutarate-dependent oxygenase activity.* Mol Cell Biol, 2004. **24**(3): p. 954-65.

204. Halliwell, B., *Reactive oxygen species and the central nervous system.* J Neurochem, 1992. **59**(5): p. 1609-23.

205. Harris, Z.L., *Aceruloplasminemia.* J Neurol Sci, 2003. **207**(1-2): p. 108-9.

206. Enerson, B.E. and L.R. Drewes, *The rat blood-brain barrier transcriptome.* J Cereb Blood Flow Metab, 2006. **26**(7): p. 959-73.

207. Moos, T. and E.H. Morgan, *Transferrin and transferrin receptor function in brain barrier systems.* Cell Mol Neurobiol, 2000. **20**(1): p. 77-95.

208. Fishman, J.B., et al., *Receptor-mediated transcytosis of transferrin across the blood-brain barrier.* J Neurosci Res, 1987. **18**(2): p. 299-304.

209. Roberts, R., et al., *Studies of the mechanism of iron transport across the blood-brain barrier.* Ann Neurol, 1992. **32 Suppl**: p. S43-50.

210. Burdo, J.R., et al., *Mechanisms and regulation of transferrin and iron transport in a model blood-brain barrier system.* Neuroscience, 2003. **121**(4): p. 883-90.

211. Deane, R., W. Zheng, and B.V. Zlokovic, *Brain capillary endothelium and choroid plexus epithelium regulate transport of transferrin-bound and free iron into the rat brain.* J Neurochem, 2004. **88**(4): p. 813-20.

212. Ueda, F., et al., *Rate of 59Fe uptake into brain and cerebrospinal fluid and the influence thereon of antibodies against the transferrin receptor.* J Neurochem, 1993. **60**(1): p. 106-13.

213. Moos, T. and E.H. Morgan, *The significance of the mutated divalent metal transporter (DMT1) on iron transport into the Belgrade rat brain.* J Neurochem, 2004. **88**(1): p. 233-45.

214. Beard, J.L., et al., *Brain iron uptake in hypotransferrinemic mice: influence of systemic iron status.* J Neurosci Res, 2005. **79**(1-2): p. 254-61.

215. Wu, L.J., et al., *Expression of the iron transporter ferroportin in synaptic vesicles and the blood-brain barrier.* Brain Res, 2004. **1001**(1-2): p. 108-17.

216. Connor, J.R., et al., *Iron and iron management proteins in neurobiology.* Pediatr Neurol, 2001. **25**(2): p. 118-29.

217. Malecki, E.A., et al., *Transferrin is required for normal distribution of 59Fe and 54Mn in mouse brain.* J Neurol Sci, 1999. **170**(2): p. 112-8.

218. Laterra, J. and G.W. Goldstein, *Ventricular organization of cerebrospinal fluid: blood-brain barrier, brain edema, and hydrocephalus*, in *Principles of neural science*, E.R. Kandel, J.H. Schwartz, and T.M. Jessell, Editors. 2000, McGraw-Hill. p. 1288-1300.

219. Felgenhauer, K., *Protein size and cerebrospinal fluid composition.* Klin Wochenschr, 1974. **52**(24): p. 1158-64.

220. Bleijenberg, B.G., H.G. Van Eijk, and B. Leijnse, *The determination of non-heme iron and transferrin in cerebrospinal fluid.* Clin Chim Acta, 1971. **31**(1): p. 277-81.

221. Del Principe, D., A. Menichelli, and C. Colistra, *The ceruloplasmin and transferrin system in cerebrospinal fluid of acute leukemia patients.* Acta Paediatr Scand, 1989. **78**(2): p. 327-8.

222. Lamoureux, G., et al., *Cerebrospinal fluid proteins in multiple sclerosis.* Neurology, 1975. **25**(6): p. 537-46.

223. Faucheux, B.A., et al., *Expression of lactoferrin receptors is increased in the mesencephalon of patients with Parkinson disease.* Proc Natl Acad Sci U S A, 1995. **92**(21): p. 9603-7.

224. Qian, Z.M. and Q. Wang, *Expression of iron transport proteins and excessive iron accumulation in the brain in neurodegenerative disorders.* Brain Res Brain Res Rev, 1998. **27**(3): p. 257-67.

225. Moos, T. and E.H. Morgan, *Evidence for low molecular weight, non-transferrin-bound iron in rat brain and cerebrospinal fluid.* J Neurosci Res, 1998. **54**(4): p. 486-94.

226. Beard, J.L., et al., *Moderate iron deficiency in infancy: biology and behavior in young rats.* Behav Brain Res, 2006. **170**(2): p. 224-32.

227. Cooperman, S.S., et al., *Microcytic anemia, erythropoietic protoporphyria, and neurodegeneration in mice with targeted deletion of iron-regulatory protein 2.* Blood, 2005. **106**(3): p. 1084-91.

228. Mittal, B., et al., *Expression of a membrane-bound form of the ferroxidase ceruloplasmin by leptomeningeal cells.* Glia, 2003. **41**(4): p. 337-46.

229. Thompson, K.J., S. Shoham, and J.R. Connor, *Iron and neurodegenerative disorders.* Brain Res Bull, 2001. **55**(2): p. 155-64.

230. Burdo, J.R. and J.R. Connor, *Brain iron uptake and homeostatic mechanisms: an overview.* Biometals, 2003. **16**(1): p. 63-75.

231. Mancuso, M., et al., *Hereditary ferritinopathy: a novel mutation, its cellular pathology, and pathogenetic insights.* J Neuropathol Exp Neurol, 2005. **64**(4): p. 280-94.

232. Vidal, R., et al., *Intracellular ferritin accumulation in neural and extraneural tissue characterizes a neurodegenerative disease associated with a mutation in the ferritin light polypeptide gene.* J Neuropathol Exp Neurol, 2004. **63**(4): p. 363-80.

233. Cozzi, A., et al., *Characterization of the l-ferritin variant 460InsA responsible of a hereditary ferritinopathy disorder.* Neurobiol Dis, 2006. **23**(3): p. 644-52.

234. Swaiman, K.F., *Hallervorden-Spatz syndrome.* Pediatr Neurol, 2001. **25**(2): p. 102-8.

235. Hayflick, S.J., *Unraveling the Hallervorden-Spatz syndrome: pantothenate kinase-associated neurodegeneration is the name.* Curr Opin Pediatr, 2003. **15**(6): p. 572-7.

236. Zhou, B., et al., *A novel pantothenate kinase gene (PANK2) is defective in Hallervorden- Spatz syndrome.* Nat Genet, 2001. **28**(4): p. 345-9.

237. Perry, T.L., et al., *Hallervorden-Spatz disease: cysteine accumulation and cysteine dioxygenase deficiency in the globus pallidus.* Ann Neurol, 1985. **18**(4): p. 482-9.

238. Kuo, Y.M., et al., *Deficiency of pantothenate kinase 2 (Pank2) in mice leads to retinal degeneration and azoospermia.* Hum Mol Genet, 2005. **14**(1): p. 49-57.

239. Patel, P.I. and G. Isaya, *Friedreich ataxia: from GAA triplet-repeat expansion to frataxin deficiency.* Am J Hum Genet, 2001. **69**(1): p. 15-24.

240. Campuzano, V., et al., *Frataxin is reduced in Friedreich ataxia patients and is associated with mitochondrial membranes.* Hum Mol Genet, 1997. **6**(11): p. 1771-80.

241. Priller, J., et al., *Frataxin gene of Friedreich's ataxia is targeted to mitochondria.* Ann Neurol, 1997. **42**(2): p. 265-9.

242. Babcock, M., et al., *Regulation of mitochondrial iron accumulation by Yfh1p, a putative homolog of frataxin.* Science, 1997. **276**(5319): p. 1709-12.

243. Koutnikova, H., et al., *Studies of human, mouse and yeast homologues indicate a mitochondrial function for frataxin.* Nat Genet, 1997. **16**(4): p. 345-51.

244. Radisky, D.C., M.C. Babcock, and J. Kaplan, *The yeast frataxin homologue mediates mitochondrial iron efflux. Evidence for a mitochondrial iron cycle.* J Biol Chem, 1999. **274**(8): p. 4497-9.

245. Gerber, J., U. Muhlenhoff, and R. Lill, *An interaction between frataxin and Isu1/Nfs1 that is crucial for Fe/S cluster synthesis on Isu1.* EMBO Rep, 2003. **4**(9): p. 906-11.

246. Martelli, A., et al., *Frataxin is essential for extramitochondrial Fe-S cluster proteins in mammalian tissues.* Hum Mol Genet, 2007.

247. Muhlenhoff, U., et al., *Components involved in assembly and dislocation of iron-sulfur clusters on the scaffold protein Isu1p.* Embo J, 2003. **22**(18): p. 4815-25.

248. Bulteau, A.L., et al., *Frataxin acts as an iron chaperone protein to modulate mitochondrial aconitase activity.* Science, 2004. **305**(5681): p. 242-5.

249. Chen, O.S., S. Hemenway, and J. Kaplan, *Inhibition of Fe-S cluster biosynthesis decreases mitochondrial iron export: evidence that Yfh1p affects Fe-S cluster synthesis.* Proc Natl Acad Sci U S A, 2002. **99**(19): p. 12321-6.

250. Stehling, O., et al., *Iron-sulfur protein maturation in human cells: evidence for a function of frataxin.* Hum Mol Genet, 2004. **13**(23): p. 3007-15.

251. Richardson, D.R., et al., *Development of potential iron chelators for the treatment of Friedreich's ataxia: ligands that mobilize mitochondrial iron.* Biochim Biophys Acta, 2001. **1536**(2-3): p. 133-40.

252. Wong, A., et al., *The Friedreich's ataxia mutation confers cellular sensitivity to oxidant stress which is rescued by chelators of iron and calcium and inhibitors of apoptosis.* Hum Mol Genet, 1999. **8**(3): p. 425-30.

253. Boddaert, N., et al., *Selective iron chelation in Friedreich ataxia: biologic and clinical implications.* Blood, 2007. **110**(1): p. 401-8.

254. Miyajima, H., et al., *Familial apoceruloplasmin deficiency associated with blepharospasm and retinal degeneration.* Neurology, 1987. **37**(5): p. 761-7.

255. Harris, Z.L., et al., *Aceruloplasminemia: molecular characterization of this disorder of iron metabolism.* Proc Natl Acad Sci U S A, 1995. **92**(7): p. 2539-43.

256. Morita, H., et al., *Hereditary ceruloplasmin deficiency with hemosiderosis: a clinicopathological study of a Japanese family.* Ann Neurol, 1995. **37**(5): p. 646-56.

257. Royle, N.J., et al., *Human genes encoding prothrombin and ceruloplasmin map to 11p11-q12 and 3q21-24, respectively.* Somat Cell Mol Genet, 1987. **13**(3): p. 285-92.

258. Daimon, M., et al., *Fine structure of the human ceruloplasmin gene.* Biochem Biophys Res Commun, 1995. **208**(3): p. 1028-35.

259. Logan, J.I., et al., *Hereditary caeruloplasmin deficiency, dementia and diabetes mellitus.* Qjm, 1994. **87**(11): p. 663-70.

260. Dunaief, J.L., et al., *Macular degeneration in a patient with aceruloplasminemia, a disease associated with retinal iron overload.* Ophthalmology, 2005. **112**(6): p. 1062-5.

261. Miyajima, H., Y. Takahashi, and S. Kono, *Aceruloplasminemia, an inherited disorder of iron metabolism.* Biometals, 2003. **16**(1): p. 205-13.

262. Yoshida, K., et al., *A mutation in the ceruloplasmin gene is associated with systemic hemosiderosis in humans.* Nat Genet, 1995. **9**(3): p. 267-72.

263. Miyajima, H., et al., *CSF abnormalities in patients with aceruloplasminemia.* Neurology, 1998. **51**(4): p. 1188-90.

264. Kohno, S., et al., *Defective electron transfer in complexes I and IV in patients with aceruloplasminemia.* J Neurol Sci, 2000. **182**(1): p. 57-60.

265. Harris, Z.L., et al., *Targeted gene disruption reveals an essential role for ceruloplasmin in cellular iron efflux.* Proc Natl Acad Sci U S A, 1999. **96**(19): p. 10812-7.

266. Jeong, S.Y. and S. David, *Age-related changes in iron homeostasis and cell death in the cerebellum of ceruloplasmin-deficient mice.* J Neurosci, 2006. **26**(38): p. 9810-9.

267. Patel, B.N., et al., *Ceruloplasmin regulates iron levels in the CNS and prevents free radical injury.* J Neurosci, 2002. **22**(15): p. 6578-86.

268. Hahn, P., et al., *Disruption of ceruloplasmin and hephaestin in mice causes retinal iron overload and retinal degeneration with features of age-related macular degeneration.* Proc Natl Acad Sci U S A, 2004. **101**(38): p. 13850-5.

269. LaVaute, T., et al., *Targeted deletion of the gene encoding iron regulatory protein-2 causes misregulation of iron metabolism and neurodegenerative disease in mice.* Nat Genet, 2001. **27**(2): p. 209-14.

270. Smith, S.R., et al., *Severity of neurodegeneration correlates with compromise of iron metabolism in mice with iron regulatory protein deficiencies.* Ann N Y Acad Sci, 2004. **1012**: p. 65-83.

271. Kim, S. and P. Ponka, *Control of transferrin receptor expression via nitric oxide-mediated modulation of iron-regulatory protein 2.* J Biol Chem, 1999. **274**(46): p. 33035-42.

272. Galy, B., et al., *Iron homeostasis in the brain: complete iron regulatory protein 2 deficiency without symptomatic neurodegeneration in the mouse.* Nat Genet, 2006. **38**(9): p. 967-9; discussion 969-70.

273. Wilms, H., et al., *Inflammation in Parkinson's diseases and other neurodegenerative diseases: cause and therapeutic implications.* Curr Pharm Des, 2007. **13**(18): p. 1925-8.

274. Sofic, E., et al., *Increased iron (III) and total iron content in post mortem substantia nigra of parkinsonian brain.* J Neural Transm, 1988. **74**(3): p. 199-205.

275. Bartzokis, G., et al., *MRI evaluation of brain iron in earlier- and later-onset Parkinson's disease and normal subjects.* Magn Reson Imaging, 1999. **17**(2): p. 213-22.

276. Becker, G., et al., *Degeneration of substantia nigra in chronic Parkinson's disease visualized by transcranial color-coded real-time sonography.* Neurology, 1995. **45**(1): p. 182-4.

277. Berg, D., et al., *Echogenicity of the substantia nigra: association with increased iron content and marker for susceptibility to nigrostriatal injury.* Arch Neurol, 2002. **59**(6): p. 999-1005.

278. Gotz, M.E., et al., *The relevance of iron in the pathogenesis of Parkinson's disease.* Ann N Y Acad Sci, 2004. **1012**: p. 193-208.

279. Alam, Z.I., et al., *Oxidative DNA damage in the parkinsonian brain: an apparent selective increase in 8-hydroxyguanine levels in substantia nigra.* J Neurochem, 1997. **69**(3): p. 1196-203.

280. Dexter, D.T., et al., *Basal lipid peroxidation in substantia nigra is increased in Parkinson's disease.* J Neurochem, 1989. **52**(2): p. 381-9.

281. Pratico, D., *In vivo measurement of the redox state.* Lipids, 2001. **36 Suppl**: p. S45-7.

282. Stadtman, E.R., *Protein oxidation in aging and age-related diseases.* Ann N Y Acad Sci, 2001. **928**: p. 22-38.

283. Wood-Kaczmar, A., S. Gandhi, and N.W. Wood, *Understanding the molecular causes of Parkinson's disease.* Trends Mol Med, 2006. **12**(11): p. 521-8.

284. Golts, N., et al., *Magnesium inhibits spontaneous and iron-induced aggregation of alpha-synuclein.* J Biol Chem, 2002. **277**(18): p. 16116-23.

285. Hashimoto, M., et al., *Oxidative stress induces amyloid-like aggregate formation of NACP/alpha-synuclein in vitro.* Neuroreport, 1999. **10**(4): p. 717-21.

286. Ohnishi, S. and K. Takano, *Amyloid fibrils from the viewpoint of protein folding.* Cell Mol Life Sci, 2004. **61**(5): p. 511-24.

287. Bartzokis, G., et al., *In vivo evaluation of brain iron in Alzheimer disease using magnetic resonance imaging.* Arch Gen Psychiatry, 2000. **57**(1): p. 47-53.

288. Connor, J.R., et al., *A histochemical study of iron, transferrin, and ferritin in Alzheimer's diseased brains.* J Neurosci Res, 1992. **31**(1): p. 75-83.

289. Deibel, M.A., W.D. Ehmann, and W.R. Markesbery, *Copper, iron, and zinc imbalances in severely degenerated brain regions in Alzheimer's disease: possible relation to oxidative stress.* J Neurol Sci, 1996. **143**(1-2): p. 137-42.

290. Todorich, B.M. and J.R. Connor, *Redox metals in Alzheimer's disease.* Ann N Y Acad Sci, 2004. **1012**: p. 171-8.

291. Garzon-Rodriguez, W., A.K. Yatsimirsky, and C.G. Glabe, *Binding of Zn(II), Cu(II), and Fe(II) ions to Alzheimer's A beta peptide studied by fluorescence.* Bioorg Med Chem Lett, 1999. **9**(15): p. 2243-8.

292. Mantyh, P.W., et al., *Aluminum, iron, and zinc ions promote aggregation of physiological concentrations of beta-amyloid peptide.* J Neurochem, 1993. **61**(3): p. 1171-4.

293. Bodovitz, S., et al., *Iron levels modulate alpha-secretase cleavage of amyloid precursor protein.* J Neurochem, 1995. **64**(1): p. 307-15.

294. Rogers, J.T., et al., *An iron-responsive element type II in the 5'-untranslated region of the Alzheimer's amyloid precursor protein transcript.* J Biol Chem, 2002. **277**(47): p. 45518-28.

295. Honda, K., et al., *Oxidative stress and redox-active iron in Alzheimer's disease.* Ann N Y Acad Sci, 2004. **1012**: p. 179-82.

296. Walker, F.O., *Huntington's Disease.* Semin Neurol, 2007. **27**(2): p. 143-50.

297. Hilditch-Maguire, P., et al., *Huntingtin: an iron-regulated protein essential for normal nuclear and perinuclear organelles.* Hum Mol Genet, 2000. **9**(19): p. 2789-97.

298. Bartzokis, G., et al., *Increased basal ganglia iron levels in Huntington disease.* Arch Neurol, 1999. **56**(5): p. 569-74.

299. Chen, J.C., et al., *MR of human postmortem brain tissue: correlative study between T2 and assays of iron and ferritin in Parkinson and Huntington disease.* AJNR Am J Neuroradiol, 1993. **14**(2): p. 275-81.

300. Rutledge, J.N., et al., *Study of movement disorders and brain iron by MR.* AJR Am J Roentgenol, 1987. **149**(2): p. 365-79.

301. Bartzokis, G. and T.A. Tishler, *MRI evaluation of basal ganglia ferritin iron and neurotoxicity in Alzheimer's and Huntingon's disease.* Cell Mol Biol (Noisy-le-grand), 2000. **46**(4): p. 821-33.

302. Lumsden, A.L., et al., *Huntingtin-deficient zebrafish exhibit defects in iron utilization and development.* Hum Mol Genet, 2007.

303. Rosen, D.R., et al., *Mutations in Cu/Zn superoxide dismutase gene are associated with familial amyotrophic lateral sclerosis.* Nature, 1993. **362**(6415): p. 59-62.

304. Julien, J.P. and J. Kriz, *Transgenic mouse models of amyotrophic lateral sclerosis.* Biochim Biophys Acta, 2006. **1762**(11-12): p. 1013-24.

305. Barber, S.C., R.J. Mead, and P.J. Shaw, *Oxidative stress in ALS: a mechanism of neurodegeneration and a therapeutic target.* Biochim Biophys Acta, 2006. **1762**(11-12): p. 1051-67.

306. Williamson, T.L., et al., *Absence of neurofilaments reduces the selective vulnerability of motor neurons and slows disease caused by a familial amyotrophic lateral sclerosis-linked superoxide dismutase 1 mutant.* Proc Natl Acad Sci U S A, 1998. **95**(16): p. 9631-6.

307. Rothstein, J.D., *Excitotoxicity and neurodegeneration in amyotrophic lateral sclerosis.* Clin Neurosci, 1995. **3**(6): p. 348-59.

308. Julien, J.P., *Amyotrophic lateral sclerosis. unfolding the toxicity of the misfolded.* Cell, 2001. **104**(4): p. 581-91.

309. Ross, C.A. and M.A. Poirier, *Protein aggregation and neurodegenerative disease.* Nat Med, 2004. **10 Suppl**: p. S10-7.

310. Urushitani, M., S.A. Ezzi, and J.P. Julien, *Therapeutic effects of immunization with mutant superoxide dismutase in mice models of amyotrophic lateral sclerosis.* Proc Natl Acad Sci U S A, 2007. **104**(7): p. 2495-500.

311. Imon, Y., et al., *Low intensity areas observed on T2-weighted magnetic resonance imaging of the cerebral cortex in various neurological diseases.* J Neurol Sci, 1995. **134 Suppl**: p. 27-32.

312. Oba, H., et al., *Amyotrophic lateral sclerosis: T2 shortening in motor cortex at MR imaging.* Radiology, 1993. **189**(3): p. 843-6.

313. Yasui, M., K. Ota, and R.M. Garruto, *Concentrations of zinc and iron in the brains of Guamanian patients with amyotrophic lateral sclerosis and parkinsonism-dementia.* Neurotoxicology, 1993. **14**(4): p. 445-50.

314. Kasarskis, E.J., et al., *Aluminum, calcium, and iron in the spinal cord of patients with sporadic amyotrophic lateral sclerosis using laser microprobe mass spectroscopy: a preliminary study.* J Neurol Sci, 1995. **130**(2): p. 203-8.

315. Danzeisen, R., et al., *Superoxide dismutase 1 modulates expression of transferrin receptor.* J Biol Inorg Chem, 2006. **11**(4): p. 489-98.

316. Leveugle, B., et al., *The iron-binding protein lactotransferrin is present in pathologic lesions in a variety of neurodegenerative disorders: a comparative immunohistochemical analysis.* Brain Res, 1994. **650**(1): p. 20-31.

317. Goodall, E.F., et al., *Association of the H63D polymorphism in the hemochromatosis gene with sporadic ALS.* Neurology, 2005. **65**(6): p. 934-7.

318. Wang, X.S., et al., *Increased incidence of the Hfe mutation in amyotrophic lateral sclerosis and related cellular consequences.* J Neurol Sci, 2004. **227**(1): p. 27-33.

319. Brett, F.M., et al., *Evolution of neuropathologic abnormalities associated with blood-brain barrier breakdown in transgenic mice expressing interleukin-6 in astrocytes.* J Neuropathol Exp Neurol, 1995. **54**(6): p. 766-75.

320. Chiang, C.S., et al., *Reactive gliosis as a consequence of interleukin-6 expression in the brain: studies in transgenic mice.* Dev Neurosci, 1994. **16**(3-4): p. 212-21.

321. Castelnau, P.A., et al., *Abnormal iron deposition associated with lipid peroxidation in transgenic mice expressing interleukin-6 in the brain.* J Neuropathol Exp Neurol, 1998. **57**(3): p. 268-82.

322. Mukhopadhyay, C.K., Z.K. Attieh, and P.L. Fox, *Role of ceruloplasmin in cellular iron uptake.* Science, 1998. **279**(5351): p. 714-7.

323. Richardson, D.R., *Role of ceruloplasmin and ascorbate in cellular iron release.* J Lab Clin Med, 1999. **134**(5): p. 454-65.

324. Young, S.P., M. Fahmy, and S. Golding, *Ceruloplasmin, transferrin and apotransferrin facilitate iron release from human liver cells.* FEBS Lett, 1997. **411**(1): p. 93-6.

325. Csere, P., R. Lill, and G. Kispal, *Identification of a human mitochondrial ABC transporter, the functional orthologue of yeast Atm1p.* FEBS Lett, 1998. **441**(2): p. 266-70.

326. Lill, R. and G. Kispal, *Mitochondrial ABC transporters.* Res Microbiol, 2001. **152**(3-4): p. 331-40.

327. David, S. and B.N. Patel, *Ceruloplasmin: Structure and function of an essential ferroxidase*, in *Advances in structural biology*, S.K. Malhotra, Editor. 1999, JAI press Inc.: Stamford, CT. p. 213-39.

328. Xu, X., et al., *Aceruloplasminemia: an inherited neurodegenerative disease with impairment of iron homeostasis.* Ann N Y Acad Sci, 2004. **1012**: p. 299-305.

329. Mackenzie, B. and M.D. Garrick, *Iron Imports. II. Iron uptake at the apical membrane in the intestine.* Am J Physiol Gastrointest Liver Physiol, 2005. **289**(6): p. G981-6.

330. Mims, M.P. and J.T. Prchal, *Divalent metal transporter 1.* Hematology, 2005. **10**(4): p. 339-45.

331. Anderson, G.J. and D.M. Frazer, *Recent advances in intestinal iron transport.* Curr Gastroenterol Rep, 2005. **7**(5): p. 365-72.

332. Latunde-Dada, G.O., et al., *Molecular and functional roles of duodenal cytochrome B (Dcytb) in iron metabolism.* Blood Cells Mol Dis, 2002. **29**(3): p. 356-60.

333. Ferreira, G.C. and J.S. Zhang, *Mechanism of 5-aminolevulinate synthase and the role of the protein environment in controlling the cofactor chemistry.* Cell Mol Biol (Noisy-le-grand), 2002. **48**(8): p. 827-33.

334. Schranzhofer, M., et al., *Remodeling the regulation of iron metabolism during erythroid differentiation to ensure efficient heme biosynthesis.* Blood, 2006. **107**(10): p. 4159-67.

335. Ajioka, R.S., J.D. Phillips, and J.P. Kushner, *Biosynthesis of heme in mammals.* Biochim Biophys Acta, 2006. **1763**(7): p. 723-36.

336. De Domenico, I., et al., *Iron overload due to mutations in ferroportin.* Haematologica, 2006. **91**(1): p. 92-5.

337. Ganz, T., *Molecular control of iron transport.* J Am Soc Nephrol, 2007. **18**(2): p. 394-400.

338. Pandolfo, M., *Iron and Friedreich ataxia.* J Neural Transm Suppl, 2006(70): p. 143-6.

339. Wilson, R.B., *Iron dysregulation in Friedreich ataxia.* Semin Pediatr Neurol, 2006. **13**(3): p. 166-75.

340. Latunde-Dada, G.O., et al., *Haem carrier protein 1 (HCP1): Expression and functional studies in cultured cells.* FEBS Lett, 2006. **580**(30): p. 6865-70.

341. Kikuchi, G., T. Yoshida, and M. Noguchi, *Heme oxygenase and heme degradation.* Biochem Biophys Res Commun, 2005. **338**(1): p. 558-67.

342. Koizumi, S., *Human heme oxygenase-1 deficiency: a lesson on serendipity in the discovery of the novel disease.* Pediatr Int, 2007. **49**(2): p. 125-32.

343. Celec, P., *Hemojuvelin: a supposed role in iron metabolism one year after its discovery.* J Mol Med, 2005. **83**(7): p. 521-5.

344. Krijt, J., et al., *Expression of Rgmc, the murine ortholog of hemojuvelin gene, is modulated by development and inflammation, but not by iron status or erythropoietin.* Blood, 2004. **104**(13): p. 4308-10.

345. Hugman, A., *Hepcidin: an important new regulator of iron homeostasis.* Clin Lab Haematol, 2006. **28**(2): p. 75-83.

346. Anderson, G.J., et al., *The ceruloplasmin homolog hephaestin and the control of intestinal iron absorption.* Blood Cells Mol Dis, 2002. **29**(3): p. 367-75.

347. Lee, D.W. and J.K. Andersen, *Role of HIF-1 in iron regulation: potential therapeutic strategy for neurodegenerative disorders.* Curr Mol Med, 2006. **6**(8): p. 883-93.

348. Wallander, M.L., E.A. Leibold, and R.S. Eisenstein, *Molecular control of vertebrate iron homeostasis by iron regulatory proteins.* Biochim Biophys Acta, 2006. **1763**(7): p. 668-89.

349. Ward, P.P., E. Paz, and O.M. Conneely, *Multifunctional roles of lactoferrin: a critical overview.* Cell Mol Life Sci, 2005. **62**(22): p. 2540-8.

350. Shaw, G.C., et al., *Mitoferrin is essential for erythroid iron assimilation.* Nature, 2006. **440**(7080): p. 96-100.

351. Courville, P., R. Chaloupka, and M.F. Cellier, *Recent progress in structure-function analyses of Nramp proton-dependent metal-ion transporters.* Biochem Cell Biol, 2006. **84**(6): p. 960-78.

352. Fortier, A., et al., *Single gene effects in mouse models of host: pathogen interactions.* J Leukoc Biol, 2005. **77**(6): p. 868-77.

353. Quigley, J.G., et al., *Investigation of a putative role for FLVCR, a cytoplasmic heme exporter, in Diamond-Blackfan anemia.* Blood Cells Mol Dis, 2005. **35**(2): p. 189-92.

354. Gomme, P.T., K.B. McCann, and J. Bertolini, *Transferrin: structure, function and potential therapeutic actions.* Drug Discov Today, 2005. **10**(4): p. 267-73.

355. Aisen, P., *Transferrin receptor 1.* Int J Biochem Cell Biol, 2004. **36**(11): p. 2137-43.

356. Ponka, P., *Cellular iron metabolism.* Kidney Int Suppl, 1999. **69**: p. S2-11.

357. Ponka, P. and C.N. Lok, *The transferrin receptor: role in health and disease.* Int J Biochem Cell Biol, 1999. **31**(10): p. 1111-37.

358. Kuo, Y., et al. *Zyklopen, a new member of the multi-copper ferroxidase family, is expressed in multiple tissues.* in *The second congress of the International BioIron Society*. 2007. Kyoto, Japan.

1.10 Figures and tables

Figure 1

Alternative splicing in DMT1. Alternative splicing in 5' and 3' ends generate 4 transcripts of DMT1. 5' splicing generates 1A and 1B forms; the 1A form having a longer N terminus. 3' splicing generates +IRE and -IRE isoforms of DMT1.

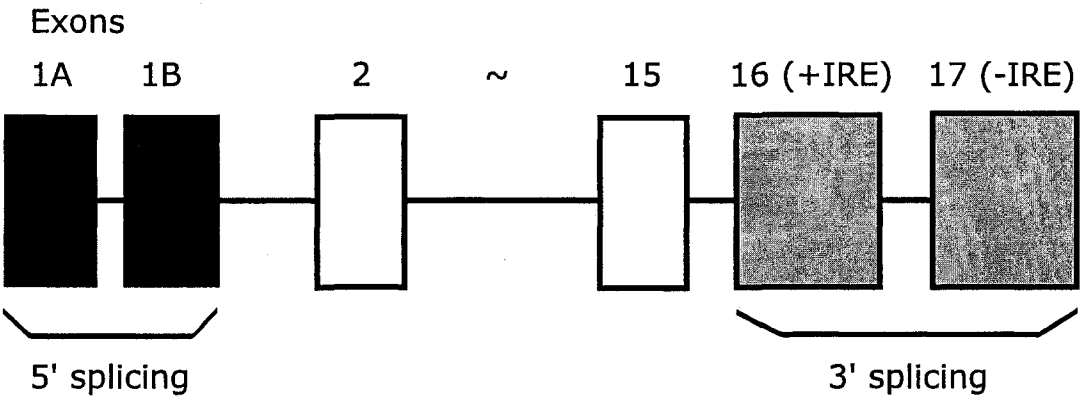
Exons
1A
1B
2
~
15
16 (+IRE)
17 (-IRE)
5' splicing
3' splicing

Figure 2

Copper centers in human ceruloplasmin. Cu 2, 4, and 6 represent mononuclear copper atoms in domains 2, 4, and 6. Cu 10, 20, and 30 indicate coppers in the trinuclear center located between domains 1 and 6. Ferrous iron binds to a site near Cu 4 and the arrows represent transfer of electrons from the mononuclear copper Cu 4 to the trinuclear copper center where it reduces bound oxygen molecules to water.

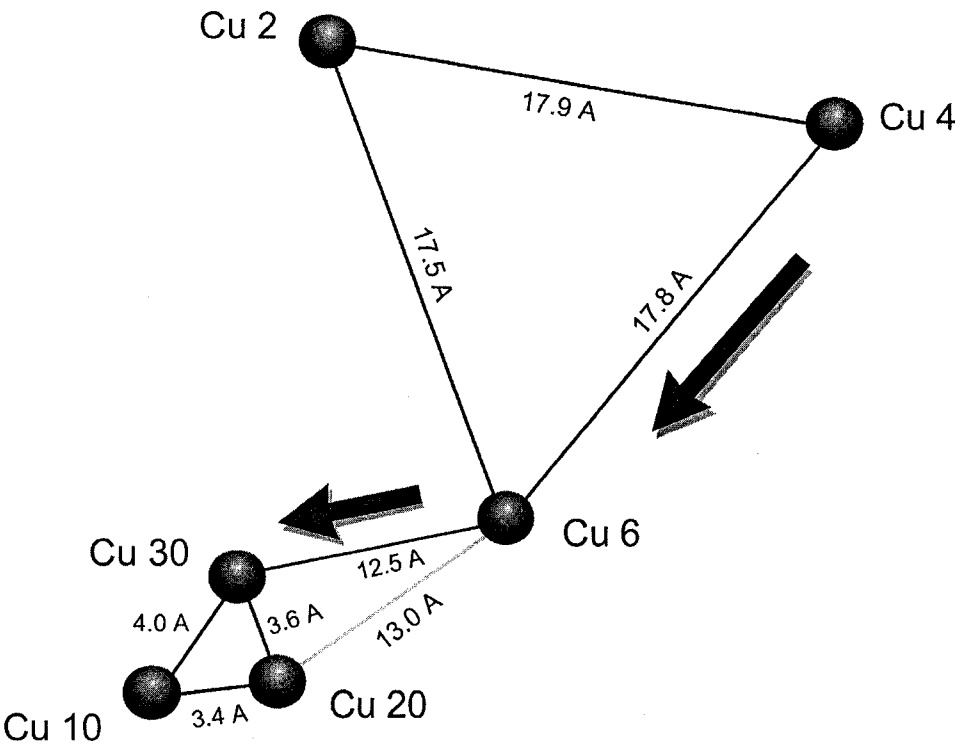
Cu 2
17.9 A
Cu 4
17.5 A
17.8 A
Cu 6
Cu 30
12.5 A
4.0 A
3.6 A
13.0 A
Cu 10
3.4 A
Cu 20

Figure 3

The transferrin cycle. Holotransferrin (HOLO-TF) binds to the transferrin receptor (TfR) and the complex is internalized by clathrin-coated pit mediated endocytosis. Specialized endosomes are made, and proton pump acidification releases iron from the TF-TfR complex. Steap3 converts released Fe^{3+} to Fe^{2+} and DMT1 transports iron into the cytoplasm. The APO-TF/TfR complexes are then recycled to the cell membrane. On encountering neutral pH on the cell surface, APO-TF is released from the TfR and recycled.

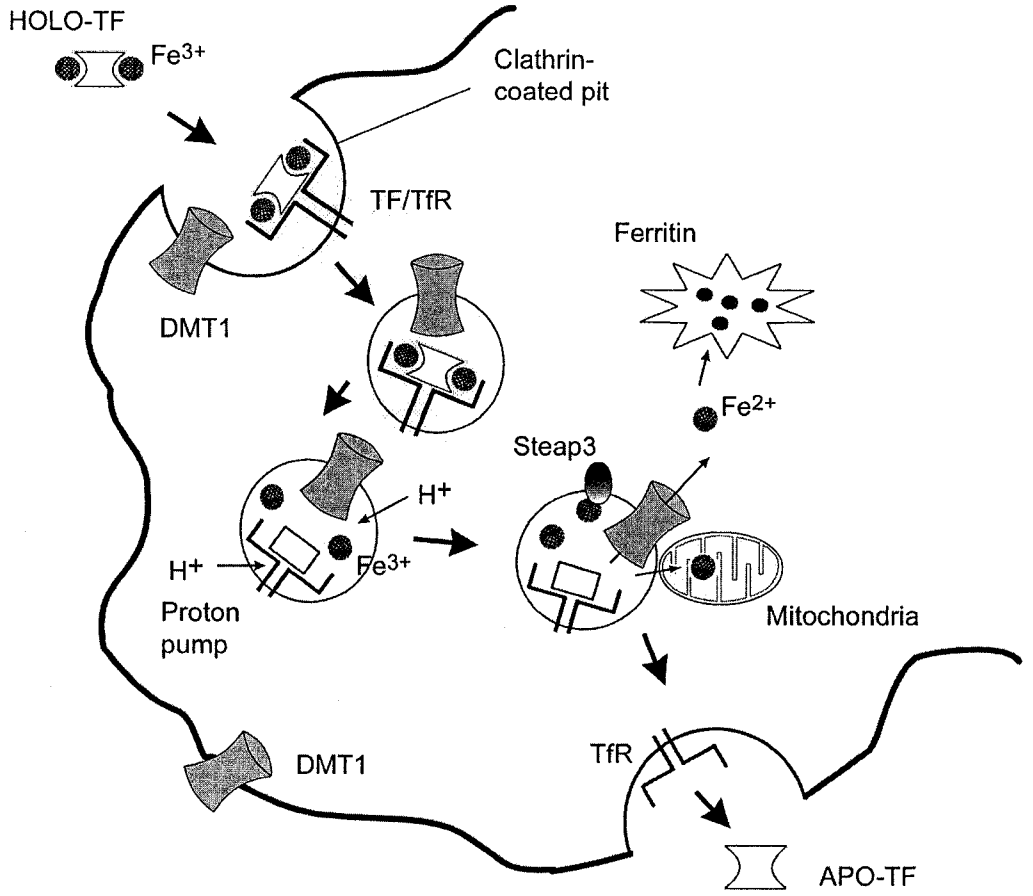
HOLO-TF
Fe3+
Clathrin-
coated pit
TF/TfR
DMT1
Ferritin
Fe2+
Steap3
H+
H+
Fe3+
Proton
pump
Mitochondria
DMT1
TfR
APO-TF

Figure 4

Non-transferrin mediated iron uptake and release in duodenal enterocytes. Non-heme iron from the diet is reduced by the ferric reductase (DCYTB) at the brush border and transported through DMT1. Some iron is stored in ferritin, and the remainder is transported out through a transporter FPN on the basolateral membrane. Ferrous iron (Fe^{2+}) that is transported through FPN is converted into ferric iron (Fe^{3+}) by ferroxidases (HP and/or CP) and loaded onto transferrin.

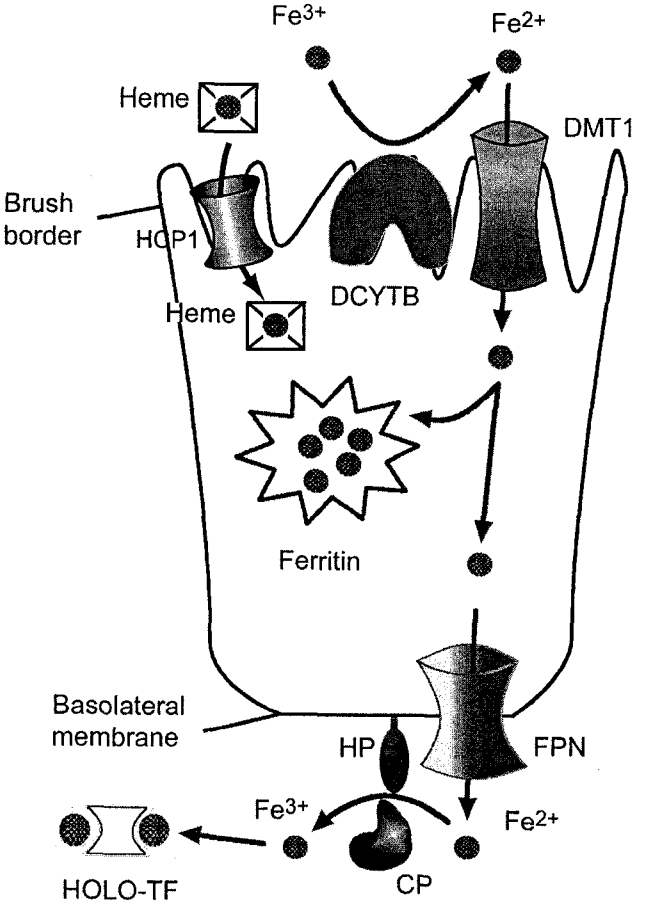
Fe3+
Fe2+
Heme
DMT1
Brush
border
HCP1
DCYTB
Heme
Ferritin
Basolateral
membrane
HP
FPN
Fe3+
Fe2+
HOLO-TF
CP

Figure 5

Regulation of iron protein expression by IRP. IRP binding affinity to IRE increases under conditions of iron starvation and decreases under conditions of excess iron. **(A)** In the case of ferritin mRNA, IRP binding to 5' IRE inhibits translation and ferritin synthesis is decreased. **(B)** In the case of TfR1, IRP binding to the 3' IREs stabilizes TfR1 mRNA and increases the mRNA that is translated. On the other hand, transferrin mRNA is degraded when there is excess iron.

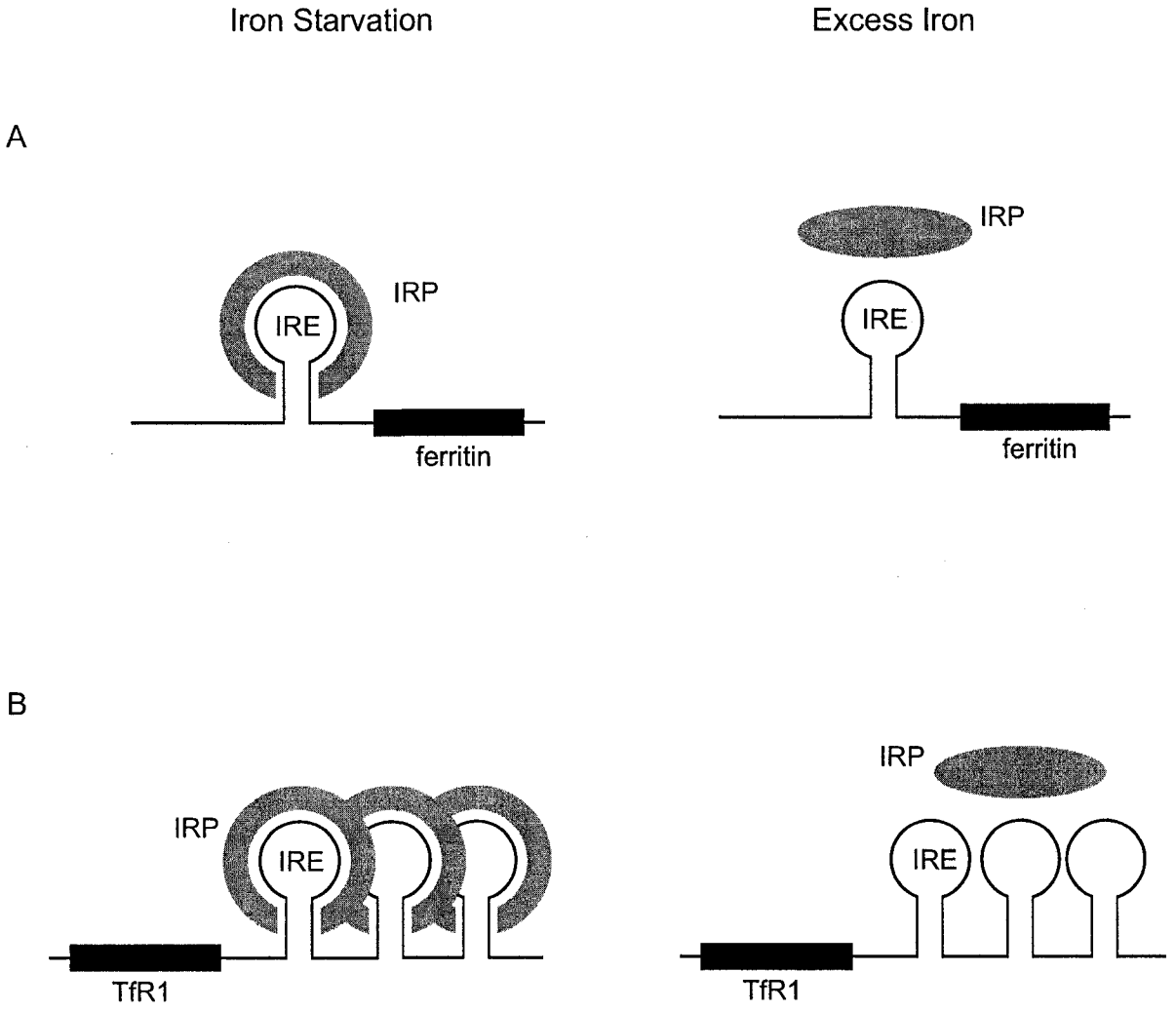
Iron Starvation
Excess Iron
A
IRP
IRE
ferritin
IRP
IRE
ferritin
B
IRP
IRE
TfR1
IRP
IRE
TfR1

Table 1 Proteins involved in iron homeostasis in mammals.

Protein	Function	References
ABCG2 (BCRP/MXR/ABCP)	Heme or porphyrin exporter	[166, 167]
ATP-binding cassette transporter 7 (ABC7)	Mitochondrial Fe exporter	[325, 326]
Ceruloplasmin (CP)	Ferroxidase, helping Fe efflux	[327, 328]
Dexras1	DMT1 regulation in neuron by NMDA	[51]
Divalent metal-ion transpoter 1 (DMT1)	Iron uptake iron into cells, release of TF-bound endosomal Fe	[329, 330]
Duodenal cytochrome B (DCYTB)	Ferrireductase, helps DMT1 to import Fe	[331, 332]
Erythroid 5-aminolevulinate synthase (eALAS)	Erythroid specific heme synthesis protein	[333, 334]
Ferritin (FTL & FTH)	Cellular iron storage	[80]
Ferrochelatase	Inserting Fe for heme synthesis	[335]
Ferroportin (FPN)	Iron efflux	[336, 337]
Frataxin	Handling mitochondrial Fe involved in Fe-S cluster formation	[338, 339]
Heme carrier protein 1 (HCP1)	Duodenal heme importer	[161, 340]
Heme oxygenase (HO)	Release Fe from heme	[341, 342]
Hemojuvelin (HJV)	Unknown, HEPC regulation?	[343, 344]
Hepcidin (HEPC, LEAP1)	Negative Fe regulator	[337, 345]
Hephaestin (HEPH)	Ferroxidase, helping duodenal Fe efflux	[346]
HFE (HFE)	TfR1-mediated Fe uptake regulation	[30]
Hypoxia-inducible factor 1 (HIF1)	Binds to HIF-responsive element	[347]

Iron-regulatory protein (IRP)	Regulate expression of IRE containing proteins	[180, 348]
Lactoferrin (LF)	Binds to circulating iron	[349]
Mitochondrial ferritin (MtF)	Iron storage in mitochondria	[93]
Mitoferrin	Mitochondrial iron uptake in erythroid cells	[350]
Natural resistance-associated macrophage protein 1 (Nramp1)	Fe release from macrophage	[351, 352]
Receptor for feline leukemia virus, subgroup C (FLVCR)	Heme exporter	[163, 353]
Six-transmembrane epithelial antigen of the prostate 3 (Steap3)	Ferrireductase, helps endosomal Fe release	[56]
T cell immunoglobulin-domain and mucin-domain 2 (TIM-2)	H ferritin receptor	[75]
Transferrin (TF)	Iron transport in plasma	[32, 354]
Transferrin receptor (TfR)	Iron uptake into cells	[355-357]
Zyklopen (ZP)	Ferroxidase	[358]

CHAPTER 2

The Regulation of Iron Efflux from Astrocytes by GPI-anchored Ceruloplasmin and the Iron Export Transporter Ferroportin

** Much of the work presented in this chapter was published in J. Biol. Chem. (*S.Y. Jeong and David, S. (2003) Glycosylphoshatidylinositol-anchored ceruloplasmin is required for iron efflux from cells in the central nervous system. J. Biol. Chem. 278:27144-27148*). The last part of this work dealing with the lipid rafts are new experiments that have not been submitted yet for publication.

2.1 Preface

Ceruloplasmin is an essential ferroxidase involved in iron metabolism. Lack of this protein cause abnormal iron accumulation in the CNS and liver in human patients and animal models. We have reported the membrane bound form of CP, but the role of this protein in astrocytes iron metabolism is not clear. In this chapter, I examined the role of GPI-CP in maintaining iron homeostasis in astrocytes purified from CP null mice and wildtype control mice. I also studied the localization of an iron exporting protein ferroportin (FPN) under different iron condition in vitro. Data shown in Figures 1,2, and 4 are done for my Master's work and presented in this chapter only for the sake of completeness.

2.2 Summary

Ceruloplasmin (CP) is a ferroxidase that converts highly toxic ferrous iron to its non-toxic ferric form. A glycosylphosphatidylinositol (GPI)-anchored form of this enzyme is expressed by astrocytes in the mammalian central nervous system (CNS), while the secreted form is expressed by the liver and found in serum. Lack of this enzyme results in iron accumulation in the brain and neurodegeneration in human patients and the mouse model. In this chapter, we show using astrocytes purified from the cerebral cortex of *CP* null mice and wildtype mice that GPI-CP is essential for iron efflux and not involved in regulating iron influx. This work also shows that GPI-CP co-localizes on the astrocyte cell surface with the iron exporter ferroportin (FPN) and is also physically associated with it. In addition, FPN alone is unable to efflux iron from astrocytes in the absence of GPI-CP or secreted CP. We provide evidence that the divalent metal influx transporter DMT1 is expressed by astrocytes and is likely to mediate iron influx into these glial cells. We also show using sucrose-density gradient separation of membrane preparations that like other GPI-anchored proteins GPI-CP is located in the lipid raft regions of the astrocyte cell membrane. On the other hand, under control media conditions, FPN is spread out in both lipid raft and non-lipid raft regions. However, when cells are cultured in high iron containing medium, FPN is rapidly mobilized into the lipid rafts from adjacent non-lipid raft regions. Such relocation of FPN would allow for increased GPI-CP/FPN interactions and allow for more iron efflux. These data suggest that the coordinated action of GPI-CP and FPN is required for iron efflux from neural cells and disruption of this balance could lead to iron accumulation in the CNS and neurodegeneration.

2.3 Introduction

Mechanisms to maintain iron homeostasis at the cellular level are crucial for the viability of cells. Excess or inappropriately shielded cellular iron can lead to cell death. The effects of this toxicity are especially noticeable in the brain, spinal cord and other parts of the central nervous system (CNS), as the mature CNS lacks regenerative capabilities. Although iron is essential for a variety of biological functions such as oxygen transport, mitochondrial respiration and DNA synthesis, it can generate highly toxic free radicals because it is a redox-active metal.

In its divalent state (Fe^{2+}), iron is highly toxic as it reacts with hydrogen peroxide and molecular oxygen to produce free radicals. Free radical formation can promote lipid peroxidation, DNA strand breaks, degradation of biomolecules, and eventually cause cell death [1]. Therefore, organisms have developed mechanisms to prevent increase of the iron-pool while maintaining sufficient levels for metabolic use. However, these homeostatic mechanisms can get dysregulated and cause iron deficiency or iron overload. The safe conversion of Fe^{2+} to Fe^{3+} is catalyzed predominantly by a copper-binding glycoprotein, ceruloplasmin [CP, EC 1.16.3.1, [2]]. Humans with mutations of the *CP* gene (aceruloplasminemia) show iron accumulation in various organs including the liver and brain, which is noticeable by the age of 45-55 years [3, 4]. *CP* null mutant mice also show accumulation of iron in the liver [5, 6] and CNS [6]. Moreover, increased levels of iron and lipid peroxidation have been observed in the cerebrospinal fluid (CSF) of these patients [7]. The accumulation of iron in the CNS correlates with neurodegeneration in humans and mice [3, 6]. We have shown previously that the rat brain expresses mainly the GPI-anchored form of ceruloplasmin (GPI-CP), which is predominantly expressed by astrocytes [8]. Human GPI-CP was also cloned recently [9].

DMT1 (also Nramp2/DCT1/SLC11A2) is a divalent metal transporter found in duodenal enterocytes [10]. Mutations in DMT1 seen in *mk* mice with microcytic anemia and the Belgrade (*b*) rat cause defects in iron transport from the lumen of the gut into enterocytes, and from plasma transferrin into erythroid precursors [11, 12]. DMT1 transports non-heme, ferrous iron (Fe^{2+}) instead of ferric (Fe^{3+}) iron, which is relatively more soluble and bioavailable. Therefore, the existence of a membrane reductase to convert ferric iron to ferrous iron was proposed. A mammalian ferric reductase, duodenal cytochrome b (DCYTB/Cybrd1) was cloned recently from mouse duodenum [13]. In the gut, DCYTB is mainly localized in the brush border membrane and proposed to function as a ferric reductase. An iron exporter called ferroportin (FPN/MTP1/IREG1/SLC11A3) is found on the basolateral side of mouse duodenal enterocytes, and several other cell types [14-16]. Although much is known about iron absorption and efflux in enterocytes in the gut, the mechanisms controlling iron homeostasis in neural cells in the CNS is still not well understood.

Here, we report on experiments done to assess how GPI-CP, which is expressed predominantly by astrocytes in the CNS, regulates iron levels in astrocytes and to determine its interactions with two divalent metal ion transporters DMT1 and FPN. We also show how the interaction between GPI-CP and FPN in lipid raft microdomains in membranes is regulated by cellular iron status to maintain iron homeostasis.

2.4 Experimental procedures

Iron influx/efflux studies: Astrocytes were purified from neonatal wildtype ($Cp^{+/+}$) and CP null mice ($Cp^{-/-}$) littermates [6] and cultured as described previously [20]. The *CP* null

mice were generated in this laboratory as previously reported [6]. Cultured astrocytes were plated on poly-L-lysine (PLL, Sigma)-coated 24-well plates two days before the experiment at a density of $3x10^5$cells/well. Cells were washed with serum-free Dulbecco's Modified Eagle Medium (DMEM, Invitrogen) twice and incubated in DMEM containing vitamins and penicillin/streptomycin for 1 hour at 37°C to remove any transferrin-bound iron.

Influx study: After 1 hour, DMEM was replaced with Sato's modified chemically-defined serum free medium [21] without transferrin. Radiolabeled iron ($^{59}FeCl_3$, 1 μCi / well, Perkin Elmer Lifescience) mixed with non-labeled $FeCl_3$ (total of 40μM), and L-ascorbate (Sigma) was added to keep iron in its ferrous form (molar ratio of $FeCl_3$ to L-ascorbate = 1:44). After different culture periods, cells were treated with Pronase (Calbiochem) for 1 hour at 4°C to remove membrane-bound iron and then lysed in 1N NaOH. Additional experiments with EDTA (500 μM) and Pronase treatment proved to be similar to Pronase alone. The amount of radioactivity bound non-specifically to the cells or the culture substrate was estimated by adding the radiolabeled-iron containing media to culture wells and removing it within 1-2 minutes, washing the wells and measuring with a γ-counter (LKB Wallac). This radioactivity level, which was found to be extremely low, was considered as background value and subtracted from all values at each data point. This value is considered as zero at the 0 hour time point. Cells were cultured in 5% CO_2 at 37°C in the radiolabeled-iron containing media until the desired time points (i.e., 12, 24, 48 hours). Sister cultures were treated in the same manner without radioactive iron and viable cell numbers were estimated by trypan blue exclusion. The amount of radioactivity that was taken up by the cells was converted into picomoles of iron using a

standard graph and normalized to value per 10^6 cells. The standard graph was plotted using counts per minute versus serial dilution of 1 μl $^{59}FeCl_3$.

Efflux study: Cultured astrocytes in 24 well plates were washed and incubated in serum-free medium for 1 hour as was done for the influx study. Cells were then loaded with radiolabeled-iron containing medium for 24 hours (same condition as above). After 24 hours, cells were washed twice with DMEM and serum-free Sato's chemically defined medium without transferrin was added to the cultures. At each time points (0, 12, 24, 48 hours) cells were detached, pelleted, and lysed in 1N NaOH. In addition, 200μl aliquot of culture medium from each time point was collected to measure the amount of iron released into the medium. Radioactivity in both cell pellet and culture medium was measured.

All radioactivity measurements at each time point were done in quadruplicate and repeated in three separate experiments. Results are shown in mean ± s.e.m (n=3). Two-sample Student's t-test was used to determine statistical significance.

RT-PCR: Total RNA was purified from rat neonatal astrocyte cultures by RiboPure kit (Ambion) following the manufacture's protocol. RT-PCR was performed using the GeneAmp RNA PCR kit (PerkinElmer Life Sciences). Primers used were as follows: DMT1_for: 5'-ACC GGG CCA ATA AGC AGG AAG TTC-3', DMT1_rev: 5'-GGC AAA GCG CGA CCA TTT TAG GTT-3', FPN_for: 5'-TGG CCT TGT TCG GAC TGG TCT G-3', FPN_rev: 5'-TCA GGA TTT GGG GCC AAG ATG AC-3', DCYTB_for: 5'-CGC GGT GAC CGG CTT CGT C-3', and DCYTB_rev: 5'-CGA GGG GCG TTT CAG GAC AAA GA-3' (Invitrogen custom-made primer). PCR was performed under the

following conditions: step 1, 2:30 min at 95°C × 1 cycle; step 2, 0:45 min at 95°C; 0:45 min at 61.5°C (58°C for FPN and 60.2°C for DCYTB); 1:30 min at 72°C × 35 cycles; step 3, 7 min at 72 °C × 1 cycle. RT-PCR for glyceraldehyde-3-phosphate dehydrogenase (GAPDH) was performed for the equal use of RNA according to the conditions previously described [22].

Western blotting: Cultured neonatal rat astrocytes were washed and pelleted. Total proteins were extracted with 1% Nonidet-40 (Sigma), 1% sodium deoxycholate (BDH Chemicals), 2% SDS, 0.15M sodium phosphate (pH 7.2), 2mM EDTA, containing a cocktail of protease inhibitors (Roche Diagnostics). Proteins were separated by SDS-PAGE, transferred to PVDF membrane (Bio-Rad), and incubated with anti-FPN (1:4000, Alpha Diagnostics) or anti-DMT1 (1:4000, Alpha Diagnostics, NRAMP24-S which recognizes DMT1 with and without IRE), or anti-actin polyclonal antibodies for loading control (Santa Cruz Biotechnology). Blots were washed and incubated with peroxidase-conjugated IgG, (1:200,000, Jackson Immunoresearch). Antibodies were detected with an enhanced chemiluminescence (ECL) kit (NEN Life Science Products).

Immunocytochemistry: Purified neonatal rat astrocytes were plated on PLL-coated round glass coverslips and cultured in DMEM containing 10 % fetal bovine serum. Cells were washed in Hank's balanced salt solution and stained with anti-CP monoclonal antibody (1A1, which was generated in our laboratory; 1:100) for 30min at room temperature. Cells were washed and rhodamine-conjugated goat anti-mouse IgG was added for 30 min. Cells were fixed and permeabilized in acetic acid:ethanol (5:95, v/v) at –20°C for 20 min. Permeabilized cells were stained with either anti-FPN or anti-DMT1 polyclonal rabbit antibodies (1:200, Alpha diagnostics) for 30 min at room temperature

and visualized by fluoresceine-conjugated goat anti-rabbit IgG (all secondary antibodies from Jackson Immunoresearch). Confocal microscopy was used to generate 0.8 μm sectioned images of cells.

Co-immunoprecipitation assay: Purified rat astrocytes were sonicated and centrifuged at 500*g* for 10 min to pellet the nuclei. Supernatant was centrifuged at 137,000*g* for 1hr at 4°C to pellet membrane faction. The pellet was resuspended in extraction buffer (10 mM Tris/HCl pH. 7.4, 150 mM NaCl, 5 mM EDTA, 1.25 % Triton X-100, and protease inhibitors). Protein concentration in the extracts was measured (DC Protein Assay kit, Bio-Rad). CP was immunoprecipitated using 200μg of the mouse monoclonal anti-ceruloplasmin antibody (1A1) conjugated to an immunoprecipitation column (Pierce) and 300μg of the protein extract is incubated overnight. After washing steps, the bound protein was eluted according to the manufacturer's protocol. Immunoprecipitated samples were denatured and separated on 7.5 % SDS-PAGE gel and Western blotted to detect Cp, DMT1 and FPN. A column without conjugated primary antibody was used to obtain the negative control.

Iron treatment and lipid raft fractionation: Purified rat astrocytes were washed and changed into different iron containing media: (i) control medium contained 3% bovine serum in DMEM: (ii) iron–rich medium consisted of the control medium with an additional 40μM of non-transferrin bound iron mixed with L-ascorbate as described above; (iii) iron-deprived medium consisted of the control medium containing 400μM of a highly lipophilic iron chelator, salicylaldehyde isonicotinoyl hydrazone (SIH). Cells were incubated for 3 hours in these media and then washed with cold PBS 3 times. Lipid raft and non-lipid raft components of the membranes were purified by sucrose gradient

fractionation modified from a previously described protocol [23]. Briefly, cells were pelleted and re-dissolved in cold TNE (25mM Tris-HCl/0.15M NaCl/5mM EDTA) buffer with 1% Triton X-100, sonicated briefly, and incubated at 4°C for 30 minutes. The cell extracts were mixed with 2M sucrose solution and 1M and 0.2M sucrose solutions were then layered carefully and centrifuged for 17 hours at 4°C (200,000g). A total of 10 fractions were collected and pelleted by centrifugation for 10 minutes at 4°C (13,000g). Pellets were washed with 2mM EGTA twice and proteins were extracted using 1% SDS extraction buffer. Fractions were separated on a 4-10% gradient SDS-PAGE for analysis. Rabbit polyclonal anti-TfR1 (1:500, Zymed) and anti-caveolin (1:200, Santa-Cruz Biotechnology) antibodies were used to detect lipid raft fractions by non-overlapping lanes for these two antibodies. Rabbit polyclonal anti-FPN (1:1000, Alpha diagnostics) and anti-CP (1:000, Dako Cytomation) antibodies were used to detect FPN and CP in these fractions on Western blots which was done as described above. A horseradish peroxidase (HRP)-conjugated goat anti-rabbit secondary antibody and the ECL kit was used to detect signals.

Quantitative reverse transcriptase polymerase chain reaction (QRT-PCR): Total RNA was purified from astrocytes with different iron treatments using RNeasy Lipid Tissue kit (Qiagen, Mississauga, Ontario, Canada), and QRT-PCR was performed using the Brilliant Probe-based QRT-PCR Reagents and MX4000 (Stratagene, La Jolla, CA), both following the protocols of the manufacturer. Gene-specific primers and a Taqman probe designed against FPN were used as previously described [24]. Peptidylprolyl isomerase A (PPIA) was used as a loading control [25]. For data analysis, the sample cycle threshold values were normalized to that of PPIA and expressed as fold increase.

Results are shown as the mean relative ratio (fold increase) of mRNA ± SD of the mean from three separate experiments ($n = 3$) compared with control media treated cells. Two-sample Student's t test was used to determine statistical significance between groups.

Gel retardation assay: A gel retardation assay was performed to assess the cytosolic iron level after different iron treatments by assessing the interaction between iron regulatory proteins (IRPs) and iron response elements (IREs). 30μg of total protein extracts from different cells were mixed with ^{32}P-labeled ferritin IRE RNA probe (obtained from Dr. K. Pantopoulos, McGill University, Montreal, Canada), which was *in vitro* transcribed from a linearized plasmid template using T7 RNA polymerase. The samples were incubated for 10min at room temperature with heparin (5mg/ml) to prevent non-specific binding. Unbound probe was degraded by RNase T1 incubation. The formation of RNA-protein complexes was then detected by gel electrophoresis using 6% non-denaturing polyacrylamide gels. The gels were scanned with STORM860 (phosphoimager) for analysis.

2.5 Results

The aim of these experiments was to determine how does GPI-CP regulate iron levels in neural cells so that in its absence iron accumulates in cells in the CNS as seen in aceruloplasminemia and $Cp^{-/-}$ mice. GPI-CP may regulate normal iron levels in the CNS by either limiting how much iron enters the cell, or facilitating iron efflux. To distinguish between these two possibilities we assessed iron influx and efflux with ^{59}Fe *in vitro* using astrocytes purified from the $Cp^{-/-}$ and $Cp^{+/+}$ mice. Astrocytes were used because our earlier work indicated that GPI-CP is expressed mainly in astrocytes in the rat CNS [26].

For the influx studies, astrocytes were cultured in medium containing ^{59}Fe/ascorbate in Sato's modified serum-free medium. At various time intervals the cells were harvested and the amount of radiolabeled iron within the cells estimated. These studies showed that the amount of iron influx is similar in $Cp^{-/-}$ and $Cp^{+/+}$ mice (Figure 1). The rate of influx is 0.1pmol/10^6 cells/hour, which is about 1/50 of influx reported for macrophages via the transferrin receptor [27]. For efflux studies, astrocyte cultures were first loaded with ^{59}Fe in medium for 24 hours. The radiolabeled medium was then removed, cultures washed and replaced with fresh medium. The supernatant and cells were sampled at varying intervals for up to 48 hours. In cultures of wildtype astrocytes, almost 70% of the iron within the cell was effluxed within 48 hours (Figure 2A). In contrast, iron efflux was severely impaired in astrocyte cultures from $Cp^{-/-}$ mice. Less than 5% of the iron effluxed in the 48-hour period (Figure 2B). To assess if the secreted form of CP can compensate for the lack of GPI-CP, cultures of astrocytes from $Cp^{-/-}$ mice were first loaded with ^{59}Fe for 24 hours as noted above. After removing the radiolabeled medium, fresh medium containing soluble CP was added to the cultures. Ceruloplasmin at 1μg/ml, i.e., the concentration found in cerebrospinal fluid (CSF) increased iron efflux minimally by 9% (Figure 3), while ceruloplasmin at 300 μg/ml, i.e., the concentration in serum, enhanced efflux to 50% (Figure 3). Increasing the CP concentration to 400μg/ml increased efflux further to 65% showing dose-dependent effect. These results indicate that the low amount of CP in CSF is insufficient to mediate iron efflux and concentrations of soluble CP equal to or higher than serum levels are needed to efflux iron to the levels achieved by GPI-CP.

As CP is a ferroxidase, it must regulate iron efflux via iron transporters. We first carried out experiments to assess if the iron efflux transporter FPN, and the iron influx

transporter DMT1 are expressed by astrocytes. RT-PCR and Western blotting analysis showed that DMT1 and FPN mRNA and protein are expressed by astrocytes (Figure 4A, B, D). RT-PCR analysis also indicates that the ferrireductase DCYTB is expressed by these cells, which could make soluble ferrous iron available for influx via DMT1 over prolonged periods *in vitro* [13] (Figure 4C). Confocal microscopy of double-immunofluorescence labeling of cultured astrocytes showed that FPN but not DMT1 is co-localized with GPI-CP on the surface of astrocytes (Figure 5). These data suggest that there might be a specific interaction of GPI-CP with the iron exporter FPN. To confirm these immunoflurorescence results and to assess if there is a direct physical interaction between these two molecules, GPI-CP was immunoprecipitated with the monoclonal antibody against CP (1A1) and Western blotted to detect DMT1 and FPN. These results showed that FPN but not DMT1 is co-immunoprecipitated with GPI-CP indicating a direct interaction of this GPI-anchored ferroxidase with FPN (Figure 6A). Given the evidence of interaction between GPI-CP and FPN, it is possible that the lack of iron efflux in cultures of astrocytes from $Cp^{-/-}$ mice could be due to a down-regulation of the expression of FPN in $Cp^{-/-}$ mice. To determine if this is the case, total protein from the brains of $Cp^{-/-}$ and $Cp^{+/+}$ mice were Western blotted to detect FPN. The level of expression of FPN protein is similar in total brain extracts of $Cp^{-/-}$ and $Cp^{+/+}$ mice (Figure 6B). However, more recent studies we did on purified astrocytes in collaboration with Jerry Kaplan's laboratory indicate that FPN is lost from the cell membrane in the absence of CP [28]. These results suggest that the interaction of FPN with GPI-CP is required for it to be retained on the cell surface.

GPI-CP is expected to be localized to the lipid raft domains of the cell membrane where the majority of GPI-anchored proteins are present. On the other hand, FPN is a

multi-pass integral membrane protein which would not be expected to be localized selectively to the lipid rafts. The work presented above suggests that GPI-CP and FPN interact to form complexes, and that these complexes are required for iron efflux from cells. We therefore assessed if one way in which the cell might regulate the formation of GPI-CP/FPN complexes depending upon the need for iron efflux would be to control the movement of FPN from non-lipid raft regions of the membrane into the lipid rafts domains in which GPI-CP is localized. To test this, purified rat astrocytes were cultured in normal culture medium, high iron, or low iron containing medium as described in the Experimental Methods section. As expected, GPI-CP was also localized to the lipid raft domains (Figure 7A lanes 1-3). On the other hand, in control media condition FPN was present in both lipid raft and non-lipid raft fractions (Figure 7A lanes 1-5). Interestingly, in cells cultured in high iron containing medium, FPN was exclusively localized to the lipid raft fractions (Figure 7A, lanes 1-3). Densitometry analysis did not show any changes in total amount of the FPN under these conditions at this time point, i.e., cultured for 3 hours in these media conditions (Figure 7B), therefore suggesting rapid re-localization of the protein by increased amount of iron. In contrast, cells cultured in low iron medium, i.e., containing the iron chelator SIH, showed an overall reduction of FPN from all fractions (Figure 7A lanes 1-5, 7B). However, the localization and amount of CP expression on the cell membrane was not altered by iron level in the culture medium (Figure 7A, B).

We next assessed by double-immunofluorescence the changes in FPN localization in the lipid raft in cells cultured under the different iron concentrations. For this, the lipid raft regions of the cell membrane were identified by staining with fluorescin-labeled cholera toxin B subunit (CtxB, Figure 8B) and the cultures double labeled with anti-FPN

and a rhodamine conjugated secondary antibody. Both flurorescent microscopy and confocal microscopy revealed that in astrocytes cultured in the normal control medium the FPN staining was diffusely spread throughout the cell membrane with some localization of FPN staining to the margins of the lipid rafts stained wth CtxB (Figure 8A, B, J). In contrast, cultures incubated in high iron medium showed strong co-localization of FPN to the margins as well as within the patches stained with CtxB indicating active mobilization of FPN into the lipid raft domains (Figure 8E, F). Confocal laser microscopy showed a marked increase in the number of CtxB patches (lipid rafts) with FPN co-localization in high iron conditions as compared to control medium conditions (Fig 8J). No detectable signal for FPN was detected in the SIH-treated cells (Figure 8G, J), possibly due to internalization and degradation of the protein as previously reported to happen under high hepcidin conditions [29].

Since cellular iron homeostasis is mostly maintained by intracellular iron concentration through the IRE/IRP mechanism (see section 1.5.2), we tested whether our extracellular treatments changed the intracellular iron pool. A gel retardation assay showed that there is decreased binding of IRPs in the iron treated group and increased binding of IRPs in the SIH treated group (Figure 9B) therefore reflecting changes in the intracellular iron pool due to the treatments. Interestingly mRNA expression of FPN is also changed in the different iron treatment groups (Figure 9A). However, as FPN mRNA contains IRE sequences in the 5' untranslated region (UTR) FPN is expected to be regulated translationally at the protein level not the mRNA level. These data therefore suggest that other factors may be involved in regulation of FPN mRNA expression along with the IRE/IRP mechanism. IRP-independent regulation of ferritin, which also contains 5'-UTR IRE, was also reported recently [30]. Therefore, both the increase in mRNA level

and release of IRP from IRE will increase protein levels of FPN under iron overload conditions and help cells to export iron.

2.6 Discussion

Although there has been an increase in our understanding of iron transport and regulation of iron levels in hematopoietic tissue, macrophages and enterocytes in the gut, there is little direct evidence for the molecular mechanisms underlying iron transport across neural cell membranes in the CNS [reviewed in [31]]. Once iron gets past the endothelial cells in the CNS, their uptake into neural cells could occur via transferrin and/or non-transferrin-mediated mechanisms. TfR are expressed by oligodendrocytes and neurons in the CNS while their expression in astrocytes has been more difficult to detect, although some recent studies suggest its presence in astrocytes [32]. However, TF levels in the CSF which reflects the amount available to CNS tissue is extremely low [about 1/100 compared to serum, 0.2-0.6 μM in human [33]], suggesting that under normal conditions, transferrrin-mediated uptake may not be significant, particularly in astrocytes. This is further supported by the findings in hypotransferrinemic mice, which show a normal distribution of iron in the brain [34, 35]. These data suggest that non-transferrrin-mediated mechanisms are likely to be involved in iron influx into cells in the brain. We show here that astrocytes can indeed take up iron though non-transferrin mediated mechanisms. We also show that astrocytes express both the divalent metal transporter DMT1, which has specificity for divalent metals including ferrous iron, as well as the ferricreductase DCYTB, indicating a role for these molecules in mediating iron uptake in the CNS. Our data show that the rate of iron uptake into astrocytes is about 1/50 that of macrophages [27] and about 1/30 that of hepatocytes [36]. This slow rate of uptake into

astrocytes might explain the slow accumulation of iron and late onset of neurological symptoms in aceruloplasminemia.

Iron deficiency in the body does not appear primarily to affect the brain, suggesting that it is capable of possibly retaining iron or mobilizing iron from other sources to maintain normal physiological functions. In addition, high levels of serum iron as occurs in hemochromatosis does not lead to iron accumulation in the CNS (reviewed in [37]) indicating possibly a unique homeostatic mechanism either at the level of the endothelial cells in the CNS or in cells that surround CNS capillaries, namely astrocytes. In contrast, iron accumulates in the brain in aceruloplasminemia in humans and mice [3-6], in which serum iron and serum transferrrin saturation levels are very low [5, 6]. We show here that a lack of CP expression by astrocytes leads to disruption of iron efflux. The requirement of GPI-CP for iron efflux from astrocytes indicates that oxidation of ferrous iron transported across the cell membrane likely via the transmembrane transporter FPN is an essential step. Moreover, soluble CP was shown to be essential for iron transport across the oocyte membranes when FPN was expressed in these cells *in vitro* [16]. Earlier studies on the yeast showed that a transmembrane multi-copper oxidase Fet3 with homology to CP interacts with an iron permease Ftr1p to transport iron across the cell membrane [38, 39]. We now show that FPN is expressed by astrocytes from the brain and is physically associated with GPI-CP. Furthermore, we also provide evidence that the expression of FPN alone is insufficient to allow iron efflux in the absence of GPI-CP. Since FPN transports ferrous iron that is highly toxic, CP as the major ferroxidase in the CNS might play a crucial role in detoxifying it to the ferric state. The inability of FPN to efflux ferrous iron in the absence of CP may therefore serve as a protective mechanism to prevent efflux of toxic ferrous iron leading to the rapid generation of free radicals.

Although the slow accumulation of iron intracellularly may eventually surpass the ability of the intracellular sequestering capacity of the cell and lead to cell damage and death.

Since soluble CP in the CSF, which is produced by the choroid plexus, is extremely low (1μg/ml compared to 300μg/ml in the serum), it is likely to contribute minimally to the ferroxidase activity in the CNS. Besides meningeal cells that are outlining the CNS, astrocytes are known to be the only cell type in the CNS to express CP [26, 40], which is of the GPI-anchored form [8, 26]. The severe accumulation of iron in the brain in cases of aceruloplasminemia indicates that CP expressed on the surface of astrocytes plays an important role in the maintenance of normal iron levels in the CNS and its mobilization out of the CNS. One advantage of the GPI-anchored form of CP in the brain is that it reduces the need to have high levels of CP in the CSF. Our results indicate that at least 300-400μg/ml of CP in the CSF would be needed to efflux iron from astrocytes. This contrasts sharply with the total protein concentration of 350μg/ml in human CSF [41]. Some of the other features that GPI-anchors confer to proteins may also aid in the physiological function of CP, e.g., GPI-anchored proteins, most of which are localized in lipid-rich microdomains have a much greater degree of lateral mobility [42], and may also help serve as an apical targeting signal [43]. The latter feature may lead to the targeting of GPI-CP *in vivo* to the astrocytic endfeet that surround capillaries in the CNS, and thus position the iron efflux mechanism in close proximity to blood vessels via which iron can be mobilized out of the CNS.

In order to maintain iron homeostasis at the cellular level, the import and export of iron has to be tightly regulated depending on the level of iron within the cell. Under low iron conditions, hepcidin, a negative iron regulator, has been shown to bind to FPN

and cause its internalization and degradation [29]. This removal of FPN from the cell surface prevents unwanted loss of iron from iron starved cells as we have seen in our present experiments with astrocytes cultured in the presence of the iron chelator SIH. On the other hand, under high iron load one might expect increased expression of FPN and GPI-CP so that the cells can rapidly efflux the excess iron. Our data shows that after the 3 hour period, only FPN mRNA expression increases and is accompanied by decreased binding of IRP. This type of compensatory upregulation of FPN expression would not be immediate and would take a few hours. We propose that a novel mechanism to rapidly increase the GPI-CP/FPN complexes in response to iron overload is the lateral movement of FPN from non-lipid raft regions of the membrane to the lipid rafts domains where GPI-CP resides. We suggest that this might be the cell's first initial response to excess iron, followed later by increased *de novo* synthesis of FPN. The mechanism underlying the lateral translocation of FPN into the lipid rafts is not known at present. However, there are other examples in the literature of such movement of proteins, e.g., the glycoprotein agrin has been shown to mediate the translocation of the acetylcholine receptor into the lipid raft and cause clustering at the neuromuscular junction [44]. How intracellular iron levels cause translocation of FPN is currently under investigation in our laboratory.

This work provides the basis for understanding why iron accumulates in the CNS in aceruloplasminemia and may have implications for understanding the pathogenesis of other neurodegenerative diseases in which iron accumulation occurs, such as Parkinson's disease, amyotrophic lateral sclerosis and Alzheimer's disease.

2.7 References

1. Halliwell, B. and J.M. Gutteridge, *Oxygen toxicity, oxygen radicals, transition metals and disease.* Biochem J, 1984. **219**(1): p. 1-14.
2. Osaki, S., D.A. Johnson, and E. Frieden, *The possible significance of the ferrous oxidase activity of ceruloplasmin in normal human serum.* J Biol Chem, 1966. **241**(12): p. 2746-51.
3. Miyajima, H., et al., *Familial apoceruloplasmin deficiency associated with blepharospasm and retinal degeneration.* Neurology, 1987. **37**(5): p. 761-7.
4. Yoshida, K., et al., *A mutation in the ceruloplasmin gene is associated with systemic hemosiderosis in humans.* Nat Genet, 1995. **9**(3): p. 267-72.
5. Harris, Z.L., et al., *Targeted gene disruption reveals an essential role for ceruloplasmin in cellular iron efflux.* Proc Natl Acad Sci U S A, 1999. **96**(19): p. 10812-7.
6. Patel, B.N., et al., *Ceruloplasmin regulates iron levels in the CNS and prevents free radical injury.* J Neurosci, 2002. **22**(15): p. 6578-86.
7. Miyajima, H., et al., *CSF abnormalities in patients with aceruloplasminemia.* Neurology, 1998. **51**(4): p. 1188-90.
8. Patel, B.N., R.J. Dunn, and S. David, *Alternative RNA splicing generates a glycosylphosphatidylinositol- anchored form of ceruloplasmin in mammalian brain.* J Biol Chem, 2000. **275**(6): p. 4305-10.
9. Hellman, N.E., et al., *Biochemical analysis of a missense mutation in aceruloplasminemia.* J Biol Chem, 2002. **277**(2): p. 1375-80.
10. Gunshin, H., et al., *Cloning and characterization of a mammalian proton-coupled metal-ion transporter.* Nature, 1997. **388**(6641): p. 482-8.

11. Fleming, M.D., et al., *Microcytic anaemia mice have a mutation in Nramp2, a candidate iron transporter gene.* Nat Genet, 1997. **16**(4): p. 383-6.

12. Fleming, M.D., et al., *Nramp2 is mutated in the anemic Belgrade (b) rat: evidence of a role for Nramp2 in endosomal iron transport.* Proc Natl Acad Sci U S A, 1998. **95**(3): p. 1148-53.

13. McKie, A.T., et al., *An iron-regulated ferric reductase associated with the absorption of dietary iron.* Science, 2001. **291**(5509): p. 1755-9.

14. Abboud, S. and D.J. Haile, *A novel mammalian iron-regulated protein involved in intracellular iron metabolism.* J Biol Chem, 2000. **275**(26): p. 19906-12.

15. Donovan, A., et al., *Positional cloning of zebrafish ferroportin1 identifies a conserved vertebrate iron exporter.* Nature, 2000. **403**(6771): p. 776-81.

16. McKie, A.T., et al., *A novel duodenal iron-regulated transporter, IREG1, implicated in the basolateral transfer of iron to the circulation.* Mol Cell, 2000. **5**(2): p. 299-309.

17. Allen, J.A., R.A. Halverson-Tamboli, and M.M. Rasenick, *Lipid raft microdomains and neurotransmitter signalling.* Nat Rev Neurosci, 2007. **8**(2): p. 128-40.

18. Hering, H., C.C. Lin, and M. Sheng, *Lipid rafts in the maintenance of synapses, dendritic spines, and surface AMPA receptor stability.* J Neurosci, 2003. **23**(8): p. 3262-71.

19. Pediconi, M.F., et al., *Metabolic cholesterol depletion hinders cell-surface trafficking of the nicotinic acetylcholine receptor.* Neuroscience, 2004. **128**(2): p. 239-49.

20. Mittal, B., et al., *Expression of a membrane-bound form of the ferroxidase*

ceruloplasmin by leptomeningeal cells. Glia, 2003. **41**(4): p. 337-46.

21. Bottenstein, J.E. and G.H. Sato, *Growth of a rat neuroblastoma cell line in serum-free supplemented medium.* Proc Natl Acad Sci U S A, 1979. **76**(1): p. 514-7.

22. Ousman, S.S. and S. David, *MIP-1alpha, MCP-1, GM-CSF, and TNF-alpha control the immune cell response that mediates rapid phagocytosis of myelin from the adult mouse spinal cord.* J Neurosci, 2001. **21**(13): p. 4649-56.

23. Kramer, E.M., et al., *Compartmentation of Fyn kinase with glycosylphosphatidylinositol-anchored molecules in oligodendrocytes facilitates kinase activation during myelination.* J Biol Chem, 1999. **274**(41): p. 29042-9.

24. Jeong, S.Y. and S. David, *Age-related changes in iron homeostasis and cell death in the cerebellum of ceruloplasmin-deficient mice.* J Neurosci, 2006. **26**(38): p. 9810-9.

25. Feroze-Merzoug, F., et al., *Peptidylprolyl isomerase A (PPIA) as a preferred internal control over GAPDH and beta-actin in quantitative RNA analyses.* Biotechniques, 2002. **32**(4): p. 776-8, 780, 782.

26. Patel, B.N. and S. David, *A novel glycosylphosphatidylinositol-anchored form of ceruloplasmin is expressed by mammalian astrocytes.* J Biol Chem, 1997. **272**(32): p. 20185-90.

27. Kim, S. and P. Ponka, *Control of transferrin receptor expression via nitric oxide-mediated modulation of iron-regulatory protein 2.* J Biol Chem, 1999. **274**(46): p. 33035-42.

28. De Domenico, I., et al., *Ferroxidase activity is required for the stability of cell surface ferroportin in cells expressing GPI-ceruloplasmin.* Embo J, 2007. **26**(12): p. 2823-31.

29. Nemeth, E., et al., *Hepcidin regulates cellular iron efflux by binding to ferroportin and inducing its internalization.* Science, 2004. **306**(5704): p. 2090-3.

30. Mikhael, M., et al., *Iron regulatory protein-independent regulation of ferritin synthesis by nitrogen monoxide.* Febs J, 2006. **273**(16): p. 3828-36.

31. Burdo, J.R. and J.R. Connor, *Brain iron uptake and homeostatic mechanisms: an overview.* Biometals, 2003. **16**(1): p. 63-75.

32. Qian, Z.M., et al., *Transferrin receptors on the plasma membrane of cultured rat astrocytes.* Exp Brain Res, 1999. **129**(3): p. 473-6.

33. Bradbury, M.W., *Transport of iron in the blood-brain-cerebrospinal fluid system.* J Neurochem, 1997. **69**(2): p. 443-54.

34. Dickinson, T.K. and J.R. Connor, *Cellular distribution of iron, transferrin, and ferritin in the hypotransferrinemic (Hp) mouse brain.* J Comp Neurol, 1995. **355**(1): p. 67-80.

35. Dickinson, T.K. and J.R. Connor, *Immunohistochemical analysis of transferrin receptor: regional and cellular distribution in the hypotransferrinemic (hpx) mouse brain.* Brain Res, 1998. **801**(1-2): p. 171-81.

36. Richardson, D.R., *Role of ceruloplasmin and ascorbate in cellular iron release.* J Lab Clin Med, 1999. **134**(5): p. 454-65.

37. Anderson, G.J. and L.W. Powell, *HFE and non-HFE hemochromatosis.* Int J Hematol, 2002. **76**(3): p. 203-7.

38. Askwith, C., et al., *The FET3 gene of S. cerevisiae encodes a multicopper oxidase required for ferrous iron uptake.* Cell, 1994. **76**(2): p. 403-10.

39. Stearman, R., et al., *A permease-oxidase complex involved in high-affinity iron uptake in yeast.* Science, 1996. **271**(5255): p. 1552-7.

40. Klomp, L.W., et al., *Ceruloplasmin gene expression in the murine central nervous system.* J Clin Invest, 1996. **98**(1): p. 207-15.

41. Fishman, R.A., *Cerebrospinal Fluid in Diseases of the Nervous System.* 2nd ed. 1992, Philadelphia, PA: Saunders W B Co. 416.

42. Udenfriend, S. and K. Kodukula, *How glycosylphosphatidylinositol-anchored membrane proteins are made.* Annu Rev Biochem, 1995. **64**: p. 563-91.

43. Lisanti, M.P., et al., *A glycophospholipid membrane anchor acts as an apical targeting signal in polarized epithelial cells.* J Cell Biol, 1989. **109**(5): p. 2145-56.

44. Zhu, D., W.C. Xiong, and L. Mei, *Lipid rafts serve as a signaling platform for nicotinic acetylcholine receptor clustering.* J Neurosci, 2006. **26**(18): p. 4841-51.

2.8 Figures and tables

Figure 1

Role of ceruloplasmin in iron influx in astrocytes. Graph shows non-transferrin-mediated uptake of ^{59}Fe into astrocytes at 12, 24 and 48 hours after addition of radiolabeled iron containing serum-free medium to cultures. Iron uptake is similar in cultures from *CP* $^{+/+}$ (■) and *CP* $^{-/-}$ (□) mice. The results are shown as means ± s.e.m.

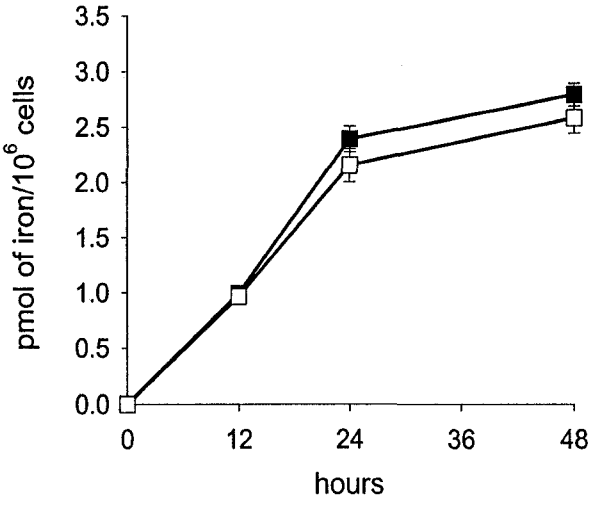
3.5
3.0
2.5
2.0
1.5
1.0
0.5
0.0
pmol of iron/10^6 cells
0
12
24
36
48
hours

Figure 2

Role of ceruloplasmin in iron efflux from astrocytes. **(A)** *Iron efflux from astrocytes from CP $^{+/+}$ mice.* Cells were loaded with ^{59}Fe for 24 hours, washed and cultured in non-radioactive, serum-free, transferrin-free medium. The amount of radiolabeled iron was measured in the cell pellet and culture medium at 0, 12, 24 and 48 hours. About 70% of the radiolabeled iron in the cells is effluxed by 48 hours (●). A corresponding increase in radiolabeled iron is detected in the culture medium (○), indicating iron efflux. Results are shown as means ± s.e.m (n=3). **(B)** *Iron efflux from astrocytes from CP $^{-/-}$ mice.* Cells were loaded with ^{59}Fe and cultured as in A. The percentage of radiolabeled iron in the cells remains unchanged through out the 48 h period (●). Radiolabeled iron is also not detected in the culture medium (○) during this period, indicating that iron does not efflux from astrocyte from *CP* $^{-/-}$ mice. Efflux at each time point was compared for statistical significance with the corresponding cell pellet or supernatant values from *CP*$^{+/+}$ mice shown in panel A using a two-sample Student's t-test. * ; $p<0.02$.

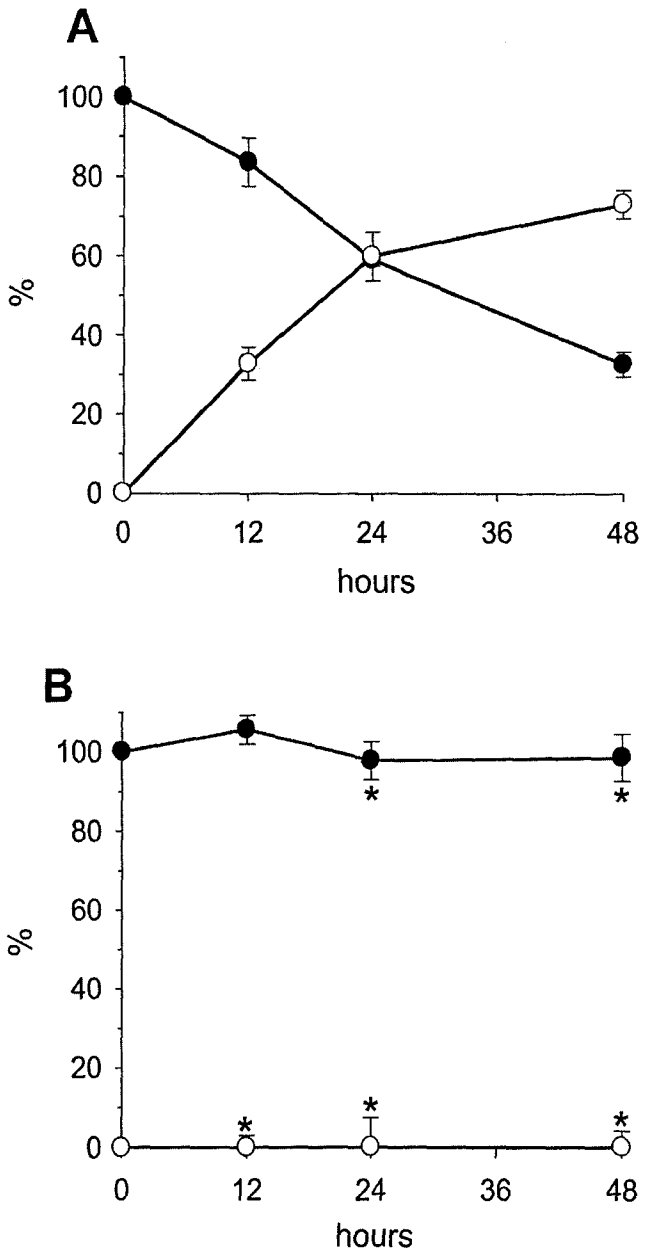
A
100
80
60
40
20
0
%
0
12
24
36
48
hours
B
100
80
60
40
20
0
%
*
*
*
*
*
0
12
24
36
48
hours

Figure 3

Effect of soluble CP on iron efflux from astrocytes from* $CP^{-/-}$ *mice. To assess if secreted ceruloplasmin can compensate for GPI-CP to efflux iron, astrocytes from $CP^{-/-}$ mice were loaded with iron as in Figure 2 and cultured serum-free, transferrin-free medium to which was added serum ceruloplasmin at a concentration of 1μg/ml (equivalent to CSF levels) and 300 μg/ml (equivalent to serum levels). Control $CP^{-/-}$ cells (●) were cultured in the same medium without CP. Very minimal iron efflux occurred with 1μg/ml of ceruloplasmin (■), whereas a 50% efflux was seen with 300μg/ml of ceruloplasmin (▲). Only excess amount of CP (400μg/ml) showed similar effect to GPI-CP (♦). Results represent means ± s.e.m. * ; $p<0.02$.

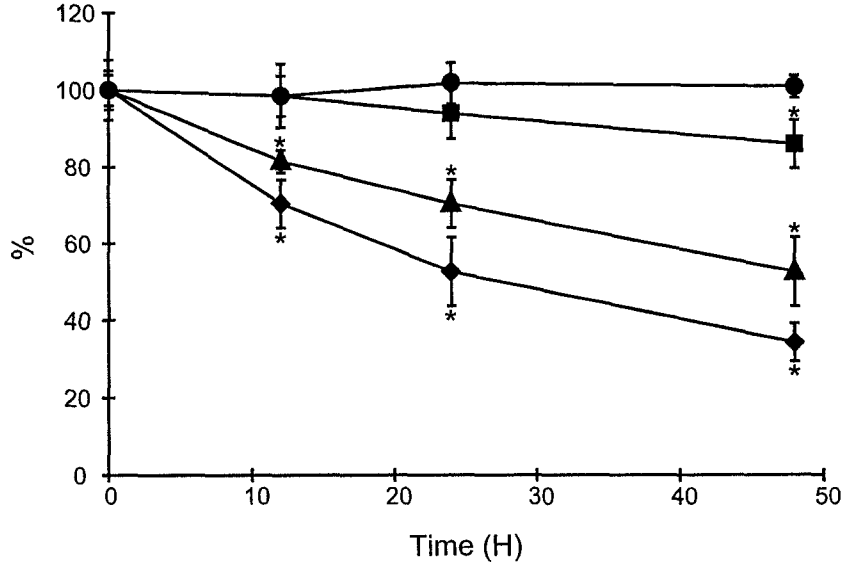
120
100
80
60
40
20
0
%
0
10
20
30
40
50
Time (H)

Figure 4

Iron transporters are expressed in astrocytes. mRNA expression of DMTI **(A)**, FPN **(B)** and the ferric reductase DCYTB **(C)**. GAPDH RT-PCRs were used as RNA controls. **(A)** Lane 1 shows DMT1 mRNA expression in rat astrocytes. Lane 2 shows wildtype CHO cells, and lane 3 shows CHO cells stably transfected with DMT1 cDNA (positive control). **(B)** Lane 1 shows FPN mRNA expression in rat astrocytes. Lane 2 shows rat duodenum (positive control) and lane 3 shows rat heart (negative control). **(C)** Lane 1 shows mRNA expression of the ferric reductase DCYTB in mouse astrocytes. Lane 2 shows mouse duodenum, and lane 3 shows heart (negative control). **(D)** Western blots of rat astrocyte proteins showing DMT1 protein (65 kDa) in lane 1, and FPN protein (66 kDa) in lane 2. Equal protein loading was confirmed with anti-actin Western blots.

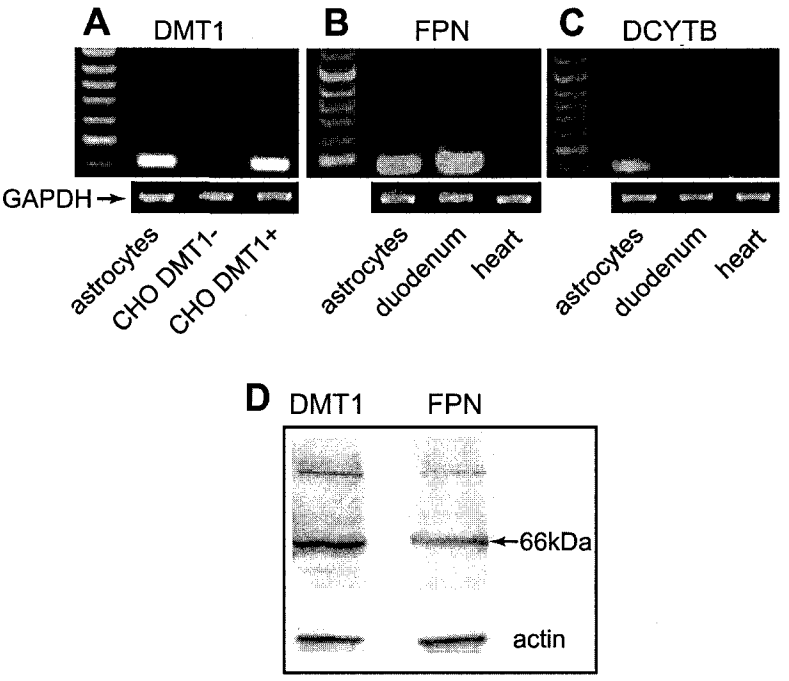
A
DMT1
B
FPN
C
DCYTB
GAPDH
astrocytes
CHO DMT1-
CHO DMT1+
astrocytes
duodenum
heart
astrocytes
duodenum
heart
D
DMT1
FPN
66kDa
actin

Figure 5

GPI-CP is associated with FPN. **(A)** Confocal microscopy of cultured astrocytes showing double-immunofluorescence labeling for cell surface GPI-CP and FPN. These two molecules are co-localized (arrows in panel labeled "Double"). **(B)** In contrast, cell surface ceruloplasmin and DMT1 are not co-localized.

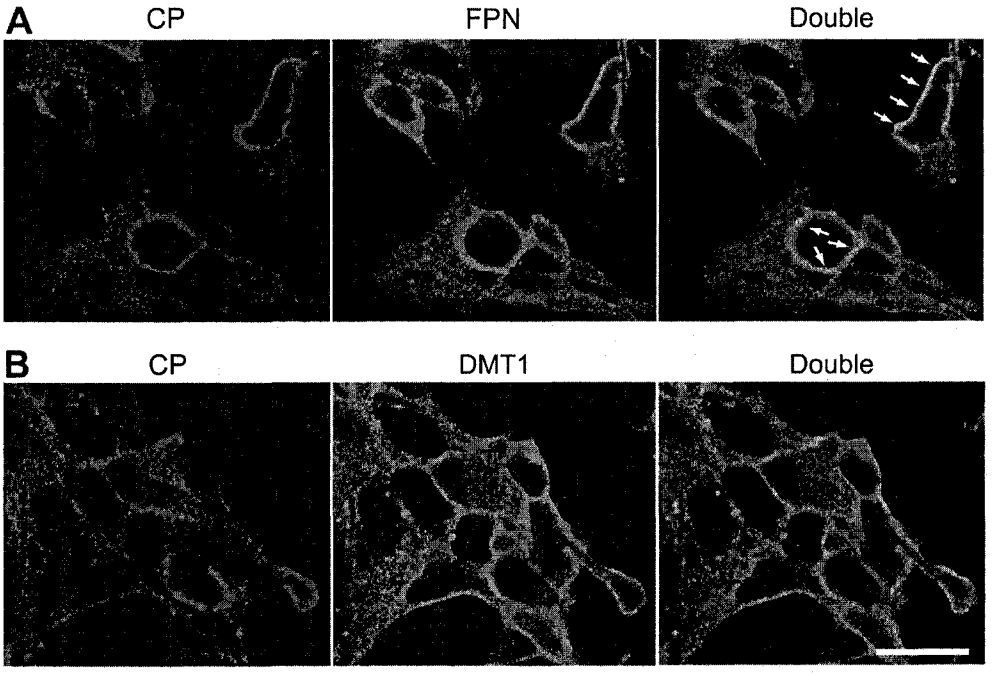
A
CP
FPN
Double
B
CP
DMT1
Double

Figure 6

GPI-CP is immunoprecipitated with FPN **(A)** Astrocyte proteins immunoprecipitated with the monoclonal CP antibody, 1A1, were separated on SDS-PAGE and Western blotted for CP (lanes 3), DMT1 (4) and FPN (5). FPN but not DMT1 was co-immunoprecipitated with CP antibodies. Columns without conjugated primary antibody and immunoblotted for CP (lane 1) and FPN (lane 2) were used as negative controls. Lane 3 was used as a positive. **(B)** FPN expression remains unchanged in $CP^{+/+}$ and $CP^{-/-}$ mouse brain. Protein extracts of brains from $CP^{+/+}$ (lane 1) and $CP^{-/-}$ (lane 2) mice were Western blotted for FPN and actin (loading control).

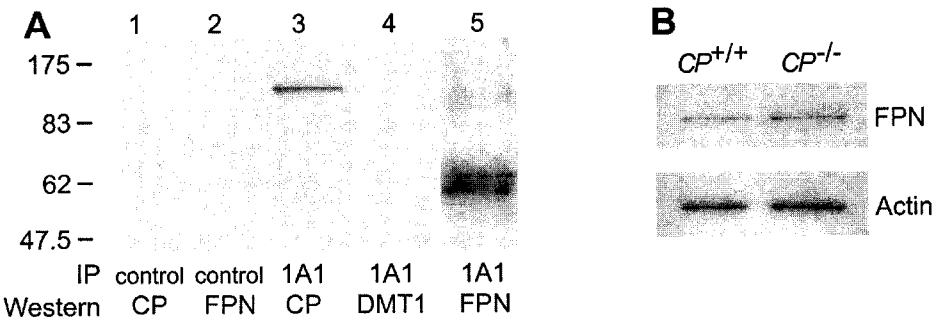
A
1
2
3
4
5
175 –
83 –
62 –
47.5 –
IP control control 1A1 1A1 1A1
Western CP FPN CP DMT1 FPN
B
CP+/+
CP-/-
FPN
Actin

Figure 7

Iron drives FPN into the lipid rafts. **(A)** Purified rat astrocytes were incubated with 3% serum containing media with either 40μM of non-transferrin-bound iron (Fe/ascorbate) or 400μM salicylaldehyde isonicotinoyl hydrazone (SIH, iron chelator) for 3 hours. Protein was extracted using non-continuous sucrose gradient fractionation and separated on SDS-PAGE and Western blot was performed. After treatment with Fe, FPN was exclusively localized to the lipid raft area (Fe, lanes 1-3) where CP normally resides (row 5). The control group showed wider distribution of FPN on raft and non-raft area (Ctl). SIH treatment caused FPN to diminish (SIH). Lipid raft was defined by non-overlapping lanes between TfR1 and caveolin bands (rows 6 and 7). **(B)** FPN1 bands in panel A were quantified using ImageQuant (n=3) for densitometry. Total amount of FPN did not change between the control and Fe-treated groups, but FPN1 was concentrated in lipid raft fraction in cultures treated with 40μM iron. *; $p<0.05$, Student's t-test. **(C)** Western blots for CP were quantified. The expression and localization of CP in the membrane was not affected by the iron levels in the culture medium.

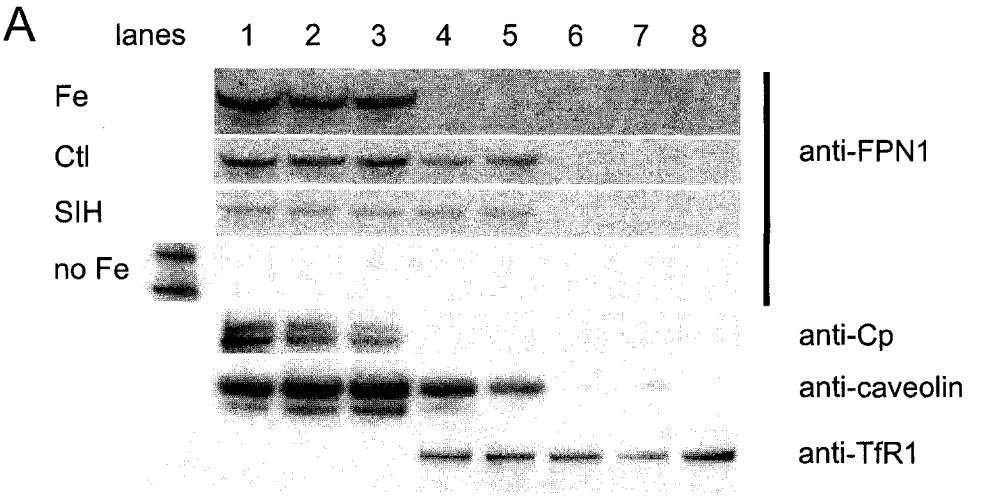
A
lanes 1 2 3 4 5 6 7 8
Fe
Ctl
SIH
no Fe
anti-FPN1
anti-Cp
anti-caveolin
anti-TfR1

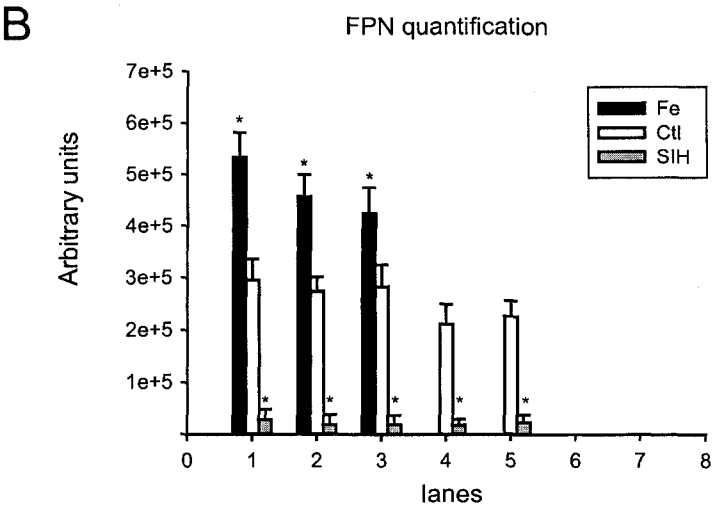
B
FPN quantification
Arbitrary units
7e+5
6e+5
5e+5
4e+5
3e+5
2e+5
1e+5
Fe
Ctl
SIH
0 1 2 3 4 5 6 7 8
lanes

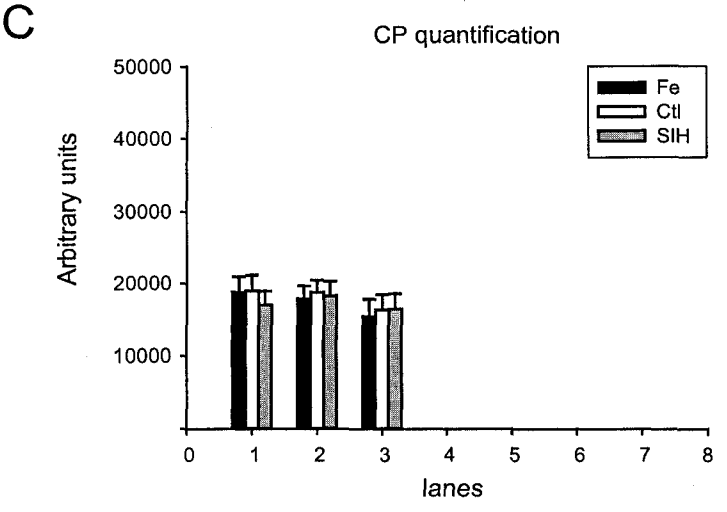
C
CP quantification
Arbitrary units
50000
40000
30000
20000
10000
Fe
Ctl
SIH
0 1 2 3 4 5 6 7 8
lanes

Figure 8

Localization of FPN in lipid rafts. **(A-I)** Rat astrocytes incubated with different media were stained with anti-FPN (red), FITC-conjugated cholera toxin B (CtB, green, lipid raft marker), and DAPI for nuclei. **(A-C)** The control cells showed homogeneous distribution of FPN and lipid rafts. **(D-F)** Fe-treated cells showed marked increase of clusters of FPN and CtB staining on the cell surface. **(G-I)** SIH treated cells showed diminished FPN staining. Lipid raft remained similar to the control group. Scale bar = 25μm. **(J)** Confocal microscope images of cells in the 3 different groups. Control cells showed some co-localization of FPN and CtB, which was markedly increased in the Fe-treated cells. Note that the size of the lipid raft cluster was also increased. SIH-treated cells showed very minimal FPN staining.

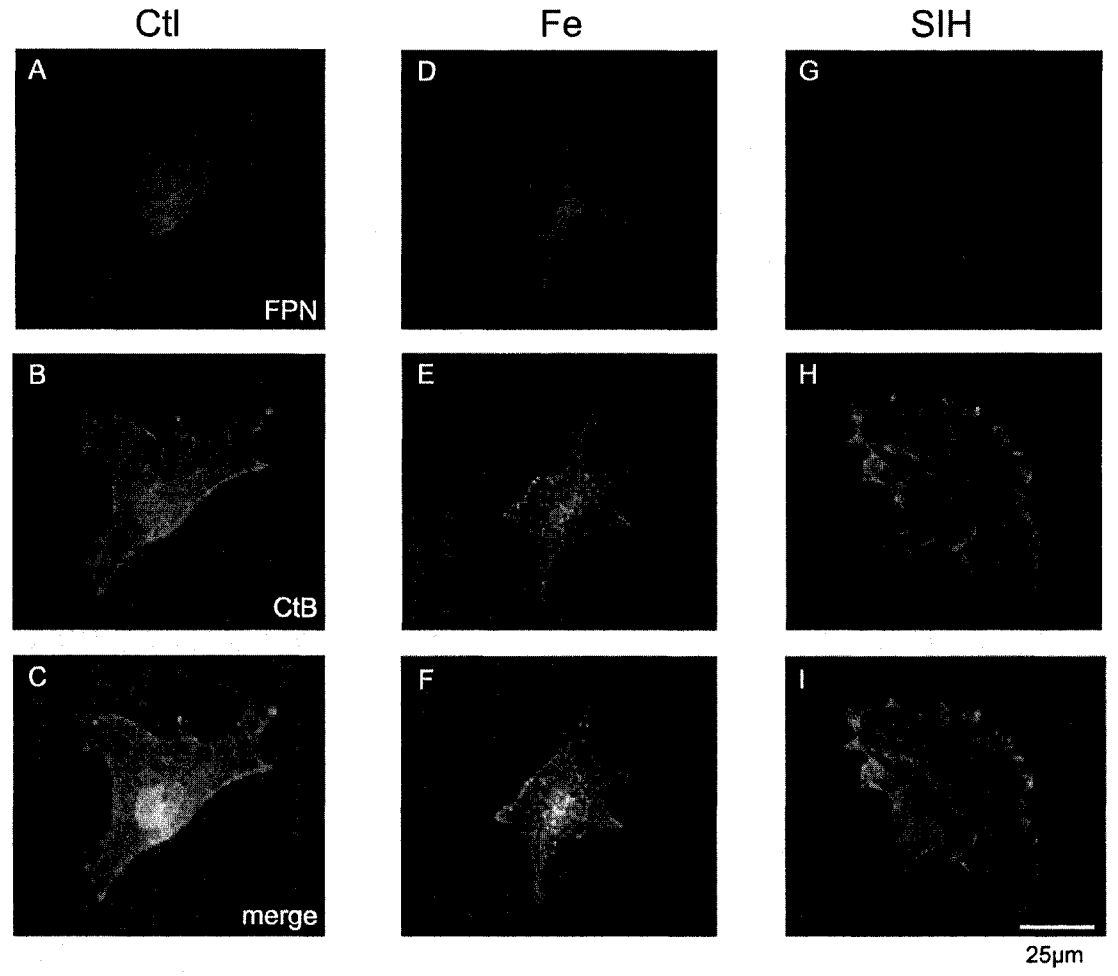
Ctl
Fe
SIH
A
D
G
FPN
B
E
H
CtB
C
F
I
merge
25μm
J
Ctl
Fe
SIH

Figure 9

Regulation of FPN expression under different cellular iron concentration. **(A)** Qauntitative real time RT-PCR for FPN shows a 150% increase in mRNA compared to the control in the Fe-treated group, and the SIH group showed a 60% reduction. CP mRNA expression was not affected by treatments. *; $p<0.05$, Student's t-test. **(B)** Electron mobility shift assay shows decreased IRP1 and IRP2 in the Fe-treated group and increased IRP1 and IRP2 in the SIH group reflecting the cellular iron status of each group.

A

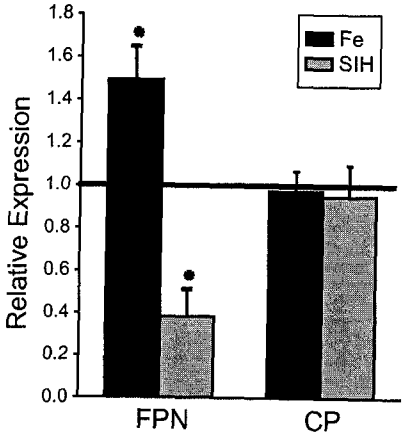
Relative Expression
1.8
1.6
1.4
1.2
1.0
0.8
0.6
0.4
0.2
0.0
Fe
SIH
FPN
CP

B

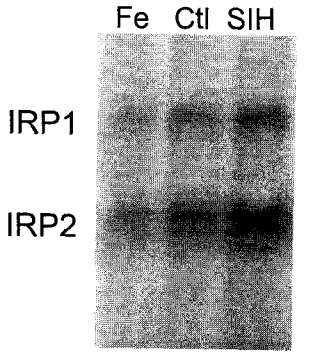
Fe
Ctl
SIH
IRP1
IRP2

CHAPTER 3

Age-related Changes In Iron Homeostasis and Cell Death in the Cerebellum of Ceruloplasmin Deficient Mice

** The work presented in this chapter was published in J. Neurosci (*S.Y. Jeong and David, S. (2006) Age-related Changes In Iron Homeostasis and Cell Death in the Cerebellum of Ceruloplasmin Deficient Mice. J. Neurosci. 26:9810-9819).*

3.1 Preface

In the previous chapter, I examined the role of GPI-anchored ceruloplasmin and generation of an efflux complex with an iron efflux protein ferroportin (FPN) *in vitro*. GPI-CP is essential for astocytic iron efflux and we have reported that there is abnormal CNS tissue iron accumulation in the *CP* null mice (patel et al.). Therefore, I wanted to characterize the role of GPI-CP *in vivo* and understand which cells accumulate iron and also how neurodegeneration occur. In this chapter, I have examined accumulation of iron in *CP* null mice and also disregulation of proteins involved in iron homeostasis during aging. Furthermore, I have reported two different types of cell death in the *CP* null mice.

3.2 Summary

Iron is essential for a variety of cellular functions but its levels and bioavailability must be tightly regulated because of its toxic redox activity. A number of transporters, binding proteins, reductases and ferroxidases help maintain iron homeostasis to prevent cell damage. The multi-copper ferroxidase ceruloplasmin (CP) converts toxic ferrous iron to its non-toxic ferric form and is required for iron efflux from cells. Absence of this enzyme in humans leads to iron accumulation and neurodegeneration in the central nervous system. Here we report on the changes that occur in the cerebellum of CP null ($CP^{-/-}$) mice with aging. We show that iron accumulation, which is reflected in increased ferritin expression, occurs mainly in astrocytes by 24 months in $CP^{-/-}$ mice and is accompanied by a significant loss of these cells. In contrast, Purkinje neurons and the large neurons in the deep nuclei of $CP^{-/-}$ mice do not accumulate iron but express high levels of the iron importer, divalent metal transporter 1 (DMT1), suggesting that these cells may be iron deprived. This is also accompanied by a significant reduction in the number of Purkinje neurons. These data suggest that astrocytes play a central role in the acquisition of iron from the circulation; and that two different mechanisms underlie the loss of astrocytes and neurons in $CP^{-/-}$ mice. These findings provide a better understanding of the degenerative changes seen in humans with aceruloplasminemia, and have implications for normal aging and neurodegenerative diseases in which iron accumulation occurs.

3.3 Introduction

Iron is an essential metal that is involved in many metabolic processes. Iron serves as a cofactor for various heme and non-heme proteins, including the cytochromes of the mitochondrial oxidative chain for ATP generation, enzymes for DNA repair and neurotransmitter synthesis [1]. Although these functions depend upon the redox active nature of iron, free radicals can also be produced if iron is in excess or inappropriately shielded [2]. A number of transporters, binding proteins, oxidases and reductases exist that tightly regulate iron homeostasis [3]. Lack or dysregulation of the expression of these molecules can lead to iron overload or iron deficiency. Interestingly, alterations of iron levels in non-central nervous system (CNS) tissue, as happens in hemochromatosis, do not generally affect CNS iron levels [4] suggesting that the CNS is shielded by the blood-brain barrier (BBB). Nevertheless, changes in the expression of these iron homeostasis proteins in the CNS can lead to CNS pathology [5].

Ceruloplasmin (CP) is a ferroxidase that safely converts toxic ferrous (Fe^{2+}) iron to its non-toxic ferric (Fe^{3+}) form [6, 7]. A secreted form of CP is expressed mainly by the liver, and a glycosylphosphatidylinositol (GPI)-anchored form is expressed in the CNS by astrocytes [8]. Null mutations of the CP gene in humans (aceruloplasminemia) result in iron accumulation in various organs including the liver and CNS [9-11]. Iron accumulation and neurodegeneration in this condition occurs between 45-55 years of age [12-14]. Mice deficient in CP ($CP^{-/-}$) also show iron accumulation in the liver and other organs [15, 16]. In an earlier report we provided a preliminary biochemical characterization of iron accumulation in various regions of the CNS in $CP^{-/-}$ mice with age [16]. Iron accumulation has also been reported in the retina of mice lacking both CP and the CP homologue hephaestin [17]. We have also shown in *in vitro* studies that CP is

required for iron efflux from astrocytes and that GPI-CP is bound to the efflux transporter ferroportin1 (FPN) [18].

It is not known if the absence of CP alters the expression of other molecules involved in iron homeostasis. In addition, since GPI-CP is expressed only in astrocytes, it is of interest to know whether iron deposition occurs in astrocytes as well as neurons and whether both cell types undergo degeneration. Studies of the mechanisms controlling iron homeostasis in the CNS will have implications for neurological disorders such as Alzheimer's and Parkinson's disease in which iron accumulation occurs [19], in addition to providing insights into iron accumulation in the CNS through aging. We now present data on the age related accumulation of iron, expression of iron homeostasis proteins, and selective death of neurons and astrocytes in the cerebellum of $CP^{-/-}$ and wildtype mice.

3.4 Experimental procedures

Animals. $CP^{+/+}$ and $CP^{-/-}$ mice at 6, 12, 18 and 24 months of age were used. $CP^{-/-}$ mice on a C57BL/6 background were generated in our laboratory as previously described [16]. All procedures used were approved by the McGill University Animal Care committee.

Iron histochemistry. $CP^{+/+}$ and $CP^{-/-}$ mice were perfused with 0.1M phosphate buffer followed by 4% paraformaldehyde in 0.1M phosphate buffer (pH 7.2). Modified Perl's histochemistry was preformed on 14μm thick cryostat sections of the cerebellum to detect iron accumulation as described previously [20]. Briefly, sections were incubated with 4% potassium ferrocyanide and 4% HCl, followed by a series of incubations with diaminobenzidine and hydrogen peroxide and counterstained with 0.02% methyl green (all from Sigma-Aldrich, Oakville, ON).

Flame atomic absorption spectrometry (fAAS). Iron concentration in the cerebellum of 12 and 24 month-old $CP^{-/-}$ and $CP^{+/+}$ mice was measured by fAAS. Tissue samples were prepared according to a previously described protocol [21]. Briefly, the whole cerebellum from individual animals was weighed wet, and then dried for 20 hours at 106°C, and the dry weight measured. Dried samples were ashed at 500°C for 17 hours and solublized in 6N HCl. Extracted samples were diluted with demineralized water to an HCl concentration of 1.2 N. The iron level in each sample was measured by fAAS using an AAnalyst 400 (Perkin Elmer, Wellesley, MA). Duplicate readings were obtained for each sample. Data is shown as the mean ± SD of the iron concentration in μg per gram dry tissue weight (n = 3).

Quantitative real-time RT-PCR (QRT-PCR). Total RNA was purified from the cerebella of $CP^{+/+}$ and $CP^{-/-}$ mice at different ages using the RNeasy Lipid Tissue Kit (Qiagen, Mississauga, ON), and QRT-PCR was performed using the Brilliant® Probe-based QRT-PCR Reagents and MX4000 (Stratagene, La Jolla, CA), both following manufacturer's protocols. Gene specific primers and Taqman® probes were generated using PrimerQuest (Integrated DNA Technology, Coralville, IA) (Table 1). QRT-PCR for peptidylprolyl isomerase A (PPIA) was performed for use as an internal control [22]. For data analysis, the sample Ct values were normalized to that of PPIA and expressed as fold increase. Results are shown as the mean relative ratio (fold-increase) of mRNA ± standard deviations (SD) of the mean from 3 separate experiments (n=3) compared to the wildtype value at the same age. Two-sample Student's t-test was used to determine statistical significance.

Gel retardation assay. A gel retardation assay was performed to assess the interaction between iron regulatory proteins (IRPs) and iron response elements (IREs) following an established technique [23]. Briefly, 20μg of total protein extract of whole cerebellum from 24 month old $CP^{-/-}$ or $CP^{+/+}$ mice was mixed with ^{32}P-labeled ferritin IRE RNA probe (obtained from Dr. K. Pantopoulos, McGill University, Montreal, Canada), which was *in vitro* transcribed from a linearized plasmid template using T7 RNA polymerase. The samples were incubated for 10 min at room temperature with heparin (5mg/ml) to prevent non-specific binding. Unbound probe was degraded by 10 min incubation with RNase T1. The formation of RNA-protein complexes was then detected by gel electrophoresis using 6% non-denaturing polyacrylamide gels. The gels were scanned with a STORM860 (phosphoimager) and analyzed with ImageQuant for densitometry (GE Healthcare, Uppsala, Sweden). Tissue homogenates of the cerebellum from 3 $CP^{-/-}$ and 3 $CP^{+/+}$ mice were tested.

Western blotting. Cerebella from mice at different ages were dissected out and total protein extracted as described previously [18]. Proteins were separated by SDS polyacrylamide gel electrophoresis (PAGE), transferred to polyvinylidene fluoride (PVDF) membrane (Millipore, Billerica, MA), and incubated with either rabbit anti-ferroportin (FPN, 1:4000, Alpha Diagnostics, San Antonio, TX), rabbit anti-divalent metal transporter1 (DMT1, 1:4000, Alpha Diagnostics; recognizes both forms of DMT1), rabbit anti-transferrin receptor 1 (TfR1, 1:500, Zymed, Burlington, ON), rabbit anti-ferritin (1:500, DakoCytomation, Carpinteria, CA), or mouse anti-glial fibrillary acidic protein (GFAP, 1:100, Sigma-Aldrich, Oakville, ON). Blots were washed and incubated with peroxidase-conjugated IgG, (1:200,000, Jackson Immunoresearch, West Grove, PA),

and detected with enhanced chemiluminescence (Perkin Elmer, Wellesley, MA). Equal loading of proteins was assessed using rabbit anti-actin antibodies (1:200, Sigma-Aldrich, Oakville, ON).

Immunofluorescence and Immunohistochemistry. $CP^{+/+}$ and $CP^{-/-}$ mice were perfused with 0.1M phosphate buffer followed by 4% paraformaldehyde in 0.1M phosphate buffer (pH. 7.2), and 14μm cryostat sections obtained. Double immunofluorescence labeling of tissue sections was carried out as described previously [24]. Briefly, the tissue sections were incubated with phosphate buffered saline containing 2% normal goat serum and 1% ovalbumin to block non-specific binding of antibodies. This was followed by an overnight incubation with rabbit anti-DMT1 polyclonal antibody (1:400, Alpha Diagnostics, San Antonio, TX) or a rabbit anti-ferritin antibody (1:100, DakoCytomation, Carpinteria, CA). After washing, the tissue sections were incubated with either monoclonal anti-glial fibrillary acid protein (GFAP) (for astrocytes, 1:100, Sigma-Aldrich, Oakville, ON) or SMI-32 (an anti-neurofilament antibody for neurons, 1:500, Sternberger Monoclonal, Berkeley, CA). In other experiments, sections were incubated with rabbit anti-GFAP (1:100, DakoCytomation, Carpinteria, CA) and monoclonal anti-S100β (1:250, Sigma-Aldrich, Oakville, ON) for quantifying astrocytes. The binding of polyclonal rabbit antibodies was visualized with fluoresceine-conjugated goat anti-rabbit IgG (1:200, Jackson Immunoresearch, West Grove, PA), and mouse monoclonal antibodies with rhodamine-conjugated goat anti-mouse IgG (1:200, Jackson Immunoresearch, West Grove, PA). Sections were also labeled with 100ng/ml 4'-6-diamidino-2-phenylindole (DAPI, Vector Laboratories, Burlingame, CA) and viewed with a Zeiss Axioskop 2 plus microscope (Carl Zeiss

Canada, Toronto, ON). Immunohistochemistry using Vectastain ABC kit (Vector Laboratories, Burlingame, CA) was used to detect expression of transferrin receptor 1 (TfR1) because of its low abundance in the CNS. A standard technique was used as previously described [25]. TfR1 was detected in the tissue samples using a monoclonal anti-TfR1 antibody (1: 200, Zymed, Burlington, ON, Canada) and a goat anti-mouse biotinylated secondary antibody (1:400; Jackson Immunoresearch). Binding of the primary antibody was revealed by using diaminobenzidine as the chromogen. Tissue sections were counterstained with 0.1% cresyl violet.

Quantification. Cell counts were done using BioQuant Nova Prime (BioQuant Image Analysis Corp, Nashville, TN). The mean number of astrocytes per $10^4\mu m^2$ of white matter, and the mean number of Purkinje cells in a 500μm linear distance in the Purkinje cell layer was estimated from 24 tissue sections per animal (n = 3), each section being at least 100μm apart. Results are presented as the mean number of cells ± SD. The statistical significance was determined by a two-sample Student's t-test and two-way ANOVA.

3. 5 Results

Increased iron accumulation in the cerebellum of Cp null mice. We first assessed iron accumulation in the cerebellum of $CP^{-/-}$ and $CP^{+/+}$ mice at 6, 12 and 24 months of age using enhanced Perl's histochemistry. At 6 months, there is no visible iron accumulation detected in either $CP^{-/-}$ or $CP^{+/+}$ mice (data not shown). At 12 months increased iron accumulation is detected in cells adjacent to the lining of the fourth ventricle in $CP^{-/-}$ but not in wildtype mice (Figure 1A, B). By 24 months of age, a large number of cells show iron accumulation in the cerebellar cortex (Figure 1C) and deep nuclei (Figure 1E) in CP^{-}

$^{-/-}$mice. In contrast, wildtype mice show weaker Perl's staining for iron in a few cells in the cerebellar cortex (Figure 1D) and deep nuclei (Figure 1F) indicating that a low level of iron accumulation occurs in the CNS with aging. The increased iron accumulation in 12 and 24 month old $CP^{-/-}$ mice was further confirmed and quantified by flame atomic absorption spectrometry. This analysis shows a 2-fold increase in iron levels in the cerebellum of 12 month old $CP^{-/-}$ mice as compared to wildtype mice, and a much greater increase in iron of about 4.5-fold in $CP^{-/-}$ mice at 24 months of age compared to age-matched wildtype controls (Figure 1G). The iron-loaded cells seen with Perl's staining in the cerebellar cortical white matter are glia. Iron staining is also detected occasionally in some small round cells (Figure 1C, arrows; 2A) and also in elongated cells (Figure 2A) in the granule cell layer, which based on their morphology, are likely to be granule neurons and Bergmann glia, respectively. Iron accumulation is not seen in Purkinje cells in either the *CP* null or wildtype mice (Figure 2A, B). However, there appear to be a substantial loss of Purkinje neurons in *CP* null mice compared to wildtype mice at this age (Figure 2A, B). The deep nuclei of $CP^{-/-}$ mice at 24 months contain cells intensely labeled for iron (Figure 1E, 2C), which based on their size and morphology are likely to be mainly glia (Figure 2C), and possibly also small neurons. However, the large neurons, which can be identified with the methyl green staining, did not show signs of iron accumulation (Figure 2C). In contrast to the findings in $CP^{-/-}$ mice, only a few small cells weakly stained for iron are seen in the deep nuclei of $CP^{+/+}$ mice (Figure 2D). The absence of CP therefore causes a marked accumulation of iron in the gray matter and white of the cerebellum with aging.

Changes in expression of iron homeostasis proteins. We next assessed the changes in expression of eight iron transporters and binding proteins in $CP^{-/-}$ and $CP^{+/+}$ mice with aging. Changes in mRNA expression in the cerebellum were assessed by quantitative real-time RT-PCR at 6, 12, 18 and 24 months of age and compared to wildtype levels at these ages. At 6 months of age there is no difference between *CP* null and wildtype mice in the mRNA levels of any of the iron binding proteins and transporters examined (Figure 3A). By 12 months, when the first indication of iron overload is detected, there is a small but significant increase in ferritin L chain, and a decrease in TfR1 mRNA (Figure 3A). Changes in these mRNAs are particularly interesting as ferritin and transferrin receptor1 mRNAs contain iron response elements (IREs) in the 5' and 3' untranslated regions, respectively. IREs are hairpin loop structures that interact with two types of iron-regulatory proteins (IRP1 and IRP2) in iron replete conditions. In the presence of excess iron, the failure of IRPs to bind to the IREs results in increased stability and translation of ferritin mRNA, and breakdown of transferrin receptor mRNA. Therefore changes in ferritin mRNA is a more sensitive indicator of iron accumulation than Perl's histochemistry as no obvious staining for iron was seen at 12 months except along the lining of the fourth ventricle. This induction of ferritin mRNA can be also achieved by inflammation. By 18 months of age there is an even further increase in the mRNA expression of DMT1 and ferritin L chain. As DMT1 isoforms with and without IRE are known to be expressed in neural cells [26], we used two sets of PCR primers to assess the expression of these two types of DMT1 transcripts. Quantitative real-time RT-PCR analysis revealed that the increase is in the mRNA coding for DMT1 without IRE (Figure 3A). In addition, there is also a significant increase in mRNA expression of ferritin H chain. By 24 months, the mRNA levels of both ferritin H and L chains show a 4-fold

increase, which reflects the fold change in iron detected by fAAS; while TfR1 mRNA shows a 60% reduction (Figure 3A). There is also a 2.5-fold increase in mRNA for DMT1 and DMT1 without IRE at 24 months (Figure 3A).

As the IRP-IRE system plays an important role in regulating the mRNA levels of key proteins involved in binding and transport of iron, we employed a gel retardation assay using a ^{32}P-labeled ferritin IRE RNA probe to assess the levels of activated IRPs in tissue homogenates of 24 month old $CP^{-/-}$ and $CP^{+/+}$ mice. Densitometric analysis shows ~40% decrease in IRP1 activity in $CP^{-/-}$ mice compared to the wildtype age-matched controls (Figure 3C), thus providing further confirmation of iron accumulation in the CNS. In contrast to IRP1, IRP2 activity was barely detectable in these samples. The mRNA levels of hephaestin, a ceruloplasmin homologue, as well as FPN do not show significant changes with age in CP null mice compared to wildtype controls (Figure 3A).

We also assessed if there are any changes in mRNA expression in wildtype mice with age. To do this, we plotted the fold-increase or decrease in mRNA levels in 12, 18 and 24 month-old $CP^{+/+}$ mice as compared to the levels at 6 months of age (Figure 3B). No changes are detected at 12 months; at 18 months there is small but significant increase in both ferritin chains; and at 24 months, there is an increase of 1.9 fold in the mRNA for ferritin H, 1.5 fold for ferritin L, and 1.2 fold for DMT1 (-IRE form); and a small but significant decrease in TfR1 mRNA, relative to the values at 6 months (Figure 3B). Interestingly, there is also a small but significant decrease in ceruloplasmin mRNA in 24-month old wildtype mice (Figure 3B). The data presented in Figure 3A therefore indicate changes in mRNA expression in Cp null mice that are over and above the normal increases seen with aging in wildtype mice. Western blot analysis shows that there is a corresponding increase at the protein level of DMT1 and ferritin, reduction in TfR1 but

no change in FPN protein in the cerebellum of 24 month-old $CP^{-/-}$ mice as compared to wildtype controls (Figure 3D).

Given the accumulation of iron, the increase in the expression of the iron importer DMT1 was unexpected. We therefore assessed which cell types express increased levels of DMT1 in 24 month-old $CP^{-/-}$ mice by double immunofluorescence labeling for DMT1 combined with cell type specific antibodies against neurons (monoclonal antibody SMI32), and astrocytes (anti-GFAP). DMT1 immunoreactivity is markedly increased in Purkinje neurons in the cortex (Figure 4A-C), and in the large neurons of the deep nuclei (Figure 5A-C) as compared to wildtype controls (Fig 4D-F and Fig 5D-F). On the other hand, astrocytes do not show any increase in DMT1 expression in $CP^{-/-}$ mice (data not shown). Unlike previous reports [27] we were unable to detect expression of transferrin receptor 1 (TfR1), the other iron uptake mechanism, in Purkinje neurons in our mice. Interestingly, although expression of TfR1 is not changed in Purkinje cells in 24-month old $CP^{-/-}$ mice, it appears to be elevated in endothelial cells as compared to age-matched controls (Figure 4G-H). This suggests that the endothelial cells of the blood-brain barrier increase iron uptake in the presence of iron accumulation in neural cells in the CNS. These data also suggest that DMT1 may play an important role in iron trafficking in Purkinje neurons at this age in *CP* null mice. DMT1 on the cell surface may play a role in iron influx into cells, and DMT1 on the endosomal membrane has been shown to be required for the transport of iron from the endosome into the cytosol. Therefore, the increase in DMT1 expression in Purkinje neurons and the large neurons in the deep nuclei, both of which do not show evidence of iron accumulation, suggests that these cells in $CP^{-/-}$ mice may be deprived of iron and are trying to increase iron uptake by up-regulating DMT1.

Since iron levels directly regulate ferritin synthesis in cells [28], an increase in ferritin immunoreactivity can be used to indirectly assess increases in iron levels in particular cell populations. We therefore carried out immunofluorescence staining for ferritin combined with cell type specific markers. In the cerebellar cortex, Purkinje neurons did not show ferritin immunostaining in either *CP* null or wildtype mice, suggesting that these neurons do not accumulate iron (Figure 6A-C and D-F), which is consistent with the absence of Perl's staining of these neurons. However, there is evidence of ferritin immunoreactivity in glial cells in the cerebellar cortex (Figure 6A) and occasionally some granule neurons. In the deep nuclei, astrocytes are the most abundant ferritin positive cell type but some small neurons are also ferritin positive (Figure 6G-I). In contrast, the large neurons in the deep nuclei do not show evidence of ferritin immunoreactivity (Figure 6G-I). GFAP positive astrocytes in the white matter of $CP^{-/-}$ mice show strong ferritin immunoreactivity (Figure 7A-C, insert), and are therefore likely to be the cell type that is labeled for iron by Perl's staining. There is also a significant reduction in GFAP immunoreactivity in the $CP^{-/-}$ mice as compared to wildtype mice at 24 months of age (Figure 7B and E). The reduction in GFAP in $CP^{-/-}$ mice was further confirmed by Western blot analysis (Figure 7G).

Glial and neuronal loss in *Cp* null mice. The reduction in GFAP immunoreactivity in $CP^{-/-}$ mice may be due either to a reduction in the expression levels of this intermediate filament protein or to a loss of astrocytes. We therefore quantified the number of astrocytes in the white matter at 24 months of age in tissue sections labeled with anti-GFAP. There is a marked reduction in the number of $GFAP^+$ astrocytes in $CP^{-/-}$ mice compared to wildtype mice as assessed by the number of $GFAP^+/DAPI^+$ cellular profiles

(Figure 8A, D). Quantification of the number of these $GFAP^+$ cells revealed a 61% loss in *CP* null mice compared to controls (Figure 8G). To further ascertain whether this change represents a loss of astrocytes or simply a reduction in GFAP expression, we carried out double immunofluorescence labeling for GFAP and S100β, another astrocyte marker, which labels astrocytic cell bodies. This analysis shows a 55% reduction in the number of $S100\beta^+/DAPI^+$ cells, and a 57% reduction in the number of $S100\beta^+/GFAP^+$ double-labeled cells, with DAPI stained nuclei (Figure 8G). The reduction in GFAP and S100β immunoreactivity was also detected in other regions of the cerebellum including the cortical gray matter and deep nuclei but was not quantified. These data indicate that there is a marked loss of astrocytes in $CP^{-/-}$ mice with age. We were unable to detect activated caspase 3 immunoreactivity in astrocytes, which may be due to the slow rate of cell death that occurs over a period of many months. The excessive amount of iron accumulation in astrocytes, however, is likely to lead to increased death of these cells in *CP* null mice. It is also possible that the loss of astrocytes in 24 month-old $CP^{-/-}$ mice may be further exacerbated by a reduction in cell proliferation and an inability for renewal of the astrocyte population due to a lack of iron, which is required for cell proliferation.

The data presented above in Figures. 2A, 4B, 6B suggests that there is a loss of Purkinje neurons in 24-month old mice. To rigorously assess this, we quantified the number of Purkinje cells in tissue sections immunostained for non-phosphorylated neurofilament subunits, which labels neuronal cell bodies. These results show that there is a gradual loss of Purkinje neurons in $CP^{-/-}$ mice between 12 and 24 months of age. At 12 months there is a 30% loss of Purkinje neurons, which increases to a 48% loss at 24 month of age (Figure 9). As with astrocytes, we were unable to detect activated caspase 3

immunoreactivity in Purkinje neurons. There is no difference in Purkinje cell number between wildtype and Cp null mice at 6 months of age (Figure 9). In addition, there is no detectable loss of Purkinje cells in wildtype mice with age. The loss of Purkinje neurons in $CP^{-/-}$ mice may underlie the loss of motor co-ordination on a rotor-rod test, which we have previously reported [16].

3. 6 Discussion

We have studied the role of the ferroxidase, ceruloplasmin, in iron homeostasis in the CNS with aging. The cerebellum was selected for this study because it is one of the regions of the CNS that is affected in humans with aceruloplasminemia. In particular, we have assessed the changes in iron accumulation, expression of various molecules involved in cellular iron homeostasis, as well as loss of neurons and glia in the cerebellum from 6 to 24 months of age. These data indicate that astrocytes play an important role in iron trafficking in the CNS and suggest that astroglial and neuronal death in *CP* null mice may occur via different mechanisms.

Role of astrocytes in iron trafficking in the CNS. Iron that is required for cellular metabolism in the CNS is acquired from the circulation where it is largely in the form of transferrin-bound diferric iron [29, 30]. Entry of iron into the CNS first involves transferrin receptor mediated uptake from the serum into capillary endothelial cells [31, 32], although some non-transferrin receptor mediated uptake may also occur [33-35]. Iron taken up into the endosomal compartment of endothelial cells via TF-TfR1 complexes is released from this receptor complex after acidification of the endosome and then effluxed into the cytosol via DMT1 that is present on the endosomal membrane [36].

How iron is released from endothelial cells is still not fully known. Endothelial cells express the efflux transporter FPN [37] but there is as yet no clear evidence that these cells also express CP, which we have previously shown is required for FPN mediated iron efflux [18]. Furthermore, the fact that we do not see iron accumulation in endothelial cells in $CP^{-/-}$ mice suggests that CP is not required for iron efflux from these cells.

Unlike other tissues, almost 95% of the capillary surface in the CNS is surrounded by astrocytic processes called perivascular end-feet [38]. These astrocytic processes contribute to the formation of tight junctions between endothelial cells, which comprise the blood-brain barrier (BBB) and thus limit the free flow of cells and macromolecules from the circulation into the CNS parenchyma [39]. Apart from astrocytes, other types of glial cells and neurons do not have direct access to the capillary surface. Furthermore, electron microscope analysis and recent studies on the localization of the aquaporin-4 water channel, which is exclusively localized to astrocytic processes, reveals that astrocytes extend a network of thin cytoplasmic processes around neuronal cell bodies and their processes, and around axon-dendritic synaptic complexes, in addition to the perivascular end-feet [40]. Astrocytes occupy discrete non-overlapping domains, with blood vessels lying along the boundaries of these domains [41] while neurons lie within and between these domains. We have shown previously that astrocytes are capable of non-transferrin-bound iron uptake *in vitro* [18], which may be mediated via the influx transporter DMT1 [18, 42, 43] or also possibly TfR1, although there is conflicting evidence for the latter [27, 44, 45], and our own immunostaining does not show expression of TfR1 in these glia *in vivo*. In addition, astrocytes also express FPN [46] and GPI-CP [8, 16, 18] which are required for iron efflux. Astrocytes, therefore, possess iron influx and efflux mechanisms. They are therefore ideally positioned around blood vessels

to acquire iron from the circulation via endothelial cells, and deliver it to neurons via the network of astrocytic processes surrounding neurons. Astrocytes can also take up iron released by cells in the CNS parenchyma, and possess the mechanisms required to efflux iron and load it on to transferrin at the capillary surface, from where it can be cleared into the circulation or reutilized in the CNS.

Our current data show that there is a slow accumulation of iron in astrocytes especially over a period of 12-24 months of age in $CP^{-/-}$ mice. A slow time course of the neuropathology is also seen in humans with aceruloplasminemia [47, 48]. Since GPI-CP is essential for iron efflux from astrocytes, the slow accumulation of iron in $CP^{-/-}$ mice and people with aceruloplasminemia suggest that there are either additional mechanisms *in vivo* that help clear iron from astrocytes albeit not completely efficiently or that the turnover of iron in the CNS is very slow. The eventual accumulation of iron in astrocytes is cytotoxic and leads to a 57% reduction in the number of astrocytes in the cerebellum of 24 month-old $CP^{-/-}$ mice. Oligodendrocytes do not appear to be affected in *CP* null mice, as myelination appears to be normal (data not shown).

Previous studies have reported that iron accumulates in the human CNS with normal aging [49-51]. This accumulation of iron occurs in astrocytes and microglia in the cerebral cortex, cerebellum, hippocampus, basal ganglia and amygdala in people between 60-90 years of age [52]. This age-related iron accumulation may be caused by increased leakiness of the blood-brain barrier or a reduction in the ability of astrocytes to efflux iron, or to other factors. Our present work shows that there is a low level of iron accumulation in the cerebellum of wildtype mice at 24 months. We also detected a corresponding increase in the mRNA expression of both ferritin H and L chains and reduction in TfR1 mRNA in the cerebellum of wildtype mice, which are sensitive

indicators of iron overload in cells and tissues. Interestingly, we also detected a small but significant reduction in the expression of CP in the cerebellum of 24 month-old wildtype mice as compared to 6 month-old wildtype mice. These changes in iron accumulation and mRNA expression therefore appear to be a milder version of what is seen in $CP^{-/-}$ mice, and suggests that reduction in the expression of CP in the CNS may contribute to the iron accumulation in normal aging.

Potential mechanisms underlying astrocyte and neuronal loss in $CP^{-/-}$ mice. Surprisingly, Purkinje neurons, large neurons in the deep nuclei, and the majority of other neurons in 24 month-old $CP^{-/-}$ mice did not show any evidence of iron accumulation. This finding is consistent with the possibility that these neurons receive iron mainly from astrocytes via astrocytic processes, which abut neuronal cell bodies. The inability of astrocytes to efflux iron in $CP^{-/-}$ mice would then result in iron remaining within astrocytes and not being made available to neurons. The accumulation of iron in astrocytes of $CP^{-/-}$ mice would thus be expected to result in neuronal iron deprivation. The increased expression of DMT1 in Purkinje neurons and neurons in the deep nuclei may therefore be an attempt by these iron starved neurons to increase their ability to acquire iron, possibly from the CSF where iron is found at very low levels, i.e., about 38-fold less than serum [53].

Despite the absence of iron accumulation in Purkinje cells, there is a significant loss of these neurons in $CP^{-/-}$ mice by 24 months of age, suggesting that this cell death is not due to iron-mediated free radicals generated within neurons. It is possible that free radicals generated in iron-loaded astrocytes may damage the neighboring neurons. However, the marked loss of astrocytes raises the possibility that the neuronal death may

be secondary to loss of the metabolic support normally provided by astrocytes. Selective ablation of astrocytes after cortical stab wounds and spinal cord lesions have also been shown to increase neuronal death suggesting a neuroprotective role for these glia [54, 55]. Astrocytes play an important role in maintaining the ionic and molecular homeostasis of the CNS microenvironment. Astrocytes maintain local levels of K^+, Ca^{2+}, iron and other metals, maintain pH, and provide glucose and metabolic substrates to neurons [41, 56]. Astrocytes also clear neurotransmitters such as glutamate released from synapses, and other molecules, which can be toxic to cells [41, 57]. Our results therefore suggest that different mechanisms may underlie the loss of astrocytes and neurons in *CP* null mice. Astrocytes, which show clear evidence of iron accumulation, are likely to die from iron toxicity, whereas the loss of Purkinje neurons may be secondary to the loss of the metabolic support provided by astrocytes. More direct in vitro experiments would help to firmly establish whether the loss of metabolic or trace metal coupling between astrocytes and neurons underlie Purkinje cell death. These results, however, provide new insights into the possible mechanisms that may mediate the loss of neurons and astrocytes in *CP* null mice. Similar mechanisms may also play a role in humans with aceruloplasminemia, and may have wider implications for aging and other neurodegenerative diseases in which iron accumulation occurs.

3.7 References

1. Rouault, T.A. and W.H. Tong, *Iron-sulphur cluster biogenesis and mitochondrial iron homeostasis.* Nat Rev Mol Cell Biol, 2005. **6**(4): p. 345-51.
2. Aisen, P., C. Enns, and M. Wessling-Resnick, *Chemistry and biology of eukaryotic iron metabolism.* Int J Biochem Cell Biol, 2001. **33**(10): p. 940-59.
3. Hentze, M.W., M.U. Muckenthaler, and N.C. Andrews, *Balancing acts: molecular control of mammalian iron metabolism.* Cell, 2004. **117**(3): p. 285-97.
4. Pietrangelo, A., *Hereditary hemochromatosis--a new look at an old disease.* N Engl J Med, 2004. **350**(23): p. 2383-97.
5. Ponka, P., *Hereditary causes of disturbed iron homeostasis in the central nervous system.* Ann N Y Acad Sci, 2004. **1012**: p. 267-81.
6. Williams, D.M., G.R. Lee, and G.E. Cartwright, *Ferroxidase activity of rat ceruloplasmin.* Am J Physiol, 1974. **227**(5): p. 1094-7.
7. Calabrese, L., M. Carbonaro, and G. Musci, *Presence of coupled trinuclear copper cluster in mammalian ceruloplasmin is essential for efficient electron transfer to oxygen.* J Biol Chem, 1989. **264**(11): p. 6183-7.
8. Patel, B.N., R.J. Dunn, and S. David, *Alternative RNA splicing generates a glycosylphosphatidylinositol-anchored form of ceruloplasmin in mammalian brain.* J Biol Chem, 2000. **275**(6): p. 4305-10.
9. Morita, H., et al., *Hereditary ceruloplasmin deficiency with hemosiderosis: a clinicopathological study of a Japanese family.* Ann Neurol, 1995. **37**(5): p. 646-56.
10. Yoshida, K., et al., *A mutation in the ceruloplasmin gene is associated with systemic hemosiderosis in humans.* Nat Genet, 1995. **9**(3): p. 267-72.

11. Harris, Z.L., et al., *Aceruloplasminemia: molecular characterization of this disorder of iron metabolism.* Proc Natl Acad Sci U S A, 1995. **92**(7): p. 2539-43.

12. Okamoto, N., et al., *Hereditary ceruloplasmin deficiency with hemosiderosis.* Hum Genet, 1996. **97**(6): p. 755-8.

13. Takahashi, Y., et al., *Characterization of a nonsense mutation in the ceruloplasmin gene resulting in diabetes and neurodegenerative disease.* Hum Mol Genet, 1996. **5**(1): p. 81-84.

14. Gitlin, J.D., *Aceruloplasminemia.* Pediatr Res, 1998. **44**(3): p. 271-6.

15. Harris, Z.L., et al., *Targeted gene disruption reveals an essential role for ceruloplasmin in cellular iron efflux.* Proc Natl Acad Sci U S A, 1999. **96**(19): p. 10812-7.

16. Patel, B.N., et al., *Ceruloplasmin regulates iron levels in the CNS and prevents free radical injury.* J Neurosci, 2002. **22**(15): p. 6578-86.

17. Hahn, P., et al., *Disruption of ceruloplasmin and hephaestin in mice causes retinal iron overload and retinal degeneration with features of age-related macular degeneration.* Proc Natl Acad Sci U S A, 2004. **101**(38): p. 13850-5.

18. Jeong, S.Y. and S. David, *Glycosylphosphatidylinositol-anchored ceruloplasmin is required for iron efflux from cells in the central nervous system.* J Biol Chem, 2003. **278**(29): p. 27144-8.

19. Zecca, L., et al., *Iron, brain ageing and neurodegenerative disorders.* Nat Rev Neurosci, 2004. **5**(11): p. 863-73.

20. Smith, M.A., et al., *Iron accumulation in Alzheimer disease is a source of redox-generated free radicals.* Proc Natl Acad Sci U S A, 1997. **94**(18): p. 9866-8.

21. Santos, M.M., et al., *Iron overload and heart fibrosis in mice deficient for both beta2-microglobulin and Rag1.* Am J Pathol, 2000. **157**(6): p. 1883-92.

22. Feroze-Merzoug, F., et al., *Peptidylprolyl isomerase A (PPIA) as a preferred internal control over GAPDH and beta-actin in quantitative RNA analyses.* Biotechniques, 2002. **32**(4): p. 776-8, 780, 782.

23. Kim, S. and P. Ponka, *Control of transferrin receptor expression via nitric oxide-mediated modulation of iron-regulatory protein 2.* J Biol Chem, 1999. **274**(46): p. 33035-42.

24. Kalyvas, A. and S. David, *Cytosolic phospholipase A2 plays a key role in the pathogenesis of multiple sclerosis-like disease.* Neuron, 2004. **41**(3): p. 323-35.

25. Ousman, S.S. and S. David, *Lysophosphatidylcholine induces rapid recruitment and activation of macrophages in the adult mouse spinal cord.* Glia, 2000. **30**(1): p. 92-104.

26. Roth, J.A., et al., *Differential localization of divalent metal transporter 1 with and without iron response element in rat PC12 and sympathetic neuronal cells.* J Neurosci, 2000. **20**(20): p. 7595-601.

27. Moos, T., *Immunohistochemical localization of intraneuronal transferrin receptor immunoreactivity in the adult mouse central nervous system.* J Comp Neurol, 1996. **375**(4): p. 675-92.

28. Hentze, M.W., et al., *Identification of the iron-responsive element for the translational regulation of human ferritin mRNA.* Science, 1987. **238**(4833): p. 1570-3.

29. Moos, T. and E.H. Morgan, *Transferrin and transferrin receptor function in brain barrier systems.* Cell Mol Neurobiol, 2000. **20**(1): p. 77-95.

30. Burdo, J.R. and J.R. Connor, *Brain iron uptake and homeostatic mechanisms: an overview.* Biometals, 2003. **16**(1): p. 63-75.

31. Jefferies, W.A., et al., *Transferrin receptor on endothelium of brain capillaries.* Nature, 1984. **312**(5990): p. 162-3.

32. Descamps, L., et al., *Receptor-mediated transcytosis of transferrin through blood-brain barrier endothelial cells.* Am J Physiol, 1996. **270**(4 Pt 2): p. H1149-58.

33. Deane, R., W. Zheng, and B.V. Zlokovic, *Brain capillary endothelium and choroid plexus epithelium regulate transport of transferrin-bound and free iron into the rat brain.* J Neurochem, 2004. **88**(4): p. 813-20.

34. Burdo, J.R., et al., *Mechanisms and regulation of transferrin and iron transport in a model blood-brain barrier system.* Neuroscience, 2003. **121**(4): p. 883-90.

35. Ueda, F., et al., *Rate of 59Fe uptake into brain and cerebrospinal fluid and the influence thereon of antibodies against the transferrin receptor.* J Neurochem, 1993. **60**(1): p. 106-13.

36. Fleming, M.D., et al., *Nramp2 is mutated in the anemic Belgrade (b) rat: evidence of a role for Nramp2 in endosomal iron transport.* Proc Natl Acad Sci U S A, 1998. **95**(3): p. 1148-53.

37. Wu, L.J., et al., *Expression of the iron transporter ferroportin in synaptic vesicles and the blood-brain barrier.* Brain Res, 2004. **1001**(1-2): p. 108-17.

38. Kandel, E., J. Schwartz, and T. Jessell, *Principles of Neural Science.* 4th ed. 2000: McGraw-Hill.

39. Saunders, N.R., M.D. Habgood, and K.M. Dziegielewska, *Barrier mechanisms in the brain, I. Adult brain.* Clin Exp Pharmacol Physiol, 1999. **26**(1): p. 11-9.

40. Vitellaro-Zuccarello, L., et al., *Distribution of Aquaporin 4 in rodent spinal cord: relationship with astrocyte markers and chondroitin sulfate proteoglycans.* Glia, 2005. **51**(2): p. 148-59.

41. Nedergaard, M., B. Ransom, and S.A. Goldman, *New roles for astrocytes: redefining the functional architecture of the brain.* Trends Neurosci, 2003. **26**(10): p. 523-30.

42. Burdo, J.R., et al., *Cellular distribution of iron in the brain of the Belgrade rat.* Neuroscience, 1999. **93**(3): p. 1189-96.

43. Williams, K., M.A. Wilson, and J. Bressler, *Regulation and developmental expression of the divalent metal-ion transporter in the rat brain.* Cell Mol Biol (Noisy-le-grand), 2000. **46**(3): p. 563-71.

44. Roskams, A.J. and J.R. Connor, *Transferrin receptor expression in myelin deficient (md) rats.* J Neurosci Res, 1992. **31**(3): p. 421-7.

45. Qian, Z.M., et al., *Transferrin receptors on the plasma membrane of cultured rat astrocytes.* Exp Brain Res, 1999. **129**(3): p. 473-6.

46. Burdo, J.R., et al., *Distribution of divalent metal transporter 1 and metal transport protein 1 in the normal and Belgrade rat.* J Neurosci Res, 2001. **66**(6): p. 1198-207.

47. Miyajima, H., et al., *Familial apoceruloplasmin deficiency associated with blepharospasm and retinal degeneration.* Neurology, 1987. **37**(5): p. 761-7.

48. Xu, X., et al., *Aceruloplasminemia: an inherited neurodegenerative disease with impairment of iron homeostasis.* Ann N Y Acad Sci, 2004. **1012**: p. 299-305.

49. Hallgren, B. and P. Sourander, *The effect of age on the non-haemin iron in the human brain.* J Neurochem, 1958. **3**(1): p. 41-51.

50. Connor, J.R., et al., *A quantitative analysis of isoferritins in select regions of aged, parkinsonian, and Alzheimer's diseased brains.* J Neurochem, 1995. **65**(2): p. 717-24.

51. Zecca, L., et al., *Iron, neuromelanin and ferritin content in the substantia nigra of normal subjects at different ages: consequences for iron storage and neurodegenerative processes.* J Neurochem, 2001. **76**(6): p. 1766-73.

52. Connor, J.R., et al., *Cellular distribution of transferrin, ferritin, and iron in normal and aged human brains.* J Neurosci Res, 1990. **27**(4): p. 595-611.

53. Mizuno, S., et al., *CSF iron, ferritin and transferrin levels in restless legs syndrome.* J Sleep Res, 2005. **14**(1): p. 43-7.

54. Bush, T.G., et al., *Leukocyte infiltration, neuronal degeneration, and neurite outgrowth after ablation of scar-forming, reactive astrocytes in adult transgenic mice.* Neuron, 1999. **23**(2): p. 297-308.

55. Faulkner, J.R., et al., *Reactive astrocytes protect tissue and preserve function after spinal cord injury.* J Neurosci, 2004. **24**(9): p. 2143-55.

56. Volterra, A. and J. Meldolesi, *Astrocytes, from brain glue to communication elements: the revolution continues.* Nat Rev Neurosci, 2005. **6**(8): p. 626-40.

57. Rao, K.V., et al., *Astrocytes protect neurons from ammonia toxicity.* Neurochem Res, 2005. **30**(10): p. 1311-8.

3. 8 Figures and Table

Figure 1

Iron accumulation in the cerebellum of $CP^{-/-}$ and $CP^{+/+}$ mice with age. Access iron in tissue sections are visualized by enhanced Perl's staining and counterstained with methyl green. **(A-B)** 12-month-old cerebellum. **(C-F)** 24-month-old cerebellum. **(A)** The region adjacent to the lining of the fourth ventricle shows the first evidence of iron accumulation (arrows) seen as brown staining in $CP^{-/-}$ mouse at 12 months of age. **(B)** No iron accumulation is detected in wildtype mouse at this age. **(C)** The white matter (wm) of the cerebellar cortex of a $CP^{-/-}$ mouse shows marked accumulation of iron in the glial cells. Some iron-positive cells (arrows) are also seen in the granular cell layer (gcl). **(D)** A few iron positive cells (arrowhead) are seen in the cortical white matter (wm) and granule cell layer (gcl) in a wildtype mouse. **(E)** Low magnification micrograph of the deep nuclei of a $CP^{-/-}$ mouse shows severe iron accumulation. **(F)** A small number of iron positive cells are seen in the deep nuclei of a wildtype mouse. Inserts show higher magnification of some of the iron containing cells. Scale bar: A-D = 100μm; E and F = 400μm; inserts = 50μm. **(G)** Changes in iron concentration in cerebellum of $CP^{-/-}$ (KO) and $CP^{+/+}$ (Wt) mice obtained by fAAS analysis. Data are presented as average ± SD. *$p<0.05$, n=3.

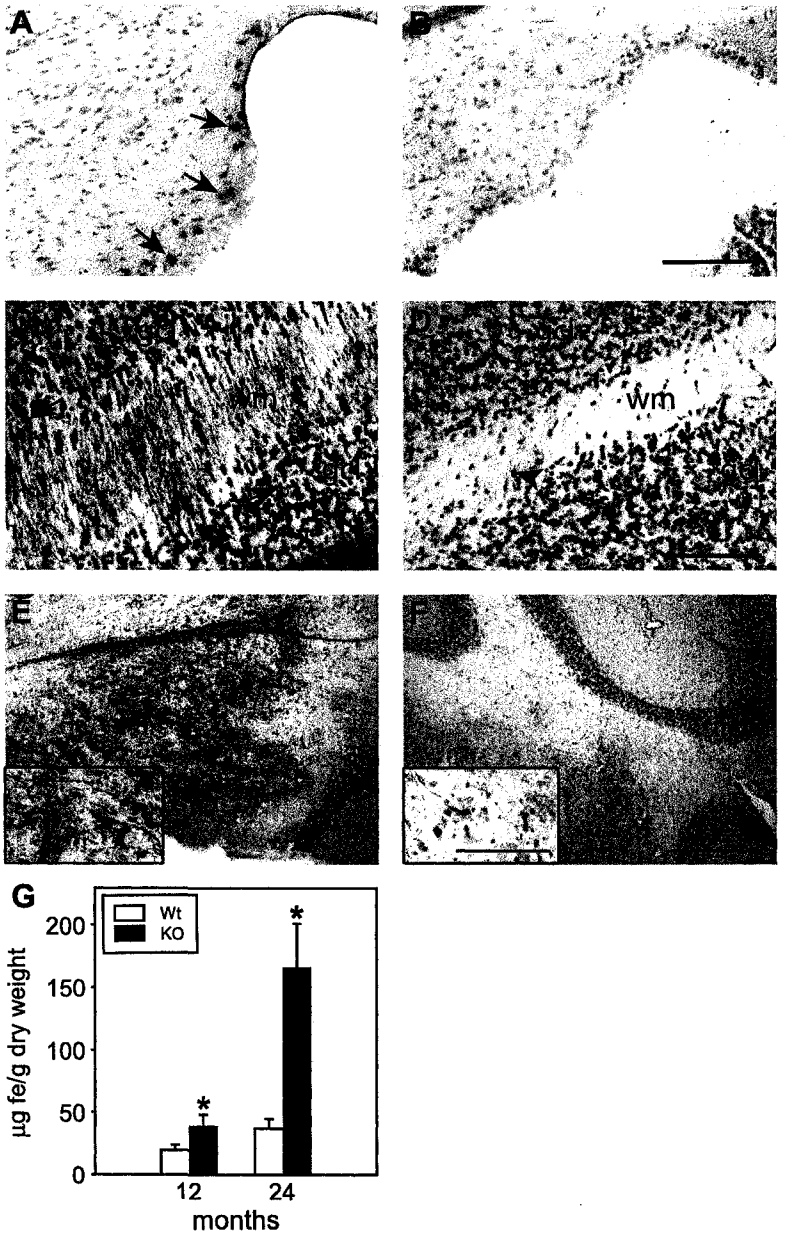
A
B
C
wm
D
wm
E
F
G
Wt
KO
200
150
100
50
0
µg fe/g dry weight
*
*
12
24
months

Figure 2

Iron accumulation in the cerebellar gray matter. **(A-B)** cortical gray matter. **(C-D)** deep nuclei. Purkinje neurons (arrowheads) in the cerebellar cortex of a $CP^{-/-}$ mouse **(A)** and wildtype mouse **(B)** do not show any evidence of iron accumulation. However, small iron-positive cells (arrows) which are likely to be either glia or granule neurons are also seen in the granule cell layer in the $CP^{-/-}$ cerebellum (A). Note the loss of Purkinje neurons (arrowheads) in the $CP^{-/-}$ mouse (A) as compared to the wildtype mouse (B). **(C)** A high magnification micrograph of the deep nucleus of a $CP^{-/-}$ mouse shows that iron accumulates in small cells (arrows) located adjacent to the large neurons that are detectable with the methyl green counter-stain. The large neurons do not show evidence of iron accumulation. **(D)** Micrograph of a deep nucleus of a wildtype mouse shows less iron accumulation than that seen in *CP* null mice. Note the few iron-positive cells (arrows) in the wildtype mouse are also small in size. Scale bar = 50μm.

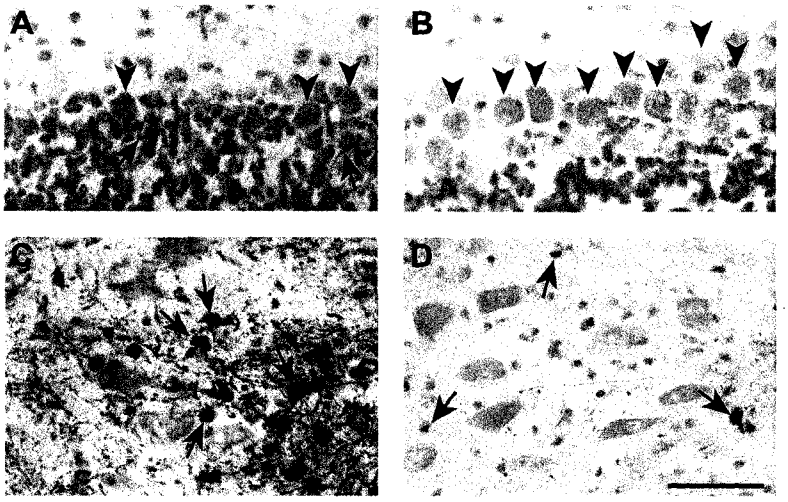
A
B
C
D

Figure 3

Changes in mRNA and protein expression of molecules involved in iron homeostasis. **(A)** Graph showing changes in mRNA expression in $CP^{-/-}$ mice with age detected by quantitative real-time RT-PCR. The data shows fold increase over wildtype levels (horizontal line at 1). The earliest change in mRNA expression is detected at 12 months when there is a small but significant increase in the expression of DMT1 and ferritin L (FTL), and a decrease in transferrin receptor 1 (TfR1). By 18 months there is a further increase in the expression of DMT1 and ferritin L chain as compared to 12 months. In addition, there is a significant increase in expression of DMT1 without IRE (-IRE) and FTH. By 24 months the changes in expression are much more pronounced. DMT1 and DMT1 -IRE are increased greater than 2-fold, FTL and H chains increase over 4-fold, and TfR1 mRNA levels are reduced more than at 12 and 18 months. Values shown are mean ± SD normalized to the wildtype mice at each time points; $n = 3$ for both $Cp^{-/-}$ and $Cp^{+/+}$ mice ($*p < 0.05$, $**p < 0.03$; Student's t test). **(B)** Graph showing changes in mRNA expression in wildtype mice at 12, 18 and 24 months of age compared to their levels at 6 months (horizontal line at 1). Significant increases are first detected in FTL and H chains at 18 months. By 24 months increases are detected in DMT1, DMT1 -IRE, FTL and H, as well as small but significant decreases in expression of TfR1 and CP. Values shown are mean ± SD normalized to the wildtype mice at 6 months old; $n = 3$ for each time point ($*p < 0.05$; Student's t test). **(C)** Gel retardation assay shows a marked decrease in IRP1 in the $CP^{-/-}$ mice cerebellum. **(D)** Western blot of 24 month-old cerebellum shows increase in protein expression for DMT1 and ferritin, decrease in TfR1, and no change in the expression of FPN in $CP^{-/-}$ mice (KO) compared to wildtype controls (Wt). β-actin was used as a loading control. Wt = wildtype; KO = $CP^{-/-}$ mice.

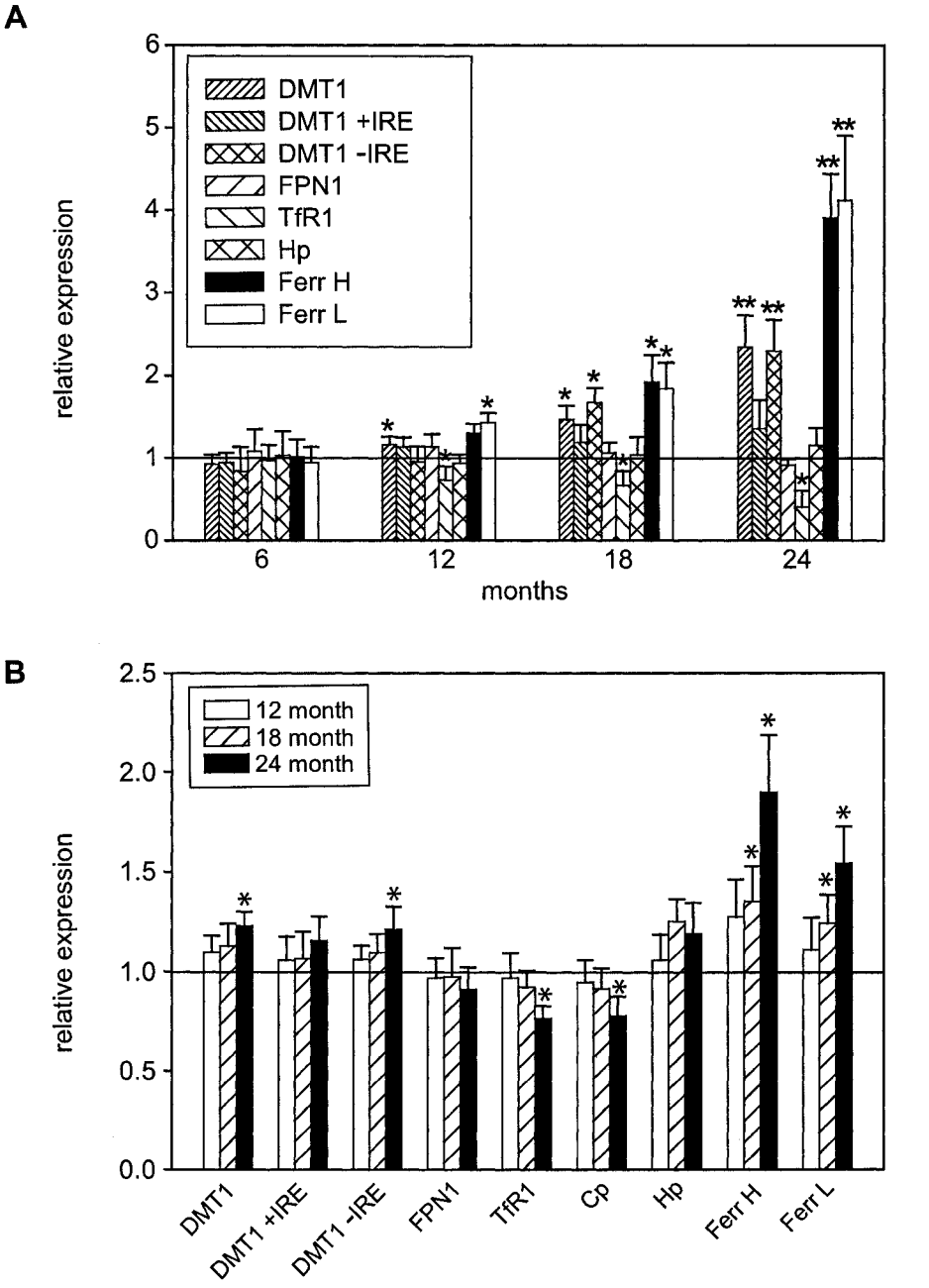
A
relative expression
DMT1
DMT1 +IRE
DMT1 -IRE
FPN1
TfR1
Hp
Ferr H
Ferr L
months
B
relative expression
12 month
18 month
24 month
DMT1
DMT1 +IRE
DMT1 -IRE
FPN1
TfR1
Cp
Hp
Ferr H
Ferr L
C
Wt
KO
IRP1
IRP2
free probe
D
DMT1
FPN1
TfR1
Ferritin
β-actin
Wt
KO

Figure 4

Immunostaining for DMT1 and TfR1 in Purkinje cells. **(A-F)** Double immunofluorescence labeling for DMT1 and SMI32 (neuronal marker). In $CP^{-/-}$ mice, DMT1 immunoreactivity is markedly increased in Purkinje neurons (A, arrows), which are double-labeled with an anti-neurofilament antibody SMI32 (B). Tissue sections of similar areas from control, wildtype mice show weak DMT1 immunoreactivity (D). Panels C, F show merged images of DMT1, SMI32 and DAPI staining. **(G-H)** Shows that there is no change in expression of TfR1 in Purkinje neurons in $CP^{-/-}$ (G, arrows), which is not detectable in these cells (arrows) in wildtype controls (H, arrows). Scale bars = 50μm.

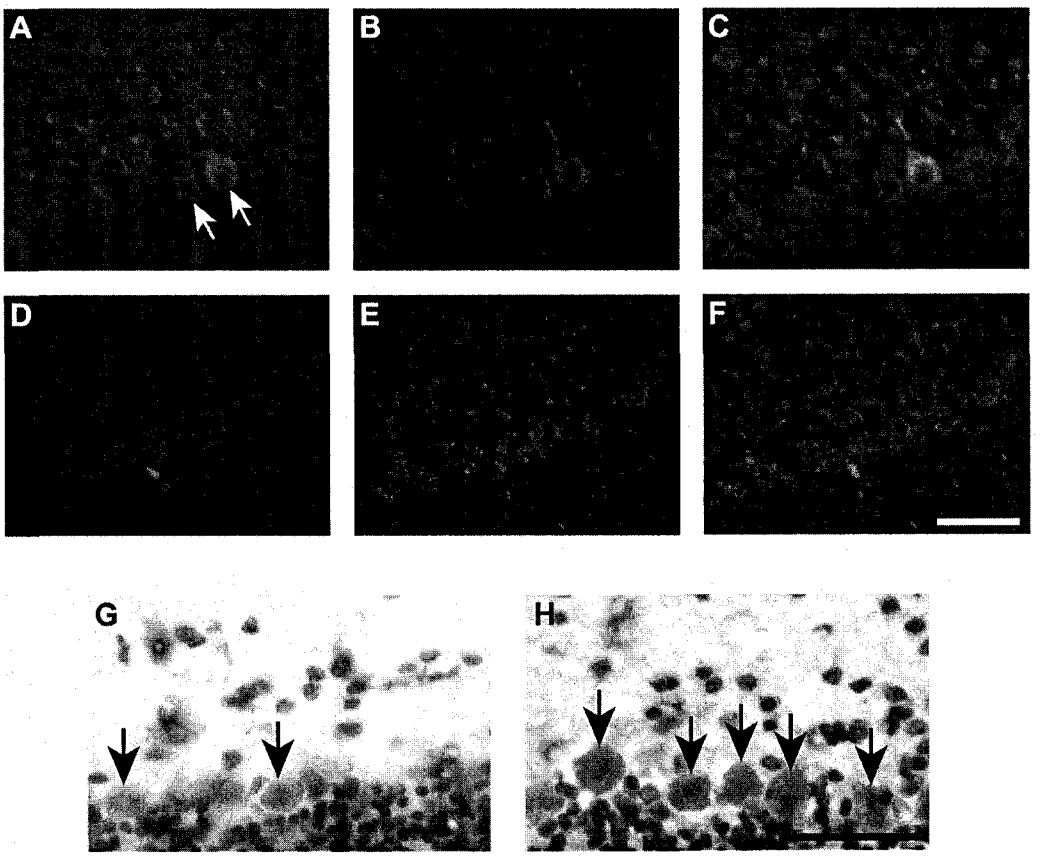
A
B
C
D
E
F
G
H

Figure 5

Expression of DMT1 in cerebellar deep nuclei. In 24-month old $CP^{-/-}$ mice, DMT1 immunoreactivity is markedly increased (A, arrows) in large neurons, which are double-labeled with SMI32 (B). Tissue sections of similar areas from control mice show weak DMT1 immunoreactivity (D). Panels C and F show merged images of DMT1, SMI32 and DAPI staining. Scale bar = 50μm.

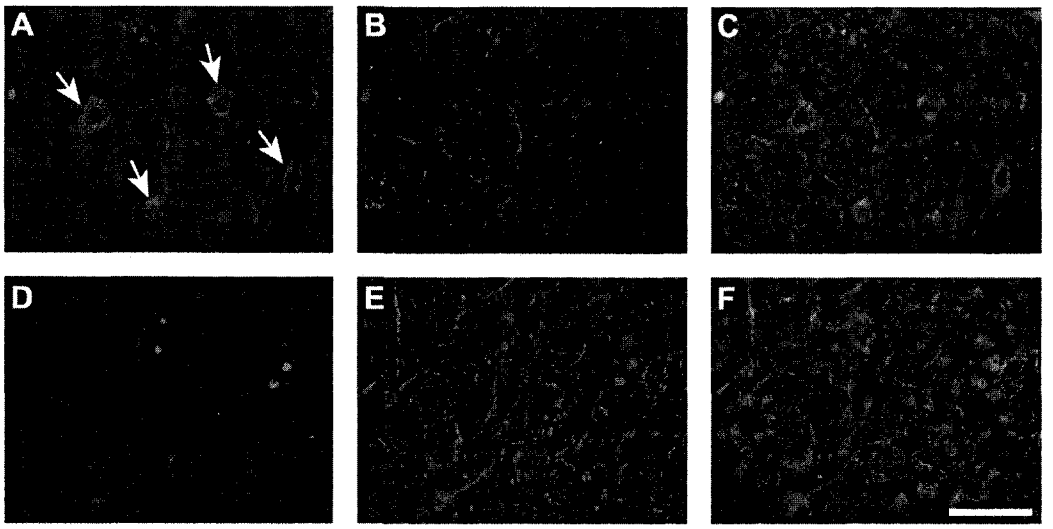
A
B
C
D
E
F

Figure 6

Large neurons do not accumulate iron. Double immunofluorescence labeling of cerebellar gray matter at 24-months of age with anti- ferritin and anti-neurofilament (SMI32) antibodies. **(A-F)** Cerebellar cortex including Purkinje cell layer. **(G-L)** Cerebellar deep nuclei. **(A and D)** There is no ferritin labeling in Purkinje neurons in either $Cp^{-/-}$ (A) or $Cp^{+/+}$ (D) mice. Purkinje neurons were detected with the neurofilament/SMI32 antibody (B and E). A ferritin-positive cell (arrow in A) is likely to be a glial cell as it is negative for neurofilament. In the deep nuclei of $Cp^{-/-}$ mice (G and H), the large neurons (arrows in H) also did not show evidence of ferritin immunolabeling. Ferritin immunoreactivity is, however, seen in some small neurons (arrows in G) and cells that were SMI32-negative (arrowhead in G), possibly glia. Anti-ferritin labeled cells are not seen in the deep nuclei of wildtype mouse (J and K). Panels, C, F, I and L are the merged images of corresponding ferritin, SMI32, and DAPI staining. Scale bar = 50μm.

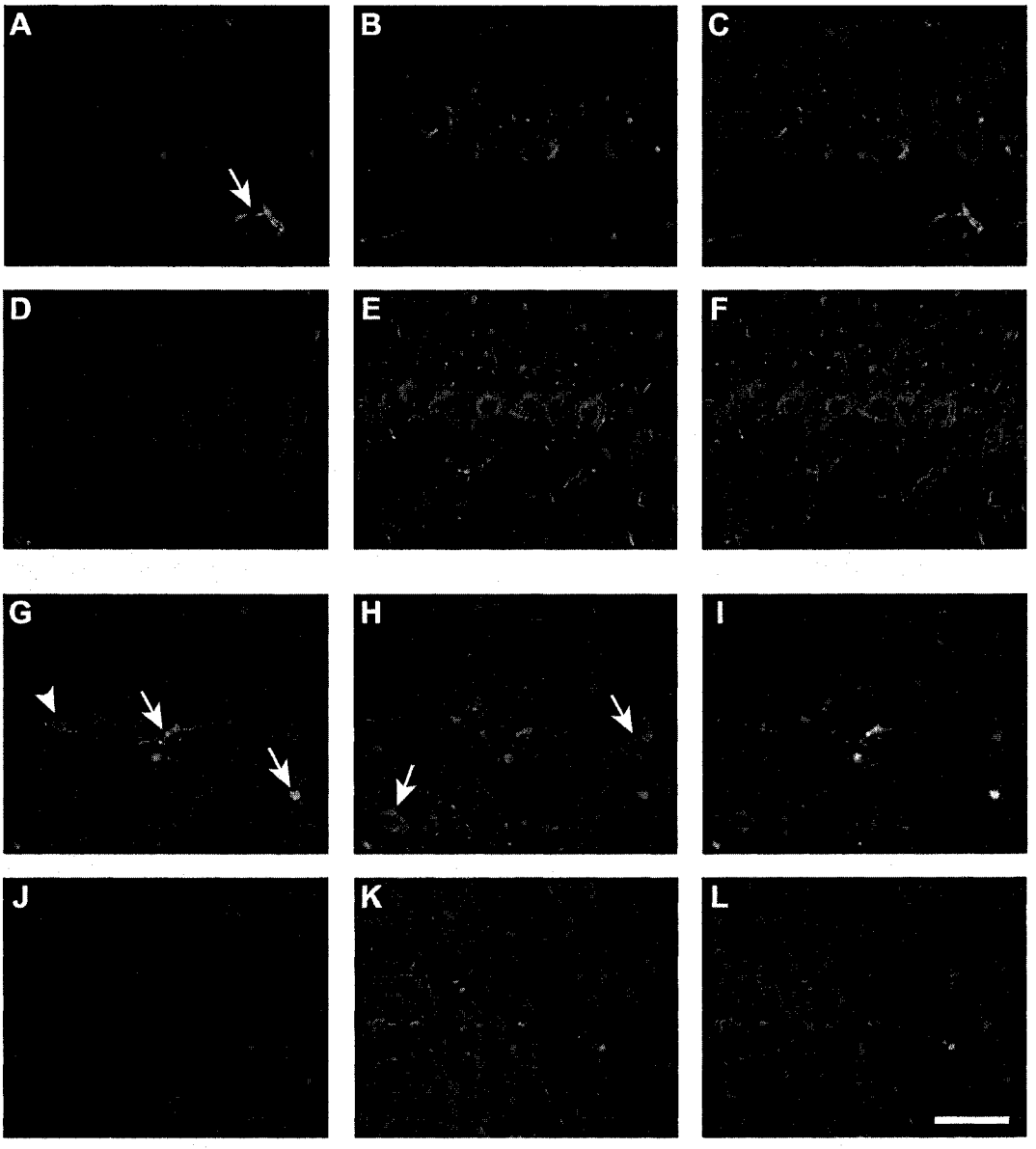
A
B
C
D
E
F
G
H
I
J
K
L

Figure 7

Astrocytes accumulate iron. **(A-F)** Double immunofluorescence labeling of cerebellar white matter at 24-months of age with anti-ferritin and anti-GFAP antibodies. Tissue section through the white matter of a $Cp^{-/-}$ mouse shows numerous ferritin-positive cells (A) that are double labeled with anti-GFAP (B), indicating that they are astrocytes. Panel C shows merged images of ferritin, GFAP and DAPI staining. The boxed area in C is shown at higher magnification in the insert. An occasional ferritin-positive cell is seen in the white matter of wildtype mouse (D). Note that the extent and intensity of the GFAP labeling is markedly diminished in the $Cp^{-/-}$ mouse compared to the wildtype (B and E). Panel F shows merged images of ferritin, GFAP and DAPI staining. Scale bar: F = 50μm; Insert in C = 20μm. **(G)** Western blot shows a reduction in GFAP in $Cp^{-/-}$ (KO) compared to control wildtype (Wt) mouse at 24 months of age.

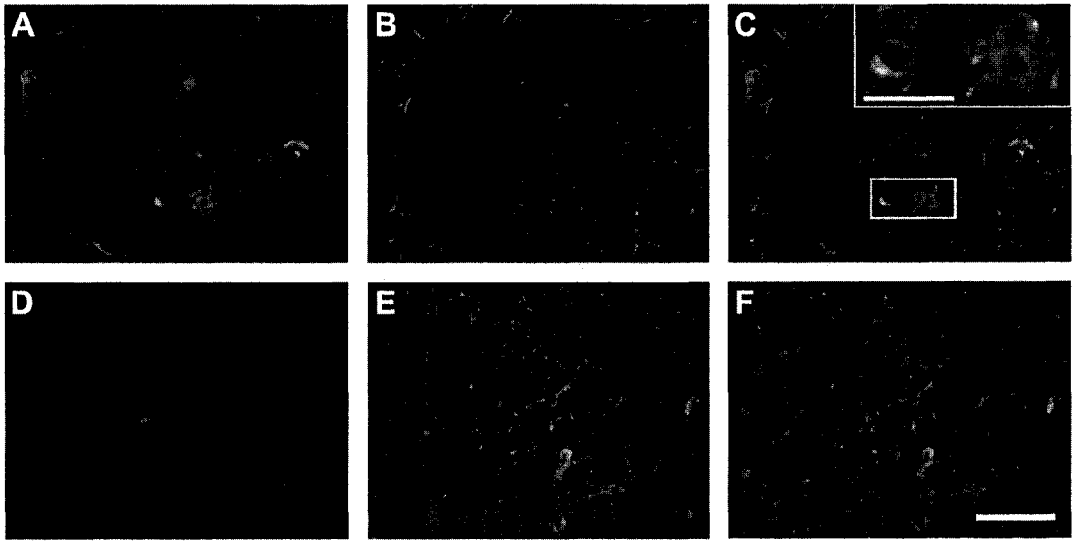
A
B
C
D
E
F

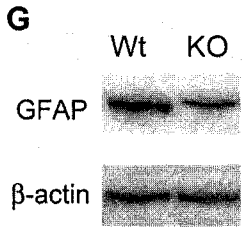
G
Wt
KO
GFAP
β-actin

Figure 8

Astrocyte loss in $Cp^{-/-}$ mice at 24 months. Tissue section though the cerebellar white matter of a $Cp^{-/-}$ mouse shows markedly reduced immunoreactivity for anti-GFAP (A) and S100β (B) as compared to wildtype mouse (D and E). The reduction in GFAP and S100β immunoreactivity in the $Cp^{-/-}$ mouse is associated with a reduction in the number of cells as seen with the DAPI staining (C) as compared to the wildtype mouse (F). The area above the dotted line in C and F is the white matter and below the line is the granule cell layer. Scale bar = 50μm. **(G)** Quantification of the $GFAP^{+}$, $S100\beta^{+}$ and GFAP/S100β double-labeled cells all show marked loss of astrocytes in $Cp^{-/-}$ mice (KO) compared to wildtype mice (Wt) at 24 months of age.

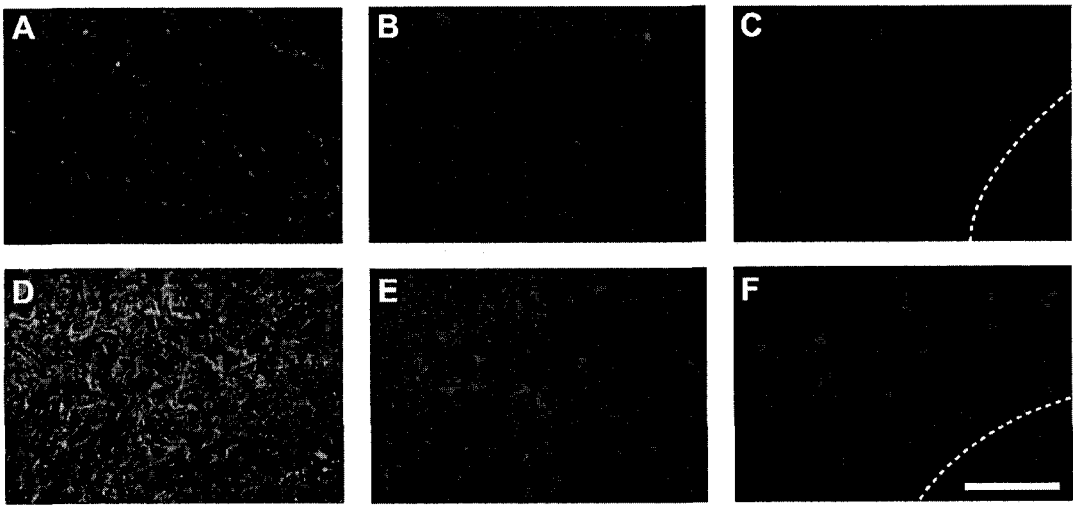
A
B
C
D
E
F

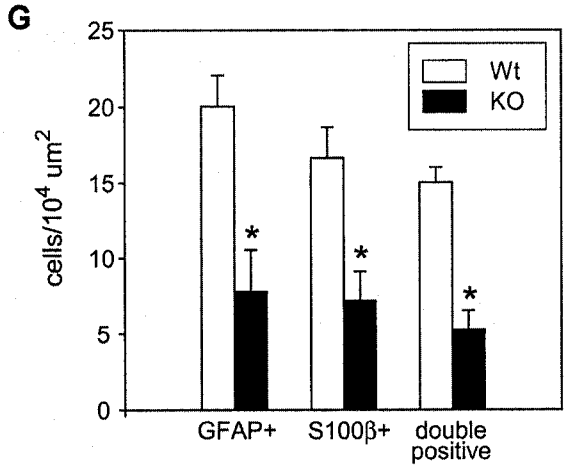
G
25
20
15
10
5
0
cells/10^4 um^2
Wt
KO
*
*
*
GFAP+
S100β+
double positive

Figure 9

Loss of Purkinje neurons in $Cp^{-/-}$ mice. SMI32 stained Purkinje neurons were quantified at 6, 12 and 24 months of age in both strains of mice. The number of Purkinje neurons begins to decrease in $Cp^{-/-}$ mice (KO) at 12 month of age as compared to wildtype mice (Wt), and is reduced further at 24 months of age ($*p < 0.05$; Student's *t* test).

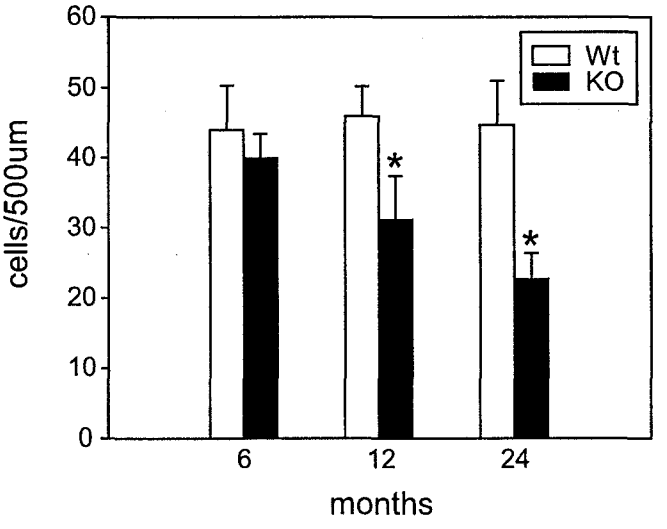
60
50
40
30
20
10
0
cells/500um
Wt
KO
*
*
6
12
24
months

Table 1 Gene-specific primers used in the study

Gene	Forward primer	Reverse primer	Probe
DMT1	TGAATCGGGCCAAT AAGCAGG A	TCAGCAAAGACGGA CACGACAA	TCCTGCATCGCGCTC TTTGTTTCCTT
DMT1 (+IRE)	ACAGCCCAGGAGAC CTTAAGAACA	ACCTTTGAACAAGCT CACCTCCGA	TAAGCCCTTTCGGGC CAAGTGCCTGTTA
DMT1 (-IRE)	TAGGCTGTGCTCAA ACCTACAGCA	TACATGACAGCCAG GCATGGTAGA	ACCTAAGCTCCTGA GTGCTGGGCCA
FPN	AGAGCTGACCTGGC ACCTTA	GGCCCAAGTCAGTG AAGGTA	AGGCAGAAAGCGGC CACA
TfR1	TGGCTCTCACACTCT CTCAGCTTT	AGGGCATTTGCGAC TCCCTGAATA	AAACCCTCTTCAGA AACCAGTTGGCCCT
CP	TGCTCTGAACCCGA GAAAGT	CTGGGAGGCTTCCA AATGTA	CCAGGAAAGCAACA GGATGT
HEPH	GCTGAGGGTCCTAA GGAATGGATA	GCCCACAGTACTTTG AGAAACAGG	CATGTGACTGTACCT GTGTTTCACCAGT
FTH	TAAAGAACTGGGTG ACCACGTGAC	AAGTCAGCTTAGCTC TCATCACCG	ATCTCTTTGACAAGC ACACCCTGGGA
FTL	TGGCCATGGAGAAG AACCTGAATC	GGCTTTCCAGGAAG TCACAGAGAT	TCTTGGATCTGCATG CCCTGGGTTCT
PPIA	AGCATACAGGTCCT GGCATC	TTCACCTTCCCAAAG ACCAC	AAGACTGAATGGCT GGATGG

CHAPTER 4

Alteration in Iron Homeostasis Contributes to Disease Progression in a Mouse Model of Amyotrophic Lateral Sclerosis

** The work presented in this chapter was performed by myself except for the sciatic nerve ligation experiment shown in Figure 8 which was done by another graduate student in the lab, Khizr. I. Rathore.

4.1 Preface

In the previous chapter, I showed abnormal iron accumulation and disruption of iron homeostasis during aging in *CP* null mice. Ceruloplasmin is a ferroxidase directly involved in maintaining iron homeostasis. There are also reports of abnormal iron accumulation in the CNS of neurodegenerative disease patients without mutations in iron homeostasis protein. In this chapter I examined disruption of iron homeostasis in a mouse model for Amyotrophic lateral sclesosis. This model is generated by overexpressing a mutant form of superoxide dismutase 1 (SOD1). Abnormal accumulation of iron in these mice and mechanism of how iron might be accumulated in the motor neurons are presented in this chapter.

4.2 Summary

Amyotrophic Lateral Sclerosis (ALS), which is characterized by degeneration of spinal motor neurons, consists of sporadic and familial forms. One of the known causes of familial ALS is missense mutations in the superoxide dismutase1 (*SOD1*) gene. There is evidence of iron accumulation in the CNS of both forms of ALS. However, the role of iron in the pathogenesis of the disease is still not clear. We examined the role of iron in a transgenic mouse line overexpressing the human $SOD1^{G37R}$ mutant. We show that iron accumulation occurs in the cell bodies of large spinal motor neurons as well as glia in the 12-month old transgenic mice but not in controls. Quantitative RT-PCR analysis of iron homeostasis proteins at 12-month (end-stage) and 4-month (pre-symptomatic) old mice showed that DMT1 and ferritin mRNA were markedly up-regulated, while there was moderate increase in ceruloplasmin (CP) and ferroportin (FPN) as compared to control mice. At 12 months, these differences were more pronounced in the cervical than in the lumbar cord. In contrast, at 4-months of age the lumbar region showed a greater increase in DMT1 and FPN mRNA, while no changes were detected in the cervical cord, suggesting a caudal to rostral alteration in the expression of iron homeostasis proteins corresponding with the caudal to rostral progression of the disease.

Immunofluorescence analysis showed increased DMT1 expression in neurons, while glia showed increased TfR1 expression. Interestingly, increased mitochondrial ferritin was detected in transgenic mice by Western blot and appeared by immunofluorescence to be high in spinal motor neurons and astrocytes. We also provide evidence that blockage of axonal transport, which occurs in human patients with ALS and *SOD1* transgenic mice, may contribute to the accumulation of iron in the neuronal

cytoplasm. Finally, we provide evidence that treatment of *SOD1*^{G37R} mice with a lipophilic iron chelator starting at 8 months of age extends lifespan by 4.8 weeks. This was accompanied by marked sparing of motor neurons in the spinal cord. These data provide evidence for the important involvement of iron in neurodegeneration and the progression of the disease in this transgenic mouse model of ALS.

4.3 Introduction

Amyotrophic lateral sclerosis (ALS) is one of the most common neurodegenerative disorders, characterized by progressive paralysis of skeletal muscles and degeneration of motor neurons in the spinal cord, brain stem, and cortex. Although 90% of the cases are of the sporadic form, the rest being familial, they share similar clinical and pathological features (reviewed in [1]). Discovery of genetic mutations in free radical-scavenging protein copper/zinc superoxide dismutase 1 (SOD1) in 20% of familial cases led to the generation of transgenic mouse models to study the disease [2, 3]. Mutant SOD1 causes cell death by as yet an unknown toxic gain-of-function effect [1, 2]. Several mechanisms for this toxicity have been suggested, including cytoskeletal abnormalities [4], glutamate toxicity [5], protein aggregation (reviewed in [6, 7]), oxidative stress (reviewed in [8]), mitochondrial dysfunction (reviewed in [4]), and extracellular SOD1 toxicity [9]. All of these factors may contribute to the pathogenesis of ALS.

High iron levels in the CNS of ALS patients have also been reported [10-12] but its contribution to the progression of the disease has not been studied. Iron is essential for life as it serves an important co-factor for various enzymes, such as those involved in DNA, RNA, and protein synthesis, mitochondrial oxidation reactions, neurotransmitter synthesis and a variety of other metabolic processes in many cellular processes. However, its redox active nature means that it can generate free radicals and cause cell damage if not properly regulated or shielded. Genetic disruptions of proteins involved in iron homeostasis cause neurodegeneration in the CNS (reviewed in [13, 14]). There is increased oxidative damage in both sporadic and familial ALS cases and also in animal models of ALS [15]. Whether this increase in oxidative damage is due to improperly

shielded copper from mutant SOD1 is not known, but no alteration of total copper is observed [16]. On the other hand, there are reports of high iron levels in the CNS of both familial and sporadic forms of ALS [10-12]. How and why iron accumulates and its contribution to the progression of the disease has not been studied.

Here we report that there is accumulation of iron in the spinal cord of *SOD1*^{G37R} transgenic mice, and show that disruption of iron homeostasis mechanisms accompanies the onset and progression of the disease. In addition we provide evidence that blockage of axonal transport may contribute to some of the iron accumulation seen in motor neurons. Furthermore, treatment with an iron chelator slows disease progression and extends life in this mouse model of ALS.

4.4 Experimental procedures

Animals. Heterozygous transgenic mice expressing G37R mutant *SOD1* (*SOD1*^{G37R}, line 29) and littermate wildtype mice obtained from Jackson Laboratories were used in this study. Mice were maintained on a C57Bl/6 background. All procedures used were approved by the McGill University Animal Care committee and followed the guidelines of the Canadian Council on Animal Care.

Iron histochemistry. *SOD1*^{G37R} and control mice were deeply anesthetized with ketamine:xylazine:acepromazine (50mg/ml: 5mg/ml: 1mg/ml) and perfused with 0.1 M phosphate buffer, followed by 4% paraformaldehyde in 0.1 M phosphate buffer, pH 7.2. Modified Perl's histochemistry was performed on 14 μm-thick cryostat sections of the spinal cords to detect iron accumulation as described previously [17]. Briefly, sections were incubated with 4% potassium ferrocyanide and 4% HCl, followed by a series of

incubations with diaminobenzidine and hydrogen peroxide and counterstained with 0.02% methyl green (all from Sigma-Aldrich, Oakville, Ontario, Canada).

Quantitative real-time reverse transcription-PCR. Total RNA was purified from cervical, thoracic and lumbar segments of the spinal cord using the RNeasy Lipid Tissue kit (Qiagen, Mississauga, Ontario, Canada), and quantitative real-time reverse transcription (QRT)-PCR was performed using the Brilliant Probe-based QRT-PCR Reagents and MX4000 (Stratagene, La Jolla, CA), both following the protocols of the manufacturer. Gene-specific primers and Taqman probes were used as previously described [18]. QRT-PCR for peptidylprolyl isomerase A (PPIA) was performed for use as an internal control [19]. For data analysis, the sample cycle threshold values were normalized to that of PPIA and expressed as fold increase. Results are shown as the mean relative ratio (fold increase) of mRNA ± SD of the mean from three separate experiments ($n = 3$). The two-sample Student's t test was used to determine statistical significance.

Western blotting. Spinal cord segments from *SOD1*^{G37R} and control mice were removed and total protein was extracted as described previously [20]. Proteins were separated by SDS-PAGE, transferred to polyvinylidene fluoride membrane (Millipore, Billerica, MA), and incubated with rabbit anti-FPN (1:4000; Alpha Diagnostics, San Antonio, TX), rabbit anti-DMT1 (1:4000; Alpha Diagnostics; recognizes both forms of DMT1), rabbit anti-TfR1 (1:500; Zymed, Burlington, Ontario, Canada), or rabbit anti-CP (1:1000, DakoCytomation, Carpinteria, CA). Blots were washed and incubated with peroxidase-conjugated IgG (1:200,000; Jackson ImmunoResearch, West Grove, PA) and detected with enhanced chemiluminescence (PerkinElmer). Equal loading of proteins was assessed using rabbit anti-β actin antibodies (1:400; Sigma-Aldrich).

Double immunofluorescence. *SOD1*^{G37R} and control mice were deeply anesthetized as above and perfused with 0.1 M phosphate buffer, followed by 4% paraformaldehyde in 0.1 M phosphate buffer, pH 7.2, and 14μm cryostat sections were obtained. Double-immunofluorescence labeling of tissue sections was performed as described previously [18]. Briefly, the tissue sections were incubated with PBS containing 2% normal goat serum and 1% ovalbumin to block nonspecific binding of antibodies. This was followed by an overnight incubation with rabbit anti-DMT1 antibody or rabbit anti-FPN antibody (1:400; both from Alpha Diagnostics) or a rabbit anti-ferritin antibody (1:100; DakoCytomation) or a rabbit anti-mitochondrial ferritin antibody (1:100, from Dr. Paolo Arosio, University of Brescia, Brescia, Italy). After washing, the tissue sections were incubated with either monoclonal anti-GFAP for astrocytes (1:100; Sigma-Aldrich) or NeuN (for neurons, Chemicon, Temecula, CA) or Mac-1 (for macrophages, 1:200) as a cell specific marker. The binding of antibodies was visualized with either fluorescein or rhodamine-conjugated secondary antibodies (1:200; Jackson ImmunoResearch). Sections were also counterstained with 100 ng/ml 4'-6-diamidino-2-phenylindole (DAPI) (Vector Laboratories, Burlingame, CA) and viewed with a Zeiss (Toronto, Ontario, Canada) Axioskop 2 plus microscope.

Immunohistochemistry. Vectastain ABC kit (Vector Laboratories, Burlingame, CA) was used to detect transferrin receptor 1 (TfR1) expression due to its low abundance in the CNS. TfR1 was stained in the tissue samples using a monoclonal anti-TfR1 antibody (1: 200, Zymed) and a goat anti-mouse biotinylated secondary antibody (1:400; Jackson Immunoresearch). Binding of the primary antibody was visualized by using diaminobenzidine (DAB) as the chromogen.

Sciatic Nerve Ligation. Three-month old C57BL/6 mice were deeply anesthetized as above and the left sciatic nerve cut and ligated at the mid-thigh level. The right sciatic nerve was exposed and closed to serve as a sham control. After 30 days, animals were perfused with fixative as described above and Perl's immunohistochemistry for iron was performed to detect iron in the lumbar spinal cord. The large ventral horn motor neurons were examined on both the ligated and control sides.

Gel retardation assay. A gel retardation assay was performed to assess the interaction between IRPs and IREs following an established technique [18, 21]. Briefly, 30μg of total protein extract of cervical spinal cord segment from 12-month-old $SOD1^{G37R}$ and wildtype mice was mixed with ^{32}P-labeled ferritin IRE RNA probe (obtained from Dr. K. Pantopoulos, McGill University, Montreal, Quebec, Canada), which was transcribed *in vitro* from a linearized plasmid template using T7 RNA polymerase. The samples were incubated for 10 min at room temperature with heparin (5 mg/ml) to prevent nonspecific binding. Unbound probe was degraded by a 10 min incubation with RNase T1. The formation of RNA–protein complexes was then detected by gel electrophoresis using 6% non-denaturing polyacrylamide gels. The gels were scanned with a STORM860 (phosphoimager) and analyzed with ImageQuant for densitometry (GE Healthcare, Uppsala, Sweden).

Mitochondrial ferritin. Spinal cords from 12-month old $SOD1^{G37R}$ transgenic and wildtype mice were processed immediately for mitochondrial purification using the Mitochondria Isolation kit for Tissue (Pierce, Rockford, IL) following the manufacturer's protocol. Isolation of purified mitochondria was verified on Western blots with the anti-COX IV antibody (1:1000, Cell Signaling). The mitochondrial preparation was then

solublized in 2% SDS and 40μg of the protein samples were loaded on to each lane and separated on 4-12% SDS-PAGE and blotted on to PVDF membranes. The membranes were incubated with a rabbit anti-mitochondrial ferritin antibody (1:500, from Dr. Paolo Arosio, University of Brescia, Brescia, Italy).

Iron Chelator Treatments and blood sample analysis. *SOD1*^{G37R} mice were treated with the iron chelator salicylaldehyde isonicotinoyl hydrazone (SIH) as previously described [22]. Briefly, the SIH solution (50mg/kg) was prepared fresh every time and used within 30min. Mice (n=12) were injected intraperitoneally starting at 8 months of age and treated either once or twice a week. The control group of mice were treated with the vehicle solution (SIH). n=18. Analysis of survival was carried out blind. The survival of the mice was analyzed by plotting Kaplan-Meier graphs. Two-way ANOVA was used to determine statistical significance. Blood samples from different groups of mice (n=4 for each group) were collected via the heart at the end of experiments and a full blood analysis was done by the McGill University Animal Resources Centre's Diagnostic and Research Support Service.

Histological analysis of motor neuron survival after SIH treatment. SIH and vehicle treated mice were sacrificed at 50 weeks of age (end-stage for the vehicle treated mice) by intracardiac perfusion with 4% paraformaldehyde. The spinal cord segments were removed and frozen 14μm thick tissue sections were obtained on gelatin-coated glass slides. The tissue sections were stained with 0.1% cresyl violet and the survival of the motor neurons was examined in the lumbar, thoracic and cervical segments.

4. 5 Results

Two different patterns of iron accumulation in motor neurons and glia. We first examined whether there is iron accumulation in the spinal cord of *SOD1*^{G37R} transgenic mice. At 12 months of age, we detected iron accumulation in the cell bodies of the large ventral horn motor neurons (Figure 1C-D, G-I), while no such accumulation was detected in wildtype mice of the same age (Figure 1A-B, E-F). The iron staining in these neurons appeared to be small, rounded cytoplasmic inclusions (Figure 1G-I). In addition, some glial cells in the gray and white matter were also positive for iron, showing a more diffuse type of labeling of the entire cell (Figure 2C-E).

Dysregulation of expression of iron homeostasis proteins. As cellular iron levels are regulated by a number of proteins involved in iron transport and storage we next assessed their expression in *SOD1*^{G37R} transgenic and wildtype mice.

***(i) Transporters and ferroxidases*:** We first assessed the mRNA expression of three iron transporters (divalent metal transporter1 [DMT1], transferrin receptor 1 [TfR1] and iron exporter [FPN]) and two ferroxidases (ceruloplasmin [CP] and hephaestin [HEPH]) in the cervical, thoracic and lumbar regions by quantitative real-time RT-PCR (QRT-PCR). This was first done at the end-stage of the disease, namely 12 months of age. A striking finding is that there is a caudal to rostral gradient in the mRNA levels of these molecules with the highest levels being rostrally in the cervical region (Figure 3A). DMT1 mRNA transcripts with (+IRE) and without (-IRE) iron response elements are found in the CNS. In the cervical region, there was about a 5-fold increase in DMT1 (-IRE) mRNA, while the DMT1 (+IRE) and TfR1 showed about a 1.6-fold increase (Figure 3A). In contrast, in

the lumbar region the mRNA levels of DMT1 (–IRE) and TfR1 were below the normal range. The increase in DMT1 (-IRE) mRNA suggests that factors other than cellular iron levels play a role in regulating their expression. On the other hand the small but significant increase in TfR1 mRNA which contain IREs suggest that changes in intracellular iron levels may also play a role in regulating the expression of some of these iron homeostasis genes.

The iron exporter FPN also showed a caudal to rostral gradient with ~3.5-4-fold increase in the cervical region and a 2-fold increase in the lumbar region (Figure 3A). A similar caudal to rostral pattern was also seen with the mRNA expression of the ferroxidase, ceruloplasmin in 12 month old $SOD1^{G37R}$ transgenic mice (Figure 3A). The cervical region showed a 3.5-fold increase while in the lumbar region the levels were below 2-fold and not statistically significant. No changes were detected in the expression of hephaestin, a ceruloplasmin homologue (data not shown).

The caudal to rostral pattern of mRNA expression described above, correlates with the caudal to rostral progression of neurodegeneration and functional disability in the $SOD1^{G37R}$ transgenic mice. Since the neurodegeneration is not yet fully underway in the cervical and thoracic spinal cord at 12 months of age, while it is well-advanced in the lumbar region, we reasoned that there would be a reverse gradient in mRNA expression of these iron homeostasis proteins at 4 months of age (pre-symptomatic stage). As expected at 4 months of age, the mRNA expression of DMT1 (-IRE) and FPN was highest in the lumbar region (3.5-fold for DMT1 (-IRE) and 2-fold for FPN, Figure 3B) and lowest in the cervical region (both unchanged). At this age, DMT1 (+IRE) mRNA did not show changes in any region, while TfR1 mRNA was slightly reduced in the

lumbar and thoracic regions (Figure 3B). As the relative increase in DMT1 mRNA appears to be higher than that of FPN, this dysregulation may contribute to an overall increase in iron uptake into cells in the spinal cord of $SOD1^{G37R}$ transgenic mice. At 4 months, CP was also highest in the lumbar region (Figure 3B).

The increased expression of DMT1, FPN and CP in the cervical cord at 12 months of age was also confirmed by Western blot analysis (Figure 4). The increase in DMT1 was ~2-fold greater than that of FPN and CP. However, no difference in TfR1 protein expression was detected in $SOD1^{G37R}$ transgenic mice by Western blot analysis.

We next carried out double immunofluorescence labeling to examine which cells in the spinal cord upregulate expression of DMT1 and FPN in $SOD1^{G37R}$ transgenic and wildtype mice at 12 months of age. The expression of DMT1 was increased in motor neurons (Figure 5D-E) in the ventral horn of the spinal cord as well as in some GFAP+ astrocytes (data not shown). FPN, however was increased in motor neurons (Figure 5J-K) as well as in other cells possibly glia. On the other hand, TfR1 expression was reduced in the large motor neurons but increased in glia (Figure 6). This experiment was done using an HRP-conjugated secondary antibody and DAB enhancement method due to the low abundance of TfR1 in the CNS. Since the mRNA data showed that the change in DMT1 was in the –IRE transcripts, these data suggest that inflammatory mediators such as cytokines might increase the expression of this iron importer in neurons, while the IRE/IPR mechanism may underlie the increases in the other iron importer TfR1 in glia.

(ii) ***Iron storage protein ferritin*:** Ferritin is a sensitive indicator of cellular iron status and increase in ferritin reflects iron accumulation. A similar caudal to rostral pattern of

increasing mRNA expression was also seen with ferritin heavy (FTH) and light (FTL) chains in 12 month old *SOD1*^{G37R} transgenic mice (Figure 7A). In the cervical region there is a 4-fold increase in FTH and a 9-fold increase in FTL, while their levels in the lumbar region were either reduced (FTH) or unchanged (FTL). Double immunofluorescence labeling showed that increased cytosolic ferritin expression was seen in glia, mainly microglia and some astrocytes, but not in neurons (Figure 7E-F, K-L). The morphology of iron positive inclusions along with the lack of cytosolic ferritin staining in motor neurons suggests that these inclusions are not due to iron stored in cytosolic ferritin, but some other cytosolic compartment that is not recognized by the IRE/IRP mechanism. These data also suggest that in *SOD1*^{G37R} transgenic mice neurons and glia accumulate iron via different mechanisms: glia via TfR1 and ferritin and neurons via DMT1. Another factor that can influence the accumulation of iron in the large motor neurons in *SOD1*^{G37R} transgenic mice is disruption of axonal transport.

Iron accumulation induced by disruption of anterograde axonal transport. Since alteration of axonal transport is reported in ALS and in the *SOD1* transgenic mice [23-25], we assessed whether disruption of axonal transport will result in accumulation of iron in the neuronal cell bodies. To test this we ligated the sciatic nerve on one side in adult mice (Figure 8A). After 30 days, the spinal cord was assessed for iron accumulation using Perl's histochemistry. Large ventral horn motor neurons on the ligated side showed granular iron accumulation in the cell bodies (Figure 8B). The ventral horn neurons on the control side did not show any signs of iron accumulation (data not shown). These data suggest strongly that blockade of axonal transport which is known to occur in the

experimental model of ALS is also likely to contribute to the iron accumulation in the motor neurons in *SOD1*^{G37R} transgenic mice.

Changes in the iron regulatory system. Another mechanism that increases iron uptake into cells is binding of iron regulatory protein (IRP) to IREs, which regulate the mRNA levels of several iron homeostasis proteins including TfR1 mRNA. We have seen the increase of TfR1 mRNA in the cervical and thoracic regions in 12-month old *SOD1*^{G37R} transgenic mice. Recent *in vitro* studies have shown that transfection of mutant SOD1 (*SOD1*^{G93A}) into a human astrocytoma cell line led to an increase in TfR1 expression and increases in IRP1 [26]. We therefore carried out an electromobility gel-shift assay to assess the IRP1 levels in the spinal cord of 12-month old *SOD1*^{G37R} transgenic mice. An approximately 2-fold increase in IRP1 was seen in the spinal cord of *SOD1*^{G37R} transgenic mice as compared to wildtype controls (Figure 9). This change in the IRP1 binding activity is specific for spinal cords from *SOD1* transgenic mice, as no difference is seen in the liver. Since TfR1 is increased in glia not neurons, the increased IRP1 is likely to underlie the increased accumulation of iron in glia.

Increase in mitochondrial iron in *SOD1*^{G37R} mice. A number of lines of evidence indicate mitochondrial abnormalities in the spinal cord in ALS and in transgenic mice expressing different SOD1 mutants [27-31]. Mutant SOD1 has also been shown to preferentially associate with spinal cord mitochondria via tight association or cross-linking to the outer mitochondrial membrane [32]. Additionally, the *SOD1*^{G37R} mutant protein was found to also be associated with the inner mitochondrial membrane,

suggesting abnormal import of this mutant protein into the mitochondria [32]. Such association of the mutant SOD1 protein with mitochondrial membranes is thought to lead to disruption of mitochondrial function [32]. Much of the iron that normally enters cells is likely to be transported to the mitochondria as it is the site of generation of iron-sulfur clusters [33-35]. Iron-sulfur clusters which serve as important co-factors are inserted into mitochondrial proteins such as those of the oxidative chain or exported into the cytosol for incorporation into proteins and enzymes that serve a variety of metabolic functions [33, 35]. *In vitro* studies have shown that over-expression of $SOD1^{G37R}$ causes increases in mitochondrial superoxide and a shift in the redox potential [36, 37]. Furthermore, *in vitro* work has also shown that oxidation of iron-sulfur clusters by superoxide can cause release of iron [38]. Therefore, breakdown of iron-sulfur clusters in the mitochondria could lead to accumulation of iron in mitochondria. It is also possible that abnormal breakdown of ferritin in neurons within lysosomes may make more iron available to mitochondria. We therefore assessed if there is iron accumulation in mitochondria in the spinal cord of 12-month old $SOD1^{G37R}$ mice. As ferritin is a very sensitive indicator of iron status, we carried out Western blot analysis for mitochondrial ferritin. Mitochondria were purified by subcellular fractionation from the spinal cord of 12-month old $SOD1^{G37R}$ and wildtype mice. There was a 2-fold increase in mitochondrial ferritin in the $SOD1^{G37R}$ mice as compared to the wildtype (Fig 10A). Additionally, immunofluorescence staining with this antibody showed that there was indeed a marked increase in mitochondrial ferritin in the ventral horn motor neurons and astrocytes in 12-month old $SOD1^{G37R}$ transgenic mice as compared to wildtype mice of the same age (Figure 10E-F, K-L). These data suggest that there is a significant increase in mitochondrial iron accumulation

in the motor neurons in the spinal cord in this mouse model of ALS. Iron accumulation in mitochondria could lead to neurodegeneration in these mice as occurs in Fredrick's ataxia which results from mutations in the mitochondrial protein frataxin [39].

Protective effects of iron chelator treatment. As there is disruption of iron homeostasis and iron accumulation in $SOD1^{G37R}$ transgenic mice, we assessed the effects of an iron chelator on the progression of the disease. The high affinity, lipophilic iron chelator, salicylaldehyde isonicotinoyl hydrazone (SIH) [22, 40] was administered intraperitoneally starting at 8 months (late pre-symptomatic age) at two dosing regimens. When SIH (50mg/kg) treatment was started at 8 months of age and given once a week, it increased the average life span by 3.5 weeks (Figure 11A; 49.56±1.89 vs 53.08±2.54 weeks, $p<0.01$). Furthermore, when SIH was given twice a week starting at 8 months of age, the average life span increased by 4.8 weeks (Figure 11A, 54.42±2.84, $p<0.01$), showing a dose-dependent effect. There were more surviving neurons at 50 weeks in SIH treated $SOD1^{G37R}$ transgenic mice compared to the wildtypes (Figure 11B). This four-month treatment was well tolerated, as these mice did not show hematological signs of anemia (Table 1). These data provide strong evidence that the disruption of iron homeostasis and increased iron accumulation in the CNS contributes to the progression of the disease in $SOD1^{G37R}$ transgenic mice.

4. 6 Discussion

We have studied the role of iron in the progression of disease in *SOD1*^{G37R} transgenic mice, a mouse model of ALS. We show that iron accumulation occurs in both neurons and glia in 12 month-old transgenic mice but not in wildtype controls of the same age. We also show that the expression of the iron importer DMT1 is increased in neurons while TfR1 is increased in glia. We also provide evidence that disruption of anterograde axonal transport in wildtype mice leads to iron accumulation in the cell bodies of the large motor neurons in the spinal cord and may also contribute to iron accumulation in the motor neurons in *SOD1*^{G37R} transgenic mice. We assessed IRP1 binding activity in the spinal cord of *SOD1*^{G37R} transgenic mice by electromobility shift assays and show that it is increased compared to wildtype mice. Increased mitochondrial ferritin was also detected in the spinal cord of transgenic mice indicating increased iron load in mitochondria. Excess mitochondrial iron may lead to free radical damage and dysfunction of mitochondrial metabolism. Finally, the ability of the iron chelator treatment to increase the lifespan of the *SOD1*^{G37R} transgenic mice provides clear evidence of the important detrimental role of iron in the pathogenesis of this disease.

Iron accumulation in the CNS of ALS and *SOD1*^{G37R} transgenic mice. There is evidence from the clinical literature of iron accumulation in the CNS of patients with ALS [10-12]. Although this has been known for some time, direct evidence of a role for iron in ALS has not been demonstrated thus far. Our data provides clear evidence that iron accumulation occurs in both neurons and glia but that different molecular mechanisms may contribute to iron accumulation in these two cellular compartments. In

glia the increase in TfR1 that is likely to be mediated by the increase in IRP1 may underlie the influx of iron at later stages of the disease. Normally, IRP1 would be expected to concomitantly reduce the expression of ferritin [41]. However, ferritin expression appears to go up mainly in microglia, which likely acquire this iron from phagocytosis of dead and dying cells. Ferritin expression has also been reported to be increased by pro-inflammatory cytokines or nitric oxide [42-46]. Since inflammation and increased cytokine expression have been reported in the spinal cord of SOD1 transgenic mice, this may underlie the increase of ferritin in microglia. The increased ferritin would lead to increased iron storage in cells. We have shown previously that astrocytes in *CP* null mice lose their ability to efflux iron [20]. Although these astrocytes markedly increase their expression of ferritin, iron-mediated toxicity eventually leads to cell death [18].

In contrast to glia, neurons in the $SOD1^{G37R}$ transgenic mice show increased expression of the DMT1 mRNA transcripts without IRE. Such transcripts are not regulated by changes in iron levels but by other factors such as pro-inflammatory cytokines, which are known to be increased in the spinal cord of $SOD1^{G37R}$ transgenic mice [47-50]. The iron efflux transporter FPN is also increased in neurons in these mice, however, the relative level of expression appears to be lower than that of DMT1. Although we do not know what relative levels of FPN and DMT1 are required to maintain normal levels of cellular iron, it is possible that the greater increase in DMT1 might contribute, in part, to the iron accumulation in neurons. Another factor that may contribute to iron accumulation in the motor neurons in the ventral horn is blockage of axonal transport. A variety of structural, metabolic and synaptic elements are transported

down the axon by anterograde transport. However, there has only been indirect evidence to suggest that iron may be transported down the axon by anterograde transport. This includes evidence that FPN is expressed in synaptic vesicles [51], and evidence of axonal ferritin staining in IRP2 null mice [52]. We now provide direct evidence that blockage of anterograde axonal transport in the sciatic nerve of wildtype mice by cut and ligation results in iron accumulation in the cell bodies of the ventral horn motor neurons. These results suggest that iron that is transported anterogradely down the axon gets returned back to the cell body via retrograde transport after being blocked at the site of ligation. Previous reports have shown that axonal aggregate formation disrupts axonal transport in ALS as well as in the transgenic mouse models [23-25]. Increased mitochondria and lysosomal accumulation has also been reported to occur in the proximal axon in ALS patients [25]. This retrogradely transported ferritin-bound iron might end up in lysosomes where ferritin gets degraded [53] and iron is released. It has also been suggested that abnormal accumulation of ubiquitinated, misfolded proteins might affect the normal proteasomal machinery and protein degradation. Lysosomal enzyme activity has been reported to be decreased in ALS [54]. Therefore, altered axonal transport of iron and proteasomal malfunction in the neurons in *SOD1*^{G37R} transgenic mice might cause the vesicular accumulation of iron that is seen in neurons.

Mechanisms of iron mediated toxicity in *SOD1*^{G37R} transgenic mice. Cells maintain iron homeostasis by regulating both influx and efflux of iron, which appear to be disrupted in *SOD1*^{G37R} transgenic mice. Mutant SOD1 can form non-soluble aggregates and specifically bind to the mitochondrial membrane in the spinal cord [32]. These

authors suggested that these aggregates may disrupt the mitochondrial import machinery and that mitochondrial dysfunction may contribute to the pathogenesis of the disease. Our current work indicates that this may also involve disruption of mitochondrial iron homeostasis leading to iron accumulation in mitochondria and iron-mediated toxicity. Mitochondria are the main sites of generation of iron-sulfur clusters, which are incorporated into a variety of proteins and serve as important co-factors for numerous enzymes [55, 56]. One important Fe-S cluster containing protein that is involved in maintaining iron homeostasis is IRP1, which is a bifunctional protein that also serves as cytosolic aconitase. When iron is low, break down of the Fe-S cluster in aconitase causes a conformational change that transforms it to IPR1, which binds to IREs. Binding of IRP1 to IRE causes more Fe influx into cells by stabilizing the mRNA of the iron importer TfR1. Disruption of mitochondrial Fe-S assembly or blockage of transport across the mitochondrial membrane would cause deprivation of Fe-S clusters in the cytosol and generate constitutively active IRP1 in its IRE binding form and lead to faulty iron sensing.

Over-expression of $SOD1^{G37R}$ can also cause an increase in mitochondrial superoxide levels and shift in the redox potentials *in vitro* [36, 37]. Moreover, *in vitro* studies have shown that superoxide can cause oxidation of Fe-S clusters and cause release of iron [38]. Therefore, breakdown of Fe-S clusters in the mitochondria can cause accumulation of iron in mitochondria. Mitochondrial iron is increased as reflected by increases in mitochondrial ferritin (Figure 10). In addition, such superoxide-mediated breakdown of Fe-S in the cytosol could also generate more of the active form of IRP1 (Figure 9). This loss in the ability to sense cellular iron levels would lead to more iron uptake and iron accumulation in cells.

The marked increase in mitochondrial ferritin in the spinal cord of $SOD1^{G37R}$ transgenic mice is an indication of mitochondrial iron accumulation. We have seen this increase of mitochondrial ferritin in both neurons and glia. Treatment with the iron chelator provides strong evidence of the important role of iron-mediated toxicity in the progression of the disease. The enhancement of lifespan by 4.8 weeks in the slow progressing $SOD1^{G37R}$ transgenic line is better than any single therapy reported thus far. Better survivals have only been seen with the use of multiple combination therapies [57]. Our work now provides a strong rationale for the inclusion of iron chelator therapy for the treatment of ALS.

4. 7 References

1. Boillee, S., C. Vande Velde, and D.W. Cleveland, *ALS: a disease of motor neurons and their nonneuronal neighbors.* Neuron, 2006. **52**(1): p. 39-59.
2. Julien, J.P. and J. Kriz, *Transgenic mouse models of amyotrophic lateral sclerosis.* Biochim Biophys Acta, 2006. **1762**(11-12): p. 1013-24.
3. Rosen, D.R., et al., *Mutations in Cu/Zn superoxide dismutase gene are associated with familial amyotrophic lateral sclerosis.* Nature, 1993. **362**(6415): p. 59-62.
4. Williamson, T.L., et al., *Absence of neurofilaments reduces the selective vulnerability of motor neurons and slows disease caused by a familial amyotrophic lateral sclerosis-linked superoxide dismutase 1 mutant.* Proc Natl Acad Sci U S A, 1998. **95**(16): p. 9631-6.
5. Rothstein, J.D., *Excitotoxicity and neurodegeneration in amyotrophic lateral sclerosis.* Clin Neurosci, 1995. **3**(6): p. 348-59.
6. Julien, J.P., *Amyotrophic lateral sclerosis. unfolding the toxicity of the misfolded.* Cell, 2001. **104**(4): p. 581-91.
7. Ross, C.A. and M.A. Poirier, *Protein aggregation and neurodegenerative disease.* Nat Med, 2004. **10 Suppl**: p. S10-7.
8. Barber, S.C., R.J. Mead, and P.J. Shaw, *Oxidative stress in ALS: a mechanism of neurodegeneration and a therapeutic target.* Biochim Biophys Acta, 2006. **1762**(11-12): p. 1051-67.
9. Urushitani, M., S.A. Ezzi, and J.P. Julien, *Therapeutic effects of immunization with mutant superoxide dismutase in mice models of amyotrophic lateral sclerosis.* Proc Natl Acad Sci U S A, 2007. **104**(7): p. 2495-500.

10. Imon, Y., et al., *Low intensity areas observed on T2-weighted magnetic resonance imaging of the cerebral cortex in various neurological diseases.* J Neurol Sci, 1995. **134 Suppl**: p. 27-32.

11. Kasarskis, E.J., et al., *Aluminum, calcium, and iron in the spinal cord of patients with sporadic amyotrophic lateral sclerosis using laser microprobe mass spectroscopy: a preliminary study.* J Neurol Sci, 1995. **130**(2): p. 203-8.

12. Oba, H., et al., *Amyotrophic lateral sclerosis: T2 shortening in motor cortex at MR imaging.* Radiology, 1993. **189**(3): p. 843-6.

13. Ponka, P., *Hereditary causes of disturbed iron homeostasis in the central nervous system.* Ann N Y Acad Sci, 2004. **1012**: p. 267-81.

14. Zecca, L., et al., *Iron, brain ageing and neurodegenerative disorders.* Nat Rev Neurosci, 2004. **5**(11): p. 863-73.

15. Carri, M.T., et al., *Neurodegeneration in amyotrophic lateral sclerosis: the role of oxidative stress and altered homeostasis of metals.* Brain Res Bull, 2003. **61**(4): p. 365-74.

16. Subramaniam, J.R., et al., *Mutant SOD1 causes motor neuron disease independent of copper chaperone-mediated copper loading.* Nat Neurosci, 2002. **5**(4): p. 301-7.

17. Smith, M.A., et al., *Iron accumulation in Alzheimer disease is a source of redox-generated free radicals.* Proc Natl Acad Sci U S A, 1997. **94**(18): p. 9866-8.

18. Jeong, S.Y. and S. David, *Age-related changes in iron homeostasis and cell death in the cerebellum of ceruloplasmin-deficient mice.* J Neurosci, 2006. **26**(38): p. 9810-9.

19. Feroze-Merzoug, F., et al., *Peptidylprolyl isomerase A (PPIA) as a preferred internal control over GAPDH and beta-actin in quantitative RNA analyses.* Biotechniques, 2002. **32**(4): p. 776-8, 780, 782.

20. Jeong, S.Y. and S. David, *Glycosylphosphatidylinositol-anchored ceruloplasmin is required for iron efflux from cells in the central nervous system.* J Biol Chem, 2003. **278**(29): p. 27144-8.

21. Kim, S. and P. Ponka, *Control of transferrin receptor expression via nitric oxide-mediated modulation of iron-regulatory protein 2.* J Biol Chem, 1999. **274**(46): p. 33035-42.

22. Klimtova, I., et al., *A study of potential toxic effects after repeated 10-week administration of a new iron chelator--salicylaldehyde isonicotinoyl hydrazone (SIH) to rabbits.* Acta Medica (Hradec Kralove), 2003. **46**(4): p. 163-70.

23. Williamson, T.L. and D.W. Cleveland, *Slowing of axonal transport is a very early event in the toxicity of ALS-linked SOD1 mutants to motor neurons.* Nat Neurosci, 1999. **2**(1): p. 50-6.

24. Zhang, B., et al., *Neurofilaments and orthograde transport are reduced in ventral root axons of transgenic mice that express human SOD1 with a G93A mutation.* J Cell Biol, 1997. **139**(5): p. 1307-15.

25. Sasaki, S. and M. Iwata, *Impairment of fast axonal transport in the proximal axons of anterior horn neurons in amyotrophic lateral sclerosis.* Neurology, 1996. **47**(2): p. 535-40.

26. Danzeisen, R., et al., *Superoxide dismutase 1 modulates expression of transferrin receptor.* J Biol Inorg Chem, 2006. **11**(4): p. 489-98.

27. Bendotti, C., et al., *Early vacuolization and mitochondrial damage in motor neurons of FALS mice are not associated with apoptosis or with changes in cytochrome oxidase histochemical reactivity.* J Neurol Sci, 2001. **191**(1-2): p. 25-33.

28. Jaarsma, D., et al., *Human Cu/Zn superoxide dismutase (SOD1) overexpression in mice causes mitochondrial vacuolization, axonal degeneration, and premature motoneuron death and accelerates motoneuron disease in mice expressing a familial amyotrophic lateral sclerosis mutant SOD1.* Neurobiol Dis, 2000. **7**(6 Pt B): p. 623-43.

29. Kong, J. and Z. Xu, *Massive mitochondrial degeneration in motor neurons triggers the onset of amyotrophic lateral sclerosis in mice expressing a mutant SOD1.* J Neurosci, 1998. **18**(9): p. 3241-50.

30. Wong, P.C., et al., *An adverse property of a familial ALS-linked SOD1 mutation causes motor neuron disease characterized by vacuolar degeneration of mitochondria.* Neuron, 1995. **14**(6): p. 1105-16.

31. Hervias, I., M.F. Beal, and G. Manfredi, *Mitochondrial dysfunction and amyotrophic lateral sclerosis.* Muscle Nerve, 2006. **33**(5): p. 598-608.

32. Liu, J., et al., *Toxicity of familial ALS-linked SOD1 mutants from selective recruitment to spinal mitochondria.* Neuron, 2004. **43**(1): p. 5-17.

33. Lill, R., et al., *Mechanisms of iron-sulfur protein maturation in mitochondria, cytosol and nucleus of eukaryotes.* Biochim Biophys Acta, 2006. **1763**(7): p. 652-67.

34. Napier, I., P. Ponka, and D.R. Richardson, *Iron trafficking in the mitochondrion: novel pathways revealed by disease.* Blood, 2005. **105**(5): p. 1867-74.

35. Rouault, T.A. and W.H. Tong, *Iron-sulphur cluster biogenesis and mitochondrial iron homeostasis.* Nat Rev Mol Cell Biol, 2005. **6**(4): p. 345-51.

36. Ferri, A., et al., *Familial ALS-superoxide dismutases associate with mitochondria and shift their redox potentials.* Proc Natl Acad Sci U S A, 2006. **103**(37): p. 13860-5.

37. Zimmerman, M.C., L.W. Oberley, and S.W. Flanagan, *Mutant SOD1-induced neuronal toxicity is mediated by increased mitochondrial superoxide levels.* J Neurochem, 2007.

38. Liochev, S.I. and I. Fridovich, *The role of O2.- in the production of HO.: in vitro and in vivo.* Free Radic Biol Med, 1994. **16**(1): p. 29-33.

39. Campuzano, V., et al., *Friedreich's ataxia: autosomal recessive disease caused by an intronic GAA triplet repeat expansion.* Science, 1996. **271**(5254): p. 1423-7.

40. Cheah, J.H., et al., *NMDA receptor-nitric oxide transmission mediates neuronal iron homeostasis via the GTPase Dexras1.* Neuron, 2006. **51**(4): p. 431-40.

41. Pantopoulos, K., *Iron metabolism and the IRE/IRP regulatory system: an update.* Ann N Y Acad Sci, 2004. **1012**: p. 1-13.

42. Kwak, E.L., et al., *Role for NF-kappa B in the regulation of ferritin H by tumor necrosis factor-alpha.* J Biol Chem, 1995. **270**(25): p. 15285-93.

43. Torti, S.V., et al., *The molecular cloning and characterization of murine ferritin heavy chain, a tumor necrosis factor-inducible gene.* J Biol Chem, 1988. **263**(25): p. 12638-44.

44. Tsuji, Y., et al., *Coordinate transcriptional and translational regulation of ferritin in response to oxidative stress.* Mol Cell Biol, 2000. **20**(16): p. 5818-27.

45. Wei, Y., et al., *Interleukin 1 induces ferritin heavy chain in human muscle cells.* Biochem Biophys Res Commun, 1990. **169**(1): p. 289-96.

46. Mikhael, M., et al., *Iron regulatory protein-independent regulation of ferritin synthesis by nitrogen monoxide.* Febs J, 2006. **273**(16): p. 3828-36.

47. Elliott, J.L., *Cytokine upregulation in a murine model of familial amyotrophic lateral sclerosis.* Brain Res Mol Brain Res, 2001. **95**(1-2): p. 172-8.

48. Ghezzi, P. and T. Mennini, *Tumor necrosis factor and motoneuronal degeneration: an open problem.* Neuroimmunomodulation, 2001. **9**(4): p. 178-82.

49. Hensley, K., et al., *Message and protein-level elevation of tumor necrosis factor alpha (TNF alpha) and TNF alpha-modulating cytokines in spinal cords of the G93A-SOD1 mouse model for amyotrophic lateral sclerosis.* Neurobiol Dis, 2003. **14**(1): p. 74-80.

50. Hensley, K., et al., *Temporal patterns of cytokine and apoptosis-related gene expression in spinal cords of the G93A-SOD1 mouse model of amyotrophic lateral sclerosis.* J Neurochem, 2002. **82**(2): p. 365-74.

51. Wu, L.J., et al., *Expression of the iron transporter ferroportin in synaptic vesicles and the blood-brain barrier.* Brain Res, 2004. **1001**(1-2): p. 108-17.

52. Zhang, P., et al., *Electron tomography of degenerating neurons in mice with abnormal regulation of iron metabolism.* J Struct Biol, 2005. **150**(2): p. 144-53.

53. Kidane, T.Z., E. Sauble, and M.C. Linder, *Release of iron from ferritin requires lysosomal activity.* Am J Physiol Cell Physiol, 2006. **291**(3): p. C445-55.

54. Kawai, H., et al., *Lysosomal enzyme activities in skeletal muscle of patients with neuromuscular diseases.* Muscle Nerve, 1995. **18**(9): p. 1009-15.

55. Kispal, G., et al., *The mitochondrial proteins Atm1p and Nfs1p are essential for biogenesis of cytosolic Fe/S proteins.* Embo J, 1999. **18**(14): p. 3981-9.

56. Lange, H., et al., *A mitochondrial ferredoxin is essential for biogenesis of cellular iron-sulfur proteins.* Proc Natl Acad Sci U S A, 2000. **97**(3): p. 1050-5.

57. Kriz, J., G. Gowing, and J.P. Julien, *Efficient three-drug cocktail for disease induced by mutant superoxide dismutase.* Ann Neurol, 2003. **53**(4): p. 429-36.

4. 8 Figures and Tables

Figure 1

Abnormal iron accumulation in neurons and glia of $SOD1^{G37R}$ mice.

(A-B) Wildtype mice at 12 months of age show no accumulation of iron in the ventral horn of the lumbar spinal cord. Large motor neurons are clearly seen (arrowheads).

(C-D) $SOD1^{G37R}$ mice show iron accumulation in cells in the ventral horn of the lumbar spinal cord, seen as brown deposits (arrows). Large motor neurons are rarely detectable suggesting atrophy of these neurons. Scale bars = 100μm, 50μm.

(E–F) Higher magnification micrographs of neurons shown in A and B. Wildtype mice at 12 months of age show no accumulation of iron.

(G–I) Higher magnification micrographs of neurons shown in C and D. $SOD1^{G37R}$ mice show marked accumulations of iron in the cell body. Scale bar = 25μm.

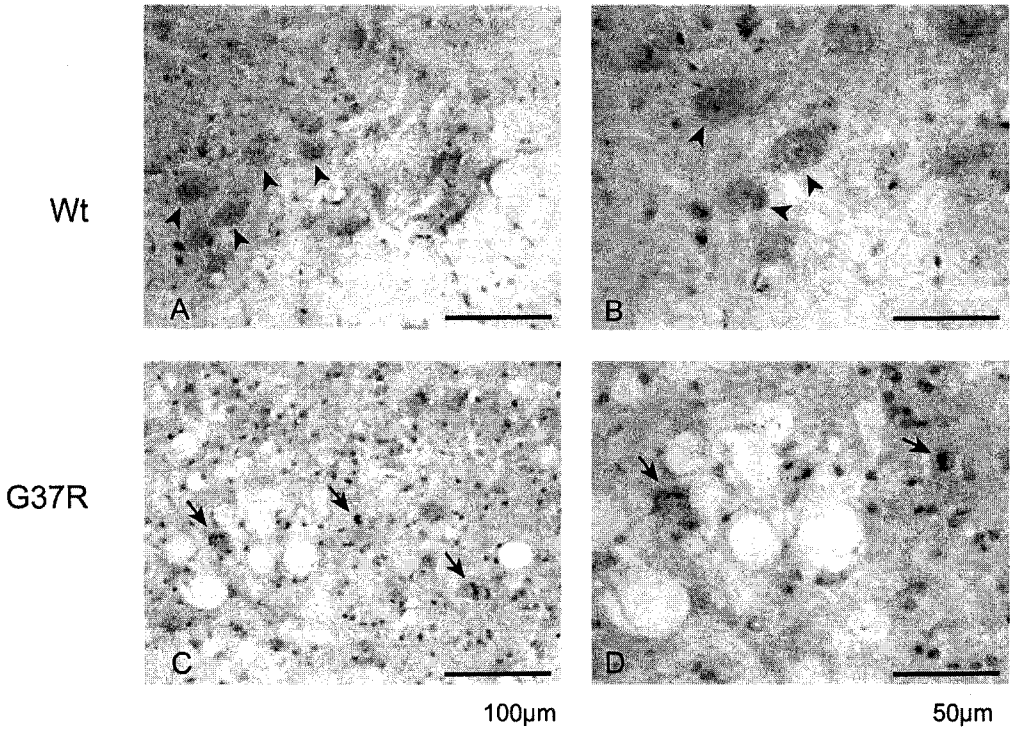
Wt
G37R
A
B
C
D
100μm
50μm

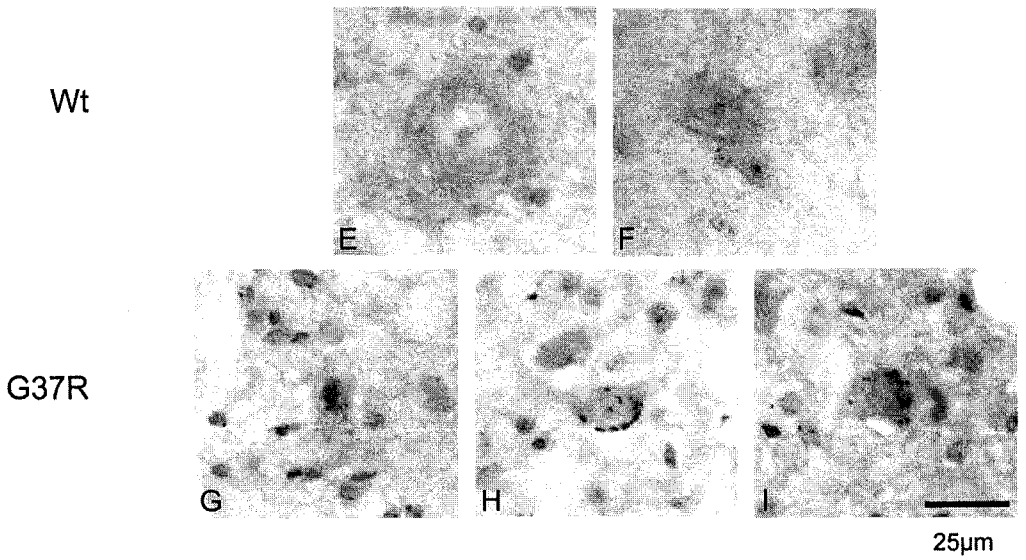
Wt
G37R
E
F
G
H
I
25μm

Figure 2

Iron accumulation in the glia of $SOD1^{G37R}$ mice.

(A-B) Glial cells from wildtype mice do not show any visible iron accumulation (arrowheads).

(C-E) Glial cells from $SOD1^{G37R}$ mice show iron accumulation in a pattern that is different from neurons (arrows). This accumulation is spread throughout the cytoplasm and not the vesiclular-type of inclusions seen in neurons. Scale bars = 100μm, 20μm.

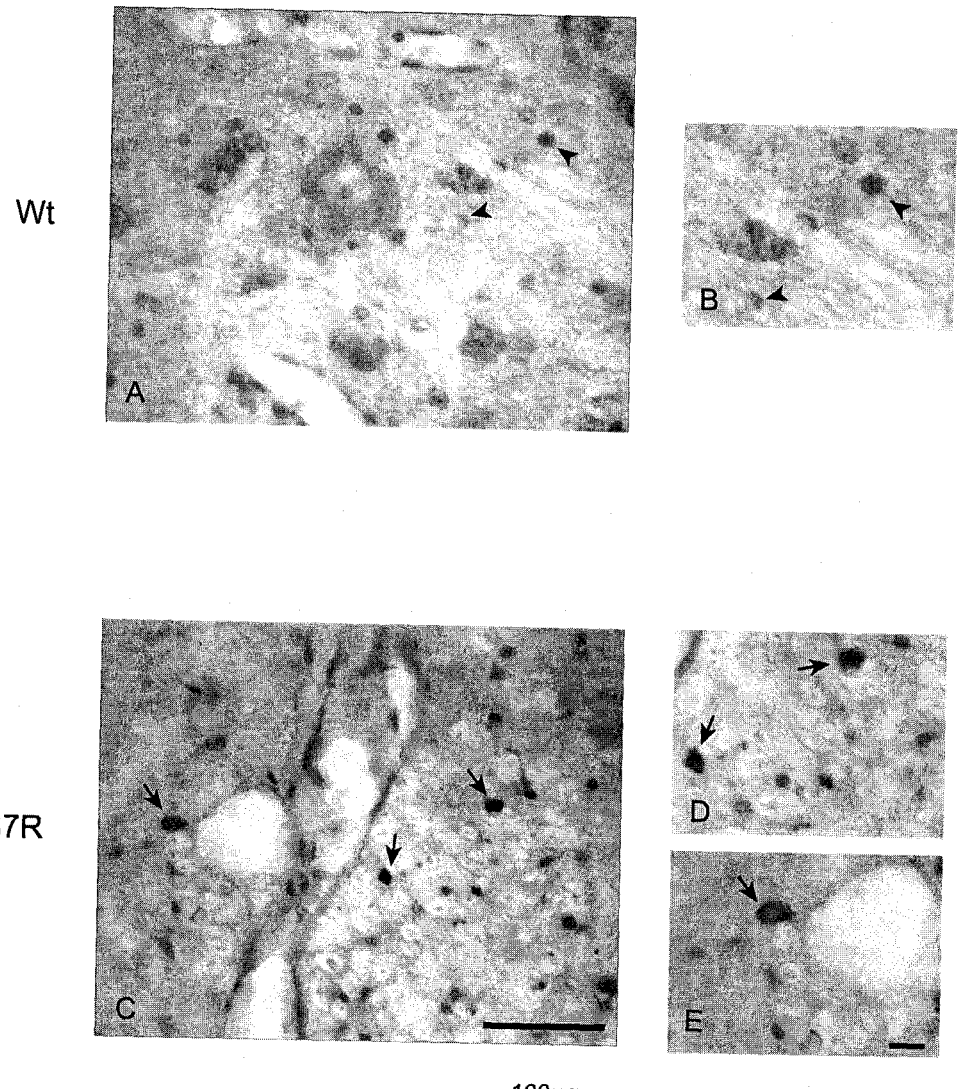
Wt
A
B
G37R
C
D
E
100µm
20µm

Figure 3

Expression of iron homeostasis proteins in SOD1^{G37R} mice.

(A) At 12 months of age the increases in DMT1, FPN, CP and TfR1 mRNA are much higher in the cervical spinal cord than in the lumbar region. The higher increase reflects the caudal to rostral progression of the disease with active degeneration still occurring in the cervical cord at this stage. The increase of DMT1 mRNA is mainly of the -IRE form. (*; $p<0.05$).

(B) QRT-PCR data at 4 month (pre-symptomatic stage) show that in early stages of the disease DMT1 –IRE, FPN and CP mRNA are higher in the lumbar than in the cervical region in the spinal cord of *SOD1^{G37R}* mice. TfR1 expression appears to be reduced in the lumbar and thoracic regions. Black bar; cervical, white bar; thoracic, grey bar; lumbar spinal cord.

A

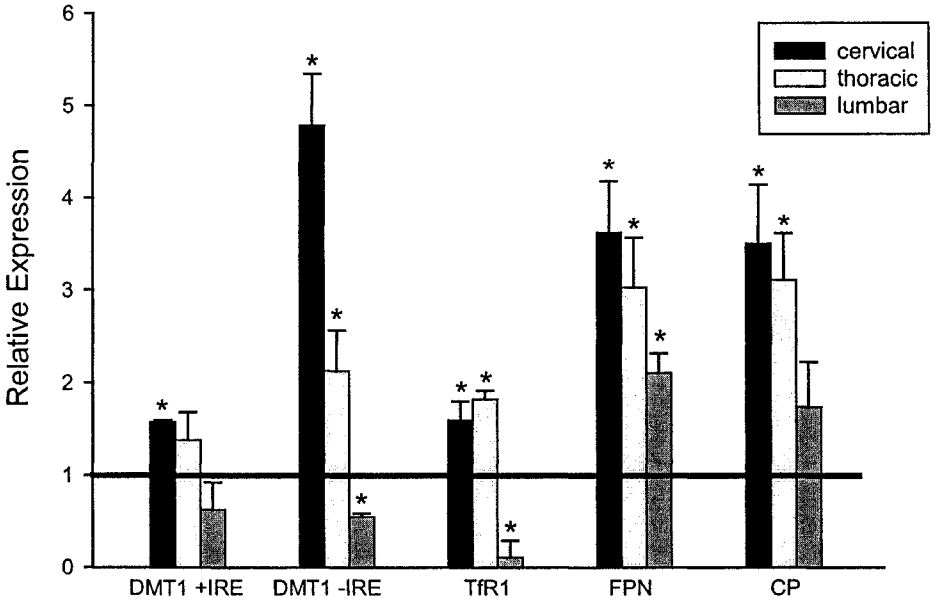
12m
Relative Expression
cervical
thoracic
lumbar
0
1
2
3
4
5
6
DMT1 +IRE
DMT1 -IRE
TfR1
FPN
CP

B

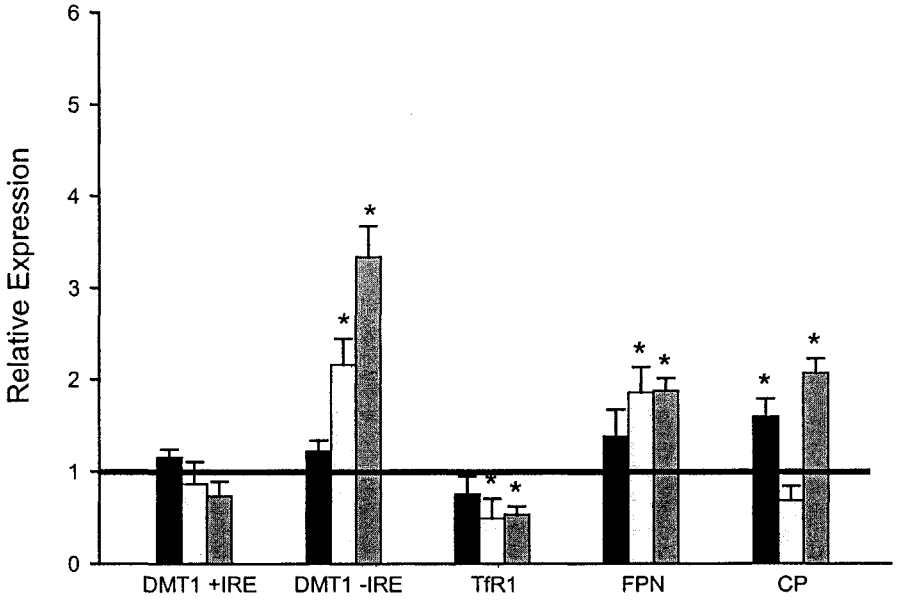
4m
Relative Expression
0
1
2
3
4
5
6
DMT1 +IRE
DMT1 -IRE
TfR1
FPN
CP

Figure 4

DMT1 is increased more than FPN in the SOD1^{G37R} mice. Western blot analysis of proteins from the cervical cord of 12-month–old mice shows that DMT1, FPN and CP are greater in the *SOD1^{G37R}* than in wildtype mice. There is a 2-fold or greater increase in DMT1 expression in *SOD1^{G37R}* mice than FPN and CP. TfR1 did not show a difference in total protein expression in *SOD1^{G37R}* mice as compared to the wildtype mice. β-actin was used as a loading control.

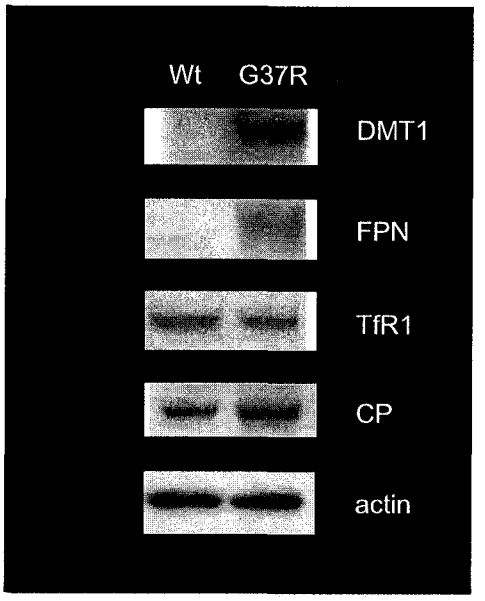
Wt
G37R
DMT1
FPN
TfR1
CP
actin

Figure 5

Motor neurons upregulate DMT1 in the SOD1^{G37R} transgenic mice.

(A-F) Double immunofluorescence labeling shows that the DMT1 is upregulated in surviving neurons (arrows) at 12 months of age in the cervical spinal cord of *SOD1^{G37R}* transgenic mice (D-E) as compared to wildtype mice (A-C).

(G-L) FPN staining is increased overall at 12 months in the cervical cod of *SOD1^{G37R}* mice but not in motor neurons (J-K, arrows). The relative increase of FPN is lower than DMT1. Scale bar = 100μm.

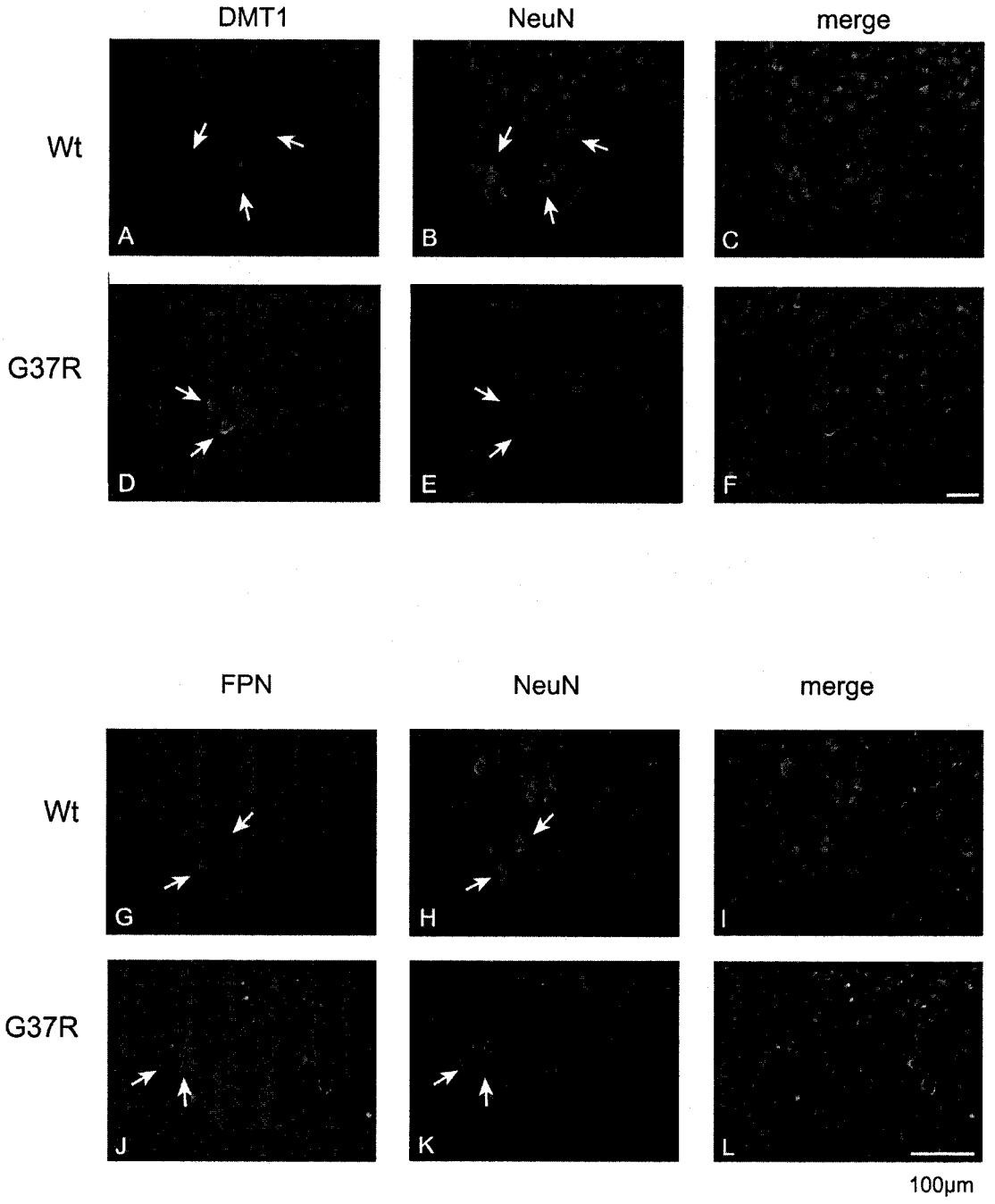
DMT1
NeuN
merge
Wt
G37R
A
B
C
D
E
F
FPN
NeuN
merge
Wt
G37R
G
H
I
J
K
L
100μm

Figure 6

TfR1 expression is decreased in motor neurons but increased in glia of SOD1^{G37R} transgenic mice.

(A-B) Surviving motor neurons in the cervical spinal cord of 12 months old *SOD1^{G37R}* transgenic mice show marked decrease in TfR1 expression (B, arrows).

(C-D) On the other hand, glial cells (arrowheads) increased TfR1 expression in the transgenic mice (D). Scale bar = 50μm.

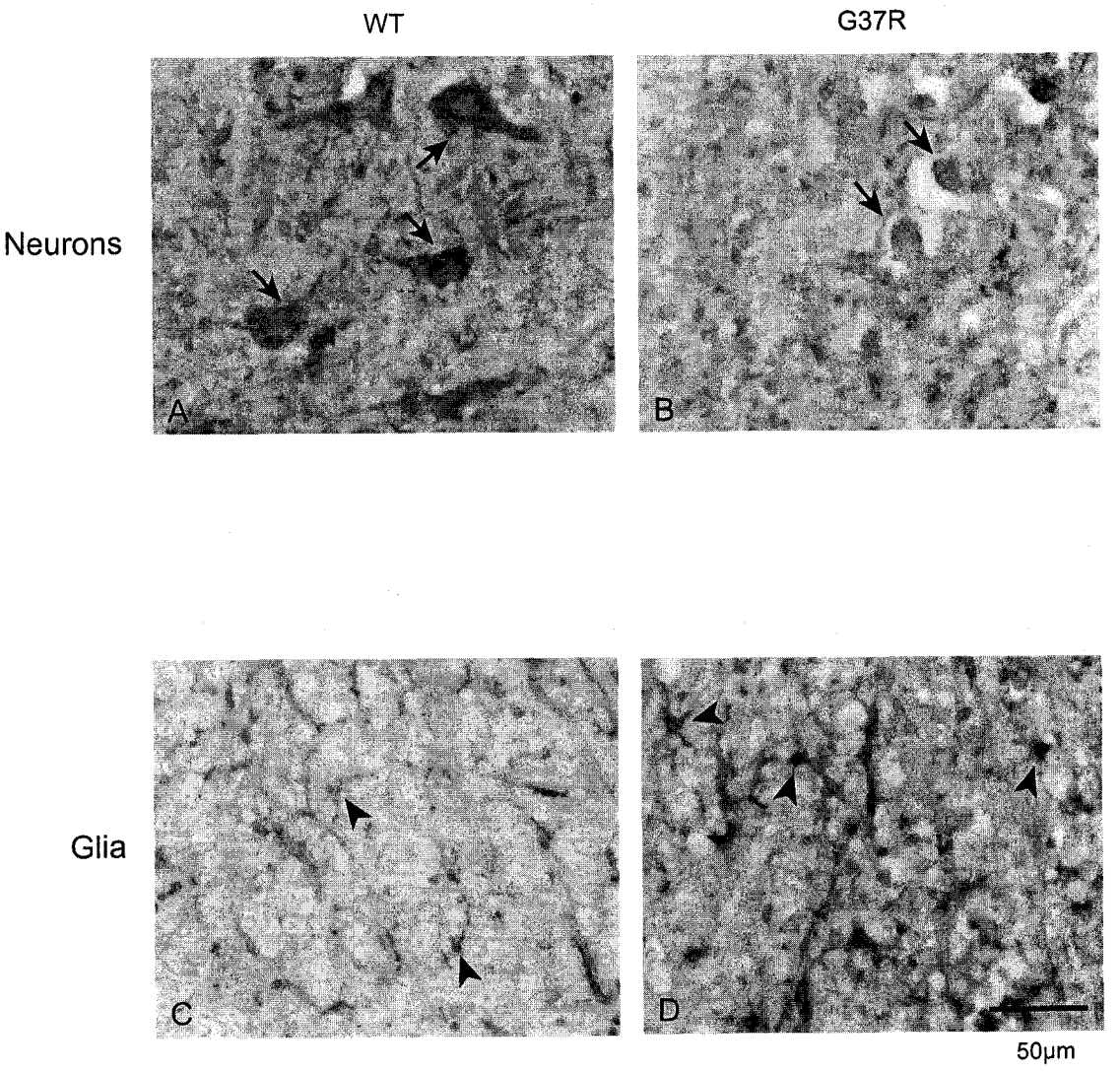
WT
G37R
Neurons
A
B
Glia
C
D
50μm

Figure 7

Ferritin is increased in the macrophages not in the motor neurons in SOD1^{G37R} mice.

(A) At 12 months of age, the mRNA expression of the heavy and light chains of ferritin is markedly increased in the cervical than lumbar region of *SOD1^{G37R}* mice. This reflects an active process of iron accumulation occurring in the cervical region, while in the lumbar the disease is well established. (*; $p < 0.05$).

(B-G) High expression of ferritin is localized to the Mac1 positive cells, a marker for activated microglia/macrophages, in the SOD1 transgenic mice (E-F, arrows). No detectable ferritin or Mac1 immunoreactivity was found in the wildtype animals.

(H-M) Although Perl's immunohistochemistry shows iron positive inclusions in the motor neurons in the SOD1 transgenic mice, there is no upregulation of ferritin in the motor neurons (K-L, arrow) indicating that the iron containing neuronal inclusions do not contain ferritin. Scale bars = 50μm, 25μm.

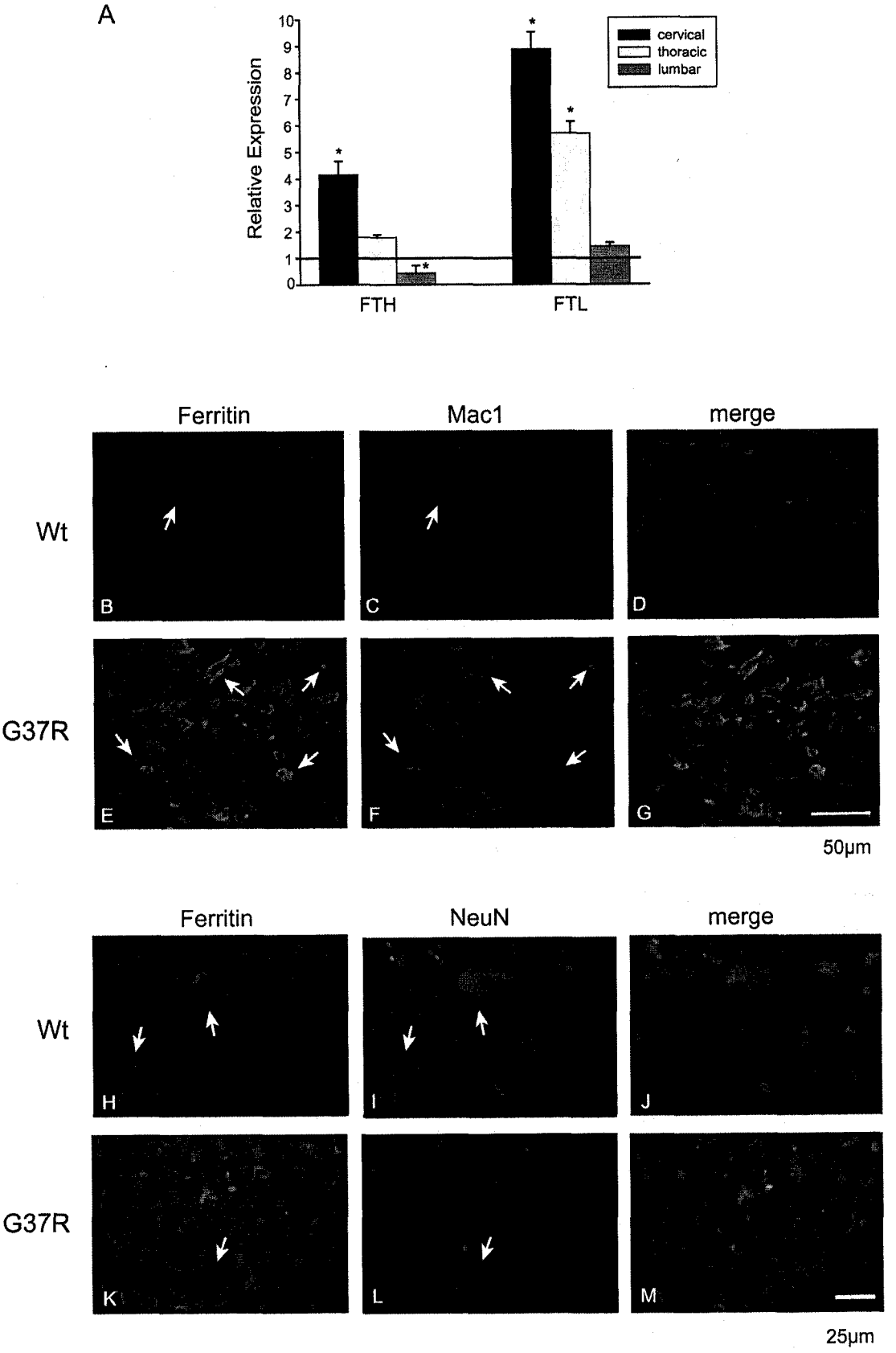
A
Relative Expression
10
9
8
7
6
5
4
3
2
1
0
cervical
thoracic
lumbar
FTH
FTL
Ferritin
Mac1
merge
Wt
G37R
B
C
D
E
F
G
50μm
Ferritin
NeuN
merge
Wt
G37R
H
I
J
K
L
M
25μm

Figure 8

Blocking axonal transport caused iron accumulation in motor neurons of normal mice. Blocking anterograde axonal transport by sciatic nerve ligation (A) resulted in accumulation of iron in the neuronal cell bodies of the large motor neurons (B). Iron staining is seen as vesicular structures (arrows) similar to that seen in the neurons in *SOD1*^{G37R} mice. The sham operated control side (right side in A) did not show any iron accumulation (data not shown).

A

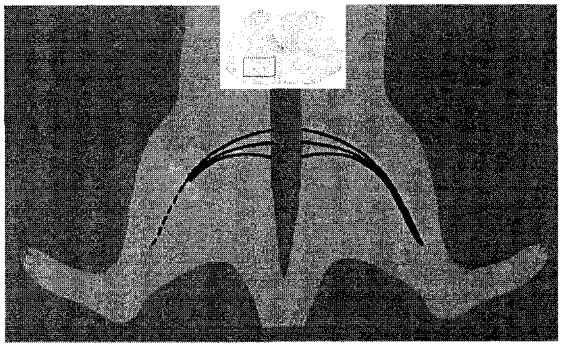

B

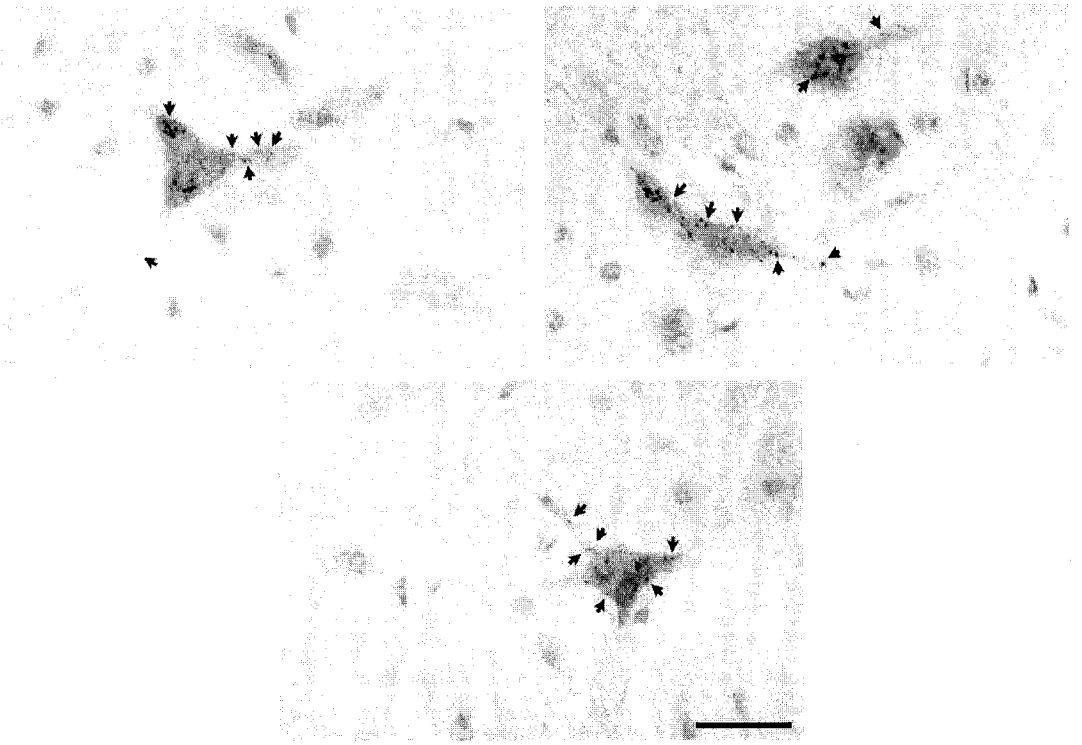

Figure 9

Changes in iron regulatory mechanism in spinal cord of SOD1^{G37R} mice. Electron mobility shift assay with protein extracts of spinal cords from *SOD1^{G37R}* and wildtype mice show that there is ~2 fold increase of IRP1 activity in the *SOD1^{G37R}* samples as compared to wildtype mice. This increase of IRP1 is only noted in the spinal cords but not in the liver samples. There was no detectable IRP2 activity in these tissues. β-mercaptoenthanol (2-ME) treated samples were used as loading controls.

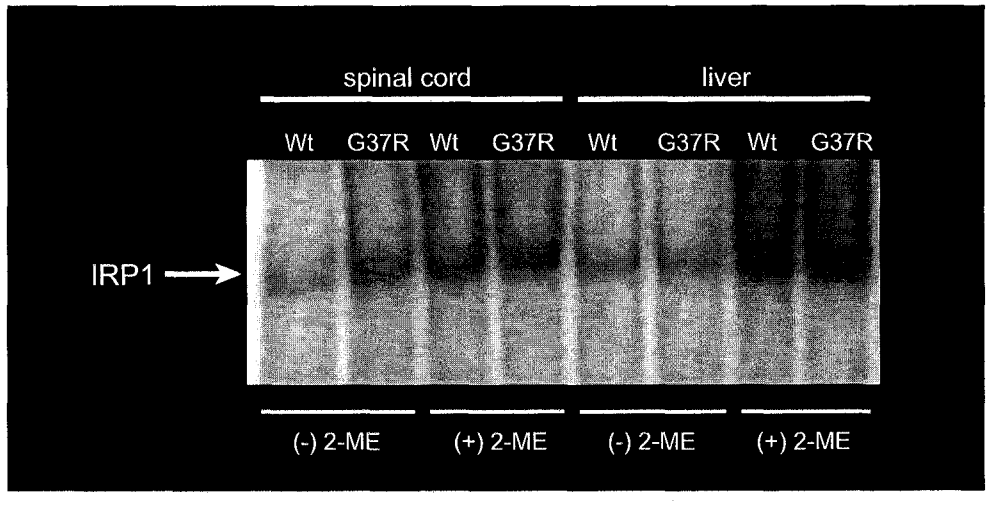
spinal cord
liver
Wt
G37R
Wt
G37R
Wt
G37R
Wt
G37R
IRP1
(-) 2-ME
(+) 2-ME
(-) 2-ME
(+) 2-ME

Figure 10

Mitochondrial ferritin is increased in motor neurons and astrocytes in SOD1^{G37R} transgenic mice.

(A) Western blotting for mitochondrial ferritin using purified mitochondrial protein shows that there is upregulation of MtF in *SOD1* transgenic animals as compared to wildtype mice. COX IV was used for loading control.

(B-G) Surviving motor neurons in the cervical spinal cords of *SOD1* transgenic mice show upregulation of MtF (E–F, arrow)

(H-M) Astrocytes also show marked increase in MtF expression (K–L, arrows). There was no detectable staining in both neurons and astrocytes in the control mice. Scale bar = 50μm.

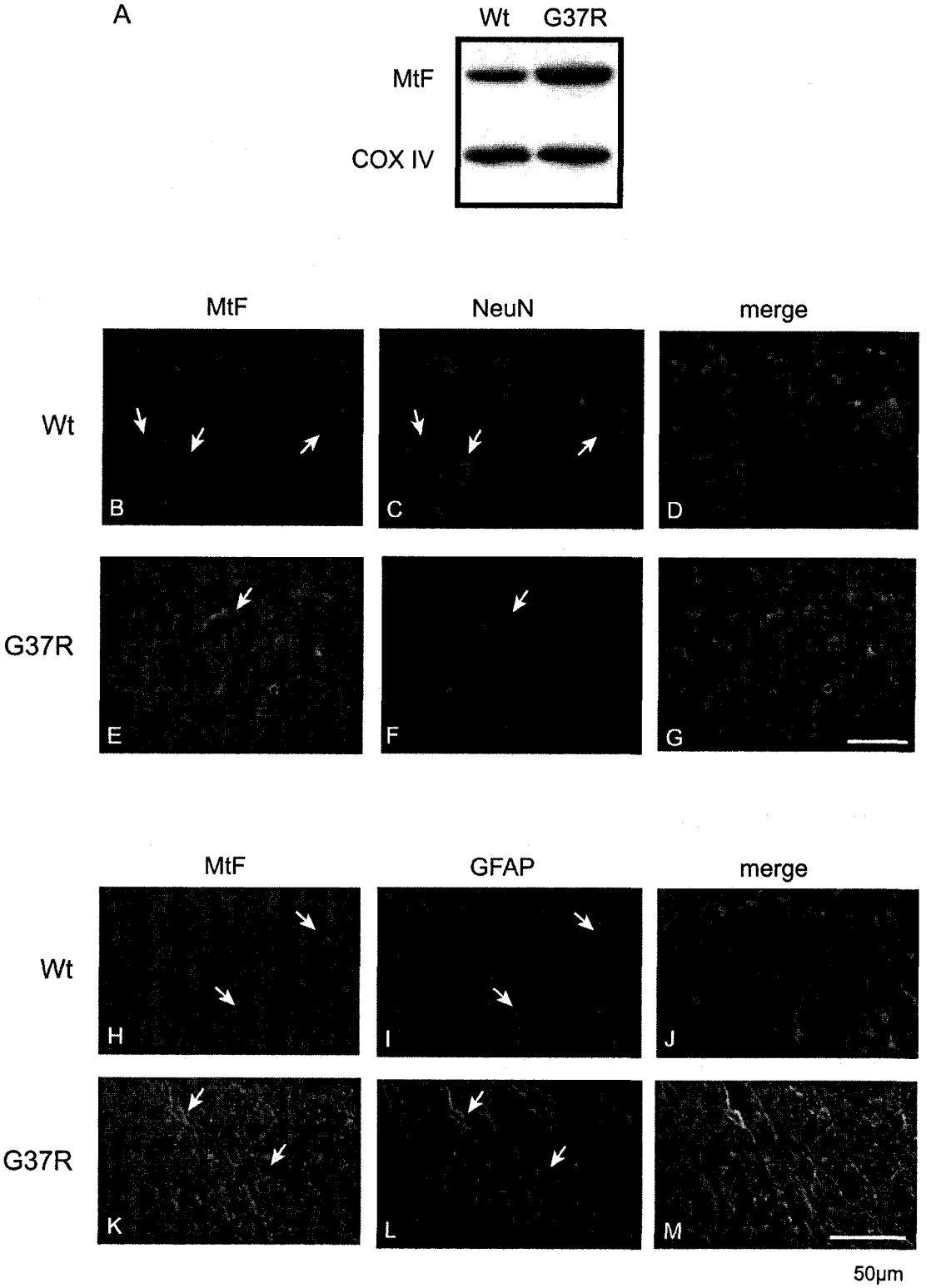
A
Wt
G37R
MtF
COX IV
MtF
NeuN
merge
Wt
B
C
D
G37R
E
F
G
MtF
GFAP
merge
Wt
H
I
J
G37R
K
L
M
50μm

Figure 11

SIH treatment is helping neurons to survive and extend the lifespan of $SOD1^{G37R}$ mice.

(A) Kaplan-Meyer graph shows percentage animals surviving in each week. Black circle line represents $SOD1^{G37R}$ transgenic animals injected with vehicle (1X PBS). n=18. Red triangles indicate mice treated with SIH once per week starting at 8 months of age (red arrow). This group showed median of 3.5 weeks lifespan extension (black line at 50%). The red squares indicate mice treated twice a week starting at 8 months. These mice showed further beneficial effect with a median increase in lifespan of 4.8 weeks. For both treatment groups, n=12. **(B)** Mice from vehicle-treated group and SIH treated group (2/week) were sacrificed at 50 weeks and stained with cresyl violet to visualize neurons. Lumbar spinal cord of vehicle treated mice shows very few surviving neurons (arrow) while SIH treated group shows striking difference in the number of surviving neurons (right panel, arrows). Scale bar = 50μm.

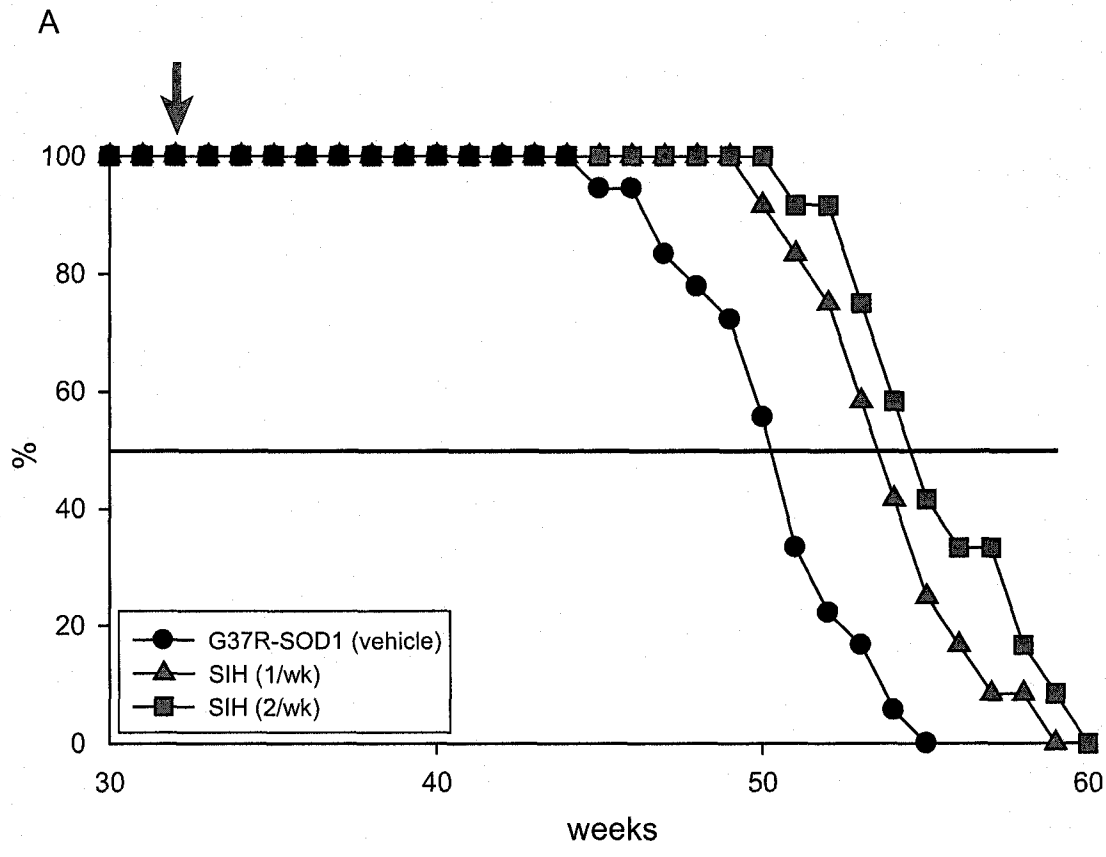
A
100
80
60
40
20
0
%
30
40
50
60
weeks
G37R-SOD1 (vehicle)
SIH (1/wk)
SIH (2/wk)

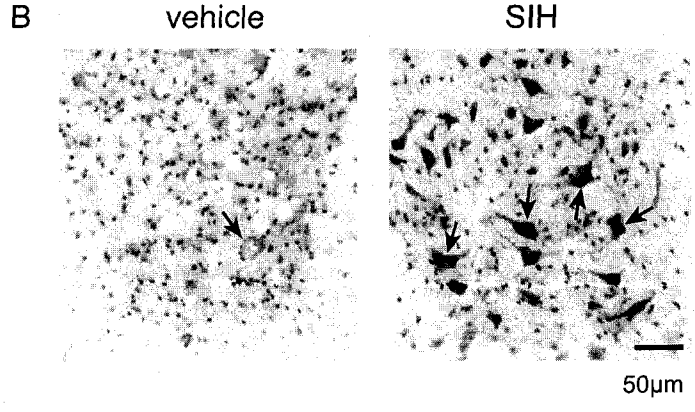
B
vehicle
SIH
50μm

Table 1

End-stage blood analysis of *SOD1*^{G37R} mice treated with vehicle and SIH

	non-SOD1 Wt	**SOD1 vehicle**	**SOD1 SIH**
hematocrit (L/L)	0.41±0.02	0.44±0.02	0.38±0.01
hemoglobin (g/L)	139.67±4.04	144±4.58	127±13.00
RBCs (x10^{12}/L)	8.94±0.53	9.28±0.53	8.02±0.69

CHAPTER 5

Summary and General Discussion

Iron plays a vital role in many essential cellular processes including DNA, RNA and protein synthesis, mitochondrial oxidation reactions and more [1]. Although iron is indispensable for cell survival, it can also be toxic if not properly shielded because of its redox-active nature and ability to generate free radicals [2]. Therefore, organisms have developed regulatory systems to keep "free iron" at its lowest level while maintaining sufficient amounts of iron to meet metabolic needs. Many studies have explored how iron is absorbed and utilized in the body, but little is known about how iron homeostasis in the central nervous system (CNS) is maintained. The CNS consumes about 20% of total body energy at a rate that is 10 times faster per gram of tissue as compared to non-CNS tissues [3]. The human brain naturally accumulates iron as a normal process of aging [4]. Moreover, iron accumulation also occurs in the CNS in many neurodegenerative diseases, although some of them are not defective in genes involved in iron homeostasis proteins ([5, 6], see also section 1.7). Therefore, assessing how iron homeostasis is achieved in the CNS is an important question not only to understand normal aging, but also to understand the pathogenesis of various neurodegenerative diseases. For my Ph. D. thesis, I have used two mouse models of neurodegenerative disease; (i) ceruloplasmin (*CP*) null mice which lack an essential ferroxidase, and is a model for aceruloplasminemia in humans (ii) $SOD1^{G37R}$ transgenic mice, which over-express the mutant form of this protein, and is a mouse model for Amyotrophic lateral sclerosis (ALS). I have assessed the dysregulation of iron homeostasis in these two models and the role of iron in the pathogenesis in the CNS. I also assessed how the ferroxidase ceruloplasmin regulates iron efflux from astrocytes.

5.1 The role of GPI-ceruloplasmin in iron efflux in astrocytes

As mentioned previously, iron is a redox-active metal. The ferrous form of iron (Fe^{2+}) is relatively soluble at neutral pH compared to the ferric form (Fe^{3+}), but it can generate toxic free radicals. Therefore, organisms have developed ferroxidases to safely oxidize ferrous iron to ferric iron that is then stored and/or transported. Ceruloplasmin (CP) is one of these ferroxidases that is abundant in serum [7]. Previously, our laboratory reported a membrane-bound GPI-anchored form of CP that is the dominant form of CP in the CNS and is expressed only by astrocytes [8]. In my work, I showed that this form of CP is essential for iron efflux from astrocytes using primary astrocyte cultures purified from *CP* null and wildtype mice. There was no difference in the iron uptake ability in astrocyte cultures from these mice, although iron efflux was impaired in astrocytes from *CP* null mice. Therefore, expression of the iron efflux protein FPN alone is not sufficient for astrocytes to efflux iron. In recent collaborative work done with Jerry Kaplan's group, I also showed that in the absence of GPI-CP, FPN gets internalized and degraded [9]. Interestingly, I also found that addition of soluble CP at the concentration found in serum (300μg/ml) was not as effective as GPI-CP in effluxing iron from *CP* null astrocytes. Therefore greater than 300μg/ml of secreted CP would be required to function as well as GPI-CP, which might be a problem since the total protein content of human CSF in the very tight extracellular space in the CNS is only 350μg/ml [10].

Although I have shown that GPI-CP is essential for iron efflux from astrocytes, it is an enzyme that is located on the external surface of the cell membrane. Therefore, GPI-CP has to be a modulator of iron efflux rather than function as a transporter. By co-immunoprecipitation using a monoclonal CP antibody, I showed that GPI-CP and the ferrous iron transporter FPN make an efflux complex on the astrocyte membrane. One of

the questions was how the formation of this efflux complex (GPI-CP/FPN) is regulated under different intracellular iron levels. One member of this complex is GPI-anchored CP and thus expected to be localized to lipid raft domains of the cell membrane, while the other (FPN) is a multipass transmembrane protein. In muscle cells, a GPI-anchored protein, agrin has been shown to be involved in translocation and clustering of acetylcholine receptors [11]. I have shown in chapter 2 that high iron concentration in astrocytes causes translocation of FPN into lipid raft microdomain where GPI-CP resides. This is a novel regulatory mechanism for the rapid redeployment of FPN that quickly generates GPI-CP/FPN complexes to help clear excess cellular iron before *de novo* synthesis of FPN by the IRE/IRP mechanism can occur (Figure 1B). Currently, the mechanism underlying the lateral movement of FPN is not known, but FPN has several possible phosphorylation sites. One of the tyrosine phosphorylation sites was reported recently to play a role in the internalization of FPN by hepcidin binding [12]. Other sites may play a role in the lateral mobility of FPN into the lipid rafts. I have also shown that treating astrocytes with a membrane permeable iron chelator causes a decrease of FPN. Thus, when there is low cytosolic iron, internalization of the iron exporter FPN might help cells to preserve iron within the cytosol (Figure 1C). This might be following the recent internalization model that binding of hepcidin induces phosphorylation of FPN and internalization of degradation of the protein [12, 13]. Interestingly, De Domenico *et al.* showed that treating C6 glioma cells with a non-membrane permeable chelator bathophenanthroline disulfonate (BPS) did not cause internalization of FPN [9], while I have shown that a membrane permeable chelator SIH caused decrease of FPN from the membrane. Therefore, intracellular iron concentration, likely via hepcidin expression, regulates FPN localization on the membrane. In other work done in collaboration with

Kaplan's group which showed that FPN gets internalized and lost from the cell membrane in the absence of GPI-CP [9], the findings presented in this thesis show that the loss of FPN from the cell surface under low iron conditions does not cause internalization of GPI-CP as its levels are unchanged. Thus FPN requires GPI-CP for its maintenance on the cell membrane but not vice versa. The data presented in Chapter 2 indicates that GPI-CP plays an important role in iron efflux from astrocytes by partnering with FPN, and also that iron levels regulate the movement of FPN into the lipid raft domains containing GPI-CP.

5.2 The role of GPI-CP in maintaining CNS iron homeostasis

The possible role of CP *in vivo* has been revealed from analysis of patients with null mutations of *CP* (aceruloplasminemia) [14]. These patients show abnormal iron accumulation in the liver and CNS and often suffer from mild anemia [15, 16]. To study the role of CP *in vivo*, our lab has generated a *CP* null mouse [17]. I carried out a detailed analysis of the cerebellum of these *CP* null mice during aging. In the cerebellum of *CP* null mice, visible iron accumulation starts at 12 months of age along the ventricles, and there was large amount of iron accumulation at 24 months of age in both in the white matter and the grey matter of the cerebellum. Iron accumulation occurred in the glia and there was no evidence of iron accumulation in the large neurons of deep nuclei nor in Purkinje neurons in the cerebellar cortex. I also showed that there is increased expression of the iron storage protein ferritin in astrocytes, which is a good indicator for iron accumulation. It was not clear from work done on tissue sections obtained from aceruloplasminemia brains which cells (astrocytes and/or neurons) accumulate iron [15]. My work on the *CP* null mice clearly shows that iron accumulation occurs in astrocytes.

This astrocytic iron accumulation in *CP* null mice is in keeping with the results presented in Chapter 2 that astrocytes from *CP* null mice are able to influx iron normally but lose their ability to efflux iron. Astrocytes cover about 95% of capillary surface in the CNS and are involved in the generation of tight junctions between endothelial cells that form the blood-brain barrier [18]. Since most of the iron that is supplied to the CNS comes through capillaries, astrocytes might play a role as the first cell to accept iron from the circulation via endothelial cells and then redistribute it to other cells in the CNS. Therefore, in *CP* null mice, astrocytes would be expected to acquire iron normally from the circulation but unable to release it to other cells in the CNS, resulting in the iron accumulation I have seen in these cells *in vivo*. The excess iron in these astrocytes is likely to contribute to the extensive loss of astrocytes in the *CP* null mice with age. Astrocytes are known to be 'housekeeping cells' in the CNS, involved in maintaining proper levels of K^+, Ca^{2+}, pH, glutamate and more [19]. The loss of this protective role of astrocytes may affect the viability of other CNS cells.

I have also reported that there is degeneration of Purkinje neurons in the *CP* null mice during aging. To our surprise, these neurons and large neurons in the deep nuclei do not accumulate iron even at 24-months of age. Double-immunofluorescence labeling showed that these neurons do not show increased ferritin expression, but upregulate the iron importer DMT1 suggesting that these cells are not iron overloaded. This finding is consistent with the idea that neurons might normally get their iron supply from astrocytes via cell/cell contact around neuronal cell bodies and processes. The inability to efflux iron from astrocytes caused iron accumulation in astrocytes and might cause iron deprivation in neurons. It is possible that the neurons increase DMT1 in an effort to acquire iron from the CSF which contains very low levels of iron (~1/38 of serum levels, [20]). Therefore

the loss of neurons in *CP* null mice is not due to iron overload toxicity but could be due to the loss of the metabolic support provided by astrocytes. It is still not clear how oligodendrocytes survive and maintain a sufficient level of iron in the *CP* null mice since myelination seems to be normal in these mice. My work suggests that two different mechanisms may mediate cell death in the CNS in *CP* null mice, and which may also occur in humans with aceruloplasminemia.

5.3 Disruption of iron homeostasis mechanisms in a mouse model for ALS

Amyotrophic lateral sclerosis (ALS) is a progressive lethal neurodegenerative disease with mainly degeneration of spinal motor neurons [21]. One of the known causes of the disease is mutations in superoxide dismutase1 (*SOD1*) that converts superoxide to molecular oxygen or hydrogen peroxide. Originally, the disease was thought to be due to a lack of dismutase activity, but later work with the *SOD1* null mice showed that it is due to a toxic 'gain of function' effect by the mutant SOD1.

Interestingly, it has been reported that abnormal iron accumulation occurs in the CNS of both familial and sporadic cases of ALS [22-24]. Although this has been known for some time, the contribution of excess iron to the progression of disease is not known. I have used one of the mutant SOD1 transgenic mouse lines ($SOD1^{G37R}$) that show slow progression of disease, with an average lifespan of around 50 weeks. Spinal cord sections from these mice showed abnormal iron accumulation in two different patterns. Ventral horn motor neurons showed round, cytoplasmic-inclusion type of iron accumulation, while glial cells showed diffuse iron accumulation in the whole cell body. Not only is the pattern of iron deposits different, but different molecular mechanisms appear to contribute to the accumulation of iron in these two cell types. I have shown that TfR1

expression is increased in glia, while motor neurons decreased expression of TfR1 but increased expression of another iron importer DMT1. Interestingly, despite clear deposits of iron accumulation in the neuronal cell bodies, I could not detect upregulation of cytoplasmic ferritin in neurons. Surprisingly, however, an antibody that specifically recognizes mitochondrial ferritin showed increased labeling of the large motor neurons and astrocytes in the spinal cord on 12-month old $SOD1^{G37R}$ transgenic mice. This was further supported by Western blot data, which showed increased expression of mitochondrial ferritin in the spinal cord of these transgenic mice as compared to wildtype controls. My data therefore provides clear evidence of increased mitochondrial ferritin which likely reflects increased iron load in mitochondria. This may contribute to the oxidative damage and mitochondrial dysfunction proposed by Cleveland's group [25].

I also provide direct evidence that the arrest of axonal transport in the sciatic nerve by ligation of the nerve results in iron accumulation in the cell bodies of the spinal motor neurons. It has been reported that axonal transport is disturbed in both familial and sporadic cases of ALS and in *SOD1* transgenic mice [26-28]. My work therefore provides strong evidence that disruption of axonal transport may also contribute to the iron accumulation seen in the motor neurons in ALS and its mouse models.

As mentioned above, the reduction of TfR1 and lack of cytosolic ferritin expression suggests that the iron accumulation in neurons in the form of the round cytoplasmic inclusion-like bodies do not appear to be sensed by the IRE/IRP regulatory mechanism. One possible explanation for this is that disruption of Fe-S clusters in mitochondria result in an improper supply of Fe-S clusters in the cytosol. This would therefore promote formation of IRP1 rather than aconitase and cause mitochondrial iron accumulation. IRP1 is a bifunctional protein that also functions as aconitase when an Fe-

S cluster is inserted into the protein. Mutant SOD1 has been shown to preferentially bind to spinal mitochondria, and this has been suggested to block the mitochondrial protein transport machinery [25]. I have shown that there is an increase in mitochondrial ferritin in *SOD1* animals suggesting mitochondrial iron accumulation. Moreover, it has been reported that mutant SOD1 can cause increased oxidative stress in mitochondria, and these reactive oxygen species are also known to breakdown Fe-S clusters *in vitro* [29-31]. Therefore, this constitutively active IRP1 might drive the down-regulation of cytosolic ferritin expression and cause disruption of the iron homeostasis mechanism in neurons despite the accumulation of iron in these cells. It is not clear yet how TfR1 is actually down-regulated and whether there is a compensatory mechanism by IRP2 in these cells.

Finally, I have shown that treating SOD1 mice with a lipophilic iron chelator salicylaldehyde isonicotinoyl hydrazone (SIH) was beneficial in extending the lifespan of $SOD1^{G37R}$ transgenic mice. This treatment showed a dose-dependent effect, and was only effective when the treatment was started before the onset of symptoms. When the SIH and vehicle treated mice are compared at 50 weeks of age when the vehicle treated group needed to be euthanized because of severe paralysis, the SIH treatment showed greatly improved motor neuron survival in all regions of the spinal cord. Moreover, the 4-month chelator treatment did not appear to cause anemia and was well tolerated by the mice. Collectively, the 4.8-week increase in lifespan in this mouse model is the best treatment in the literature for a single treatment intervention. This work therefore suggests that iron chelator therapy might be beneficial for treatment for ALS.

5.4 Conclusions

Unlike other organs, the CNS is isolated from the peripheral blood circulation and comprised of many different cell types. Different kinds of neurons are extending axons to widespread regions within the CNS, while oligodendrocytes produce the myelin sheets that wrap around axons for efficient transmission of electrical signals. Astrocytes are involved in absorbing supplies from the blood and maintaining the microenvironment in the CNS, while microglia are the resident macrophages in the CNS. In addition, the cells that line the blood vessels in the CNS form tight junctions comprising the BBB or blood-CSF-barrier, and leptomeningreal cells that line the outer surface of the CNS. Not only are there different types of cells in the CNS, but these cells are also in close contact with each other with comparatively little extracellular fluid (CSF). Therefore, understanding the iron homeostasis mechanism in the CNS cannot be achieved by studying one cell type in isolation, but by studying the more complex interactions and relationships between these cells *in vivo*. My work was therefore directed at both cell culture and *in vivo* approaches.

There are still many unanswered questions in CNS iron metabolism that need to be explored in the future. What is the role of the negative iron regulator, hepcidin, which is expressed by astrocytes and neurons? How do BBB endothelial cells crosstalk with other cells to regulate iron absorption into the CNS? What is the chemical form of iron in the CSF and the nature of iron carriers in the CSF? How do individual CNS cells uptake and efflux iron? How does iron get released and cleared from the CNS, and what mechanisms regulate this? Why does the CNS tend to retain iron even when the rest of the body is anemic?

Although many neurodegenerative diseases show iron accumulation in the CNS, it is still not very clear how this excess accumulation of iron occurs in most of these diseases. Furthermore we still do not know whether iron accumulation contributes to neurodegeneration in these conditions or is simply a by-product of cell death in the CNS. Since the mature mammalian CNS does not have the ability to regenerate effectively after damage and disease, it is very important to understand how iron accumulation occurs in the CNS in these conditions so that it can be prevented or reduced to minimize the possible cytotoxic effects of iron accumulation. My work provides some insights into how iron accumulation may occur in aceruloplasminemia and ALS, and the important contribution of iron to neurodegeneration in the mouse model of ALS.

5.5 References

1. Andrews, N.C., *Iron homeostasis: insights from genetics and animal models.* Nat Rev Genet, 2000. **1**(3): p. 208-17.
2. Halliwell, B. and J.M. Gutteridge, *Oxygen toxicity, oxygen radicals, transition metals and disease.* Biochem J, 1984. **219**(1): p. 1-14.
3. Drubach, D., *The Brain Explained.* 1999: Prentice Hall.
4. Connor, J.R., et al., *Cellular distribution of transferrin, ferritin, and iron in normal and aged human brains.* J Neurosci Res, 1990. **27**(4): p. 595-611.
5. Ponka, P., *Hereditary causes of disturbed iron homeostasis in the central nervous system.* Ann N Y Acad Sci, 2004. **1012**: p. 267-81.
6. Zecca, L., et al., *Iron, brain ageing and neurodegenerative disorders.* Nat Rev Neurosci, 2004. **5**(11): p. 863-73.
7. Holmberg, C.G. and C.B. Laurell, *Investigations in serum copper. II. Isolation of the copper containing protein, and a description of some of its properties.* Acta Chem Scand, 1948. **2**: p. 550-6.
8. Patel, B.N., R.J. Dunn, and S. David, *Alternative RNA splicing generates a glycosylphosphatidylinositol- anchored form of ceruloplasmin in mammalian brain.* J Biol Chem, 2000. **275**(6): p. 4305-10.
9. De Domenico, I., et al., *Ferroxidase activity is required for the stability of cell surface ferroportin in cells expressing GPI-ceruloplasmin.* Embo J, 2007. **26**(12): p. 2823-31.
10. Fishman, R.A., *Cerebrospinal Fluid in Diseases of the Nervous System.* 2nd ed. 1992, Philadelphia, PA: Saunders W B Co. 416.

11. Zhu, D., W.C. Xiong, and L. Mei, *Lipid rafts serve as a signaling platform for nicotinic acetylcholine receptor clustering.* J Neurosci, 2006. **26**(18): p. 4841-51.

12. De Domenico, I., et al., *The molecular mechanism of hepcidin-mediated ferroportin down-regulation.* Mol Biol Cell, 2007. **18**(7): p. 2569-78.

13. Nemeth, E., et al., *Hepcidin regulates cellular iron efflux by binding to ferroportin and inducing its internalization.* Science, 2004. **306**(5704): p. 2090-3.

14. Miyajima, H., Y. Takahashi, and S. Kono, *Aceruloplasminemia, an inherited disorder of iron metabolism.* Biometals, 2003. **16**(1): p. 205-13.

15. Morita, H., et al., *Hereditary ceruloplasmin deficiency with hemosiderosis: a clinicopathological study of a Japanese family.* Ann Neurol, 1995. **37**(5): p. 646-56.

16. Yoshida, K., et al., *A mutation in the ceruloplasmin gene is associated with systemic hemosiderosis in humans.* Nat Genet, 1995. **9**(3): p. 267-72.

17. Patel, B.N., et al., *Ceruloplasmin regulates iron levels in the CNS and prevents free radical injury.* J Neurosci, 2002. **22**(15): p. 6578-86.

18. Saunders, N.R., M.D. Habgood, and K.M. Dziegielewska, *Barrier mechanisms in the brain, I. Adult brain.* Clin Exp Pharmacol Physiol, 1999. **26**(1): p. 11-9.

19. Volterra, A. and J. Meldolesi, *Astrocytes, from brain glue to communication elements: the revolution continues.* Nat Rev Neurosci, 2005. **6**(8): p. 626-40.

20. Mizuno, S., et al., *CSF iron, ferritin and transferrin levels in restless legs syndrome.* J Sleep Res, 2005. **14**(1): p. 43-7.

21. Boillee, S., C. Vande Velde, and D.W. Cleveland, *ALS: a disease of motor neurons and their nonneuronal neighbors.* Neuron, 2006. **52**(1): p. 39-59.

22. Imon, Y., et al., *Low intensity areas observed on T2-weighted magnetic resonance imaging of the cerebral cortex in various neurological diseases.* J Neurol Sci, 1995. **134 Suppl**: p. 27-32.

23. Kasarskis, E.J., et al., *Aluminum, calcium, and iron in the spinal cord of patients with sporadic amyotrophic lateral sclerosis using laser microprobe mass spectroscopy: a preliminary study.* J Neurol Sci, 1995. **130**(2): p. 203-8.

24. Oba, H., et al., *Amyotrophic lateral sclerosis: T2 shortening in motor cortex at MR imaging.* Radiology, 1993. **189**(3): p. 843-6.

25. Liu, J., et al., *Toxicity of familial ALS-linked SOD1 mutants from selective recruitment to spinal mitochondria.* Neuron, 2004. **43**(1): p. 5-17.

26. Sasaki, S. and M. Iwata, *Impairment of fast axonal transport in the proximal axons of anterior horn neurons in amyotrophic lateral sclerosis.* Neurology, 1996. **47**(2): p. 535-40.

27. Williamson, T.L. and D.W. Cleveland, *Slowing of axonal transport is a very early event in the toxicity of ALS-linked SOD1 mutants to motor neurons.* Nat Neurosci, 1999. **2**(1): p. 50-6.

28. Zhang, B., et al., *Neurofilaments and orthograde transport are reduced in ventral root axons of transgenic mice that express human SOD1 with a G93A mutation.* J Cell Biol, 1997. **139**(5): p. 1307-15.

29. Ferri, A., et al., *Familial ALS-superoxide dismutases associate with mitochondria and shift their redox potentials.* Proc Natl Acad Sci U S A, 2006. **103**(37): p. 13860-5.

30. Liochev, S.I. and I. Fridovich, *The role of O2.- in the production of HO.: in vitro and in vivo.* Free Radic Biol Med, 1994. **16**(1): p. 29-33.

31. Zimmerman, M.C., L.W. Oberley, and S.W. Flanagan, *Mutant SOD1-induced neuronal toxicity is mediated by increased mitochondrial superoxide levels.* J Neurochem, 2007.

5.6 Figures and Tables

Figure 1

Excess iron causes FPN re-localization to the lipid rafts. **(A)** Under normal iron conditions, only some of the FPN on the cell membrane is localized to the lipid raft region where it can partner with GPI-CP. **(B)** When intracellular iron level increases, there is rapid relocalization of FPN into the lipid raft domains from non-lipid raft regions of the cell membrane. This would be expected to increase functional GPI-CP/FPN complexes to efflux the excess iron. **(C)** Under iron deprived conditions, FPN disappears from the membrane, which would help to maintain iron within the cell.

A. Normal intracellular Fe

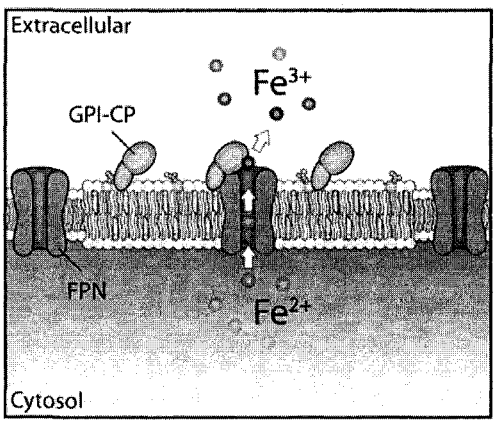

B. High intracellular Fe

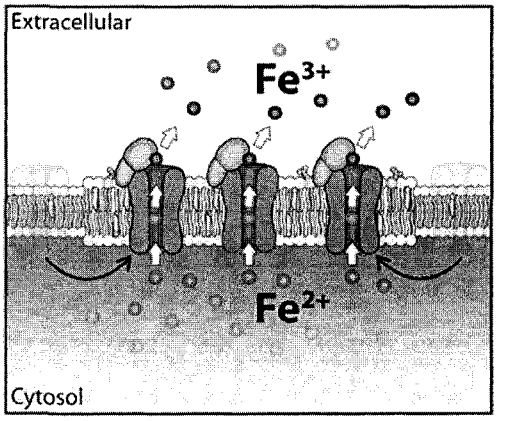

C. Low intracellular Fe

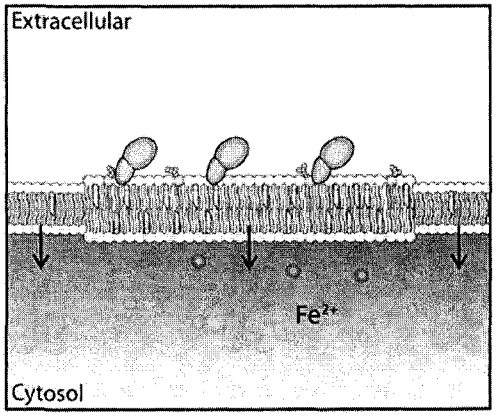

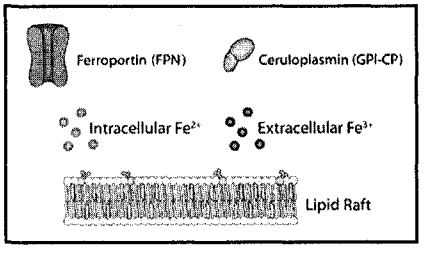

APPENDIX

McGill University Health Centre internal permit for radioactive use

McGill University animal care committee animal use protocol

Copyright waivers for published manuscripts

Copyright Permission Policy

ASBMB Journals

Journal of Biological Chemistry
Molecular and Cellular Proteomics
Journal of Lipid Research
ASBMB Today

ASBMB does not charge for and grants use without requiring your copyright permission request for:

- The Journal of Biological Chemistry is copyrighted by the American Society for Biochemistry and Molecular Biology, Inc. ASBMB grants use without requiring your copyright permission request for: Original authors wanting to reproduce figures or tables from their own work to publish in not-for-profit formats or venues, provided that full acknowledgment of the source is provided in the new work.
- Students wanting to reproduce or republish their work for educational purposes.
- Students using other authors' material for their theses.
- Reproduction or republication of abstracts only.
- Photocopying up to 5 copies for personal use.
- Non-profit educational institutions making multiple photocopies of articles for classroom use; all such reproduction must utilize institutionally owned equipment for this purpose.

Use of copyrighted material requires proper citation.

For all other uses, contact Copyright Clearance Center.

Mon, Aug 20, 2007 4:06 PM

Subject: copyright permission
Date: Monday, August 20, 2007 3:54 PM
From: Suh Young Jeong <suh.jeong@mail.mcgill.ca>
To: <mkimball@sfn.org>
Conversation: copyright permission

Dear Ms. Kimball,

Thank you for your help this afternoon. This is basically to reproduce my paper in my Ph.D. thesis. The citation is,

Jeong SY and David S
Age-related changes in iron homeostasis and cell death in the cerebellum of ceruloplasmin-deficient mice.
J Neurosci. 2006 Sep 20;26(38):9810-9.

My fax number is 1-514-934-8261

Thank you again for your help.

Regards,
Suh Young

Suh Young (Clair) Jeong, M.Sc.
Centre for Research in Neuroscience
McGill University
1650 Cedar Ave. L12-218
Montreal, QC, H3G 1A4
Canada
Tel) 1-514-934-1934 (ext. 42361)
Fax) 1-514-934-8261